

The Chemical Ecology of Protective Microbiomes

Sarah Frances Worsley

Doctor of Philosophy

School of Biological Sciences

University of East Anglia

June 2019

This copy of the thesis has been supplied on condition that anyone who consults it is understood to recognise that its copyright rests with the author and that use of any information derived therefrom must be in accordance with current UK Copyright Law. In addition, any quotation or extract must include full attribution.

Abstract

Actinobacteria are abundant in soil and well-known for producing antimicrobial compounds. Increasingly, members of this phylum are also found to form symbiotic relationships, for example with plants and insects, and provide protection against host infection. However, it remains poorly understood how Actinobacteria can be selectively recruited to the host microbiome from the environment.

Acromyrmex echinatior leafcutter ants transmit *Pseudonocardia* bacteria between generations and also recruit *Streptomyces* species to their cuticular microbiome. RNA Stable Isotope Probing (SIP) experiments demonstrated that ants supply carbon-based resources to their cuticular bacteria. In turn, RNA-sequencing showed that genes encoding *Pseudonocardia* secondary metabolites, including bacteriocins and terpenes, were expressed *in vivo* on the ant cuticle. This suggests that publicly available host resources fuel interference competition between microbial species on the cuticle, which in turn selects for antibiotic-producing bacteria.

In addition to leafcutter ants, Actinobacteria are known to be abundant in plant roots. Several plant-growth-promoting and antibiotic-producing *Streptomyces* bacteria were isolated from the root microbiome of *Arabidopsis thaliana*. Root exudates are hypothesised to play a major role in root microbiome assembly and DNA SIP, coupled with Illumina sequencing showed that these were utilised by many bacterial genera. However, *Streptomyces* appeared to be outcompeted for resources by fast-growing Proteobacteria, despite the fact that streptomycete isolates could grow on purified root exudates in the absence of competition. We found no evidence that the plant defense phytohormone salicylic acid selectively recruits *Streptomyces* to the plant root microbiome, which contradicts the conclusions made by previous published studies and suggests that they make use of other resources.

Overall, this research demonstrates that host-nutrients, coupled with priority effects, can help to define competitive outcomes within the host microbiome. Understanding factors that influence the establishment of protective bacteria has implications for the development of more consistent biocontrol strategies.

Table of Contents

Abstract	2
Table of Contents.....	3
List of Figures	9
List of Tables	13
Abbreviations	15
Acknowledgements	18
Publications arising from this work	19
Chapter 1 General Introduction	20
1.1 The microbiome	20
1.2 Protective microbiomes.....	21
1.3 Actinobacteria as protective symbionts	23
1.3.1 Features of Actinobacteria as protective symbionts	30
1.4 Mechanisms of microbiome formation	32
1.4.1 Vertical transmission of beneficial symbionts.....	33
1.4.2 Providing specific resources	34
1.4.3 Preventing colonisation by non-beneficial bacteria	35
1.5 Outline of this thesis.....	37
Chapter 2 Regulation of the leafcutter ant cuticular microbiome	40
2.1 Introduction	40
2.1.1 Leafcutter ants and their fungal cultivar.....	40
2.1.2 Parasites of the fungus garden	41
2.1.3 Vertically transmitted <i>Pseudonocardia</i> mutualists.....	42
2.1.4 Other actinomycetes on the ant cuticle.....	45
2.1.5 Building a protective microbiome.....	47
2.2 Aims	49
2.3 Materials and Methods	50
2.3.1 Ant colony collection and maintenance.....	50
2.3.2 RNA Stable Isotope Probing of the ant cuticular microbiome.....	51
2.3.2.1 RNA SIP ¹³ C feeding experiment.....	51
2.3.2.2 Preliminary isotope ratio mass spectrometry analysis.....	51

2.3.2.3	Fluorescent microscopy of ant feeding habits	52
2.3.2.4	Cuticular dissection and RNA extraction.....	53
2.3.2.5	Density gradient ultracentrifugation and fractionation.....	54
2.3.2.6	Synthesis of cDNA from RNA SIP fractions.....	55
2.3.2.7	Quantitative PCR of cDNA fractions.....	56
2.3.2.8	Sequencing and analysis	57
2.3.3	Secondary metabolite production by <i>Pseudonocardia</i> mutualists associated with <i>Acromyrmex echinatior</i> colonies	58
2.3.3.1	Isolation of <i>Pseudonocardia</i> bacteria from the ant cuticle.....	58
2.3.3.2	<i>In vitro</i> bioassays	60
2.3.3.3	Culturing <i>Pseudonocardia</i> strains on agar plates for RNA sequencing.....	60
2.3.3.4	RNA extraction from <i>Pseudonocardia</i> strains grown on agar plates.....	61
2.3.3.5	RNA isolation from ant laterocervical plates for dual RNA sequencing.....	61
2.3.3.6	Single and dual RNA sequencing	62
2.3.3.7	Processing of reads generated from RNA sequencing.....	62
2.3.3.8	Functional analysis of mapped reads.....	64
2.3.3.9	Biosynthetic gene cluster expression by <i>Pseudonocardia</i> species	64
2.3.3.10	Analysis of the <i>Pseudonocardia</i> prmABCD gene cluster	65
2.4	Results.....	65
2.4.1	RNA Stable Isotope Probing to determine the transfer of ant resources	65
2.4.1.1	Isotope Ratio Mass Spectrometry	65
2.4.1.2	Fluorescent microscopy of ants fed a labelled glucose diet	66
2.4.1.3	RNA SIP feeding experiments.....	67
2.4.1.4	The total bacterial community on <i>A. echinatior</i> laterocervical plates.....	69
2.4.1.5	Density gradient ultracentrifugation of RNA SIP samples.....	71
2.4.2	<i>Pseudonocardia</i> gene expression <i>in vitro</i> and <i>in vivo</i>	75
2.4.2.1	The bioactivity of <i>Pseudonocardia</i> mutualist species <i>in vitro</i>	75
2.4.2.2	Alignment of RNA sequencing reads	76
2.4.2.3	Normalisation of mapped reads.....	79
2.4.2.4	Expression of gene functional groups on the surface of the ant.....	80
2.4.2.5	Expression of biosynthetic gene clusters on the surface of the ant.....	83
2.4.2.6	Carbon metabolism on the surface of the ant	90
2.5	Discussion.....	94
Chapter 3 Characterisation of <i>Streptomyces</i> species isolated from the roots of		
	<i>Arabidopsis thaliana</i> plants.....	102

3.1	Introduction	102
3.1.1	The plant root microbiome	102
3.1.2	<i>Streptomyces</i> in the plant root microbiome	103
3.1.3	The role of <i>Streptomyces</i> in plant protection.....	105
3.1.4	Potential applications of plant-protective <i>Streptomyces</i> species.....	107
3.1.5	Wheat take-all fungus.....	108
3.1.6	Plant growth promoting traits.....	109
3.2	Aims	111
3.3	Materials and Methods	112
3.3.1	Plant growth and isolation of <i>Streptomyces</i> endophytes	112
3.3.2	Whole genome sequencing and analysis	116
3.3.2.1	DNA extraction for whole genome sequencing.....	116
3.3.2.2	Analysis of whole genome sequences	117
3.3.3	Screening <i>Streptomyces</i> isolates for antifungal and antibacterial activity	118
3.3.3.1	Bioassays on agar plates	118
3.3.3.2	<i>In vivo</i> bioassays against wheat take-all fungus.....	119
3.3.4	Characterisation of N2 antifungal compounds.....	120
3.3.4.1	Bioassays using filipin.....	120
3.3.4.2	Isolation of antimicrobial compounds from agar plates.....	121
3.3.4.3	Detection of the filipin complex using UPLC-MS and the purification of other compounds.....	122
3.3.5	Plant growth promotion assays	123
3.3.5.1	The effect of <i>Streptomyces</i> species on the <i>in vitro</i> growth of <i>A. thaliana</i>	123
3.3.5.2	The effect of <i>Streptomyces</i> species on the <i>in vivo</i> growth of <i>A. thaliana</i>	124
3.3.5.3	<i>In vitro</i> tests for IAA production	124
3.3.5.4	<i>In vitro</i> test for ACC production.....	125
3.4	Results	125
3.4.1	Isolation and genome sequencing of <i>Streptomyces</i> from the roots of <i>Arabidopsis</i> <i>thaliana</i>	125
3.4.1.1	Isolation of root-associated <i>Streptomyces</i> species.....	125
3.4.1.2	Whole genome sequencing of isolates	126
3.4.1.3	The identification of biosynthetic gene clusters	128
3.4.2	The bioactivity of plant-associated <i>Streptomyces</i> isolates	130

3.4.2.1	<i>In vitro</i> bioactivity of root-associated <i>Streptomyces</i> isolates.....	130
3.4.2.2	<i>In vivo</i> bioactivity of <i>Streptomyces</i> N2 against wheat take-all fungus.....	133
3.4.3	Isolation and characterisation of antimicrobials from <i>Streptomyces</i> N2.....	136
3.4.3.1	Filipin-like compounds as a potential antifungal candidates	136
3.4.3.2	Isolation of antifungal compounds.....	140
3.4.4	The impact of <i>Streptomyces</i> isolates on plant growth.....	149
3.4.5	The impact of <i>Streptomyces</i> isolates on plant biomass <i>in vitro</i>	149
3.4.6	The impact of a mixture of <i>Streptomyces</i> isolates on plant biomass <i>in vivo</i>	151
3.4.7	Production of plant-growth-promoting compounds	153
3.5	Discussion.....	157
Chapter 4 The role of root exudates in plant root microbiome establishment.....		166
4.1	Introduction	166
4.1.1	Vertical transmission.....	166
4.1.2	The role of plant root exudates	167
4.1.3	Determining the use of root exudates by bacteria in the plant root microbiome	170
4.1.4	Stable isotope probing experiments involving <i>Arabidopsis thaliana</i>	175
4.2	Aims	176
4.3	Materials and Methods	177
4.3.1	DNA Stable Isotope Probing	177
4.3.1.1	Plant growth and ¹³ C labelling.....	177
4.3.1.2	Sampling the soil, root and rhizosphere compartments	179
4.3.1.3	Density gradient ultracentrifugation and fractionation of DNA.....	180
4.3.1.4	16S rRNA gene amplification and DGGE analysis of fractions.....	181
4.3.1.5	Analysis of the 16S rRNA gene copy number across fractions using qPCR.....	184
4.3.2	16S rRNA gene amplicon sequencing of fractions	184
4.3.3	Investigating root exudates as a sole carbon source	185
4.4	Results.....	186
4.4.1	Bacterial communities in the soil, rhizosphere and roots associated with <i>Arabidopsis thaliana</i> plants	186
4.4.1.1	The total bacterial community	186
4.4.1.2	Actinobacteria in the root, rhizosphere and bulk soil compartments.....	190

4.4.2	Stable Isotope Probing to assess bacterial metabolism of <i>Arabidopsis thaliana</i> root exudates.....	192
4.4.2.1	Fraction selection	192
4.4.2.2	16S rRNA gene amplicon sequencing of density gradient fractions.....	197
4.4.3	The use of root exudates as a sole carbon and nitrogen source.....	205
4.5	Discussion.....	206
Chapter 5 Salicylic acid as a modulator of root colonisation by <i>Streptomyces</i>		213
5.1	Introduction	213
5.1.1	Plant defense phytohormones	216
5.1.2	The role of phytohormones in directing plant root microbiome establishment	216
5.1.3	Heterogeneity in the results of phytohormone studies.....	218
5.2	Aims	220
5.3	Materials and Methods	220
5.3.1	Generating eGFP-labelled <i>Streptomyces</i> strains	220
5.3.2	Root colonisation by <i>Streptomyces</i> isolates.....	222
5.3.2.1	Plant growth and inoculation of <i>Streptomyces</i> isolates.....	222
5.3.2.2	Quantifying <i>Streptomyces</i> root colonisation.....	223
5.3.3	Testing for use of salicylic acid as a sole carbon source by streptomycetes.....	223
5.3.4	Screening for salicylic acid metabolism genes in the genomes of <i>Streptomyces</i> isolates	225
5.3.5	Salicylic acid chemoattraction assays	226
5.3.6	The effect of salicylic acid on <i>Streptomyces</i> in soil microcosms.....	227
5.4	Results.....	228
5.4.1	The effect of plant genotype on plant root colonisation by <i>Streptomyces</i> species	228
5.4.2	Salicylic acid as a sole carbon source	230
5.4.3	Salicylic acid as a chemoattractant	236
5.4.4	The effect of salicylic acid on the competitiveness of <i>Streptomyces</i> in soil microcosms.....	237
5.5	Discussion.....	238
Chapter 6 General Conclusions		244
Bibliography.....		249

Supplementary Information	279
S1 Amino acid sequences of alkane monooxygenases used for phylogenetic analysis in Chapter 1.....	279
S2 Buoyant density of RNA SIP gradient fractions.....	290
S3 Biosynthetic gene clusters predicted for <i>Streptomyces</i> strain N2.....	291
S4 UPLC-MS analysis of <i>Streptomyces</i> strain N2 extracts	293
S5 Analysis of rhizosphere SIP fractions using qPCR.....	295
S6 Growth of streptomycetes on agar minimal medium.....	296

List of Figures

Figure 2.1 The <i>Acromyrmex echinaior</i> leafcutter ant system	43
Figure 2.2 A schematic of the methodology used for RNA Stable Isotope Probing.....	51
Figure 2.3 The results of Isotope Ratio Mass Spectrometry analysis	66
Figure 2.4 The distribution of a 20% glucose water diet containing green fluorescent dye, over the surface of <i>A. echinaior</i> ants.....	67
Figure 2.5 16S rRNA gene copy number across different cDNA fractions of the buoyant density gradient	68
Figure 2.6 The relative abundance (%) of bacterial phyla present in total, unfractionated RNA samples from the laterocervical plates of <i>A. echinaior</i> ants.....	69
Figure 2.7 The relative abundance (%) of bacterial genera present in total, unfractionated RNA samples from the laterocervical plates of <i>A. echinaior</i> ants	70
Figure 2.8 The average relative abundance (%) of different bacterial genera across sequenced fractions of the buoyant density gradient	72
Figure 2.9 The relative abundances (%) of bacterial genera in the “heavy” fractions of buoyant density gradients for ¹² C and ¹³ C samples	74
Figure 2.10 <i>Acromyrmex echinaior</i> ants feeding on a 20% glucose water solution.	75
Figure 2.11 The bioactivity of <i>Pseudonocardia</i> strains	76
Figure 2.12 The expression of KEGG Orthology pathway categories by <i>Pseudonocardia</i> mutualists on the laterocervical plates of <i>Acromyrmex echinaior</i> ants.....	81
Figure 2.13 The expression of KEGG Orthology pathway categories by <i>Pseudonocardia</i> mutualists on agar medium.....	82
Figure 2.14 AntiSMASH outputs for <i>Pseudonocardia</i> reference genomes	83
Figure 2.15 The expression of biosynthetic gene clusters that are shared between <i>Pseudonocardia</i> species	86
Figure 2.16 Expression of biosynthetic gene clusters that are unique to each <i>Pseudonocardia</i> species.....	88
Figure 2.17 Expression of the gene cluster <i>prmABCD</i>	91
Figure 2.18 The genetic architecture of the <i>prmABCD</i> gene cluster.....	92

Figure 2.19 Phylogenetic analysis of the PrmA protein encoded by <i>Pseudonocardia octospinosus</i> and <i>Pseudonocardia echinator</i> isolates	94
Figure 3.1 System for scoring wheat take-all (<i>G. graminis</i>) infection severity	120
Figure 3.2 Images of <i>Streptomyces</i> isolates.....	126
Figure 3.3 Biosynthetic gene cluster (BGC) predictions for genome-sequenced <i>Streptomyces</i> isolates	129
Figure 3.4 The bioactivity of <i>Streptomyces</i> strain N2	133
Figure 3.5 The inhibition of <i>G. graminis</i> by seed-coatings of <i>Streptomyces</i> strain N2	134
Figure 3.6 The effect of <i>Streptomyces</i> strain N2 on wheat plant infection severity by <i>G. graminis</i>	135
Figure 3.7 Images of <i>in vivo</i> bioassays against <i>G. graminis</i>	136
Figure 3.8 The chemical structures of different members of the filipin complex.....	137
Figure 3.9 The structure of the gene cluster encoding filipin in <i>Streptomyces</i> N2	138
Figure 3.10 The minimum inhibitory concentration (MIC) of a filipin standard.....	140
Figure 3.11 Disc-diffusion bioassays using extracts from <i>Streptomyces</i> strain N2.....	141
Figure 3.12 Mass spectra from UPLC-MS analysis of N2 extracts	143
Figure 3.13 A representative UV absorbance trace	144
Figure 3.14 The structures of filipin III, fungichromin and 14-hydroxy(iso)chainin.....	145
Figure 3.15 The structure of the predicted T1PKS-NRPS hybrid cluster in the genome of <i>Streptomyces</i> strain N2	146
Figure 3.16 Disc-diffusion bioassays using compounds purified from <i>Streptomyces</i> strain N2 against <i>Candida albicans</i> and <i>Escherichia coli</i>	148
Figure 3.17 Disc-diffusion bioassays using compounds purified from <i>Streptomyces</i> strain N2 against <i>G. graminis</i>	149
Figure 3.18 The average biomass of <i>Arabidopsis thaliana</i> plants growing on agar plates, following inoculation with different <i>Streptomyces</i> isolates	150
Figure 3.19 Plant growth phenotypes following inoculation with different streptomycete strains.....	151
Figure 3.20 Total dry weight of <i>Arabidopsis thaliana</i> plants grown in Levington compost from seeds inoculated with a mixture of L2, M2 and M3 <i>Streptomyces</i> spores	152

Figure 3.21 Plant growth promotion by a mixture of <i>Streptomyces</i> strains	152
Figure 3.22 The <i>in vitro</i> production of IAA by <i>Streptomyces</i> isolates.....	155
Figure 3.23 The use of ACC as a sole nitrogen source	156
Figure 4.1 A schematic showing the steps involved in DNA Stable Isotope Probing.....	171
Figure 4.2 Principle coordinate analyses of Bray-Curtis dissimilarities between the bulk soil, rhizosphere and root-associated communities of <i>Arabidopsis thaliana</i>	187
Figure 4.3 The relative abundance (%) of bacterial phyla in samples from the bulk soil, rhizosphere and root compartments of <i>Arabidopsis thaliana</i>	189
Figure 4.4 The relative abundance (%) of families of Proteobacteria across the soil, rhizosphere and root compartment of <i>A. thaliana</i> plants	190
Figure 4.5 The relative abundance (%) of actinobacterial families in the soil, rhizosphere and root compartment of <i>A. thaliana</i> plants.....	191
Figure 4.6 A denaturing gradient gel electrophoresis (DGGE) profile of 16S rRNA genes amplified from rhizosphere SIP fractions.	193
Figure 4.7 A denaturing gradient gel electrophoresis (DGGE) profile of 16S rRNA genes amplified from A) root fractions and B) unplanted soil samples.	194
Figure 4.8 16S rRNA gene copy number across buoyant density fractions of DNA isolated from root samples of <i>A. thaliana</i> plants.....	195
Figure 4.9 Results of a principle coordinates analysis of Bray-Curtis dissimilarities between bacterial genera present in the heavy (H) and light (L) buoyant density fractions of rhizosphere samples.....	198
Figure 4.10 Seven bacterial genera in the rhizosphere compartment of <i>A. thaliana</i> plants whose relative abundance demonstrated the greatest overall enrichment in the ¹³ CH fraction	201
Figure 4.11 Eight bacterial genera isolated from the endophytic compartment of <i>A. thaliana</i> , whose relative abundance demonstrated the greatest overall enrichment in the ¹³ CH fraction	203
Figure 4.12 The abundance of the eight bacterial genera metabolising the greatest quantities of labelled exudates in the endophytic compartment of <i>A. thaliana</i>	204
Figure 4.13 The growth of <i>Streptomyces</i> isolates on purified root exudates.....	206

Figure 5.1 Root colonisation efficiency by <i>Streptomyces</i> strains <i>S. coelicolor</i> M145 and <i>Streptomyces</i> strain M3.....	229
Figure 5.2 Isolate growth on minimal medium agarose plates	231
Figure 5.3 The growth of <i>Streptomyces</i> strains on minimal medium containing agar as the gelling agent.....	236
Figure 5.4 Salicylic acid chemoattractant assays	237
Figure 5.5 The number of colony forming units (CFU) of streptomycete inoculants retrieved from soil microcosms	238
Figure S2.1 The relationship between SIP fraction number and buoyant density	290
Figure S4.1 Ion chromatograms from UPLC-MS analysis summarising the metabolic profile of the crude ethyl acetate extract of <i>Streptomyces</i> strain N2.....	293
Figure S5.1 16S rRNA gene copy number across buoyant density fractions of DNA isolated from rhizosphere samples of <i>A. thaliana</i> plants	295
Figure S6.1 Growth of <i>Streptomyces</i> isolates on minimal medium with agar as a gelling agent	296

List of Tables

Table 1.1 Defensive symbioses in which Actinobacteria have been implicated to play a protective role.....	26
Table 2.1 Details of species and strains associated with work in Chapter 2.	50
Table 2.2 Protocol for the reverse transcription of RNA SIP fractions.....	55
Table 2.3 Primer sequences used for the partial amplification of the bacterial 16S rRNA gene	56
Table 2.4 Components and thermocycler conditions for amplification of the 16S rRNA gene using PCR.....	58
Table 2.5 Growth media used in bioassays and RNA sequencing experiments in Chapter 2. .	59
Table 2.6 Genome sequences used for alignment in RNA sequencing experiments.....	63
Table 2.7 The number of reads in each sample that uniquely mapped to each respective reference genome	78
Table 2.8 Biosynthetic gene clusters (and their classification) that are either shared by both <i>P. octospinosus</i> and <i>P. echinator</i> , or are unique to either strain	84
Table 3.1 Species and strains used in plant microbiome experiments	113
Table 3.2 Growth media used for experiments involving plant-associated streptomycetes.	114
Table 3.3 Components and thermocycler conditions for amplification of the bacterial 16S rRNA gene using colony PCR.....	116
Table 3.4 Genome features of plant-associated <i>Streptomyces</i> strains sequenced for this study	127
Table 3.5 Results of multi-locus sequence analyses of genome-sequenced isolates	128
Table 3.6 Bioactivity screens of plant-associated <i>Streptomyces</i> species	131
Table 3.7 The percentage identity of protein sequences encoded by genes found in the N2 filipin gene cluster, compared to proteins encoded by the filipin cluster of <i>S. avermitilis</i>	139
Table 3.8 The presence and absence of genes encoding enzymes involved in plant growth promotion pathways in sequenced <i>Streptomyces</i> isolates.....	154
Table 4.1 A summary of published Stable Isotope Probing (SIP) experiments.....	172

Table 4.2 Components and thermocycler conditions for the amplification of the 16S rRNA gene using PCR.	182
Table 4.3 Primers used in stable isotope probing experiments.	182
Table 4.4 Components of an 8% polyacrylamide denaturing gel, with a linear denaturant gradient of 40-80%	183
Table 4.5 Heavy (H) and Light (L) fractions of DNA selected for 16S rRNA gene amplicon sequencing	196
Table 4.6 Summary of SIP results	200
Table 5.1 Strains and plasmids used for work described in Chapter 5.	221
Table 5.2 Minimal medium recipe used for experiments in Chapter 5.	224
Table 5.3 Proteins involved in SA degradation pathways.....	225
Table 5.4 The results of BLASTp analyses comparing the amino acid sequences of genes involved in known salicylic acid degradation pathways	233
Table S3.1 Biosynthetic Gene Clusters (BGCs) predicted to be encoded in the genome of <i>Streptomyces</i> strain N2	291
Table S4.1 Compounds identified in the crude extracts of <i>Streptomyces</i> N2	294

Abbreviations

μg	Microgram
μl	Microlitre
μM	Micromolar
[M+Na]⁺	Sodium adduct in positive ion mode
%	Percent
°C	Degrees centigrade
ACC	1-aminocyclopropane-1-carboxylate
ANI	Average nucleotide identity
ANOVA	Analysis of variance
BGC	Biosynthetic gene cluster
BLAST	Basic Local Alignment Search Tool
bp	Base pairs
cDNA	Complementary DNA
CDS	Coding sequence
CFU	Colony forming units
cm	Centimeter
CsCl	Cesium chloride
CsTFA	Cesium trifluoroacetate
DEPC	Diethyl pyrocarbonate
DF	Degrees of freedom
DGGE	Denaturing gradient gel electrophoresis
DMSO	Dimethyl sulphoxide
DNA	Deoxyribonucleic acid
dNTPs	Deoxyribonucleotides
DTT	Dithiothreitol
EDTA	Ethylenediaminetetraacetic acid
eGFP	Enhanced green fluorescent protein
EtAc	Ethyl acetate
EtOH	Ethanol
g	Gram

GB	Gradient buffer
GFF	General feature format
GYM	Glucose-yeast-malt
IAA	Indole-3-acetic acid
IRMS	Isotope ratio mass spectrometry
KAAS	KEGG Automatic Annotation Server
KEGG	Kyoto Encyclopedia of Genes and Genomes
KO	Kegg Orthology
L	Litre
LB	Lennox broth
m	Metre
M	Molar
m/s	Metres per second
m/z	Mass-to-charge ratio
mAU	Milli absorbance units
MeOH	Methanol
mg	Milligrams
min(s)	Minutes(s)
ml	Milliliter
mM	Millimolar
mm	Millimeter
MRSA	Methicillin resistant <i>Staphylococcus aureus</i>
Msk	Murashige and skoog
MYM	Maltose-yeast extract-malt extract
nD-TC	Temperature adjusted average density
NCBI	National Center for Biotechnology Information
ng	Nanograms
nm	Nanometre
ORF	Open reading frame
OTU	Operational taxonomic unit
PBS-S	Phosphate buffered saline- Silwett L-77 amended
PcoA	Principle coordinate analysis

PCR	Polymerase chain reaction
PERMANOVA	Permutational analysis of variance
PGA	Potato glucose agar
PGP	Plant-growth-promotion
ppmv	Parts per million volume
qPCR	Quantitative polymerase chain reaction
RAST	Rapid Annotation using Subsystem Technology
R.I	Refractive index
RNA	Ribonucleic acid
RPKM	Reads Per Kilobase of exon model per Million reads
Rpm	Revolutions per minute
SA	Salicylic acid
SE	Standard error
sec(s)	Second(s)
SFM	Soy flour mannitol
SIP	Stable isotope probing
SOM	Soil organic matter
TAE	Tris acetate EDTA
TSB	Tryptone soy broth
UPLC-MS	Ultra-Performance Liquid Chromatographer-tandem Mass Spectrometer
v/v	Volume to volume
w/v	Weight to volume
YPD	Yeast peptone dextrose

Acknowledgements

I would like to thank my supervisors Matt Hutchings, Colin Murrell, Barrie Wilkinson and Doug Yu for providing me with this incredible opportunity and for their guidance over the four years of my PhD. I would also like to thank past and present members of the Hutchings laboratory and Pamela Salter office for their support and friendship during my time at UEA. In particular, my thanks go to Neil Holmes for introducing me to *Streptomyces* and leafcutter ants and to Elaine Patrick for her support. I am also grateful to members of the Murrell group, particularly Michael Macey, Jennifer Pratscher and Andrew Crombie for their guidance on Stable Isotope Probing. I would also like to thank Simon Moxon for his advice on RNA-seq analysis and Paul Thomas for maintaining the Biomedical Cell Imaging Laboratory. Furthermore, I would like to thank members of the John Innes Centre for their support with chemical analysis, particularly Johannes Rassbach, Sybil Batey and Daniel Heine. I would also like to thank Rachel Merton and Anne Osborne for enabling me to carry out work on the wheat Take-all fungus. I am extremely grateful to Koos Boomsma and Tabitha Innocent at the University of Copenhagen, as well as the Smithsonian Tropical Research Institute, for enabling me to undertake fieldwork in Gamboa, Panama and for providing excellent advice on working with the leafcutter ant system. I would also like to thank the EnvEast NERC Doctoral Training Partnership for funding my PhD and all members of the DTP for their valued friendship. Finally, I am also tremendously grateful to my parents and other members of the Worsley and Bowles families for their encouragement and to my fiancé Alex Bowles for his never-ending support.

Publications arising from this work

Worsley SF, Macey MC, Yu DW, Wilkinson B, Murrell JC and Hutchings MI (2019).

Investigating the role of exudates in shaping the *Arabidopsis thaliana* root microbiome using DNA stable isotope probing. (In review, *ISME J*).

Newitt JT, Prudence SMM, Hutchings MI and Worsley SF (2019). Biocontrol of cereal crop diseases using streptomycetes. *Pathogens* **8**(2): 78.

Boza G, Worsley SF, Yu D, Scheuring I (2019). Efficient assembly and long-term stability of defensive microbiomes via private resources and community bistability. *PLoS Comput Biol* **15**(5): e1007109.

Worsley SF, Innocent TM, Heine D, Murrell JC, Yu DW, Wilkinson B, Hutchings MI, Boomsma JJ and Holmes NA (2018). Symbiotic partnerships and their chemical interactions in the leafcutter ants (Hymenoptera: Formicidae). *Myrmecological News* **27**: 59-74.

Heine D[#], Holmes NA[#], Worsley SF, Alve dos Santos AC, Innocent TM, Scherlach K, Patrick E, Yu DW, Murrell JC, Boomsma JJ, Hertweck C, Hutchings MI and Wilkinson B (2018). Chemical warfare between leafcutter ant symbionts and a co-evolved pathogen. *Nat Commun* **9**: 2208.

van der Meij A[#], Worsley SF[#], Hutchings MI and van Wezel GP (2017). Chemical ecology of antibiotic production by actinomycetes. *FEMS Microbiol Rev* **41**:392-416.

Holmes NA, Innocent T, Heine D, Worsley SF, Findlay K, Murrell J.C., Wilkinson B, Boomsma JJ and Hutchings MI (2016). Genome analysis of two *Pseudonocardia* phylotypes associated with *Acromyrmex* leafcutter ants reveals their biosynthetic potential. *Front Microbiol* **7**:2073

[#] These authors contributed equally

Chapter 1 General Introduction

1.1 The microbiome

Almost all organisms, at some stage during their lifecycle, interact extensively with a complex community of microorganisms that make use of resources provided by the host niche and that are acquired from the host environment. These diverse microbial assemblages, their collective genomes as well as the host habitat, are collectively referred to as an organism's microbiome (Marchesi and Ravel 2015). It was previously thought that the assembly of the host microbiome was unpredictable, being predominantly driven by the random dispersal of microorganisms in the environment, in addition to the competitive interactions between the microbial species present in a particular habitat (Foster et al 2017, Napflin and Schmid-Hempel 2018). However, advances in next generation sequencing have demonstrated that members of the same host species often tend to associate with the same broad-scale groups of microbial taxa and that this is independent of their surrounding environmental conditions. For example, independent studies of the *Arabidopsis thaliana* plant root microbiome have shown that Proteobacteria and Actinobacteria tend to dominate the root community and that this enrichment is consistently driven by the presence of specific bacterial families (Bodenhausen et al 2013, Bulgarelli et al 2012, Lundberg et al 2012). Patterns can also be observed in the human gut microbiome, despite variation between different individuals, whereby the early-life infant gut is primarily dominated by specific species of *Bifidobacterium*, whereas the adult gut has a greater abundance of genera in the phyla Firmicutes and Bacteroidetes (Matamoros et al 2013). In addition to common patterns across members of the same host species, several microbial communities, for example those associated with plants and insects, demonstrate significant congruence with host phylogeny suggesting that certain species assemblages are being maintained and are evolving over evolutionary time along with their host (Brucker and Bordenstein 2012, Fitzpatrick et al 2018, Sanders et al 2014).

The non-random accumulation of microbial species within microbiomes suggests that host organisms play more than a passive role during microbiome assembly. In fact, hosts are expected to experience strong selection to filter the enormous pool of

microbial species available to them, to encourage the persistence of species with host-beneficial traits (Archetti et al 2011, Foster et al 2017, Scheuring and Yu 2012). Accordingly, beneficial microorganisms tend to be represented at a greater frequency within microbiomes than would be expected by chance (Scheuring and Yu 2012). Microorganisms can be advantageous to their host in a number of different ways. For example, many symbionts provide their hosts with nutritional benefits by breaking down complex, otherwise indigestible molecules, or by supplementing the host diet with essential nutrients through pathways such as nitrogen fixation or phosphate solubilisation (Kneip et al 2007, Mizrahi and Jami 2018, Tremaroli and Bäckhed 2012). Other symbionts can provide protective benefits to their host by producing antimicrobial compounds that inhibit the growth of pathogens (Clay 2014, Ford and King 2016, Haine 2008, Kaltenpoth 2009, Seipke et al 2012b), or by directing immune system development to prime its response to pathogenic organisms (Cordovez et al 2015, Kabat et al 2014, Pieterse et al 2014).

1.2 Protective microbiomes

As mentioned above, one of the mechanisms by which microbes can enhance the fitness of their host, is by providing protection against diseases caused by pathogen and parasite infection. Protection can arise through a variety of different mechanisms. Firstly, antimicrobial compounds or toxins that are produced by symbionts can directly inhibit the growth of pathogenic species. Such compounds are often produced as a by-product of interference competition occurring between strains within the microbiome; symbionts produce toxic compounds in the fight for resources and these, in turn, inhibit the growth of pathogens (Clay 2014, Ford and King 2016, Scheuring and Yu 2012). Inhibitory microbial compounds have been found to play a key role in host protection across many different host species including vertebrates, invertebrates and plants (Barke et al 2010, Berg 2009, Clay 2014, Ford and King 2016, Viaene et al 2016). For example, hoopoe birds (*Upupa epops*) are known to culture high densities of *Enterococcus* bacteria in their uropygial (preen) glands; these bacteria produce volatile antimicrobial substances that are known to inhibit the growth of feather-degrading microorganisms (Martin-Platero et al 2006, Martin-Vivaldi et al 2010). Similarly, embryos of several species of crustacean are coated in a dense growth of Gram-

negative bacteria that produce antifungal compounds against the fungal pathogen *Lagenidium callinectes* (Gil-Turnes et al 1989, Gil-Turnes and Fenical 1992).

Indirectly, strains can also inhibit the growth of pathogens via competitive exclusion and colonisation resistance. For example, if beneficial microbes have a faster growth rate or can use resources more efficiently, they will tend to dominate the use of microbiome resources such as space and nutrients, thereby excluding pathogens from exploiting the host niche (Clay 2014). The epiphytic commensal bacterial communities growing on the surface of some seaweed species have been implicated to play an important role in colonisation resistance, by preventing secondary colonisation by detrimental microorganisms (Egan et al 2013). Similarly, certain bacterial species that inhabit the mucosal and epidermal surfaces of the vertebrate gut are thought to play an important role in excluding intestinal pathogens (Buffie and Pamer 2013). For example, in mice, the commensal bacterial species, *Bacteroides thetaiotaomicron*, is known to consume carbohydrates that are required for the growth of *Citrobacter rodentium* (a mucosal pathogen of mice) and thus can exclude this pathogen from the intestinal lumen by preventing access to key resources (Buffie and Pamer 2013).

In addition to antimicrobials and competitive exclusion, members of the microbiome can also provide protection to their host via the activation of the host immune response. Evidence from mouse models suggests that commensal bacteria in the intestinal tract can enhance host immunity by directing the development of immune cell populations involved in both innate and adaptive immune processes, as well as by promoting the production of antimicrobials and pro-inflammatory factors by cells in the gut (Buffie and Pamer 2013, Hooper et al 2012). Similarly, bacterial symbionts that colonise plant roots, such as *Bacillus*, *Streptomyces* and *Pseudomonas* species, have been shown to prime the plant immune system, resulting in an elevated and accelerated response to pathogenic infection (Conn et al 2008, Cordovez et al 2015, Kurth et al 2014, Pieterse et al 2014, Selosse et al 2014). The plant host recognises residues on the surface of beneficial microbial species (called microbial associated molecular patterns, or MAMPs) which leads to the activation of signaling cascades involved in mounting an immune response (Pieterse et al 2014, Selosse et al 2014). These signals are directed by plant phytohormones such as salicylic acid, jasmonic acid

and ethylene. The local priming of these pathways can spread to distal parts of the plant leading to widespread induced systemic resistance (ISR) against foliar and root pathogens (Cordovez et al 2015, Pieterse et al 2014, Selosse et al 2014).

1.3 Actinobacteria as protective symbionts

Several microbial species have been suggested to contribute to host organism protection across a wide variety of different systems. However, increasingly, members of the phylum Actinobacteria are being found to play a key role in defensive microbiomes (Kaltenpoth 2009, Seipke et al 2012b, Viaene et al 2016). Species of Actinobacteria take part in some of the most well-characterised examples of protective symbioses and have been shown to contribute to host protection in a diverse range of species and in a variety of different ways (Table 1.1).

The phylum Actinobacteria consists of a large and diverse collection of Gram-positive bacteria with GC-rich genomes and is well-known for its contribution to both agriculture and human medicine (Hopwood 2007, van der Meij et al 2017). This contribution is mainly due to the ability of actinobacterial species to produce a huge array of secondary metabolites that have diverse functions including as antimicrobials, immunosuppressants, antivirals and anticancer compounds (Hopwood 2007, Rey and Dumas 2017, Seipke et al 2012b, van der Meij et al 2017). One of the most well-characterised groups of Actinobacteria is the genus *Streptomyces*, which is responsible for approximately 50% of the antibiotics that are presently used in the clinic (Hopwood 2007, van der Meij et al 2017). *Streptomyces* species are characterised by their secondary metabolism, saprotrophic lifestyle, filamentous growth and complex lifecycle (Chater 2006, Flärdh and Buttner 2009).

The lifecycle of a streptomycete begins with a single spore which germinates under favourable conditions to produce a number of germ tubes, which further develop into hyphae (Flärdh and Buttner 2009). These hyphae grow across and into the growth substrate, via branching and hyphal tip extension, leading to the formation of a vegetative mycelium (Flärdh and Buttner 2009). Each colony produces a diverse array of extracellular enzymes, allowing them to break down a range of substrates including complex molecules such as chitin and cellulose (Chater 2006, Chater et al 2010). Under

unfavourable conditions, such as nutrient depletion or desiccation, the colony produces aerial hyphae. Here, extensive DNA replication occurs, followed by septation and cell division, resulting in the formation of spore chains, with each spore containing a single chromosome (Flårdh and Buttner 2009). Spores are highly resistant to desiccation allowing them to disperse to new environments, in which the lifecycle resumes again under favourable conditions. The production of aerial hyphae and spores often coincides with the production of antimicrobial compounds which allow *Streptomyces* species to protect the remaining resources that have been broken down by their extracellular enzymes (Chater 2006).

It has long been known that Actinobacteria, and particularly *Streptomyces* species, are abundant in soils, in addition to a range of other environments including marine and fresh water ecosystems (van der Meij et al 2017). However, it is increasingly becoming clear that Actinobacteria are also capable of forming very close symbiotic interactions with a diverse range of other organisms including insects, marine organisms and plants (Kaltenpoth 2009, Seipke et al 2012b, Viaene et al 2016). In several of these systems there is evidence to suggest that secondary metabolites produced by Actinobacteria can provide their host with protection against infection and thus, many of these interactions are thought to represent cases of defensive mutualisms (Table 1.1). For example, Actinobacteria are known to associate with several species of fungus-farming insect, including *Acromyrmex* leafcutter ants (discussed in greater detail in Chapter 2) and the Southern pine beetle (*Dendroctonus frontalis*) (Kaltenpoth 2009, Seipke et al 2012b). Both of these species cultivate a specific species of fungus for food, however, each system is also parasitised by a specialised fungus that grows on and degrades the nutritional fungal cultivar. *Acromyrmex* leafcutter ants accumulate Actinobacteria on their cuticle which produce antimicrobials that inhibit the growth of the specialised fungal parasite *Escovopsis weberi*; the ants spread these antimicrobials over their fungus gardens to keep them free from infection (Barke et al 2010, Currie et al 2003, Currie et al 1999b). Similarly, individuals of the species *Dendroctonus frontalis*, are known to carry antibiotic-producing *Streptomyces* bacteria on their cuticle, as well as in specialised pockets known as mycangia, in which they also carry their fungal cultivar (*Entomocorticium*) around the galleries they make in the bark of pine trees (Hulcr et al 2011, Scott et al 2008). Antibiotics produced by the *Streptomyces* species associated

with the beetle can inhibit the fungal species *Ophiostoma minus* which would otherwise compete with the beetle's own fungal cultivar (Scott et al 2008). In addition to protecting a host's food source, Actinobacteria are also known to provide protection to the host itself in a diverse range of systems (Table 1.1). This can occur either through the production of antimicrobials, or by priming the host immune system to bring about an accelerated immune response to pathogen infection (Kaltenpoth et al 2005, Koehler et al 2013, Kroiss et al 2010, Viaene et al 2016).

Table 1.1 Defensive symbioses in which Actinobacteria have been implicated to play a protective role.

Host	Symbiont	Main parasites	Mechanism of protection	Mode of transmission	References
Attine (fungus-growing) ants (e.g. species of <i>Acromyrmex</i> and <i>Apterostigma</i>)	<i>Pseudonocardia</i> bacteria and other actinomycetes including <i>Streptomyces</i> species	Fungi that parasitise the ants' fungal cultivar, particularly species of <i>Escovopsis</i> which are specialised to grow on the ants' fungus gardens	Antimicrobial compounds are thought to be produced by Actinobacteria, as a by-product of interference competition on the ant cuticle. These are spread around the fungus garden	<i>Pseudonocardia</i> are vertically transmitted between generations. Other Actinobacteria are horizontally acquired	(Barke et al 2010, Barke et al 2011, Currie et al 2003, Schoenian et al 2011)
Southern pine beetle (<i>Dendroctonus frontalis</i>)	<i>Streptomyces</i> bacteria (consistently associated with	The fungal species <i>Ophiostoma minus</i> which competes with	<i>Streptomyces</i> species grow on the surface of the beetle and in specialised structures (mycangia),	Unknown	(Hulcr et al 2011, Scott et al 2008)

	beetle across North American range)	the beetles' food fungus	where they produce antimicrobials; these are spread over the galleries in pine trees in which the beetles grow their food fungus		
Female solitary digger wasps (<i>Pilanthus</i> , <i>Trachypus</i> , <i>Philanthinus</i>)	<i>Candidatus Streptomyces philanthi</i>	Fungi and bacteria that grow in the brood chamber and could infect the developing wasp larvae	<i>Streptomyces</i> are cultured in specialised antennal glands. The bacteria are spread over the surface of brood chamber walls by the female wasp and become incorporated into larval cocoons. Antimicrobials are produced on the cocoon surface	Vertically transmitted during larval cocoon spinning	(Kaltenpoth et al 2005, Kaltenpoth et al 2010b, Koehler et al 2013, Kroiss et al 2010)

Trap ants in the genus <i>Allomerus</i>	<i>Amycolatopsis</i> and <i>Streptomyces</i> bacteria	Fungal species that parasitise the traps built by the ants to ensnare insects. Traps are made from a sooty mold fungus and host plant leaves	Symbionts produce antifungals <i>in vitro</i> ; they are presumed to produce these <i>in vivo</i> to keep the ants' insect traps parasite free	Unknown	(Ruiz-Gonzalez et al 2011, Seipke et al 2012a)
Various plant species (e.g. wheat, lettuce, tomatoes, <i>Arabidopsis thaliana</i> , rice)	Various Actinobacteria, particularly <i>Streptomyces</i> species	Foliar and plant root pathogens, including bacterial and fungal species	<i>Streptomyces</i> species can provide plant host protection through the production of antimicrobials and by priming the plant immune system	Thought to be horizontal acquisition from the soil environment	(Chen et al 2016, Law et al 2017, Rey and Dumas 2017, Schrey and Tarkka 2008, Viaene et al 2016)
Marine sponges	Various actinomycetes, including <i>Streptomyces</i> species	Various microbial species	Presumed to produce antimicrobials; novel compounds have been characterised from newly isolated strains	Unconfirmed, assumed to be acquired horizontally from the environment	(Khan et al 2011) (Seipke et al 2012b)

<p>Bees (including the genera <i>Apis</i>, <i>Trigona</i> and <i>Tetragonilla</i>)</p>	<p>Various Actinobacteria including <i>Streptomyces</i> species</p>	<p><i>Paenibacillus larvae</i> and <i>Melissococcus plutonius</i> (the main causative agents of American and European foulbrood, respectively)</p>	<p>Isolates from hives have been shown to inhibit foulbrood <i>in vitro</i>. Thus, they have the potential to play a protective role <i>in vivo</i></p>	<p>Unconfirmed if the presence of Actinobacteria is adaptive for the bees</p>	<p>(Promnuan et al 2009, Promnuan et al 2013)</p>
<p>Marine cone snails</p>	<p>Various actinomycetes, including <i>Streptomyces</i> species which live and divide within the snail tissue</p>	<p>Various microbial species</p>	<p>Antifungals and other bioactive compounds have been purified from isolates, although production has not yet been confirmed <i>in vivo</i></p>	<p>Unconfirmed</p>	<p>(Peraud et al 2009)</p>

1.3.1 Features of Actinobacteria as protective symbionts

Actinobacteria are thought to be involved in approximately half of all defensive mutualisms that have been described (Kaltenpoth 2009). Several aspects of their growth and metabolism are thought to have contributed to their success as symbionts and make them particularly desirable to hosts (Chater 2006, Kaltenpoth 2009). Firstly, many Actinobacteria have the ability to subsist on a wide range of carbon sources present at very low quantities. This means that they often have access to nutrients that are inaccessible to other organisms, such as complex molecules like lignocellulose and chitin, as well as hydrocarbon-based compounds (Chater 2006, Chater et al 2010, Kaltenpoth 2009). They are also capable of persisting on metabolic waste products, potentially making them cheaper to maintain than other symbionts (Kaltenpoth 2009). Their ability to produce secondary metabolites with antimicrobial properties most likely evolved as a response to competition with other microorganisms over resources, including those present within the host niche (Kaltenpoth 2009, Seipke et al 2012b). It is likely that many actinobacterial symbionts began as commensals or even mild parasites, feeding off and fighting for host resources (Kaltenpoth 2009). The production of secondary metabolites during interference competition with other microbes may have then, in turn, become beneficial to the host by preventing pathogenic infection. These benefits are likely to have driven the evolution of mechanisms to ensure that Actinobacteria consistently colonised the microbiome (Kaltenpoth 2009).

The high abundance of Actinobacteria in soils makes it highly likely that many organisms, for example soil-burrowing insects and plant roots, encounter them on a regular basis. The spore-forming capabilities of several genera, like *Streptomyces*, may additionally aid their acquisition from the environment (horizontal transmission) as well as their transmission to later generations (vertical transmission), as it can ensure symbiont survival during these processes, or in the absence of the host organism (Chater 2006, Kaltenpoth 2009). For example, the resistance of *Streptomyces* to unfavourable conditions seems to be particularly important during symbiosis with solitary digger wasps (Table 1.1). Female solitary digger wasps (in the genera *Pilanthus*, *Trachypus* and *Philanthinus*) lay their eggs in burrows, which they dig into the soil and

provision with a paralysed honey bee; the developing larvae feed on the bee before spinning a cocoon (Kaltenpoth et al 2005, Kaltenpoth 2009). The brood chambers are humid and damp, providing optimal growth conditions for a variety of fungi and bacteria. In order to prevent their larvae from getting infected the female wasp coats the brood chamber walls with secretions containing the species *Candidatus Streptomyces philanthi* which the wasp cultures in its specialised antennal glands (Kaltenpoth et al 2005, Kaltenpoth et al 2006). These bacteria then become incorporated into the larval cocoon and produce antibiotics on the cocoon surface (Kroiss et al 2010). Remarkably, the *Streptomyces* symbiont can remain viable on the cocoon wall for up to 9 months before the larva emerges, despite the cocoon surface being a very poor environment with limited nutrients availability (Kaltenpoth et al 2010a). This long-term survival allows the *Streptomyces* bacteria to be vertically-transmitted when they are taken-up by the fully-developed females that emerge from cocoons (Kaltenpoth 2009, Kaltenpoth et al 2010a).

In several of the systems in which actinobacterial species are present as protective symbionts, they are also found to consistently dominate the host microbiome. For example in the leafcutter ant cuticular microbiome and in the solitary digger wasp antennal glands, specific species of Actinobacteria are highly abundant and other taxa are comparatively rare (Andersen et al 2013, Kaltenpoth 2009). In other systems, Actinobacteria coexist with other bacterial taxa, but are still found to be consistently enriched within the microbiome of the host organism compared to the surrounding environment. This is the case for *Streptomyces* species found to be living within the roots of certain plant species, whereby they coexist alongside other taxa such as Proteobacterial species, but are also consistently present at higher abundances in the roots compared to the surrounding soil, independent of differences in soil type (Bulgarelli et al 2012, Edwards et al 2015, Lundberg et al 2012, Viaene et al 2016). These observations suggest that there may be host mechanisms in place that restrict interactions with microbes in the environment and allow particular species of Actinobacteria access to the host microbiome. Indeed, as discussed, hosts are expected to experience strong selection to encourage the persistence of species that provide them with benefits, such as protection against disease (Archetti et al 2011,

Foster et al 2017). Unpicking host-selective mechanisms is becoming a major research focus.

1.4 Mechanisms of microbiome formation

The mechanisms underpinning microbiome formation still remain relatively elusive and may differ depending on the host species. However, developing an understanding of the signals involved will be crucial for allowing us to exploit and manipulate microbiome interactions. For example, such knowledge will enable us to develop novel methods of pest and disease control, enhance the presence of beneficial species within microbiomes and ultimately improve the health of a variety of different host organisms (Dessaux et al 2016, Ryan et al 2009). Additionally, for protective microbiomes, understanding the chemical interactions taking place between hosts, symbionts and pathogens at the molecular level, may aid the search for novel antimicrobials and enable us to decipher how to regulate the production of these molecules in a laboratory setting (van der Meij et al 2017).

The question surrounding microbiome formation is often referred to as the “partner choice” problem, since, for a host to be able to accumulate beneficial species, it must be able to distinguish between strains in its environment and limit its interactions to those that provide it with significant benefits (Archetti et al. 2011). How the host is able to identify beneficial species, particularly when interacting with hugely diverse microbial communities, remains unclear for many host-symbiont systems. However, three major hypotheses are beginning to emerge that describe mechanisms that hosts could use to bias the accumulation of microbial species, and the competitive interactions between them, in order to select specific species from their environment (Boza et al 2019, Foster et al 2017, Scheuring and Yu 2012). These mechanisms are not mutually exclusive from one another but include: firstly, the vertical transmission of specific beneficial species between host generations; secondly, the provision of resources that are preferentially metabolised by beneficial species or bias competitive interactions so that beneficial species out-compete other taxa; and thirdly, the production of compounds that reduce the competitive ability or survival of non-beneficial strains within the host microbiome. All three mechanisms will now be explored in more detail.

1.4.1 Vertical transmission of beneficial symbionts

The first mechanism by which a host could bias the outcome of microbiome accumulation is by providing beneficial species with preferential access to resources in the host niche (Boza et al 2019, Clay 2014, Foster et al 2017). The simplest way by which this can occur is via the vertical transmission of beneficial symbionts, whereby particular bacterial species are transmitted between host generations. Vertical transmission can be achieved if the host germline cells are infected with beneficial symbionts, or alternatively, non-colonised hosts are kept in isolation after birth so that they are effectively sterile before being inoculated with the parent microbiome (Boza et al 2019). By controlling the immigration of microorganisms in this way, the host gives priority to beneficial species, allowing them to proliferate in a competitor-free space (Boza et al 2019, Foster et al 2017). This can then shape subsequent microbiome acquisition and potentially prevent invasion by other unwanted species.

There are numerous examples of such priority effects occurring in nature, including in systems involving Actinobacteria (Table 1.1). For example, leafcutter ants remain sterile before they hatch from the pupal stage (Marsh et al 2014). Following hatching, they are inoculated with antibiotic-producing *Pseudonocardia* bacteria by older worker ants, within a 24 hour window (Marsh et al 2014). These filamentous Actinobacteria then bloom over the ant cuticle before receding to grow around specialised crypts which are thought to supply the cuticular microbiome with resources (Andersen et al 2013, Currie et al 1999b, Currie et al 2006, Marsh et al 2014). Similarly, solitary digger wasps inoculate their brood chambers with *Streptomyces* bacteria via antennal gland secretions; the bacteria become directly incorporated into the larval cocoon whereby they produce antibiotics and are then taken-up by emerging females (Kaltenpoth et al 2005, Kaltenpoth et al 2006, Kaltenpoth et al 2010b, Kaltenpoth et al 2012). It is possible that plant species are also capable of vertically transmitting microbial symbionts via their seeds. However, although studies have shown that a diverse community of microbes can be isolated from seeds there is, as yet, no clear consensus on whether these species are consistently transmitted across generations and what role they play during interactions with the host (Nelson 2018). The application of bacterial species to seeds as biocontrol agents attempts to replicate the process of

vertical transmission, by ensuring that protective microbial species are present at the outset of seed germination and plant microbiome formation (O'Callaghan 2016).

1.4.2 Providing specific resources

The second mechanism by which a host could drive the accumulation of beneficial microbial species is by providing their microbiome with specific nutrients that are preferentially utilised by microorganisms with the desired metabolic capabilities (Boza et al 2019, Foster et al 2017). This hypothesis can be extended, since resources can also drive interference competition between strains. Therefore, hosts could also provide their microbiome with resources that ensure beneficial microorganisms successfully outcompete other species (Archetti et al 2011, Scheuring and Yu 2012). This latter mechanism is known as the “competitive screening” hypothesis and may be particularly important for the establishment of protective microbiomes, since interference competition for resources can drive the production of compounds such as antibiotics, bacteriocins, adhesives and effector proteins that could all, in turn, be coopted for host defence (Archetti et al 2011, Foster et al 2017, Scheuring and Yu 2012).

There are several examples of specific resources being provided by hosts to recruit certain microbial species. Corals, as well as their dinoflagellate symbionts, produce large quantities of the compound dimethylsulfoniopropionate (DMSP) (Raina et al 2013). Several of the bacterial taxa that are early colonisers of coral larvae, including the genus *Pseudovibrio*, have been shown to specifically metabolise DMSP as a sole carbon and sulphur source (Raina et al 2009, Raina et al 2010, Raina et al 2016). It is thought that bacteria that can degrade DMSP may have a nutritional advantage over non-degraders and that this compound could be important in structuring the initial microbiome (Apprill et al 2009, Raina et al 2010). Interestingly, *Pseudovibrio* can also use DMSP as a precursor to produce antimicrobial compounds that inhibit the growth of coral pathogens, suggesting that DMSP may also play a role in fuelling interference competition and host protection (Raina et al 2016). In addition to corals, human breast milk is also known to contain a high density of complex oligosaccharides which are each preferentially consumed by a single species of co-adapted gut bacterium,

suggesting that private resources may also be involved in the early establishment of the human infant gut microbiome (Zivkovic et al. 2011).

Plants are also thought to recruit their microbiome from the soil environment via the use of plant-derived resources. Approximately 20-40% of photosynthetically fixed carbon leaves plants via their roots (Haichar et al 2016, Hiltner 1904). These exudates contain a complex mixture of compounds, all of which may act as resources to support the growth or competitive abilities of particular microbial taxa (Bais et al 2006). Stable isotope probing can be used to show the transfer of host resources to its microbiome by tracking the flow of isotopically-labelled metabolites produced by the host, to the nucleic acids of the microbial species that metabolise them (Dumont and Murrell 2005, Haichar et al 2016). Such experiments have shown that specific bacteria in the plant root microbiome are capable of metabolising root exudates (Bressan et al 2009, Haichar et al 2008, Haichar et al 2012). In addition to this, root exudates change with plant age and in response to abiotic and biotic stressors. In turn, changes in the levels of particular compounds are correlated with changes in the abundance of certain bacterial species in the microbiome, suggesting specific taxa may be recruited by specific root-derived substrates (Carvalhais et al 2015, Chaparro et al 2013, Chaparro et al 2014, Lanoue et al 2010). For example, foliar infection is known to cause an increase in malic acid exudation by *Arabidopsis thaliana* plants, which promotes root colonisation, binding and biofilm formation by the beneficial bacterial strain *Bacillus subtilis* FB17; this species, in turn, induces systemic resistance in the host plant (Rudrappa et al 2008). It is possible that a greater understanding of root exudate usage by different microbial taxa may enable us to exploit and manipulate plant-bacterial interactions for the purposes of improving crop health and protection (Dessaux et al 2016).

1.4.3 Preventing colonisation by non-beneficial bacteria

The third mechanism by which a host could bias microbiome establishment is by producing compounds or barriers that block the colonisation and survival of non-beneficial species, whilst still enabling or promoting colonisation by beneficial species (Boza et al 2019). A classic example of this arises during the symbiotic interaction between the bobtail squid, *Eurpryma scolopes*, and the bioluminescent bacterial

species *Vibrio fischeri* (Fang 2004, Wang and Ruby 2011). *V. fischeri* is the exclusive coloniser of the squid's light organ and is responsible for emitting light, resulting in counter-illumination of the squid and predator avoidance in moonlight (Ruby 1996). The bacteria are acquired horizontally from the environment within a 48 hour window after hatching (Ruby 1996). High levels of nitric oxide (NO), a potent oxidising agent and antimicrobial compound, can be detected in the epithelial mucus of the light organ. It has been shown that *V. fischeri* are able to tolerate high levels of NO through the action of two identified proteins, flavohemoglobin (Hmp) and a heme NO/oxygen-binding (H-NOX) protein (Graf and Ruby 2000, Poole and Hughes 2000, Wang et al 2010b, Wang and Ruby 2011). Hmp activity detoxifies NO, whereas H-NOX senses NO and suppresses the uptake of iron via hemin, as iron can elevate the damage caused by harmful superoxide radicals (Graf and Ruby 2000, Poole and Hughes 2000, Wang et al 2010a). Eliminating the genes for these proteins in *V. fischeri* leads to colonisation deficiency (Poole and Hughes 2000, Wang et al 2010a) whereas diminishing the concentration of host NO results in a greater diversity of bacterial species forming aggregates in the light organ epithelium (Davidson et al 2004). These results suggest that the presence of host-generated NO, coupled with the resistance of *V. fischeri*, normally plays an important role in the selection of this specific species from the environment.

Plants also exude a variety of toxic molecules, called allelochemicals, which inhibit a broad range of bacteria, fungi and invertebrates, as well as other plants growing in close proximity (Bais et al 2006, Hartmann et al 2009, Neal et al 2012). Beneficial microbial species must be able to tolerate allelochemicals in order to colonise the root microbiome. DIMBOA (2,4-dihydroxy-7-methoxy-1,4-benzoxazin-3-one) is an antimicrobial allelochemical that is constitutively produced by maize seedlings and is toxic to many bacterial species (Neal et al 2012). However, the plant-beneficial species, *Pseudomonas putida*, is able to degrade DIMBOA and additionally upregulates the production of the broad-spectrum antibiotic phenazine in response to detecting the compound, allowing effective colonisation of the root microbiome (Neal et al 2012). Similarly, the species *Mesorhizobium tianshanense*, which specifically forms root nodules on liquorice plants, is able to out-compete other bacteria in the soil surrounding liquorice roots, due to its tolerance of the antimicrobial compound

canavanine, which is abundant in liquorice root exudates (Cai et al 2009). Resistance is conferred through the expression of an MSiA exporter protein, allowing tolerant bacterial species to be filtered into the root microbiome (Cai et al 2009).

1.5 Outline of this thesis

It appears that, in general, there are several ways in which a host organism can direct the establishment of its own microbiome and ensure the colonisation of beneficial and protective species whilst excluding non-beneficial species. However, details of the specific mechanisms and chemical cues involved in host-symbiont interactions are only well-understood in a few cases. These tend to be systems in which interactions are limited to a very small number of beneficial microbial species, such as *V. fischeri* in the squid light organ or in the case of nitrogen-fixing rhizobia in the root nodules of leguminous plants (Liu and Murray 2016, Ruby 1996, Wang and Ruby 2011). In these cases, both host and bacterial signals are known in detail and the adaptive nature of the interaction is understood for both partners.

However, the vast majority of microbiomes consist of highly complex communities of beneficial bacteria, which are also known to be dynamic over time. There is increasing interest in being able to manipulate such microbiomes to improve host fitness, for example by directing microbiome formation to increase host protection against pathogen infection. An increased level of control over host microbiome formation could have many applications, such as enabling the establishment of a healthy human gut microbiome to reduce the incidence of human disease, or to reduce crop losses due to pathogen infection allowing us to meet the growing nutritional demands of an expanding world population. However, in order to manipulate microbiome interactions, a detailed understanding of the chemical ecology of each system is required. This includes understanding the host signals or resources that recruit protective species to the microbiome, the dynamics of these resources over time and the effect that they have on microbial interactions within diverse communities. Additionally, for many systems, a greater understanding of the protective potential of symbiont species is needed, including knowledge of the mechanisms by which each species suppresses pathogen growth *in vivo* and how gene expression and their tendency to be protective changes over time and in response to host and competitor

cues. This thesis aims to explore some of the fundamental questions surrounding the establishment of protective microbiomes, particularly those involving actinobacterial symbionts. Experiments are carried out using two model systems in which Actinobacteria are known to play a protective role, but in which they are part of microbiomes with different levels of community complexity.

In Chapter 2 I begin by investigating the *Acromyrmex echinatior* leafcutter ant cuticular microbiome, which is largely dominated by actinobacterial species (Table 1.1). This system has been well-studied as an example of a protective mutualism (Andersen et al 2013, Andersen et al 2015, Barke et al 2010, Currie et al 2003, Currie et al 1999b, Currie et al 2006), however, hypotheses surrounding the factors that enable the establishment of a cuticular microbiome that is dominated by Actinobacteria and the factors that drive antibiotic production by these symbionts *in vivo*, remain largely untested. A competitive screening model has been proposed to explain microbiome formation in this system (Scheuring and Yu 2012). The model states that publicly available resources are provided by the ant host to its cuticular microbiome. Bacterial species compete for these resources and in doing so produce antibacterial and antifungal compounds that protect the ants' fungal gardens from infection (Barke et al 2011, Scheuring and Yu 2012). In Chapter 2, I test some of the key assumptions of this model using RNA stable isotope probing to track the transfer of host resources to the cuticular microbiome. I also use RNA sequencing to determine the expression of secondary metabolites by vertically-transmitted *Pseudonocardia* symbionts *in vivo*.

In the second half of this thesis I investigate the role of Actinobacteria, particularly *Streptomyces* species, in the plant root microbiome and the factors that drive *Streptomyces*-plant interactions. In comparison to the leafcutter ant system, the establishment of the plant root microbiome is poorly understood. In Chapter 3, I particularly focus on furthering our understanding of the contribution that *Streptomyces* can make to plant host fitness via plant growth promotion but also through antimicrobial production and protection against disease. These experiments are carried out using *Arabidopsis thaliana*, since *Streptomyces* bacteria are often found to be enriched in the root microbiome of this plant species (Bulgarelli et al 2012, Lundberg et al 2012). Since *Streptomyces* are gaining increasing interest as biocontrol

agents, I evaluate the potential for *Streptomyces* strains to produce novel compounds against key pathogens, including wheat take-all fungus, which has received little focus in the literature. In Chapter four I extend my investigation of *Streptomyces*-plant root interactions to assess whether plant root exudates are important for the recruitment of Actinobacteria (as well as other microbial genera) to the *A. thaliana* root microbiome, using stable isotope probing to track the uptake of labelled exudates by host-associated bacteria. Then, in Chapter 5, I investigate the role of a specific plant phytohormone, called salicylic acid, in influencing the abundance of *Streptomyces* in the root microbiome.

Since each of the two model systems addressed in this thesis have their own complexities, both will be introduced in greater detail in their own respective chapters. The overall aim of this thesis was to establish the role that actinomycetes can play as symbionts in different host environments and the potential to use protective symbioses as a resource to unearth novel antimicrobials and biocontrol agents. Additionally, experiments described in this thesis aim to shed light on the mechanisms underpinning the establishment of Actinobacteria in the microbiomes of disparate host organisms and particularly the role that host nutrients can play in determining the final composition of the host microbiome.

Chapter 2 Regulation of the leafcutter ant cuticular microbiome

2.1 Introduction

2.1.1 Leafcutter ants and their fungal cultivar

The advent of agriculture for nutritional sustenance is considered to be a major evolutionary transition that has only occurred a handful of times in the history of the animal kingdom, but has arisen several times independently in insects (Mueller et al 2005). In particular, leafcutter ants are renowned for their ability to use vegetative material from their environment in order to grow a mutualistic food fungus. Leafcutter ants form part of a monophyletic clade of ants, called the attine ants, which first evolved fungiculture approximately 55-60 million years ago (Currie 2001, De Fine Licht et al 2010, Nygaard et al 2016, Schultz and Brady 2008). Attines are indigenous to Central and Southern America and consist of approximately 250 species, belonging to 15 classified genera (Branstetter et al 2017). Initially, attines began by cultivating a variety of fungal strains belonging to a paraphyletic clade called Leucoprineae; these cultivars grew on debris collected by the ants and were regularly switched and acquired *de novo* from their environment (Currie 2001, De Fine Licht et al 2010, Mueller et al 1998). Lineages known as the “higher attines”, evolved to become obligately dependent upon their fungal cultivars for food approximately 30 million years ago (Branstetter et al 2017, Schultz and Brady 2008). They also began to supplement their garden substrate with fresh plant material (Branstetter et al 2017). This switch culminated in the evolution of the leafcutter ant genera, *Atta* and *Acromyrmex*, approximately 15 million years ago (Branstetter et al 2017, Nygaard et al 2016, Schultz and Brady 2008). Leafcutter ants forage almost exclusively for fresh leaf material and have only ever been recorded to farm clones of a single fungal species called *Leucoagaricus gongylophorus*, which they vertically transmit via dispersing daughter queens (Currie 2001, De Fine Licht et al 2014, Schultz and Brady 2008).

Leafcutter ants are incapable of digesting fresh leaf material themselves, but instead rely on the *L. gongylophorus* cultivar and its comprehensive array of enzymes to break down plant material to usable components (De Fine Licht et al 2010). Vegetative material is brought back to the nest, chewed into a mulch by worker ants and then

added to the growing fungal biomass, along with fecal droplets, which are known to vector and concentrate enzymes involved in the degradation of plant cell wall material from the fungal cultivar (De Fine Licht et al 2014, Kooij et al 2014, Martin 1970, Schiøtt et al 2010). In turn, nutrients are supplied to the ants in the form of specialised hyphal structures called gongylidia which are rich in lipids, proteins and carbohydrates (De Fine Licht et al 2014). Gongylidia are thought to have evolved approximately 30 million years ago when the fungal cultivar became the obligate food source of the higher attines (De Fine Licht et al 2014, Schultz and Brady 2008). Clusters of gongylidia (called staphylae) are the primary food source of the ant colony, particularly the larvae, which are thought to feed almost exclusively on the fungal cultivar (Currie 2001). An expression analysis of *L. gonglyophorous* has revealed that genes encoding essential amino acids are upregulated in the gongylidia, including phenylalanine and tyrosine, both of which are required in high abundance for insect cuticle production and growth (De Fine Licht et al 2014). The gongylidia are also assumed to provide leafcutter ants with a full quota of arginine since both *Acromyrmex echinator* ants and members of the genus *Atta* are known to lack two essential genes involved in the biosynthesis of arginine, whereas *L. gonglyophorous* encodes and expresses the full set of genes (De Fine Licht et al 2014, Nygaard et al 2011, Nygaard et al 2016). Thus, a division of labour seems to have evolved, whereby ants provide the fungus with a growth substrate, but in return the fungus supplies the ants with metabolically expensive and essential amino acids, in addition to other nutrients (Worsley et al 2018).

2.1.2 Parasites of the fungus garden

Like our own agricultural crops, the ant fungal garden is susceptible to infection by parasites and pathogens, since it is an abundant and nutritious food source. The fungal cultivar may be especially prone to infection, since it is maintained as a clonal monoculture and therefore has a relatively low level of immune genetic diversity (Kost et al 2007). In particular, a specialized fungal pathogen in the genus *Escovopsis* commonly parasitises attine fungal gardens and degrades the fungal cultivar, either through direct hyphal contact or via soluble toxins and enzymes (Marfetan et al 2015, Reynolds and Currie 2004, Varanda-Haifig et al 2017, Yek et al 2012). We also recently demonstrated that *Escovopsis* produces compounds that both paralyse and kill the ants preventing them from carrying out their prophylactic behaviours, in addition to

inhibiting the ants' protective cuticular bacteria (discussed below) (Heine et al 2018). Thus, an *Escovopsis* infection can rapidly expand, eventually leading to colony collapse, whereby the ants decline in number and ultimately abandon what remains of their infected fungal crop (Currie et al 1999a). *Escovopsis* evolved to parasitise the nests of attine ants approximately 55 - 60 million years, around the time that attine ants first began to engage in agricultural activities (Nygaard et al 2016, Yek et al 2012). Recent sequencing of the *Escovopsis weberi* genome, revealed that it has undergone substantial gene loss as a result of its specialisation to grow on the attine fungal cultivar and it is now thought that the species is unable to reproduce in isolation from the ant nests (Currie et al 1999a, de Man et al 2016, Heine et al 2018, Worsley et al 2018). Often *Escovopsis* is thought to persist at low levels in fungal gardens and it is estimated to be present in approximately 50% of the *Acromyrmex echinatior* nests studied in Panama (Reynolds and Currie 2004). In addition to *Escovopsis*, several other parasitic species have also been identified in the ant fungal gardens including a range of micro-fungi and black yeasts (Little and Currie 2007, Little and Currie 2008, Worsley et al 2018).

2.1.3 Vertically transmitted *Pseudonocardia* mutualists

To prevent infections from taking hold, ants carry out a number of weeding and waste removal behaviours, in addition to secreting antimicrobial substances from their metapleural glands (Currie and Stuart 2001, Fernandez-Marin et al 2006, Worsley et al 2018). However, as an additional line of defense, attine ants have also evolved a mutualistic relationship with an antibiotic-producing genus of Actinobacteria called *Pseudonocardia* which grow as a concentrated mass on the ant cuticle, often as a visible white bloom (Figure 2.1). The ants spread the antibiotics that these bacteria produce around their fungal gardens. The exoskeleton of attine ants appears to have been modified over evolutionary time to house these mutualistic bacteria, since *Pseudonocardia* are often observed to grow in or above cavities on the ant cuticle, called foveae (Currie et al 2006). These crypts are underlain by structures that appear to be exocrine glands, consisting of a gland cell and a duct cell, the latter of which crosses the cuticle to open at the foveae (Currie et al 2006). The glands are presumed to provide some form of unidentified nutritional substance to cuticular bacteria in return for antimicrobial compounds, which is supported by the observation that the

presence of *Pseudonocardia* imposes a significant metabolic cost on the ant host (Currie et al 2006, Poulsen et al 2003, Scheuring and Yu 2012). The crypts occur in specific regions of the ant cuticle depending on the attine species (Currie et al 2006). In basal attine genera, for example *Apterostigma*, the actinomycete bacteria cluster around openings underneath the forelegs (the mesopleura), whereas in the lower attines, mutualists are concentrated on the laterocervical plates of the propleura, where they grow on protrusions called tubercles within the foveae (Currie et al 2006). Similarly, in the higher attines (such as *Acromyrmex* species), actinomycete bacteria also concentrate on the laterocervical plates, but grow on gland-associated tubercles directly on the surface of the exoskeleton (Figure 2.1) rather than within foveae (Currie et al 2006). Such specialized structures are absent in ant genera that are closely related to the attines, but are also lacking in the higher attine genus *Atta* (Mueller et al 2008). Attempts to isolate *Pseudonocardia* from the cuticle of *Atta* ants suggest that this genus also lacks this bacterial mutualist (Mueller et al 2008). *Atta* are capable of producing phenylacetic acid (a potent antifungal) in their metapleural glands which may have replaced the need to maintain antibiotic-producing symbionts (Currie et al 2006, Fernandez-Marin et al 2015, Vieira et al 2012, Worsley et al 2018).

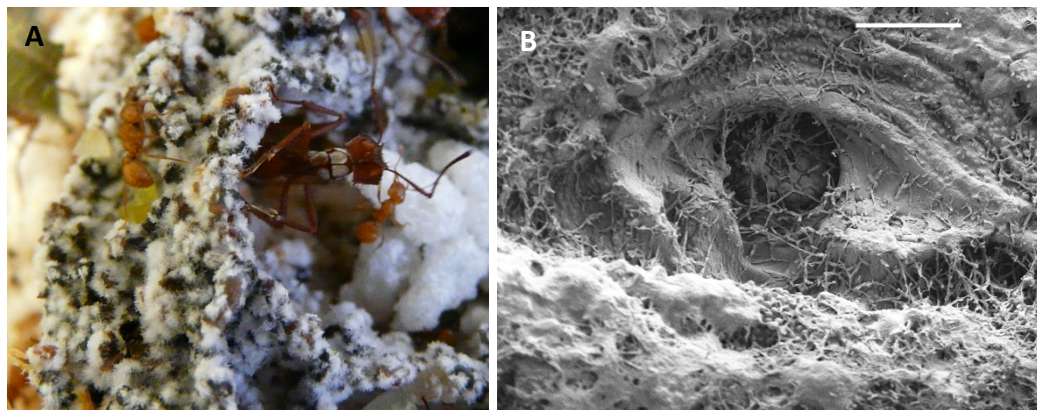


Figure 2.1 The *Acromyrmex echinatio* leafcutter ant system. **A)** An individual worker sitting within its fungal garden, with a visible white bloom of Actinobacteria on its laterocervical plates (Image: Sarah Worsley). **B)** A scanning electron micrograph of the laterocervical plate of an *Acromyrmex echinatio* worker ant, demonstrating the dense filamentous growth of Actinobacteria around a cuticular opening. Scale bar equals 20 μm (Image: Kim Findlay, John Innes Centre).

Similar to the fungal cultivar, *Pseudonocardia* bacteria are also vertically transmitted between generations resulting in a tight coevolutionary relationship between the ants and their mutualists (Currie et al 1999b). Foundress queens carry *Pseudonocardia* with them on their mating flight and use this to inoculate new daughter ants when initiating their own colony (Currie et al 1999a). Once the colony is established, workers inoculate newly eclosed workers within a 24 hour window after hatching (Marsh et al 2014, Poulsen et al 2003). Initially, *Pseudonocardia* blooms over the entire cuticle of young callow ants (individuals found mostly within the fungal garden), before shrinking back to become concentrated on the ant laterocervical plates, which coincides with workers spending a greater amount of time outside of the fungal garden (Poulsen et al 2003).

A further layer of complexity exists in the interaction between *Pseudonocardia* and *Acromyrmex* ants, since different ant colonies have been found to harbor one of two specific phlotypes of *Pseudonocardia*, originally named “PS1” and “PS2” (Andersen et al 2013, Poulsen et al 2005). It is not clear what drives the selection or maintenance of either strain, however cross-fostering experiments suggest that there may be some degree of co-adaptation, since *Pseudonocardia* strains reach lower total coverage on a non-native host and some ant prophylactic behaviours (such as self-grooming) are reduced when ants are exposed to an *Escovopsis* infection and carry a non-native *Pseudonocardia* strain (Andersen et al 2015, Armitage et al 2011). Whole genome sequencing of several different isolates of PS1 and PS2 taken from *Acromyrmex echinator* ants has now demonstrated that the two *Pseudonocardia* phlotypes are actually two distinct species, named *P. octospinosus* (PS1) and *P. echinator* (PS2) (Holmes et al 2016). Although they share several antibiotic-producing biosynthetic gene clusters, each species also encodes several unique clusters, suggesting that they may make a different cocktail of secondary metabolites on the ant surface (Holmes et al 2016).

Several new antifungal compounds have been identified and characterised from the *Pseudonocardia* mutualists associated with attine ants (Worsley et al 2018). The first to be characterised was the antifungal dentigerumycin which was isolated from a *Pseudonocardia* strain associated with the lower attine ant species *Apterostigma*

dentigerum (Oh et al 2009). It is a cyclic depsipeptide and has been shown to be selectively active against *Escovopsis* (Oh et al 2009). An additional variant of dentigerumycin has also been isolated from the same strain. The genes encoding this modified version show signatures of recent selection which may have resulted from the dynamic chemical arms race thought to exist between the *Escovopsis* parasite and the protective cuticular symbiont (Sit et al 2015). Dentigerumycin has also been isolated from *Pseudonocardia* associated with the higher attine species *Trachymyrmex* (Sit et al 2015).

In addition to dentigerumycin, the polyene antifungal, designated nystatin P1, was isolated from a *Pseudonocardia octospinosus* symbiont associated with *Acromyrmex octospinosus* ants (Barke et al 2010). This compound is similar to the clinically available antifungal drug nystatin A1, but has an additional hexose sugar potentially making it more soluble (Barke et al 2010, Lee et al 2012). Genome sequencing has demonstrated that *P. echinator* also encodes a gene cluster predicted to make a nystatin-like compound, but that this is significantly different to both nystatin A1 and P1 (Holmes et al 2016). An additional polyene antifungal compound, called selvamicin, has also been isolated from the *Pseudonocardia* strain associated with *Apterostigma* ants (Van Arnam et al 2016). Thus, the *Pseudonocardia* mutualists appear to be capable of producing a variety of antifungal compounds *in vitro*, which may be under constant selective pressure *in situ* due to the evolution of resistance by *Escovopsis*.

2.1.4 Other actinomycetes on the ant cuticle

The finding that the majority of attine ants associate with *Pseudonocardia* and that these bacteria are vertically transmitted between generations suggests that these mutualists are involved in a tight coevolutionary relationship with the ants, their fungal cultivar and the *Escovopsis* parasite. However, since the discovery of the cuticular *Pseudonocardia* bacteria, several other screens have revealed a much greater diversity of Actinobacteria on the ant laterocervical plates. This was first revealed through a survey of bacteria growing on the laterocervical plates of *A. octospinosus* ants, which found that actinobacterial diversity was much higher in this region than previously thought, and that only 15% of all of the strains isolated could be found in more than one colony, suggesting a high variability of cuticular bacteria between colonies (Kost et

al 2007). The study also found that a large percentage of the isolates could inhibit *Escovopsis in vitro*, including several *Streptomyces* strains (Kost et al 2007). *Streptomyces* are a genus of Actinobacteria that are common in soil and well-known for being prolific producers of antibiotics (van der Meij et al 2017). *Streptomyces* that produce antifungals and inhibit the parasite *Escovopsis*, have also been isolated in a range of other studies investigating the composition of attine laterocervical plates (Barke et al 2010, Haeder et al 2009). One study that carried out 454 pyrosequencing of the 16S rRNA gene, found that *Streptomyces* OTUs made up 15-29% of the bacterial community in 17 samples taken from mature *A. echinator* ants, 11 of which were collected directly from the field (Andersen et al 2013). Schoenian et al (2011) additionally demonstrated that *Streptomyces* symbionts isolated from *Acromyrmex* ants produce several antimicrobial compounds *in vitro*, including antimycins, actinomycins and valinomycins. Both valinomycins and actinomycins could be identified in the waste dumps of *A. echinator* and *A. niger* ants, and mass spectrometry imaging revealed that valinomycin could also be found over the integument of *A. echinator* ants, suggesting that these antimicrobials were ecologically relevant and expressed by the bacteria *in vivo* on the ant host (Schoenian et al 2011). Other Actinobacteria, such as *Amycolatopsis* and *Microbacterium* species have also been identified on leafcutter ant cuticles (Andersen et al 2013, Haeder et al 2009, Sen et al 2009).

The finding that a large genotypic diversity of antibiotic-producing Actinobacteria exists on the cuticle of ants, was inconsistent with the hypothesis that beneficial bacteria were purely being vertically transmitted (Barke et al 2010, Kost et al 2007). Instead, these observations suggested that actinobacterial strains can also be horizontally acquired *de novo* from the environment, for example from ant forage material or the surrounding soil (Barke et al 2010, Barke et al 2011, Kost et al 2007). *Streptomyces* species isolated from the laterocervical plates of geographically distinct populations of *Acromyrmex* ants were found to produce the well-known antifungal candidin, the genes for which are widespread amongst environmental isolates of *Streptomyces*, supporting the hypothesis that these strains are horizontally acquired (Barke et al 2010, Haeder et al 2009). In addition, bacterial diversity appears to increase with ant age and is greater in individuals that spend more time out of the nest

(such as forager ants); these ants are in greater contact with the surrounding environment which may increase their chances of acquiring a more diverse set of symbionts (Andersen et al 2013). It has also been argued that the external morphology of the cuticular crypts may have evolved to facilitate this acquisition process (Mueller et al 2008). There has been much discussion over the possible role of these additional cuticular symbionts, however the general hypothesis is that horizontal acquisition, in addition to the vertical transmission of *Pseudonocardia*, enables the ants to access a much greater diversity of secondary metabolites that can be dynamically changed over time or act as a source of horizontal gene transfer, depending on selective pressures from pathogens and parasites (Barke et al 2010, Barke et al 2011, Kost et al 2007); this multi-drug approach would in turn increase the range of pathogens and parasites that could be targeted and also help to reduce the rate at which antimicrobial resistance could evolve (Barke et al 2010, Barke et al 2011, Seipke et al 2011a).

2.1.5 Building a protective microbiome

The discovery that ants associate with a diverse community of antibiotic-producing Actinobacteria, raises interesting questions about how ants accumulate, regulate and maintain such a varied protective microbiome, allowing domination by antibiotic producers, whilst preventing colonisation by non-producers that could parasitise the system. Additionally, it is still uncertain how horizontal acquisition can be achieved when the cuticle is already densely colonised by the vertically transmitted *Pseudonocardia* strain.

The unidentified nutritional substance that is thought to be secreted from cuticular crypts has been suggested to play a key role in attine microbiome formation (Currie et al 2006). Host-derived nutrients may stabilise the interaction between ants and their vertically-transmitted *Pseudonocardia* through a process called Partner Fidelity Feedback (PFF). PFF occurs when the fitness interests of both partners are linked, for example, if ant colony productivity increases due to the bacterially-derived antimicrobial substances, this in turn improves the likelihood of bacterial transmission to the next generation (Barke et al 2011, Foster and Wenseleers 2006). However, this does not explain how a more diverse and changeable community of specifically antibiotic-producing bacteria can be selected for, and maintained on the ant cuticle.

For a host to be able to recruit beneficial symbionts with certain traits from its environment it must be able to distinguish between strains and limit its interactions (and any associated rewards) to these beneficial individuals. One possible solution occurs when partner quality is displayed via a costly phenotype, as is the case for male ornaments which only high quality individuals with desirable traits can afford to invest in (Archetti et al 2011). However, with microbial-host interactions, it seems unlikely that such signals could exist and be detected by the host, allowing discrimination between thousands of microbial species. Instead an alternative “screening hypothesis” has been proposed, whereby the host provides a particular set of conditions (for example specific types or amounts of nutrients) which are designed such that only high quality symbionts can afford to enter into an interaction (Archetti et al 2011, Scheuring and Yu 2012). Thus, beneficial symbionts screen themselves in, without the host having to directly select each individual based on quality. Competition-based screening is a further extension of this model, whereby the host environment ensures that high quality individuals are competitively superior and are able to out-compete low quality individuals (Archetti et al 2011, Scheuring and Yu 2012). As mentioned, competition-based screening may play a key role in the construction of protective microbiomes dominated by antibiotic-producing bacteria, since antibiotic production can provide a significant advantage during interference competition, and producers are also resistant to their own and often to other antibiotics (Scheuring and Yu 2012, Sen et al 2009).

Scheuring and Yu (2012) created a model to investigate which set of host-coordinated conditions might favour the growth of antibiotic producers, as well as antibiotic production, in a microbiome scenario. Their competition-based model suggested that, since antibiotic production is a costly trait, a high level of host-derived resources would be required to make this strategy affordable and allow beneficial producers to outcompete non-producers. However, under this scenario, the microbial community was also shown to be “bistable” with two possible equilibria being reached: either complete domination by non-producers or producers. Which community type prevailed depended upon which population had the higher initial abundance at the outset of competition. Therefore, for a microbiome to be dominated by antibiotic producers, a host must evolve not only to provide a high level of resources to its microbiome, but must also ensure it is initially colonised by a higher density of

antibiotic producers, so that a competitive environment with antibiotic production is already present from the outset of microbiome formation (Scheuring and Yu 2012). In the ant system this latter pre-requisite is thought to be satisfied through the vertical transmission of *Pseudonocardia* (Scheuring and Yu 2012). Worker ants are sterile when they emerge from their pupal cases but are quickly inoculated with *Pseudonocardia*, allowing it dominate on the cuticle before other bacterial species can invade (Marsh et al 2014). Other producers, such as *Streptomyces*, are then predicted to be able to colonise as they compete by producing antibiotics. This, in turn, means that they carry resistance genes (to prevent antibiotic production being suicidal) making them more resistant to many of the antibiotics produced by other strains, including *Pseudonocardia* (Holmes et al 2016, Scheuring and Yu 2012). However, although host nutrients are assumed to be provided via the cuticular crypts (Currie et al 2006), this has never been experimentally verified. In order to confirm that screening is taking place *in vivo*, it would need to be demonstrated that a public resource (available to a wide range of bacteria) is being provided by the ant host, which in turn is fuelling interference competition (and the production of antimicrobials) between the *Pseudonocardia* and all other potential colonists. The identity of the host-derived resource is of additional interest as many bacterial isolates taken from the ant system are not bioactive under laboratory conditions, despite encoding genes to produce a large number of antimicrobial compounds (Seipke et al 2011a, Seipke et al 2011b). It has been shown that some biosynthetic genes can be switched on by mimicking the conditions present in their environment of origin (van der Meij et al 2017). Thus, it is possible that ants secrete resources that can regulate the production of secondary metabolites by their symbiotic bacteria and these could be used to discover novel antimicrobial compounds *in vitro*.

2.2 Aims

In Chapter 1, experiments are described that set out to test the unconfirmed assumptions made by the screening hypothesis (discussed in 1.4.2 and 2.1.5), and therefore its validity as a model to describe protective microbiome formation in the leafcutter ant system. Firstly, the assumption that leafcutter ant hosts provide their cuticular symbionts with a publicly available resource was tested using an approach called ¹³C RNA Stable Isotope Probing (SIP). SIP allows a ¹³C heavy isotope to be

tracked from the host organism, to the nucleic acids of bacterial symbionts that are metabolising labelled-resources provided by their host (Dumont and Murrell 2005). Additionally, total (dual) RNA sequencing was used to assess whether the expression of *Pseudonocardia* genes encoding secondary metabolites (particularly those involved in interspecific interference competition) could be detected *in vivo* on the ant cuticle, as well as *in vitro* on agar plates. RNA sequencing data was also used to investigate carbohydrate metabolism by *Pseudonocardia in situ* on the ant laterocervical plates.

2.3 Materials and Methods

2.3.1 Ant colony collection and maintenance

Colonies of *Acromyrmex echinaior* leafcutter ants were originally collected from Gamboa, Panama. Colonies A.e1083 and A.e088 (Table 2.1) were maintained under controlled temperature conditions and fed a daily diet of bramble and laurel leaves.

Table 2.1 Details of species and strains associated with work in Chapter 2.

Species/strain name	Genotype and description	Origin
A.e1083	<i>Acromyrmex echinaior</i> ant colony harboring <i>Pseudonocardia octospinosus</i> .	Gamboa, Panama.
A.e088	<i>Acromyrmex echinaior</i> ant colony harboring <i>Pseudonocardia echinaior</i> .	Gamboa, Panama.
PS1083	Wild-type isolate of <i>Pseudonocardia octospinosus</i> from A.e1083.	This study
PS088	Wild-type isolate of <i>Pseudonocardia echinaior</i> from A.e088.	This study
<i>Bacillus subtilis</i> 168	Tryptophan-requiring auxotroph. Derivative of <i>B. subtilis</i> Marburg strain.	Gift from Prof. Nicola Stanley-Wall, University of Dundee
<i>Escovopsis weberi</i>	Wild-type strain, CBS 810.71, Isolated from an unknown species of attine ant from Colombia. Genbank accession number NIGB000000000.	Wester dijk Fungal Biodiversity Institute

2.3.2 RNA Stable Isotope Probing of the ant cuticular microbiome

2.3.2.1 RNA SIP ¹³C feeding experiment

Stable isotope probing was used to track the flow of a ¹³C (“heavy”) isotope from the ant host, to the RNA molecules of bacteria on ant laterocervical plates that metabolise host-derived resources (Figure 2.2). Six replicate groups of 22 mature worker ants with visible laterocervical blooms of bacteria (Figure 2.1 and Figure 2.2) were selected from the *Acromyrmex echinator* colony A.e1083 and placed in 9cm petri dishes containing a 2x2 cm square of cotton wool soaked in water. Following 24 hours of starvation, three replicate groups of 22 ants were supplied with 300 μl of a 20% ¹³C glucose solution (w/v) for 10 days, whilst the other three control groups received 300 μl of a 20% ¹²C glucose solution (w/v) for 10 days. Glucose solutions were supplied to ants in microcentrifuge tube caps and were refreshed every three days.

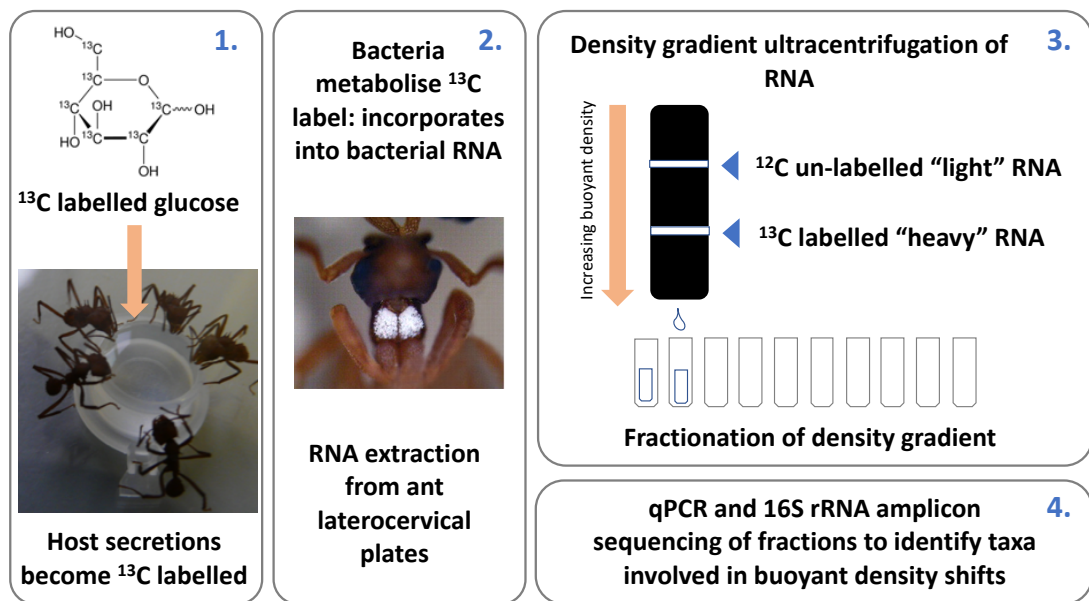


Figure 2.2 A schematic of the methodology used for RNA Stable Isotope Probing (RNA SIP) experiments investigating the leafcutter ant cuticular microbiome.

2.3.2.2 Preliminary isotope ratio mass spectrometry analysis

The ¹³C composition of ants fed on a ¹³C labelled diet was determined by using a coupled Delta plus XP Isotope Ratio Mass Spectrometer/Flash HT Plus Elemental Analyser (Thermo Finnigan) in the University of East Anglia Analytical Facility. Ants were fed on a 5% glucose solution (w/v) for 10 days; five ants were fed a ¹³C glucose

solution and five were fed on a ^{12}C glucose solution. After 10 days, ants were washed once in 70% EtOH, then sequentially in sterile dH₂O before drying on filter paper. The ants were then flash frozen and stored at -80°C until being placed in a ScanVac Coolsafe freeze dryer for 5 days. Each ant was then put into an individual 75 µl tin capsule (Elemental Microanalysis); capsules were loaded into an automatic sampler and completely converted to CO₂, N₂ and H₂O through combustion in an excess of oxygen (oxidation was carried out at 1020°C, followed by reduction at 650°C). Nitrous oxides formed during combustion were reduced using Cu. Helium was used as a carrier gas. After passing through a water trap (MgClO₄), the gases were separated chromatographically on an isothermal GC column (Thermo PTFE, 0.8m, 50°C); the resulting peaks sequentially entered the ion source of the Isotope Ratio Mass Spectrometer. Gas species were then measured using a Faraday cup universal collector array, with masses of 44, 45 and 46 being monitored for the analysis of CO₂. Casein and collagen were used to calibrate the system and normalise the data post run; these standards have been calibrated against international certified standards and have an assigned $\delta^{13}\text{C}$ value. Empty tin capsules were used as blanks. Each sample was analyzed in triplicate. The ^{13}C content of samples is reported as the ^{13}C atom percent, which was calculated using the following formula:

$$(^{13}\text{C}/^{12}\text{C}+^{13}\text{C})*100$$

2.3.2.3 Fluorescent microscopy of ant feeding habits

In order to confirm that the glucose water diet was restricted to the mouth parts of the ant and did not spread extensively over the cuticle and laterocervical plates, a fluorescently labelled 20% glucose diet was fed to ants. Fluorescent green drain tracing dye (Hydra) was used, since it was non-toxic and fluoresced brightly under an epifluorescent illuminator. 5 mg ml⁻¹ of dye was added to a 20% glucose solution, of which 300 µl was supplied to ants in the cap of a microcentrifuge tube. Ants were sampled just after taking a feed, and after 6 and 24 hours of being exposed to the dye, to trace the spread of the solution over time. After sampling, ants were carefully fixed on their backs and imaged. Brightfield and fluorescent images were acquired using a Zeiss M2 Bio Quad SV11 stereomicroscope. The samples were illuminated either with a halogen lamp (brightfield) or a 100W Hg arc lamp (fluorescence) and reflected-light

images were captured with an AxioCam HRc CCD camera and AxioVision software (Carl Zeiss, Cambridge, UK). Green fluorescence was excited with light passed through a 470 nm filter (40 nm bandpass) and the emission was collected through a 525 nm filter (50 nm bandpass).

2.3.2.4 Cuticular dissection and RNA extraction

At the end of the 10 day feeding experiment (described in 2.3.2.1), the laterocervical plates of the propleura of *Acromyrmex echinator* ants were removed using a dissection microscope and fine sterile tweezers. Laterocervical plates were placed into lysis matrix E tubes and stored on dry ice. Once the chest plates had been removed from all 22 ants in a group, the tube was snap frozen and placed at -80°C before further processing. A modified version of the QIAGEN RNeasy micro kit protocol was used for all RNA extractions. 700 µl of RLT buffer (with 1% beta mercaptoethanol) was added to each lysis matrix tube before the samples could thaw. Tubes were then placed in a FastPrep-24™ 5G benchtop homogenizer (MP Biomedicals) and disrupted for 40 seconds at 6 m/s. Samples were then centrifuged for 2 minutes at 13'000 rpm and the supernatant was collected into a QIAshredder tube. This was centrifuged for 2 minutes at 13'000 rpm to homogenise the lysate. The resulting flow-through was mixed vigorously with 700 µl acidic phenol chloroform, then allowed to rest for 3 minutes at room temperature before centrifugation for 20 minutes at 13'000 rpm. The upper phase was then collected and 50% volume of 96% ethanol was added. The mixture was then placed into a minelute column supplied with the QIAGEN RNeasy micro kit. The micro kit protocol (including the on-column DNase I treatment) was then followed through to elution of the RNA, at which point 50 µl of RNase free water (heated to 37°C) was added to the column membrane and incubated at 37°C for 5 minutes, before centrifuging for one minute at 13'000 rpm to elute the RNA. To remove any remaining DNA, RNA was treated with the turbo DNase kit: 5 µl of 10x buffer and 2 µl of Turbo DNase was added to 50 µl of RNA and incubated at 37°C for 25 minutes. RNA was then purified using the QIAGEN micro RNeasy kit cleanup protocol. The quantity and purity of all RNA samples was checked using a nanodrop spectrophotometer and a Qubit™ RNA HS assay kit (Invitrogen™).

2.3.2.5 Density gradient ultracentrifugation and fractionation

To make the RNA gradient buffer for separating labelled (“heavy”) and un-labelled (“light”) RNA (Figure 2.2) the following solutions were mixed together in diethyl pyrocarbonate (DEPC) treated glassware: 0.5 ml of 0.2 M EDTA (pH 8.0), 10 ml of 1M Tris-HCl (pH 8.0), 10 ml of 1M KCl, and 79.5 ml dH₂O (Lueders et al 2004). DEPC was used to inhibit the activity of RNase enzymes. Each of these components (apart from Tris-HCl) had been previously treated with 0.1% DEPC and incubated overnight at 37°C before autoclaving. Tris-HCl was made up in DEPC treated water and glassware. To make one complete gradient solution for the ultracentrifugation of one RNA sample, 4.5 ml of cesium trifluoroacetate (CsTFA, ~2 g ml⁻¹, GE Healthcare, Munich, Germany) was added to 850 µl of gradient buffer and 197.5 µl formamide. The refractive index (R.I) of a 60 µl aliquot of the solution was measured using a refractometer (Reichert Analytical Instruments, NY, USA) to normalize the pre-centrifugation average solution density. The R.I was adjusted to 1.3725 nD-TC ± 0.0002 (approximately 1.79 g ml⁻¹ CsTFA) by adding 50 µl aliquots of gradient buffer if the R.I was too high, or the equivalent amount of CsTFA if the R.I was too low. 270 ng of sample RNA was then added to the gradient solution and the R.I was checked and adjusted again. The total solution was then loaded into an individual polyallomer quickseal centrifuge tube (Beckman Coulter). Tubes of different samples were balanced to within 10 mg, heat sealed, and then placed into a Vti 65.2 rotar (Beckman Coulter, CA, USA). Ultracentrifugation was carried out in a Beckman Optima XL-100K ultracentrifuge for 50 hours at 20°C, 38’000 rpm with a vacuum applied. Deceleration occurred without brakes to ensure gradients remained intact.

After centrifugation, tubes were removed from the ultracentrifuge and fractionated. For fractionation, a 0.6 mm sterile needle was attached to the tubing of a peristaltic pump (cleaned with 100% EtOH and DEPC-treated water before use) and inserted into the top of the ultracentrifuge tube which was held in place by a clamp stand. The bottom of the centrifuge tube was then pierced swiftly with a sterile needle and DEPC-treated sterile dH₂O was pumped in at a rate of 450 µl min⁻¹, displacing the gradient into a 1.5 ml microcentrifuge tube that was placed beneath the clamp stand. Tubes were exchanged every minute until the water had fully displaced the gradient solution, resulting in 12 x 450 µl fractions being collected in total. The R.I of 60 µl of each

fraction was measured using a refractometer to confirm successful gradient formation. RNA was precipitated from fractions by adding 1 volume of DEPC-treated sodium acetate (1M, pH 5.2), 1 μ l (20 μ g) glycogen (from mussels, Sigma Aldrich) and 2 volumes of ice cold 96% EtOH. Fractions were incubated over night at -20°C then centrifuged for 30 minutes at 4°C, before washing with 150 μ l of ice cold 70% EtOH and centrifuging for a further 15 minutes. Pellets were then air-dried for 5 minutes and re-suspended in 15 μ l of nuclease free water.

2.3.2.6 Synthesis of cDNA from RNA SIP fractions

The RNA in each fraction was converted to cDNA before use in further downstream analysis. Synthesis of cDNA was carried out using the protocol defined in Table 2.2. Resulting cDNA was frozen at -80°C before use in qPCR and PCR reactions.

Table 2.2 Protocol for the reverse transcription of RNA SIP fractions from leafcutter ant cuticles

1. Reaction step 1	
DEPC-treated dH ₂ O	9 μ l
50 ng μ l ⁻¹ random hexamer primers (Invitrogen™)	1 μ l
10 mM dNTP mix (Invitrogen™)	1 μ l
RNA sample	1 μ l
Heat the mixture for 5 mins at 65 °C, then chill on ice. Briefly centrifuge before proceeding to step 2.	
2. Reaction step 2	
5 X first Strand Buffer (Invitrogen™)	4 μ l
0.1 M DTT (Invitrogen™)	2 μ l
RNaseOUT™ (40 units μ l ⁻¹) (Invitrogen™)	1 μ l
Incubated at room temperature for 2 minutes.	
3. Thermocycling and enzyme deactivation	
Superscript II™ reverse transcriptase (Invitrogen™)	1 μ l
Incubate the reaction in a thermocycler at : 25°C for 10 mins 42°C for 50 mins 70°C for 15 mins to inactivate the enzymes	

2.3.2.7 Quantitative PCR of cDNA fractions

To identify fractions containing labelled (^{13}C) and unlabelled (^{12}C) RNA for each sample, 16S rRNA gene copy number was quantified across cDNA fractions using qPCR.

Reactions were carried out in 25 μl volumes. 1 μl of either template cDNA, standard DNA, or dH_2O as a control, was added to 24 μl of reaction mix containing 12.5 μl of 2x Sybr Green Jumpstart Taq Ready-mix (Sigma Aldrich), 0.125 μl each of the primers PRM341F and 518R (Table 2.3), 4 μl of 25 mM MgCl_2 , 0.25 μl of 20 $\mu\text{g } \mu\text{l}^{-1}$ Bovine Serum Albumin (Sigma Aldrich), and 7 μl dH_2O . Sample cDNA, standards (a dilution series of the target 16S rRNA gene at known quantities), and negative controls were quantified in duplicate. Reactions were run under the following conditions: 95°C for 10 mins; 40 cycles of 95°C for 15 secs, 55°C for 30 secs, and 72°C for 30 secs; a plate read step at 83.5°C for 10 secs (to avoid primer dimers); 96°C for 15 secs; 100 cycles at 55°C-95°C for 10 secs, ramping 0.5°C per cycle, followed by a plate read. Reactions were performed in 96-well plates (Bio-Rad). The threshold cycle (C_T) for each sample was then converted to target molecule number by comparing to C_T values of a dilution series of target DNA standards.

Table 2.3 Primer sequences used for the partial amplification of the bacterial 16S rRNA gene

Primer name	Sequence	Description and reference
PRM341F	5'-CCTACGGG AGGCAGCAG-3'	This primer set amplifies the V3-V4 variable region of the 16S rRNA gene (Yu et al 2005).
MPRK806R	5'-GGACTACHVGGG TWTCTAAT-3'	
518R	5'- ATTACCGCGGCTGCTGG -3'	Amplifies the V3 variable region of the 16S rRNA gene in combination with PRM341F (Muyzer et al 1993).

2.3.2.8 Sequencing and analysis

Once 16S rRNA gene copy number had been quantified for each fraction using qPCR, fractions spanning the peaks in 16S rRNA gene copy number were identified. PCR was used to amplify the 16S rRNA genes in each of these fractions by using the protocol described in Table 2.4 (using the Ultra DNA polymerase mix) and primers PRK341F and 518R (Table 2.3) which amplify the V3 variable region of the 16S rRNA gene (Muyzer et al 1993). One unfractionated sample was also created for each of the ¹³C or ¹²C dietary treatments, by pooling unfractionated cDNA from each of the 3 replicate groups of ants under each treatment and using this pooled sample as the template for PCR amplification. The resulting PCR products were purified using the QIAGEN MinElute™ gel extraction kit and submitted for 16S rRNA gene amplicon sequencing using an Illumina MiSeq at Mr DNA (Molecular Research LP), Shallowater, Texas, USA. Sequence data was then processed by Mr DNA using their custom pipeline (Dowd et al 2008a, Dowd et al 2008b). As part of this pipeline, paired-end sequences were merged, barcodes were trimmed, and sequences of less than 150 bp and/or with ambiguous base calls were removed. The resulting sequences were denoised, and OTUs were assigned by clustering at 97% similarity. Chimeras were removed, and OTUs were assigned taxonomies using BLASTn against a curated database from GreenGenes, RDP II, and NCBI (DeSantis et al 2006). Plastid-like sequences were removed from the analysis. Upon receipt of the 16S rRNA gene sequencing data from Mr DNA, OTU assignments were verified using BLASTn, and statistical analysis was carried out using *R* 3.2.3 (R Core Team 2017). All 16S rRNA gene amplicon sequencing data from this experiment has been deposited in the European Nucleotide Archive public database under the study accession number PRJEB32900.

Table 2.4 Components and thermocycler conditions for amplification of the 16S rRNA gene using PCR.

Component	Volume (μ l)
2 x Ultra mix (containing Ultra DNA polymerase) (PCRBIO) or BioMix™ red (containing BIOTAQ™ DNA polymerase) (Bioline)	12.5
dH ₂ O	9
Forward Primer	0.5
Reverse Primer	0.5
Sample DNA (for colony PCR this is a single bacterial colony heated in 50% DMSO at 55°C for 45 minutes)	2.5
PCR Thermocycler reaction steps	
1. 95°C for 1 min 2. 30X cycles of 95°C for 15 secs; 55°C for 15 secs, 72°C for 15 secs 3. 72°C for 2 mins	

2.3.3 Secondary metabolite production by *Pseudonocardia* mutualists associated with *Acromyrmex echinatio* colonies

2.3.3.1 Isolation of *Pseudonocardia* bacteria from the ant cuticle

Pseudonocardia strains PS1083 and PS088 (Table 2.1) were isolated from the laterocervical plates of individual *Acromyrmex echinatio* leafcutter ants taken from colonies A.e1083 and A.e088 (Table 2.1), respectively. A sterile needle was used to scrape bacterial material off the laterocervical plates of the propleura; this was then streaked over Soya Flour Mannitol (SFM, Table 2.5) agar plates and incubated at 30°C. Resulting colonies resembling *Pseudonocardia* were purified by repeatedly streaking single colonies onto SFM agar plates. Spore stocks were created using an established protocol (described in Kieser et al 2000). Briefly, *Pseudonocardia* strains were grown as confluent lawns on Glucose Yeast Malt (GYM, Table 2.5) medium for 14 days. 5 ml of sterile 20% glycerol was added to each plate and a sterile cotton bud was used to dislodge the spores. The resulting mixture was pelleted in a centrifuge for 5 minutes at 4000 rpm. Spores were then resuspended in 500 μ l of sterile 20% glycerol and frozen at -20°C.

Table 2.5 Growth media used in bioassays and RNA sequencing experiments in Chapter 2.

Media	Component	g L ⁻¹ dH ₂ O
Glucose, Yeast, Malt (GYM) agar	Glucose	4
	Yeast extract	4
	Malt extract	10
	CaCO ₃	2
	Agar	15
Soya Flour Mannitol (SFM) agar	Soy flour	20
	Mannitol	20
	Agar	20
Potato Glucose Agar (PGA)	PGA (Sigma-Aldrich)	39
Lysogeny Broth (LB)	Tryptone	10
	NaCl	10
	Yeast extract	5

The taxonomic identity of each *Pseudonocardia* isolate was confirmed through partial amplification and sequencing of the 16S rRNA gene, using the universal primers PRM341F, MPRK806R (Table 2.3). A colony PCR protocol was used, whereby a single colony of *Pseudonocardia* (growing on an SFM plate) was added to 500 µl of 50% DMSO and heated for 45 minutes at 55°C. 2.5 µl of this mixture was then used as a template in the PCR reaction (Table 2.4, using BIOMIX™ red). PCR products were then run on a 1% agarose gel with 5% ethidium bromide. Bands of approximately 465 base pairs were excised and purified using the QIA quick gel extraction kit (QIAGEN) according to the manufacturers protocol. Sequencing of the purified product was then carried out by Eurofins Genomics, Germany. The resulting sequences were checked against the BLASTn database to confirm their identity as *Pseudonocardia*. Each sequence was also aligned to both the *Pseudonocardia octospinosus* and *Pseudonocardia echinator* 16S rRNA gene sequences (from Holmes et al 2016) to reveal their percentage identities to each of the two species. One representative colony associated with *Pseudonocardia octospinosus* bacteria (A.e1083 carrying the isolate PS1083) and one colony for *Pseudonocardia echinator* (A.e088 carrying the isolate PS088) were selected for further experimentation.

2.3.3.2 *In vitro* bioassays

Agar plate bioassays were used to evaluate antibacterial and antifungal activities associated with the *Pseudonocardia* strains A.e1083 and A.e088. 4 μ l of *Pseudonocardia* spores were spotted onto the center of GYM agar (Table 2.5) plates and allowed to dry. Plates were then grown at 30°C for 7 days. For detecting antibacterial activity, *Bacillus subtilis* was inoculated into 10 ml of Lysogeny Broth (LB, Table 2.5) and grown overnight at 30°C, shaking at 200 rpm. Overnights were then sub-cultured 1 in 20 (v/v) into 10 ml of LB and grown for another 4 hours at 30°C, 200 rpm. These cultures were then used to inoculate 100 ml of molten LB (0.5% agar), 4 ml of which was used to overlay each GYM agar plate with a growing *Pseudonocardia* colony. Plates were then placed at 30°C for 48 hours. Antibacterial activity was indicated by a zone of clearing around the *Pseudonocardia* colony. Three replicate bioassays were carried out per indicator strain.

Antifungal bioassays were carried out using *Escovopsis weberi* strain CBS 810.71, acquired from the Westerdijk Fungal Biodiversity Institute (Table 2.1). *Escovopsis weberi* was actively maintained on potato glucose agar (PGA, Table 2.5) at room temperature. Fungal mycelia were transferred to a fresh plate every month. For bioassays, a plug of actively growing *Escovopsis* mycelium was transferred from PGA plates to the edge of each GYM plate with a growing *Pseudonocardia* colony, using the end of a sterile glass Pasteur pipette; the plug was placed approximately 1cm from the edge of the plate. Plates were then left at room temperature for 2 weeks. A zone of clearing around the *Pseudonocardia* colony indicated the presence of antifungal activity. Three replicate experiments (with three replicate bioassay plates per *Pseudonocardia* strain) were carried out, whereby different *E. weberi* starter plates were used as an inoculum.

2.3.3.3 Culturing *Pseudonocardia* strains on agar plates for RNA sequencing

Pseudonocardia bacterial strains PS1083 (PS1) and PS088 (PS2) (Table 2.1) were grown as confluent lawns on sterile cellophane discs overlain on GYM agar plates (Table 2.5) supplemented with nystatin (10 μ g ml⁻¹), phosphomycin (50 μ g ml⁻¹) and

cycloheximide ($100 \mu\text{g ml}^{-1}$) to prevent contamination. Cellular material was harvested for RNA isolation after 8 days of growth at 30°C , at which point bacteria were growing as a dense lawn and aerial hyphae and spores were clearly visible on plates. A flamed, sterile metal spatula was used to scrape material from the cellophanes. Approximately $200 \mu\text{l}$ of material was collected into a microcentrifuge tube and snap frozen in liquid nitrogen before being stored at -80°C . Material was collected from three replicate plates for each of PS1083 and PS088 (Table 2.1).

2.3.3.4 RNA extraction from *Pseudonocardia* strains grown on agar plates

Total RNA extraction was carried out using a modified version of the QIAGEN RNeasy mini kit protocol. Frozen cell pellets underwent manual disruption using a hand-held micropestle, which was used to grind the pellet to a fine powder. Samples were placed on dry ice and cooled with liquid nitrogen during this process. $700 \mu\text{l}$ of QIAGEN buffer RLT (with 1% beta-mercaptoethanol) was added to ground samples before thawing. Samples were vortexed thoroughly to mix and then centrifuged for one minute at $13'000 \text{ rpm}$ to pellet remaining debris. The supernatant was added to a QIAshredder column and centrifuged for 2 minutes at $13'000 \text{ rpm}$ to homogenise. The remainder of the protocol was as described in section 2.3.2.4, except that columns from the Qiagen RNeasy mini kit were used due to the larger quantities of RNA.

2.3.3.5 RNA isolation from ant laterocervical plates for dual RNA sequencing

The laterocervical plates of *Acromyrmex echinatio* ants were removed as described in section 2.3.2.4. One sample was collected from each of the colonies A.e1083 and A.e088 (Table 2.1), respectively. Only a single sample was taken from each colony since this was a preliminary experiment designed to assess whether it was even possible to map RNA-seq reads from an ant cuticle back to the *Pseudonocardia* reference sequences. However, to try to remove as much of the inter-individual variation in a colony as possible, each sample was a pool of laterocervical plates removed from 80 mature worker ants that had visible growth of *Pseudonocardia* bacteria on their cuticle. Samples were stored at -80°C prior to processing. Extraction of RNA from cuticles was as described in section 2.3.2.4.

2.3.3.6 Single and dual RNA sequencing

The quantity and purity of all RNA samples (from plates and ant cuticles) was checked using a nanodrop spectrophotometer and Qubit™ RNA HS assay kit (Invitrogen™). Additionally, RNA integrity was assessed using an Experion™ bioanalyser with a prokaryotic RNA standard sensitivity analysis kit (Bio-Rad, California, USA). 1 µg of RNA from each of the laterocervical plate samples, as well as the three replicate samples for each *Pseudonocardia* species grown on plates, was then further processed and sequenced by Vertis Biotechnologie AG (Freising-Weihenstephan, Germany) using a Dual RNA sequencing approach (Westermann et al 2016). Briefly, rRNA molecules (both ant and bacterial) were depleted with the Ribo-Zero Magnetic Gold Kit (Epidemiology) using the manufacturer's instructions. Stranded cDNA libraries were then generated for Illumina Dual RNA sequencing (see Westermann et al 2016 for methods). Single-end sequencing (75 bp) was then performed on samples using an Illumina NextSeq500 platform. All sequencing reads have been deposited in the European Nucleotide Archive public database under the study accession number PRJEB32903.

2.3.3.7 Processing of reads generated from RNA sequencing

The quality of Illumina sequences (returned from Vertis Biotechnologie AG) was assessed using the program FastQC (Babraham Institute, Cambridge, UK), before using TrimGalore version 0.4.5 (Babraham Institute, Cambridge, UK) to trim Illumina adaptors and low quality base calls from the 3' end of reads (an average quality phred score of 20 was used as cut-off). After trimming, sequences shorter than 20 base pairs were discarded. Trimmed files were then aligned to the *Acromyrmex echinator* genome and the appropriate *Pseudonocardia* genome (Table 2.6). The genomes for *Pseudonocardia* isolates Ae707 and Ae706 (Table 2.6) were chosen as representative reference genomes for *P. octospinosus* and *P. echinator*, respectively, (Holmes et al 2016).

Table 2.6 Genome sequences used for alignment in RNA sequencing experiments.

Genome	Description	Accession number and reference
<i>Acromyrmex echinator</i>	Whole genome shotgun sequencing project of the wild-type <i>A. echinator</i> genome.	AEVX000000000, Nygaard et al (2011)
Ae707	Whole genome shotgun sequencing of a wild-type isolate of <i>Pseudonocardia octospinosus</i> , isolated from the cuticle of an <i>A. echinator</i> ant.	MCIR000000000, Holmes et al (2016)
Ae706	Whole genome shotgun sequencing of a wild-type isolate of <i>Pseudonocardia echinator</i> , isolated from the cuticle of an <i>A. echinator</i> ant.	MCIQ000000000, Holmes et al (2016)

Reads from the two laterocervical plate samples were aligned to both the *A. echinator* reference genome and their respective *Pseudonocardia* genome (either *P. octospinosus* or *P. echinator*, for samples taken from colonies A.e1083 or A.e088, respectively). All alignments were done using the splice-aware alignment program HiSat2 (Kim et al 2015) with the default settings. For cuticle samples, reads that had mapped successfully to their respective *Pseudonocardia* genome were then mapped back to the ant genome (and vice versa) to check that reads did not cross-map between the two genomes (i.e they were either uniquely ant or bacterial reads). Following alignment, the program HTSeq (Anders et al 2015) was used to count mapped reads per annotated coding sequence (CDS) using the General Feature Format (GFF) file for each genome; GFF files contain the annotated gene coordinates for each genome. Reads that mapped to multiple locations within a genome were discarded at this point and only uniquely mapped reads were used in the counting process. Read counts per CDS were then converted to reads per kilobase of exon model per million reads (RPKM), by extracting gene lengths from the GFF file. Converting reads to RPKM values normalises counts by RNA length and accounts for differences in sequencing

depth, which enables more accurate comparisons both within and between samples (Mortazavi et al 2008). Counts were converted using the following formula, whereby C is the read count for a single gene, L is the length of the gene and T is the total number of uniquely mapped reads for that sample:

$$\text{RPKM} = C / ((L/1000) * (T/1000000))$$

2.3.3.8 Functional analysis of mapped reads

In order to investigate the expression levels of different gene functional groups, a custom perl script was written (with assistance from Dr. Simon Moxon at UEA) to extract the amino acid sequences of every annotated gene in each *Pseudonocardia* genome. Protein identifier codes from the GFF file as well as the protein sequence file were used as an input for each *Pseudonocardia* strain. The extracted protein sequences were then uploaded to BlastKOALA (Kanehisa et al 2016b) which assigns K numbers to each amino acid sequence based on its relation to orthologous proteins in other organisms. A K number is a unique identifier used by the KEGG Orthology (KO) database which classifies genes by molecular function into pathway categories (Kanehisa et al 2016a, Kanehisa et al 2016b). Assigned K numbers were classified into five main KEGG pathway categories (and their associated sub-categories) using the KEGG Pathway Mapper tool. These were: cellular processes, environmental information processing, genetic information processing, primary metabolism and secondary metabolism. Each gene, with its associated K number and category assignments, was then matched to its RPKM value from the RNA sequencing dataset so that the expression levels of different KO categories could be established and the mostly highly expressed genes in certain KO categories (for example in the carbohydrate metabolism category) could be identified.

2.3.3.9 Biosynthetic gene cluster expression by *Pseudonocardia* species

To investigate the expression of biosynthetic gene clusters (BGCs) by *Pseudonocardia* on the ant cuticle and on plates, genome sequences were uploaded to antiSMASH version 4.0, which predicts the presence of BGCs based on sequence homology to known clusters (Blin et al 2017). RPKM values were then generated for each predicted

BGC, based on the length of the predicted cluster and read counts for genes situated within it.

2.3.3.10 Analysis of the *Pseudonocardia* prmABCD gene cluster

The *prmABCD* gene cluster was highly expressed on the ant surface. A phylogenetic analysis was carried out to compare the amino acid sequence of the PrmA protein encoded by *P. octospinosus* and *P. echinator* isolates (from Holmes et al 2016) to published amino acid sequences for PrmA in other species, as well as other alkane monooxygenases. Amino acid sequences used for the analysis are detailed in the supplementary information (S1). Amino acid sequences were aligned using the MUSCLE algorithm (Edgar 2004) in MEGA7 (Kumar et al 2016) using the default settings. Aligned sequences were then used to construct a Maximum Likelihood tree using Mega7. An LG model with partial deletion of gaps was used, and rates amongst sites was set as gamma distributed with invariant sites. The robustness of the phylogeny was tested using the Bootstrap method, with 500 replicates. Following phylogenetic analysis, the amino acid sequences of PrmA, PrmB, PrmC and PrmD in both PS1083 and PS088 were compared to those in the isolate *Pseudonocardia* sp. TY-7 (Kotani et al 2006) using BLASTp.

2.4 Results

2.4.1 RNA Stable Isotope Probing to determine the transfer of ant resources

2.4.1.1 Isotope Ratio Mass Spectrometry

In order to establish whether ants could internalise and metabolise a significant amount of ^{13}C labelled glucose when fed over a period of 10 days, ants receiving a ^{12}C or ^{13}C , 5% glucose solution ($n = 5$ individuals in each treatment) underwent Isotope Ratio Mass Spectrometry (IRMS) analysis. Ants fed on a ^{13}C glucose diet were found to have a greater atom percentage of ^{13}C (an average of $3.14\% \pm 0.41$ standard error) compared to ants that had been feeding on a ^{12}C glucose solution ($1.09\% \pm 0.01$) (Figure 2.3). Since ants were washed prior to the analysis, ^{13}C was assumed to have been internalised by the ant. In order to maximize the amount of labelling seen in RNA SIP experiments, glucose concentrations were increased from 5% (used for IRMS analysis) to 20% glucose (w/v) in SIP experiments.

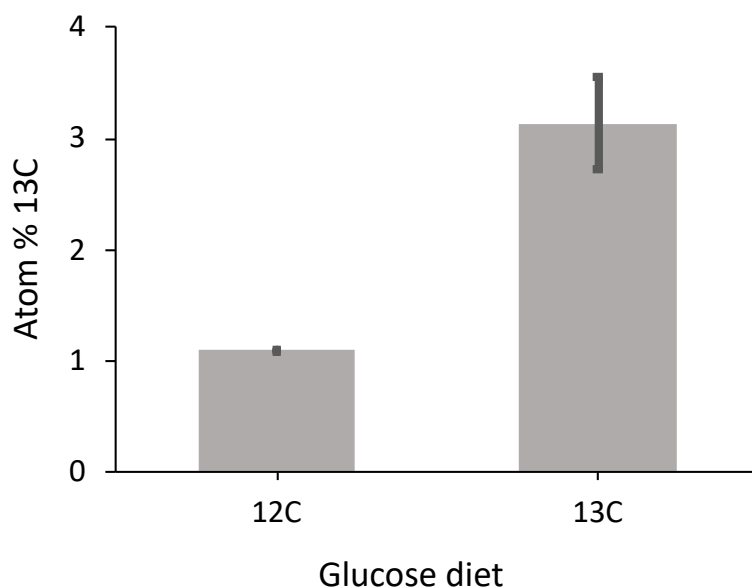


Figure 2.3 The results of Isotope Ratio Mass Spectrometry analysis measuring the atom percentage of ^{13}C in ants fed on either a ^{12}C or ^{13}C , 5% glucose diet for 10 days. N=5 ants per sample and results are shown as averages \pm standard error.

2.4.1.2 Fluorescent microscopy of ants fed a labelled glucose diet

In order to further confirm that glucose solutions were being internalised and were not spreading extensively over the surface of the ant during feeding, ants were fed a 20% glucose solution containing a green fluorescent dye. Ants were imaged under green fluorescent light, either immediately after feeding or up to 24 hours after being exposed to the solution (Figure 2.4). Imaging revealed that, when the ants first fed on the glucose diet, a small amount of the solution was spread around the mouth parts. However, this was never observed to spread onto the laterocervical chest plates, which house the dense growth of symbiotic bacteria. The only fluorescence that could be observed in this region was internal; the dye could be seen fluorescing through from the ants digestive tract, in the gap between the bottom of the head and the start of the laterocervical plates (Figure 2.4). This was also the case for ants that had been exposed to the glucose solution for up to 24 hours (Figure 2.4). In the ants that had not been imaged immediately after feeding on the glucose, the patch of fluorescence around the mandibles was either further reduced, or almost absent. Tiny amounts of the dye could sometimes be seen on the tips of the legs of some ants and it is possible

that these appeared as a result of cleaning the solution from around the mouth parts; when ants self-groom they use their front legs, which are then orally groomed through their mouth parts. In conclusion, the images show that it is unlikely that a large amount of glucose solution would have been transferred to the bacteria on the laterocervical chest plate, and so any labelling of the bacterial RNA would be more likely due to the transfer of resources from the ant host to the bacteria.



Figure 2.4 The distribution of a 20% glucose water diet containing green fluorescent dye, over the surface of *A. echinator* ants **A)** directly after taking a feed **B)** after 6 hours of being exposed to the solution and **C)** after 24 hours of exposure. DT= fluorescence shining through from the ant digestive tract, LP= laterocervical plates with growth of Actinobacteria. Brightfield and fluorescent images were acquired using a Zeiss M2 Bio Quad SV11 stereomicroscope. Green fluorescence was excited with light passed through a 470 nm filter (40 nm bandpass) and the emission was collected through a 525 nm filter (50 nm bandpass).

2.4.1.3 RNA SIP feeding experiments

To test whether the *Acromyrmex echinator* ants provide their cuticular microbiome with a specific or public resource, an RNA stable isotope probing (RNA SIP) experiment combined with 16S rRNA gene amplicon sequencing, was carried out. Three replicate groups of 22 ants (mature workers with visible bacterial growth on their laterocervical plates) were fed on either a 20% solution of ^{13}C glucose or ^{12}C glucose for 10 days, after which laterocervical plates were dissected out and used for RNA extractions. RNA underwent density gradient ultracentrifugation in CsTFA, in order to separate the ^{13}C labelled (“heavy”) RNA from the un-labelled ^{12}C (“light”) RNA (Figure 2.2). Reverse transcribed cDNA from the resulting fractions was then used in qPCR reactions to assess the distribution of 16S rRNA gene copies along the buoyant density gradient

and determine whether labelling of bacterial RNA had occurred under the ^{13}C treatment.

The qPCR experiments revealed that a high percentage of 16S rRNA gene copies had shifted to higher buoyant densities in samples derived from the ^{13}C dietary treatment (Figure 2.5). The 16S rRNA gene copy number peaked in fractions with buoyant densities spanning 1.796-1.799 g ml^{-1} in ^{13}C samples, versus fractions spanning 1.785-1.790 g ml^{-1} in ^{12}C samples (Figure 2.5). This suggested that the heavier, ^{13}C isotope had been incorporated into the RNA of many bacterial taxa on the cuticle, due to the metabolism of labelled resources from their host. Density shifts were consistent with those seen in other bacterial RNA SIP studies (Fortunato and Huber 2016, Tannock et al 2014). Fractions spanning the peaks in 16S rRNA gene copy number were selected for PCR amplification and 16S rRNA gene amplicon sequencing (diamond symbols in Figure 2.5), along with a pooled unfractionated sample from each of the ^{13}C and ^{12}C treatment replicates.

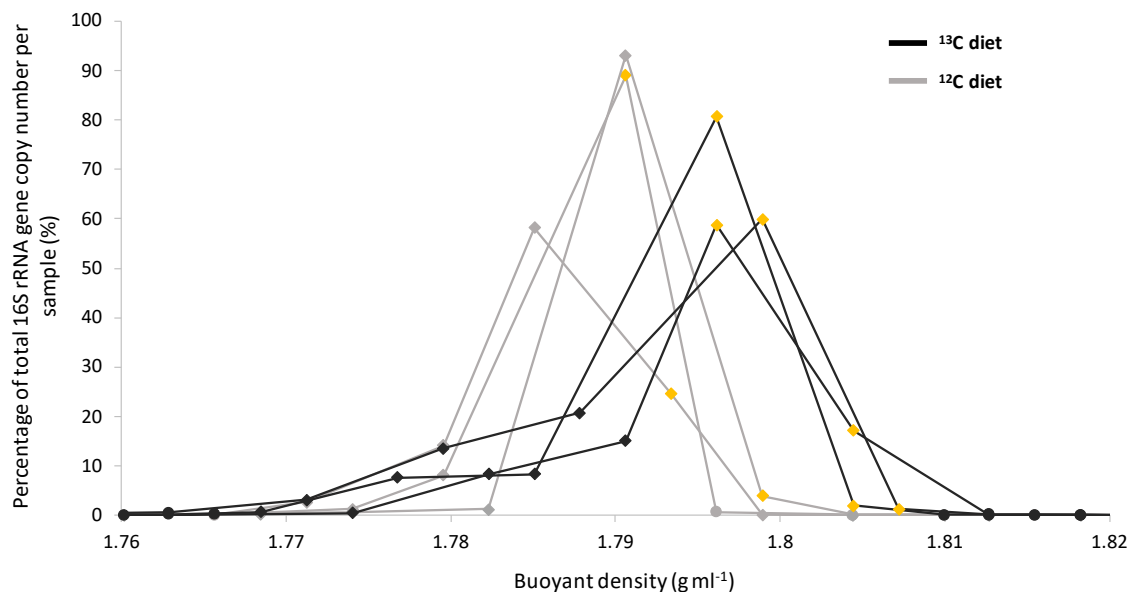


Figure 2.5 16S rRNA gene copy number across different cDNA fractions of the buoyant density gradient, as determined via qPCR. Three replicate samples were taken from ^{13}C (black) or ^{12}C (grey) fed ants. Diamonds represent fractions that were sent for 16S rRNA gene amplicon sequencing and yellow diamonds represent those designated as “heavy” fractions under the different treatments.

2.4.1.4 The total bacterial community on *A. echinator* laterocervical plates

Actinobacteria dominated the pooled unfractionated laterocervical plate samples of both ^{12}C and ^{13}C fed ants, making up 76.6% and 78.0% of these samples, respectively (Figure 2.6). Proteobacteria were the second most abundant phylum, being present at 23.3% and 20.0% of ^{12}C and ^{13}C samples, respectively (Figure 2.6).

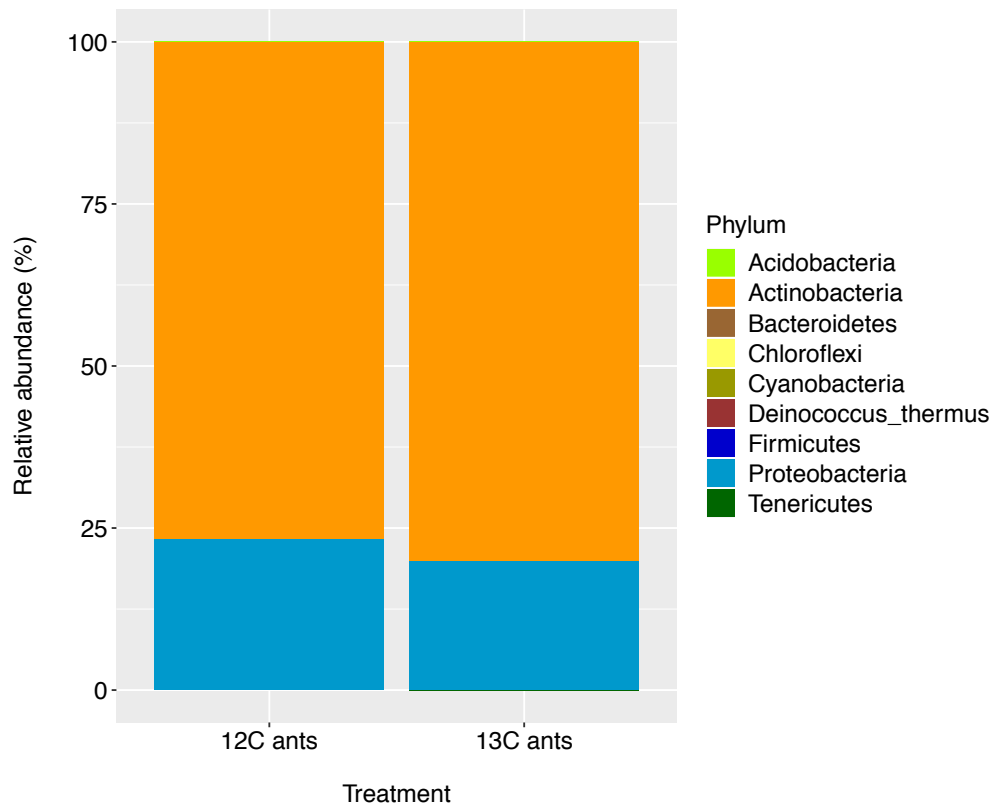


Figure 2.6 The relative abundance (%) of bacterial phyla present in total, unfractionated RNA samples from the laterocervical plates of *A. echinator* ants. Ants were provided with either a ^{12}C or ^{13}C 20% glucose diet for 10 days.

The three most abundant genera (Figure 2.7) in unfractionated cDNA samples were *Pseudonocardia* (35.8% and 38.1% in the pooled ^{12}C and ^{13}C unfractionated samples, respectively), *Streptomyces* (19.69% and 20.53%, respectively) and *Wolbachia* (22.8% and 19.6%, respectively). *Wolbachia* are intracellular parasites and are abundant in the thoracic muscles of *A. echinator* worker ants (Andersen et al 2012) and so these reads most likely come from worker ant tissue that was still attached to the laterocervical plates following dissection. *Wolbachia* was also the main genus contributing to the presence of Proteobacteria in unfractionated samples, with other proteobacterial

genera being present at extremely low abundances. Each of the genera on the laterocervical plates was present at very similar abundances between the two dietary treatment groups.

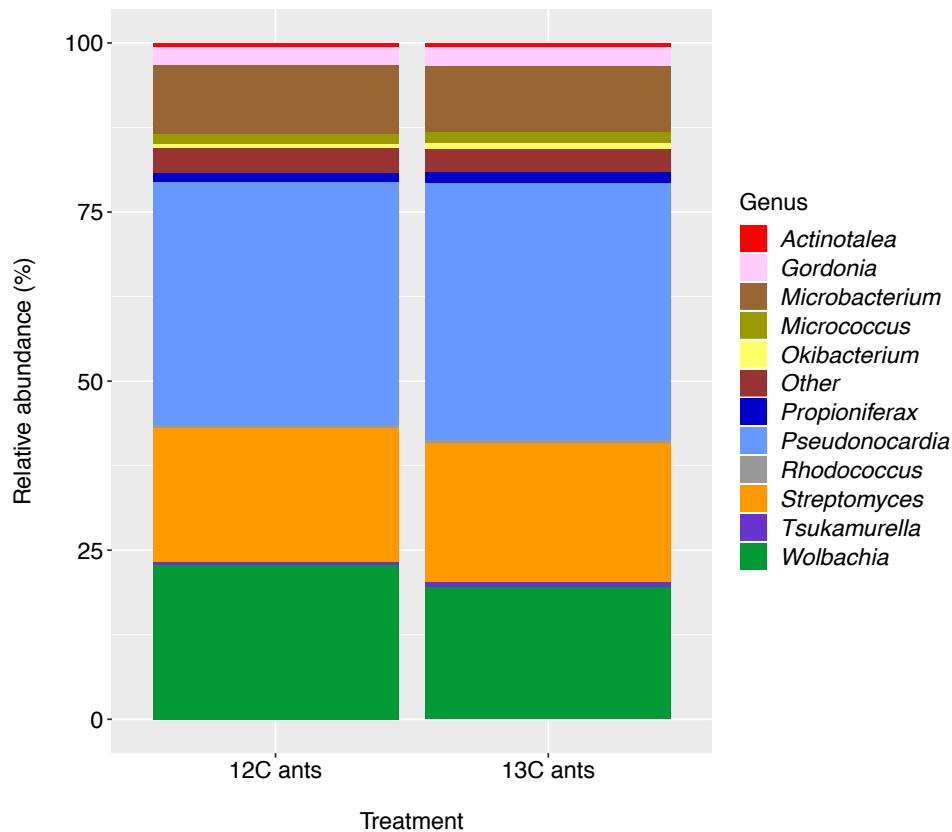


Figure 2.7 The relative abundance (%) of bacterial genera present in total, unfractionated RNA samples from the laterocervical plates of *A. echinator* ants. Ants were provided with either a ^{12}C or ^{13}C 20% glucose diet.

As discussed in (2.1.3) *Acromyrmex echinator* ants are typically associated with one of two vertically transmitted *Pseudonocardia* species, which are passed between the cuticles of worker ants and the next generation of larvae (Andersen et al 2013, Andersen et al 2015, Holmes et al 2016). Over 95% of *Pseudonocardia* 16S rRNA reads in the unfractionated SIP samples were identical to a single strain, in this case *P. octospinosus*, with none of the remaining reads mapping significantly to the 16S rRNA gene sequence of *P. echinator*. The presence of *Streptomyces* bacteria is also consistent with previous studies and their proposed role as horizontally acquired

mutualists that are screened in by their hosts (Barke et al 2010, Haeder et al 2009, Kost et al 2007, Scheuring and Yu 2012) .

2.4.1.5 Density gradient ultracentrifugation of RNA SIP samples

Analysis of density gradient fractions using qPCR, suggested that many members of the bacterial community on the laterocervical plates of *Acromyrmex echinator* ants were metabolising labelled host-derived resources, as a large percentage of 16S rRNA gene copies had shifted to higher buoyant density fractions under the ^{13}C dietary treatment (Figure 2.5). Accordingly, an analysis of the taxonomic composition of RNA SIP fractions of different buoyant densities confirmed that many actinobacterial genera were present in the higher buoyant density fractions under the ^{13}C treatment, including *Pseudonocardia* and *Streptomyces* (Figure 2.8 and Figure S2.1). For example, *Pseudonocardia* sequences had an average relative abundance of $36.30\% \pm 4.17$ (SE) and $32.30\% \pm 4.11$ in fractions 7 and 8 of the three ^{13}C samples, respectively (Figure 2.8). Fractions 7 and 8 had an average buoyant density of $1.797 \text{ g ml}^{-1} \pm 0.001$ SE and $1.805 \text{ g ml}^{-1} \pm 0.001$ SE, respectively (Figure S2.1), which coincided with the peaks in 16S rRNA gene copy number identified by qPCR (Figure 2.5); an average of $73.28\% \pm 6.31$ (SE) of 16S rRNA gene copies occurred across these fractions in the three replicate ^{13}C samples (Figure 2.5). In contrast, bacterial sequences were barely detectable in fraction 8 (buoyant density of $1.801 \text{ g ml}^{-1} \pm 0.003$) of ^{12}C samples in qPCR experiments, with only $0.30\% \pm 0.20$ of bacterial 16S rRNA gene copies occurring in this fraction across the three replicate samples (Figure 2.5). Additionally, although *Pseudonocardia* sequences were observed in fraction 7 of ^{12}C samples (Figure 2.8), only low numbers ($1.59\% \pm 1.20$) of bacterial 16S rRNA sequences could actually be amplified from this fraction number (average buoyant density of $1.796 \text{ g ml}^{-1} \pm 0.003$) in qPCR experiments (Figure 2.5). Peaks in 16S rRNA gene copy number instead occurred in fractions 5-6 of ^{12}C samples, which had average buoyant densities spanning $1.780\text{-}1.788 \text{ g ml}^{-1}$ (Figure 2.5); *Pseudonocardia* made up an average of $54.41\% \pm 5.6$ and $52.38\% \pm 3.44$ of fractions 5 and 6, in these samples, respectively. Apart from *Pseudonocardia*, other taxa had also shifted into the higher buoyant density fractions of ^{13}C samples, for example the genera *Streptomyces* and *Microbacterium* made up $19.18\% \pm 0.33$ and $8.71\% \pm 1.43$ of fraction 7, and $17.64\% \pm 0.26$ and $12.40\% \pm 0.68\%$ of fraction 8, respectively (Figure 2.5 and Figure 2.8).

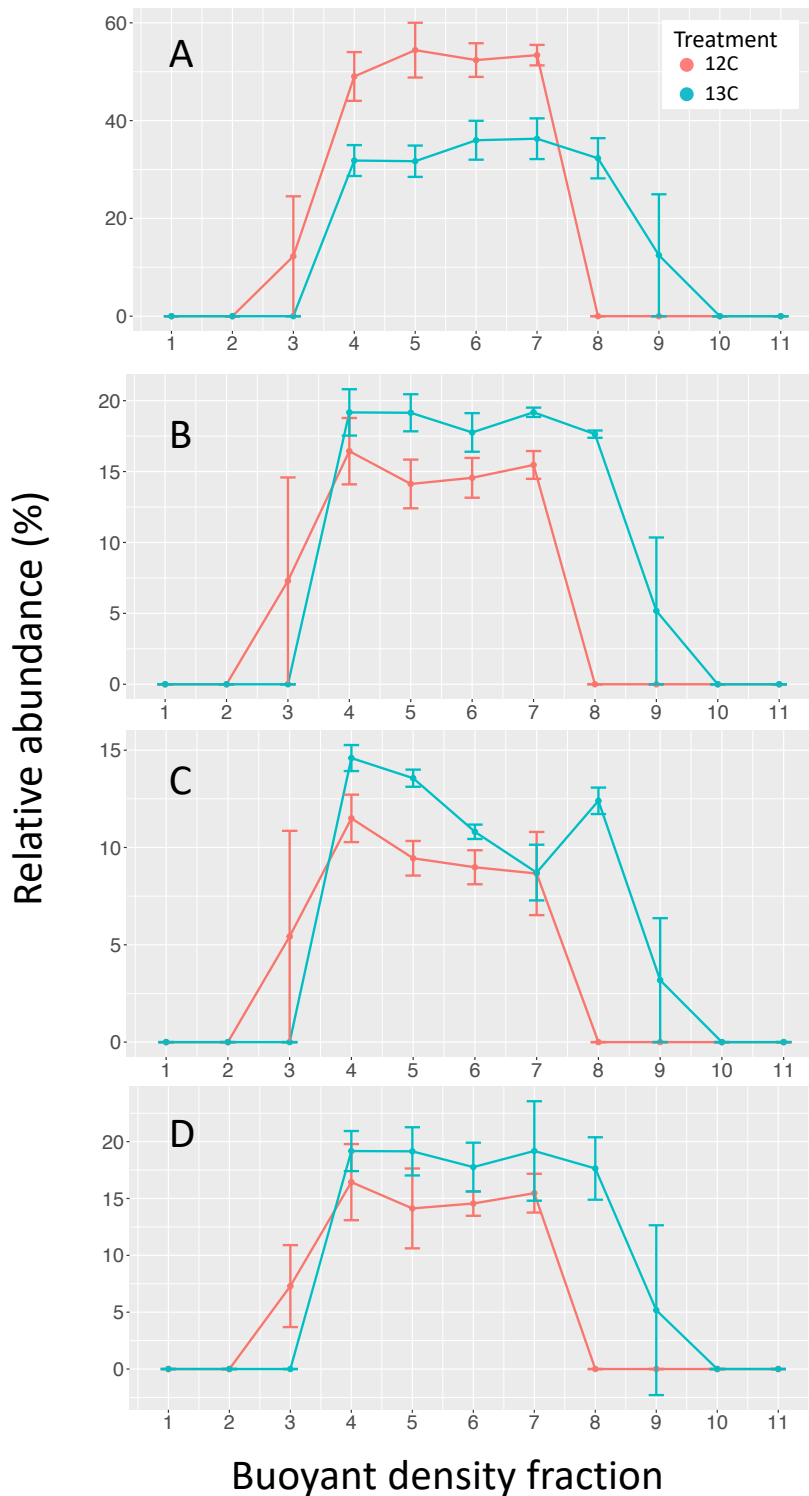


Figure 2.8 The average relative abundance (%) of different bacterial genera across sequenced fractions of the buoyant density gradient. Genera are **A)** *Pseudonocardia* **B)** *Streptomyces* **C)** *Microbacterium* and **D)** *Wolbachia*. Fractions originated from samples taken from ants fed on a ^{13}C (blue) or ^{12}C (red) glucose diet. Increasing fraction number represents increasing buoyant density (see Figure S2.1). Error bars represent standard errors and n=3 replicate samples under each treatment.

In addition to density shifts in bacterial taxa under the ^{13}C treatment, several genera were also more abundant in the “heavy” fractions of the ^{13}C samples than in the heaviest of the ^{12}C fractions (Figure 2.5 and Figure 2.9), implying that they had a slight advantage in the use of carbon-based resources derived from their host. For example, *Streptomyces* increased from an average relative abundance of $14.8\% \pm 0.33\%$ (SE) in ^{12}C heavy fractions, to $18.5\% \pm 0.29\%$ of ^{13}C heavy fractions. Several other Actinobacterial genera that had been comparatively rare in ^{12}C heavy fractions were enriched by more than 1.5 fold in the ^{13}C heavy fractions (Figure 2.9). Interestingly, although *Pseudonocardia* was abundant in the heaviest fractions of the ^{13}C samples, its relative abundance decreased from $53.65\% \pm 1.95\%$ to $34.30 \pm 3.78\%$ between the heaviest fractions of the ^{12}C treatment and ^{13}C treatment (Figure 2.9). This corresponded with a concurrent increase in the abundance of other genera and a more even community structure in the heavier ^{13}C fractions. This evenness suggests that ant-derived resources were not solely being made available to particular bacterial taxa on the ant cuticle, for example the *Pseudonocardia* mutualist, which would otherwise have dominated the ^{13}C heavy fractions if being supplied with a private resource. Instead, a buoyant density shift in the majority of the bacterial community suggests a public resource was being made available to most of the genera on the ant cuticle.

The genus *Wolbachia* also appeared to be metabolising labelled resources from the ant host in the experiment, as it was prevalent in heavier ^{13}C fractions (Figure 2.8 and Figure 2.9). The relative abundance of *Wolbachia* increased from $9.86\% \pm 1.60\%$ in the heavy ^{12}C fractions, to $19.49\% \pm 3.53\%$ in the ^{13}C heavy fractions, suggesting it was also playing a major role in resource metabolism (Figure 2.9). Since *Wolbachia* are intracellular symbionts that inhabit the tissue underlying the laterocervical plates, this observation suggests that resources were derived from the ants themselves and not directly from the glucose water. This is supported by the preliminary IRMS data which showed that the ants internalise a significant amount of the ^{13}C from their glucose diet (Figure 2.3) as well as the fluorescent microscopy images demonstrating that glucose water was not transferred to the chest plate region (Figure 2.4). Additionally, ants

were only ever observed to feed using their mandibles and their chest plates never came into direct contact with the liquid diet (Figure 2.10).

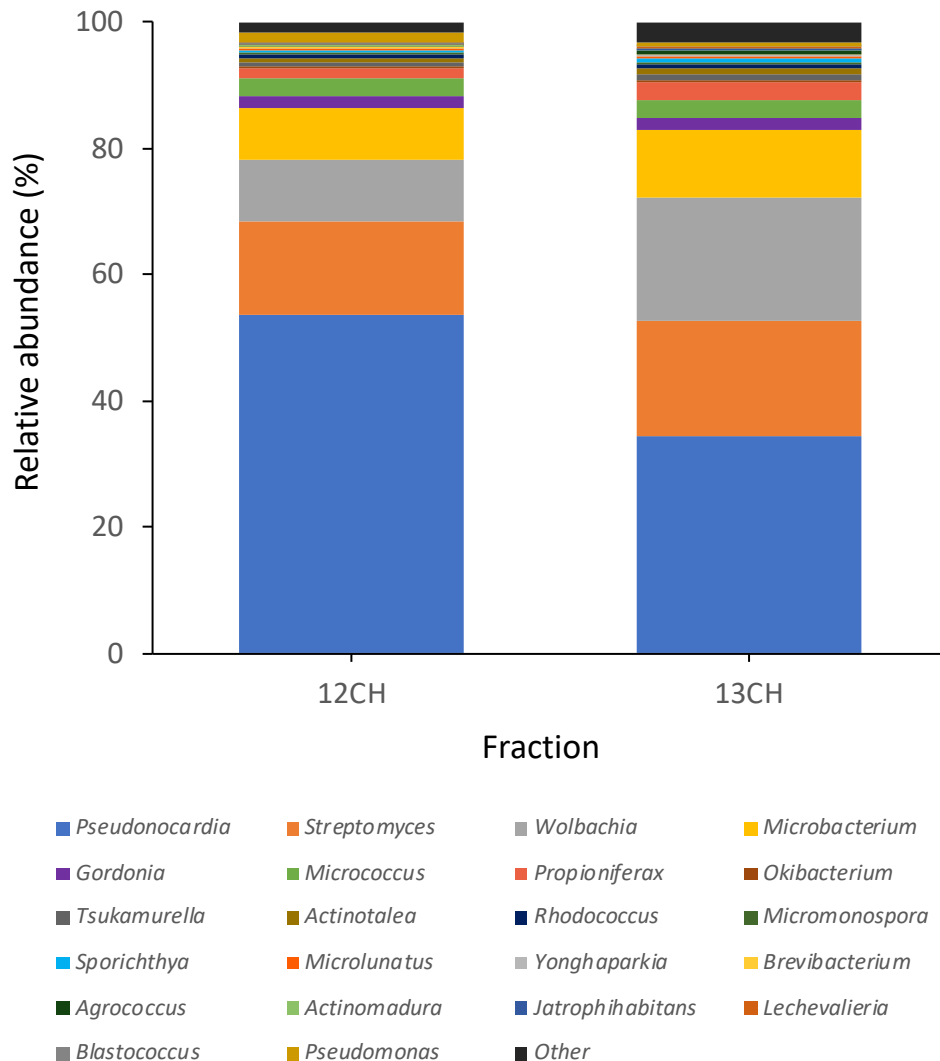


Figure 2.9 The relative abundances (%) of bacterial genera in the “heavy” fractions of buoyant density gradients for ^{12}C and ^{13}C samples, respectively. Heavy fractions were determined via qPCR, which identified peaks in 16S rRNA gene copy number in both sets of samples (see Figure 2.5).

In conclusion these results suggest that the community of bacteria living on the laterocervical plates of ants predominantly consists of Actinobacteria and these receive carbon-based resources from their ant host, that appear to be made publicly available to all bacteria on the cuticle.



Figure 2.10 *Acromyrmex echinator* ants feeding on a 20% glucose water solution.

2.4.2 *Pseudonocardia* gene expression *in vitro* and *in vivo*

In order to investigate the production of antimicrobial compounds by *Pseudonocardia* mutualists *in vitro*, bioassays were carried out using one isolate each of *P. echinator* and *P. octospinosus*. RNA sequencing experiments were also carried out to compare the expression of *Pseudonocardia* biosynthetic gene clusters, using *Pseudonocardia* grown on agar medium and samples isolated from the laterocervical plates of ants harboring either *P. octospinosus* or *P. echinator* as cuticular symbionts.

2.4.2.1 The bioactivity of *Pseudonocardia* mutualist species *in vitro*

In order to test for the ability of *Pseudonocardia* isolates PS088 (*P. echinator*) and PS1083 (*P. octospinosus*) (Table 2.1) to produce antibacterial and antifungal compounds *in vitro*, *Pseudonocardia* isolates were grown on GYM agar plates and challenged with either *Bacillus subtilis*, or the specialised nest pathogen *Escovopsis weberi*. PS088 demonstrated relatively strong antibacterial activity against *B. subtilis*, indicated by the zone of clearing around the central *Pseudonocardia* colony (Figure 2.11). This isolate also demonstrated moderate antifungal activity against *E. weberi* with a medium zone of inhibition (Figure 2.11). In comparison, PS1083 did not exhibit

antibacterial properties against *B. subtilis* on GYM agar media, but exhibited extremely strong inhibition of *E. weberi*; growth of this fungus was almost entirely prevented apart from at the very edge of the plate (Figure 2.11). The observation of stronger antifungal activity by PS1083 compared to PS088 was not due to a difference in the viability of the inoculum, since both sets of bioassays were inoculated from the same starter plate of *E. weberi*. The result was also repeatable across three independent experiments (three replicate plates in each experiment), whereby different *E. weberi* starter plates were used as an inoculum.

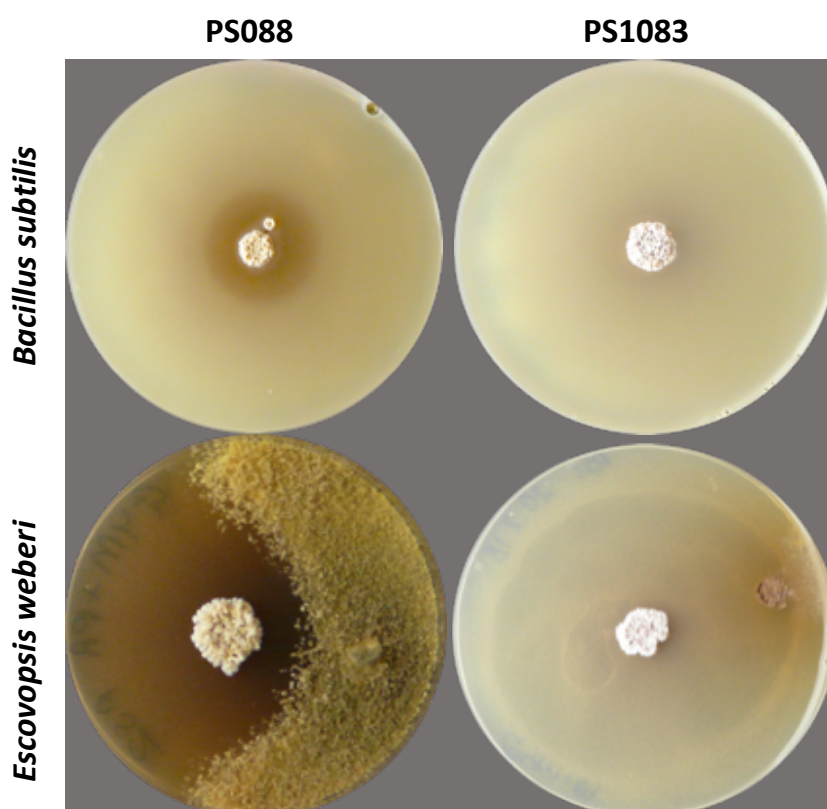


Figure 2.11 The bioactivity of *Pseudonocardia* strains against *Bacillus subtilis* (top) and the specialised nest pathogen *Escovopsis weberi* (bottom). The two *Pseudonocardia* isolates tested were PS088 (*P. echinator*, left) and PS1083 (*P. octospinosus*, right).

2.4.2.2 Alignment of RNA sequencing reads

To establish the extent to which *Pseudonocardia* biosynthetic gene clusters (BGCs) were expressed *in vitro*, RNA was extracted from three samples each of both PS1083 (*P. octospinosus*) and PS088 (*P. echinator*) grown as confluent lawns on GYM agar

plates (PS1083 or PS088 A-C, Table 2.7). To compare this to gene expression *in vivo* on the *A. echinator* cuticle, RNA was also extracted from the laterocervical plates of ants in the colonies A.e1083 and A.e088, respectively (samples C1083 and C088, Table 2.7). Only a single extraction from laterocervical plates was carried out for each colony, as it was uncertain whether it would be possible to map reads back to *Pseudonocardia* genomes when the RNA samples contain a mixture of ant and bacterial RNA, with ant RNA likely to be dominant. Despite being only a single extraction, each sample consisted of the laterocervical plates of 80 individual ants pooled together, reducing the effect of inter-ant variation. Both sets of RNA samples were sequenced using a dual RNA sequencing approach (Westermann et al 2016) generating single end Illumina reads that were 75 bp in length.

The reads generated for each sample were quality filtered and aligned to the corresponding reference genome (Table 2.6, Table 2.7). For RNA samples taken from agar grown cultures, an average of 58.6% of reads from PS1083 samples mapped uniquely to the reference genome (Table 2.7). For PS088, 65.4% mapped uniquely (Table 2.7). Reads that mapped ambiguously to multiple locations (on average 13.93% and 28.33% for PS088 and PS1083, respectively) were discarded. Samples C1083 and C088 (from laterocervical plates) were aligned to both the *A. echinator* genome (Table 2.6) and a representative genome for either *P. octospinosus* (Ae707 genome, Table 2.6) or *P. echinator* (Ae706 genome, Table 2.6), depending on the *Pseudonocardia* genotype associated with colony of origin. For both samples, a high percentage of the reads mapped uniquely to the *A. echinator*, host genome (Table 2.7); this is not surprising as samples taken from laterocervical plates would be expected to contain a high proportion of ant RNA relative to bacterial RNA due to the greater overall biomass of host cellular material. However, it was still possible to map 1% of the reads to the *P. octospinosus* genome for sample C1083, and 2% of reads to the *P. echinator* genome for sample C088. These percentages and the raw numbers of reads are in line with other dual RNA sequencing experiments (Camilios-Neto et al 2014, Mateus et al 2019, Westermann et al 2016, Westermann et al 2019). Additionally, cross-mapping showed that the vast majority of the reads that uniquely mapped to either of the *Pseudonocardia* reference genomes, did not map to the *A. echinator* genome and vice

versa, suggesting that uniquely mapped reads were mainly either bacterial or ant derived.

Table 2.7 The number of reads in each sample that uniquely mapped to each respective reference genome (details of reference genomes can be found in Table 2.6). The percentage of uniquely mapped reads for each sample is shown in brackets.

Sample	Source	Alignment		
		<i>A. echinator</i> genome	<i>P. octospinosus</i> genome Ae707	<i>P. echinator</i> genome Ae706
C1083	80 pooled laterocervical plates from ants in colony Ae1083	8,548,640 (78.7 %)	103,820 (1.0 %)	-
C088	80 pooled laterocervical plates from ants in colony Ae088	7,058,678 (73.5 %)	-	189,989 (2.0 %)
PS1083 A	PS1083 grown confluent on GYM agar	-	4,491,975 (50.5 %)	-
PS1083 B	PS1083 grown confluent on GYM agar	-	5,573,275 (58.6 %)	-
PS1083 C	PS1083 grown confluent on GYM agar	-	7,123,585 (66.7 %)	-
PS088 A	PS088 grown confluent on GYM agar	-	-	6,026,502 (63.3 %)
PS088 B	PS088 grown confluent on GYM agar	-	-	6,552,342 (67.1 %)
PS088 C	PS088 grown confluent on GYM agar	-	-	5985177 (65.8%)

2.4.2.3 Normalisation of mapped reads

In order to establish patterns of gene expression for gene functional groups and individual BGCs within samples, read counts for each individual coding sequence were converted to values of reads per kilobase of exon model per million mapped reads (RPKM). Converting counts to RPKM values controls for the fact that genes of greater length will accumulate greater numbers of reads (Mortazavi et al 2008). It also controls for differences in sequencing depth across different samples by dividing by the total number of uniquely mapped reads (Mortazavi et al 2008). However, it is important to note that quantitatively comparing RPKM values between samples, assumes that the total amount of mRNA per cell is the same in each of the samples (i.e that total expression is the same under the different conditions present across samples) (Evans et al 2018). As this could not be confirmed, and is possibly unlikely to be the case, for the different *Pseudonocardia* isolates growing on laterocervical plates and on agar media it was only possible to compare the general patterns of gene expression, specifically for BGCs, across samples and not possible to statistically measure differences in expression for each individual gene. There are other methods that allow normalisation of gene expression between samples, for example it is possible to normalise read counts by making them relative to the expression of stably expressed genes, such as housekeeping genes (Evans et al 2018). However, this again assumes that the housekeeping genes are not differentially expressed between conditions, which it was not possible to confirm for our samples.

Despite not being able to normalise values to quantitatively compare RPKM values across samples from the different conditions, the RNA-sequencing experiments could still be used as a useful indicator of the relative expression (and possible importance) of different BGCs within and across samples. It also stands as a preliminary set of experiments that confirms the ability to detect gene expression by *Pseudonocardia* *in vitro* on agar, and *in vivo* on the ant laterocervical plates. This paves the way for differential sequencing experiments using these conditions, for example it would be possible to investigate differences in gene expression by the *Pseudonocardia* mutualist on laterocervical plates in the presence or absence of nest infection, or on agar medium in the presence or absence of pathogenic cues.

2.4.2.4 Expression of gene functional groups on the surface of the ant

In order to compare the broad scale patterns of gene expression by *Pseudonocardia* across samples, genes were classified into five main KEGG pathway categories and their associated sub-categories. These five categories were: cellular processes, environmental information processing, genetic information processing, primary metabolism and secondary metabolism (Figure 2.12, Figure 2.13). Both species of *Pseudonocardia*, showed very similar patterns of gene expression on the laterocervical plates of ants across these broad-scale groupings (Figure 2.12). Of particular interest were genes involved in secondary metabolism; genes classified as being involved in the biosynthesis of antibiotic production as well as secondary metabolite production showed relatively high levels of expression in both samples from the different ant colonies. When looking at the most highly expressed genes in these categories many of them encoded proteins involved in the metabolism of amino acids, but also those involved in the production of isoprenoid units for example the proteins IspH, IspD and GcpE. Isoprenoids are important precursors for natural products such as terpenoids. Samples from *Pseudonocardia* grown on agar plates, also showed broadly similar patterns, with categories for the biosynthesis of secondary metabolites and antibiotics having similar levels of expression to those on the ant laterocervical plates (Figure 2.13).

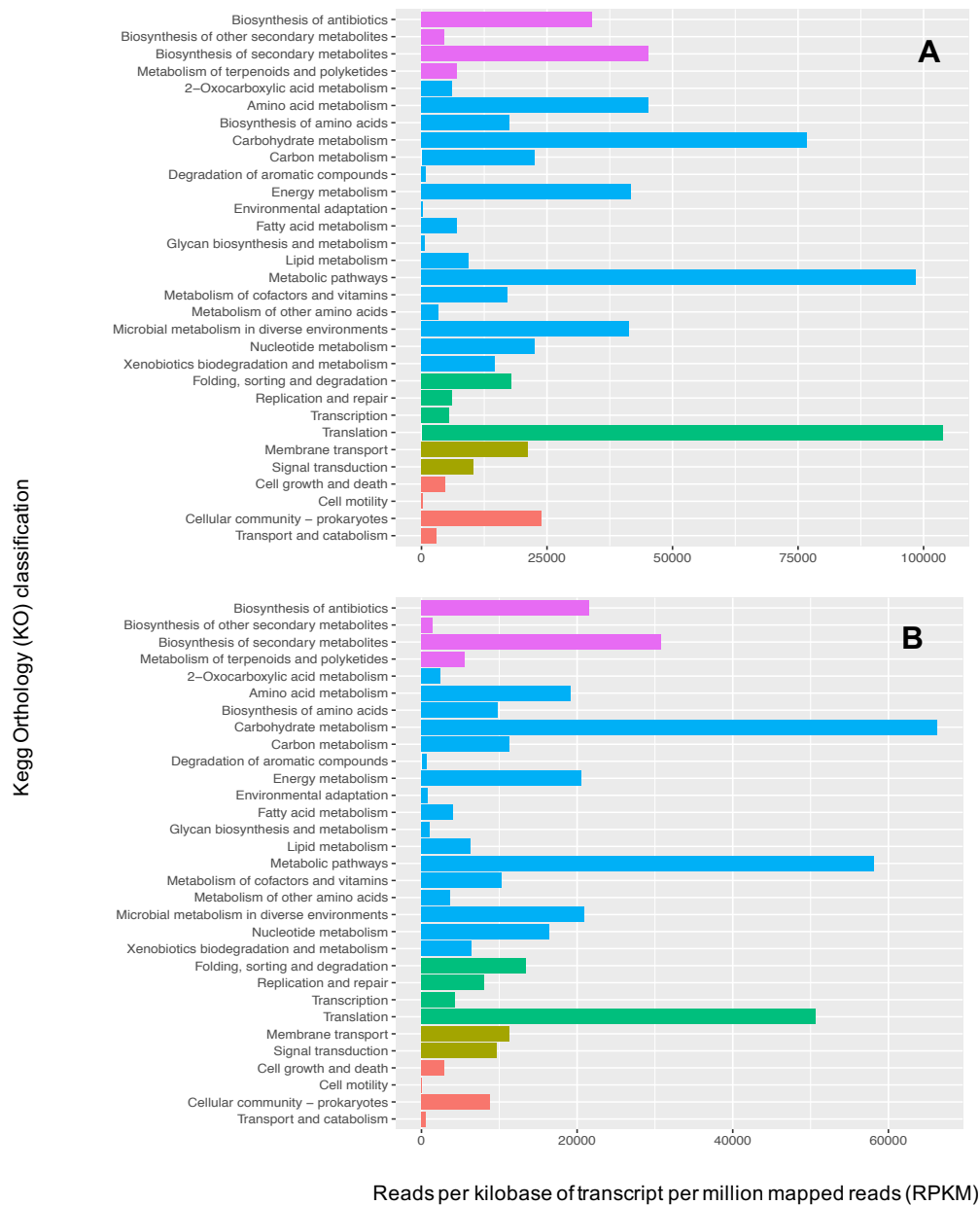


Figure 2.12 The expression of KEGG Orthology pathway categories by *Pseudonocardia* mutualists on the laterocervical plates of *Acromyrmex echinator* ants. Gene expression by **A) *Pseudonocardia octospinosus*** and **B) *Pseudonocardia echinator*** is shown in reads per kilobase of transcript per million mapped reads.

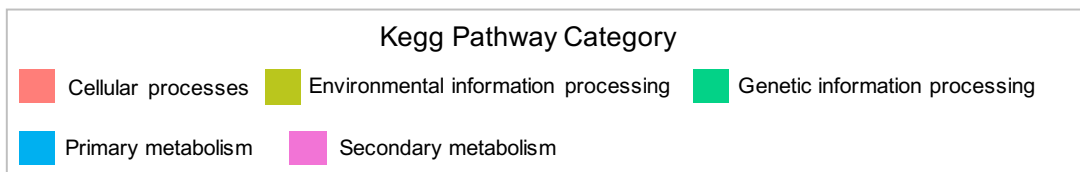


Figure 2.13 The expression of KEGG Orthology pathway categories by *Pseudonocardia* mutualists on agar medium. Expression by **A)** *Pseudonocardia octospinosus* and **B)** *Pseudonocardia echinatio* is shown in reads per kilobase of transcript per million mapped reads.

2.4.2.5 Expression of biosynthetic gene clusters on the surface of the ant

In order to assess the average expression of individual BGCs by *Pseudonocardia*, both on the leafcutter ant cuticle and on GYM agar plates, values of Reads Per Kilobase of transcript per Million mapped reads (RPKM) were generated for each individual biosynthetic gene cluster (BGC) identified in the reference genomes Ae707 and Ae706 (Table 2.6, Figure 2.14). BGC boundaries were identified and defined using AntiSMASH 4.0 (Blin et al 2017).

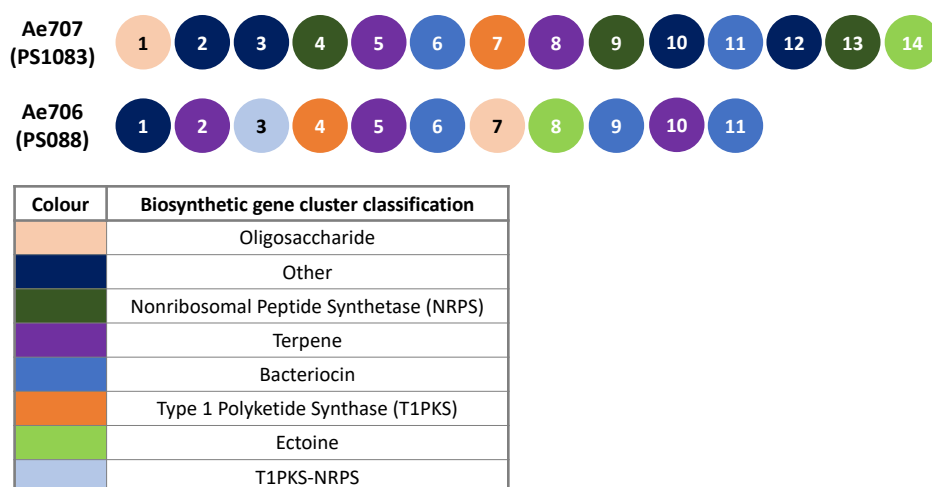


Figure 2.14 AntiSMASH outputs for *Pseudonocardia* reference genomes. The genome Ae707 (*P. octospinosus*, top) was used for alignments with samples involving the *Pseudonocardia* strain PS1083. The genome Ae706 (*P. echinator*, bottom) was used for alignments with samples involving the strain PS088. Each circle represents one predicted biosynthetic gene cluster (BGC) and all are coloured by BGC classification.

An extensive comparison of the BGCs encoded in the genomes of *P. octospinosus* and *P. echinator* isolates was previously carried out by Holmes et al 2016, whereby a MultiGeneBlast algorithm was used to align and compare each individual BGC in the genomes of five different isolates of each *Pseudonocardia* species. The genomes for Ae707 and Ae706 (used as the reference genomes for alignments) were part of this analysis. Holmes et al found that six clusters were shared between all *P. octospinosus* and *P. echinator* strains (Table 2.8). Additionally, *P. octospinosus* and *P. echinator* isolates encoded seven and five unique BGCs, respectively (Table 2.8).

Table 2.8 Biosynthetic gene clusters (and their classification) that are either shared by both *P. octospinosus* and *P. echinatio*, or are unique to either strain (table adapted from Holmes et al 2016). Cluster number relates to clusters identified by AntiSMASH (Figure 2.14).

Cluster number		Classification	Cluster code
<i>P. octospinosus</i>	<i>P. echinatio</i>		
1	7	Oligosaccharide	A
5	5	Terpene	B
7	4	Nystatin	C
8	2	Terpene	D
11	9	Bacteriocin	E
14	8	Ectoine	F
2	-	Other	G
3	-	Other	H
4	-	NRPS	I
6	-	Bacteriocin	J
9	-	NRPS	K
12	-	Other	L
13	-	NRPS	M
-	1	Other	N
-	3	T1PKS-NRPS	O
-	6	Bacteriocin	P
-	10	Terpene	Q
-	11	Bacteriocin	R

BGCs that are shared between *P. octospinosus* and *P. echinatio* displayed remarkably similar levels of expression across samples in the RNA sequencing experiment (Figure 2.15). For both *Pseudonocardia* species, BGCs encoding the compound ectoine (cluster F, Table 2.8) and a terpene compound (cluster D, Table 2.8) were the most highly expressed BGCs, both on plates and on ant laterocervical plates (Figure 2.15). Ectoine, [(4S)-2-methyl-1,4,5,6-tetrahydropyrimidine-4-carboxylic acid] is encoded by the cluster *ectABC* and is synthesised from the precursor L-aspartate β semialdehyde. The gene product of *ectD* then converts ectoine to its derivative, 5-hydroxyectoine (Czech et al 2018). Both of these compounds are highly soluble, low molecular weight compatible solutes, which can be accumulated by cells to high concentrations without interrupting cellular functions (Czech et al 2018). They are produced by a diversity of

bacterial species in response to osmotic stressors, such as high salinity, desiccation and extreme temperatures, and function to maintain cell turgor, polypeptide folding and protein stability under unfavorable conditions (Bursy et al 2008, Czech et al 2018). Terpenes on the other hand are hydrocarbons synthesized from linear isoprenoid precursors and represent an extremely diverse group of natural products with huge structural variability (Gershenzon and Dudareva 2007, Yamada et al 2015). A variety of functions have been assigned to bacterial terpenes, for example several have been documented as antifungal and antibacterial compounds and others are thought to act as a means of communication both within and between species. In this case, Cluster D carries a gene that has a high level of similarity to a lycopene cyclase gene; such enzymes are known to be important in the biosynthesis of carotenoid terpenes (Holmes et al 2016). Carotenoids are thought to have a variety of functions, including acting as protective pigments, antioxidants and scavengers of free radicals under conditions such as high light irradiation and biofilm formation in which superoxide antimicrobials may be produced (Gershenzon and Dudareva 2007, Nupur et al 2016, Richter et al 2015).

Amongst the other BGCs that are shared between *P. octospinosus* and *P. echinatio*, a cluster encoding a bacteriocin (cluster E, Table 2.8) was also expressed, although to a lesser degree, on both the laterocervical plates and agar medium (Figure 2.15). Bacteriocins are small, ribosomally synthesised peptides produced by many different species of bacteria. Different bacteriocins have been shown to demonstrate both broad and narrow spectrum antibacterial activities (Chikindas et al 2018, Cotter et al 2013, Riley and Gordon 1999). Additionally, some bacteriocins have been shown to act as quorum sensing inhibitors and can prevent the formation of biofilms by other species (Algburi et al 2017, Chikindas et al 2018).

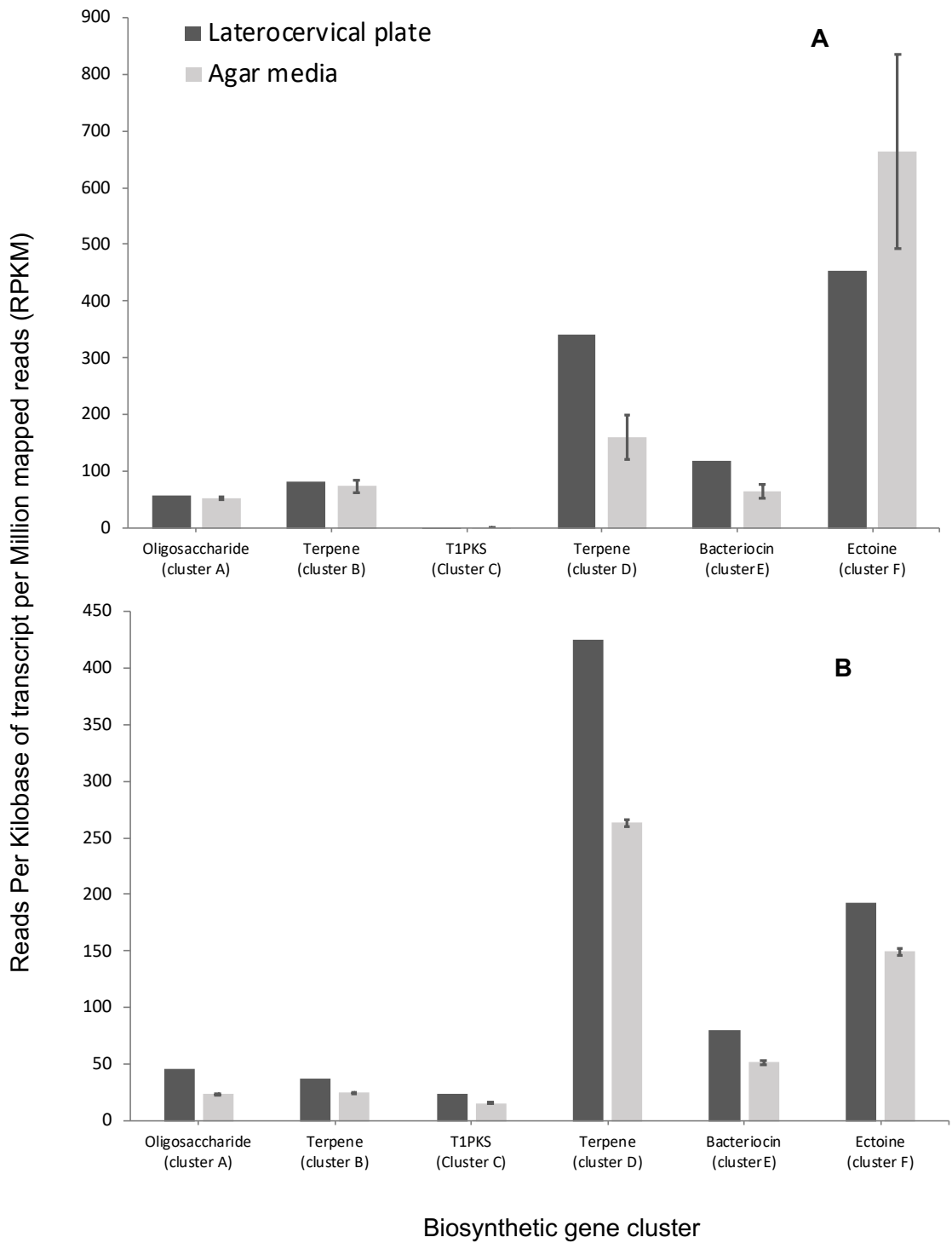


Figure 2.15 The expression of biosynthetic gene clusters that are shared between *Pseudonocardia* species. Expression is shown in reads per kilobase of transcript per million mapped reads for **A)** *P. octospinosus* and **B)** *P. echinator*. Dark grey= laterocervical plate samples, light grey= agar medium samples. Cluster codes relate to Table 2.8. For agar medium samples, values represent averages (n= 3 plate samples) and bars represent standard errors. Laterocervical plate samples are from a pool of 80 individual ants each.

In addition to the bacteriocin cluster, BGCs encoding a second terpene molecule (cluster B, Table 2.8) and an oligosaccharide (cluster A, Table 2.8) demonstrated very low levels of expression by *Pseudonocardia* species on agar media and on the ant cuticle (Figure 2.15). Like cluster D, the terpene encoded by cluster A is also thought to be a carotenoid molecule since the cluster encodes genes that have significant homology to a polyprenyl synthetase gene and a phytoene synthase gene (Holmes et al 2016), both of which have been established to play a role in carotenoid biosynthesis (Richter et al 2015). The type 1 PKS cluster (cluster C, Table 2.8) that is predicted to encode the antifungal compound nystatin also demonstrated very low levels of expression across all samples, particularly for those involving *P. octospinosus* in which expression was not detected (Figure 2.15).

For the BGCs that are unique to *P. octospinosus* (Table 2.8), the clusters H and J (Table 2.8) were the most highly expressed clusters in the laterocervical plate sample (Figure 2.16). Cluster H was classified as “other” by AntiSMASH and although two core biosynthetic genes were identified, both of these are small putative regulatory genes. Holmes et al (2016) suggest that the absence of any other predicted core biosynthetic genes makes it uncertain if this encodes a true secondary metabolite, or if it is an artifact of the algorithms used by antiSMASH to identify BGCs. Cluster J is predicted to encode a bacteriocin, due to a 273 base pair gene within the cluster showing significant homology to a gene involved in the production of a bacteriocin called linocin M18 (Holmes et al 2016). Linocin M18 is a bacteriocin, originally isolated from *Brevibacterium linens* M18, that is known to inhibit the growth of *Listeria* species and several other Gram-positive organisms (Valdes-Stauber and Scherer 1994). This appeared to be more highly expressed on the ant laterocervical plates than on agar media, although, as mentioned above, it is hard to make conclusive quantitative comparisons if total mRNA levels are unknown under the two conditions.

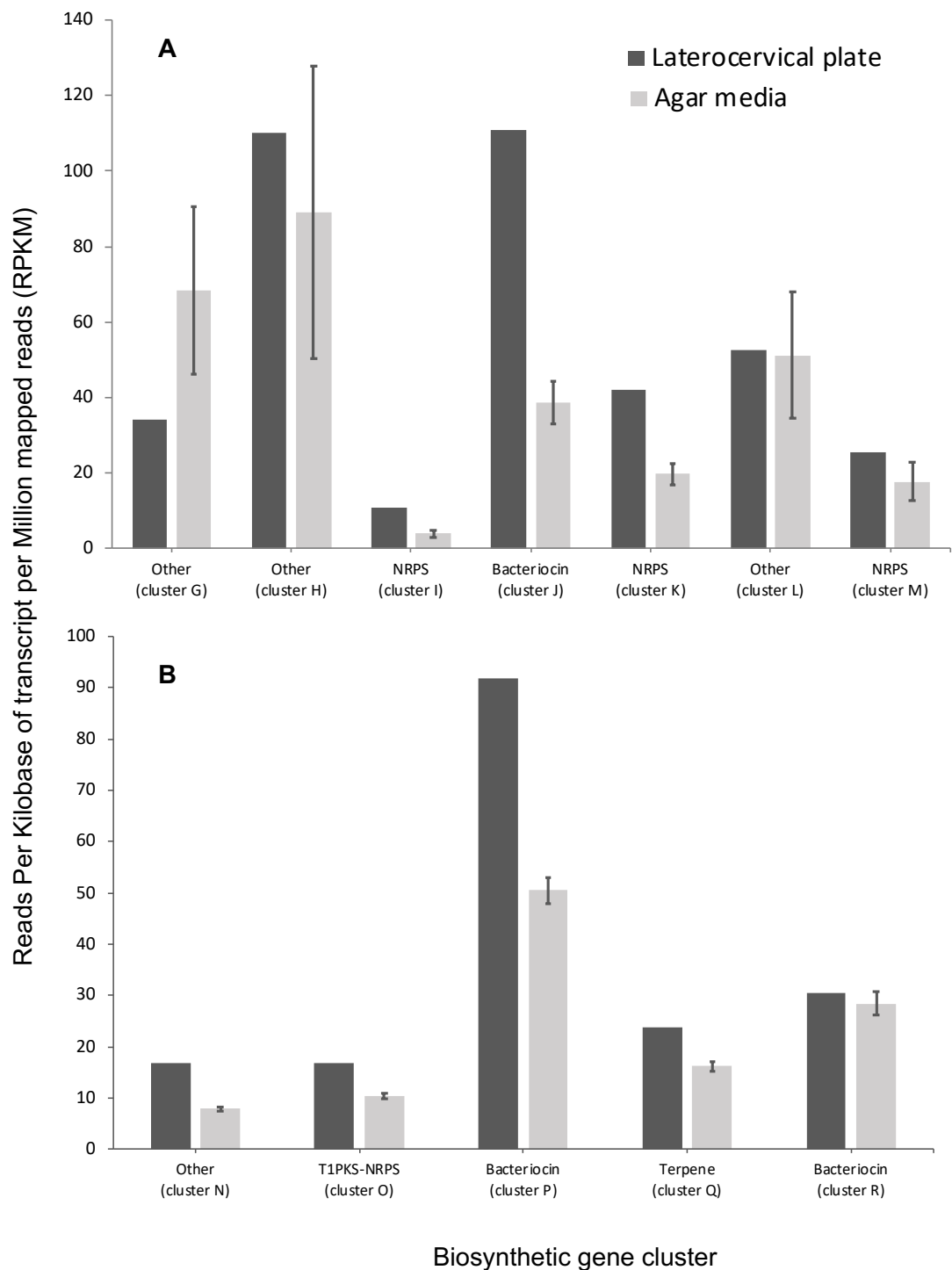


Figure 2.16 Expression of biosynthetic gene clusters that are unique to each *Pseudonocardia* species. Expression is shown as reads per kilobase of transcript per million mapped reads for **A)** *P. octospinosus* and **B)** *P. echinator*. Dark grey= laterocervical plate samples, light grey= agar medium samples. Cluster codes relate to Table 2.8. For agar medium samples, values represent averages (n= 3 plate samples) and bars represent standard errors. Laterocervical plate samples are from a pool of 80 individual ants each.

Cluster J additionally carries two adenylating enzymes, one of which shows homology to a nonribosomal peptide synthetase (NRPS), making it possible that this cluster also encodes a nonribosomal peptide product (Holmes et al 2016). Nonribosomal peptides are a group of natural products that have complex chemical structures and act in a variety of ways including as toxins, siderophores, pigments and antibiotics (Finking and Marahiel 2004, Wang et al 2014). They are synthesised independently from mRNA and the ribosome via the activity of large NRPS enzymes (Finking and Marahiel 2004, Wang et al 2014).

Cluster L (Table 2.8) was also expressed to a lesser degree in both ant and agar samples by *P. octospinosus* (Figure 2.16). This cluster was denoted as “other” by antiSMASH, however it includes a 1380 bp gene that has a high percentage homology to proteins involved in NRPS biosynthesis (Holmes et al 2016). The clusters K and M (Table 2.8), which are also predicted to encode NRPS products, were also expressed at a low level in samples (Figure 2.16). This is in addition to cluster G (Table 2.8) which encodes an unknown product but contains two genes that are homologous to a putative phenol 2-monoxygenase (involved in aromatic compound degradation) and another gene that is homologous to those involved in NRPS biosynthesis. There is quite a lot of variability in the expression of these clusters on agar plates by *P. octospinosus*, as one replicate tended to have a lower numbers of reads per BGC than the other two replicates. Cluster I (Table 2.8), which encodes an NRPS, had very low levels of expression in both sets of samples (Figure 2.16).

For BGCs that are unique to *P. echinatifior* (Table 2.8) the most highly expressed cluster on both laterocervical plates and on agar medium, was predicted to encode a bacteriocin (cluster P, Figure 2.16). As with the bacteriocin encoded by cluster J in the genome of *P. octospinosus*, cluster P contains a gene encoding a peptide with a high percentage homology to the bacteriocin linocin M18, however this only has 78% identity to the same gene in *P. octospinosus* and had different surrounding genes suggesting a different compound may be produced (Holmes et al 2016). Although, as mentioned, it is not possible to be conclusive about quantitative differences, cluster P appeared to be more highly expressed on the ant than on agar medium. The remaining clusters that were unique to *P. echinatifior* were all expressed at much lower levels

(Figure 2.16). These include clusters predicted to encode a terpene (cluster Q), a further bacteriocin peptide (cluster R), a T1PKS-NRPS (cluster O) and a cluster denoted as “other” (cluster N) but that may encode an NRPS.

2.4.2.6 Carbon metabolism on the surface of the ant

In order to identify metabolic pathways that were highly expressed by *Pseudonocardia* mutualists on the ant cuticle and that may potentially be involved in the utilisation of ant-derived resources, a closer examination of genes classified to be involved in carbohydrate metabolism (by KEGG) was undertaken. This revealed that genes involved in propanoate metabolism were very highly expressed on the ant surface. In particular, a gene cluster encoding a multicomponent propane monooxygenase (PrmABCD) contained the most highly expressed carbohydrate metabolism genes on the surface of the ant, for both *P. echinator* and *P. octospinosus* samples (Figure 2.17). Not only were they highly expressed in the category of carbohydrate metabolism genes, but they were also amongst the most highly expressed genes in the total dataset of all *Pseudonocardia* genes expressed on the ant; for *P. octospinosus*, *prmA* was the third most highly expressed gene overall (the most highly expressed genes encoded two ribosomal proteins, RPL28 and RPL36) and *prmB*, *C* and *D* were the thirteenth, nineteenth and twenty-ninth most expressed genes in the dataset, respectively. For *P. echinator*, *prmA* was the most highly expressed gene in the entire dataset and *prmB*, *C* and *D* were fourth, sixth and fifth, respectively. Interestingly, the *prmABCD* gene cluster was also expressed on plates for both *P. octospinosus* and *P. echinator*, although did not rank as highly compared to the expression of other genes (Figure 2.17).

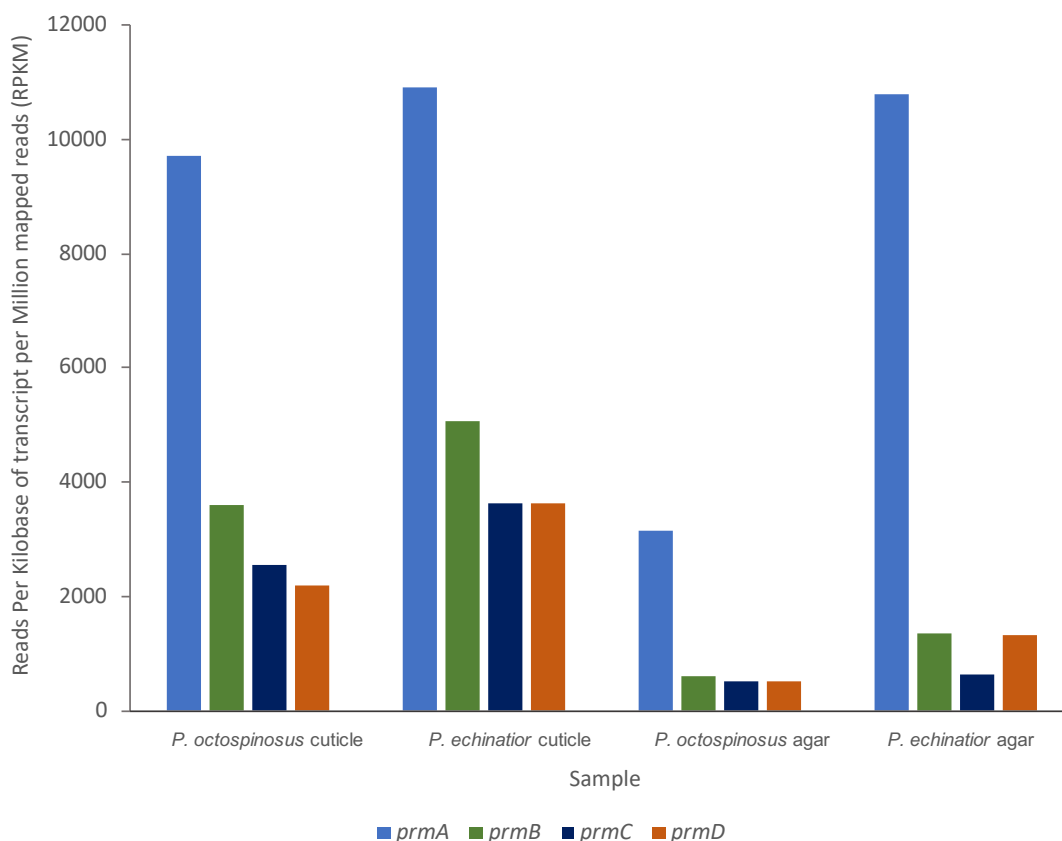


Figure 2.17 Expression of the gene cluster *prmABCD* by *P. octospinosus* (strain PS088) and *P. echinator* (strain PS1083), on the ant cuticle and on agar medium, respectively. Expression is shown as reads per kilobase of transcript per million mapped reads.

The gene cluster *prmABCD* encodes a soluble dinuclear-iron-containing monooxygenase capable of converting propane to 2-propanol via a terminal, or sub-terminal, oxidation reaction (Kotani et al 2003, Kotani et al 2006). The cluster encodes three main components (Figure 2.18) whereby *prmA* and *prmC* encode the large and small sub-unit, respectively, of a hydroxylase enzyme, *prmB* encodes an NADH-dependent acceptor oxidoreductase, and *prmD* encodes a coupling protein (Kotani et al 2003). The *prmABCD* cluster was first identified in the species *Gordonia* TY-5 which is capable of using propane as a sole carbon and energy source, in addition to several other liquid n-alkanes with C₁₃-C₂₂ carbon chains (Kotani et al 2003). Genes with significant homology to the *prmABCD* cluster encoded by *Gordonia* TY-5 have also been found in other actinobacterial species, including *Mycobacterium* TY-6 and *Pseudonocardia* TY-7, both of which can also grow on propane and a range of other long chain alkanes (Kotani et al 2006).

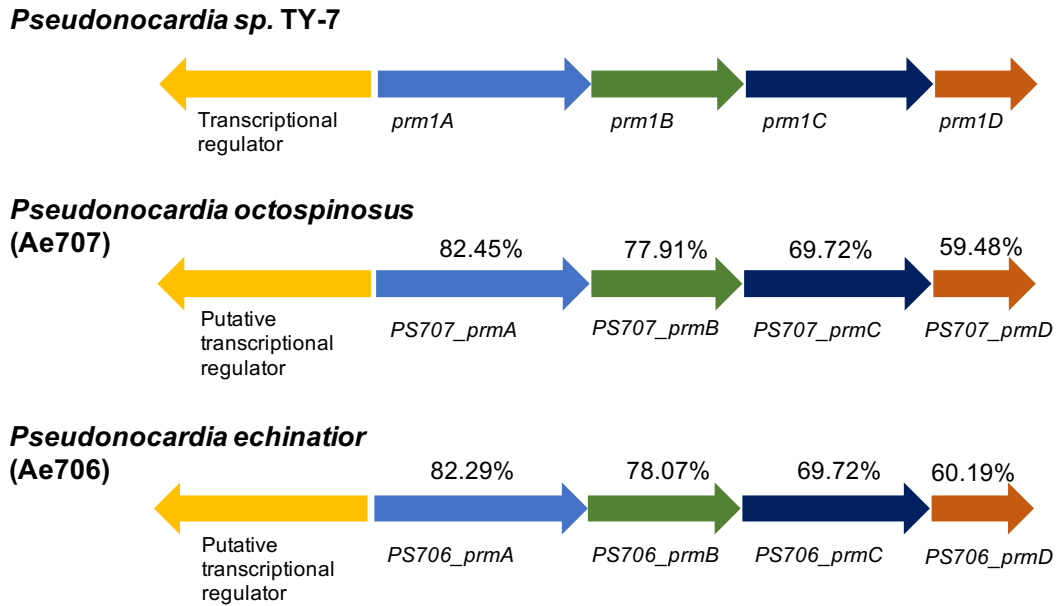


Figure 2.18 The genetic architecture of the *prmABCD* gene cluster identified in both the *P. octospinosus* (Ae707) and *P. echinaior* (Ae706) genomes. These are both compared to the published gene cluster found in *Pseudonocardia* sp. TY-7 (top). Percentages above the genes in *P. octospinosus* and *P. echinaior* clusters, represent the percentage identity of that gene to the equivalent gene found in *Pseudonocardia* sp. TY-7, as determined using BLASTn.

Phylogenetic analysis, using the amino acid sequences of published *prmA* genes as well as several other alkane monooxygenase genes, demonstrated that the PrmA amino acid sequences encoded by the five different *Pseudonocardia octospinosus* and *Pseudonocardia echinaior* mutualists (all sequenced by Holmes et al 2016 and including Ae707 and Ae706), formed their own clade, but were most closely related to the PrmA protein encoded by *Pseudonocardia* sp. TY-7 (**Error! Reference source not found.**). *Pseudonocardia* TY-7 formed a clade with *Mycobacterium* TY-6 and *Gordonia* TY-5 (**Error! Reference source not found.**). Amino acid sequences of the PrmA, B, C and D proteins in Ae707 (*P. octospinosus*) showed 82.29%, 78.07%, 69.72% and 59.41% identity to the Prm1ABCD proteins in *Pseudonocardia* TY-7 respectively, although PrmD had a lower alignment score (<200) than the other proteins (Figure 2.18). The amino acid sequences in Ae706 also had very similar percentage identities (Figure

2.18) A closer examination of sequences flanking the *prmABCD* cluster in the genomes of Ae707 and Ae706 revealed a putative Fis transcriptional regulator directly upstream of the cluster and a molecular chaperone (GroEl) directly downstream of the cluster (Figure 2.18). It was not possible to compare the regulatory genes with the one encoded by *Pseudonocardia* TY-7 as the amino acid sequence was not publicly available.

An investigation of other highly expressed carbohydrate metabolism genes revealed that a gene encoding an NAD⁺ dependent secondary alcohol dehydrogenase was also highly expressed on the ant cuticle (6th and 2nd most highly expressed carbohydrate metabolism genes by *P. octospinosus* and *P. echinaior*, respectively on the ant cuticle). This gene has significant homology to the *adh1* gene encoded by *Gordonia* TY-5 (Ae707 57.73% identity, Ae706 72.43% identity) which is essential for the strain to convert 2-propanol to acetone during the degradation of propane. Genes involved in butanoate metabolism were also highly expressed, in addition to those involved in gluconeogenesis, glycolysis and the TCA cycle. Butanoate metabolism is involved in the degradation of fats and oils, but can also be an important precursor to secondary metabolite biosynthesis.

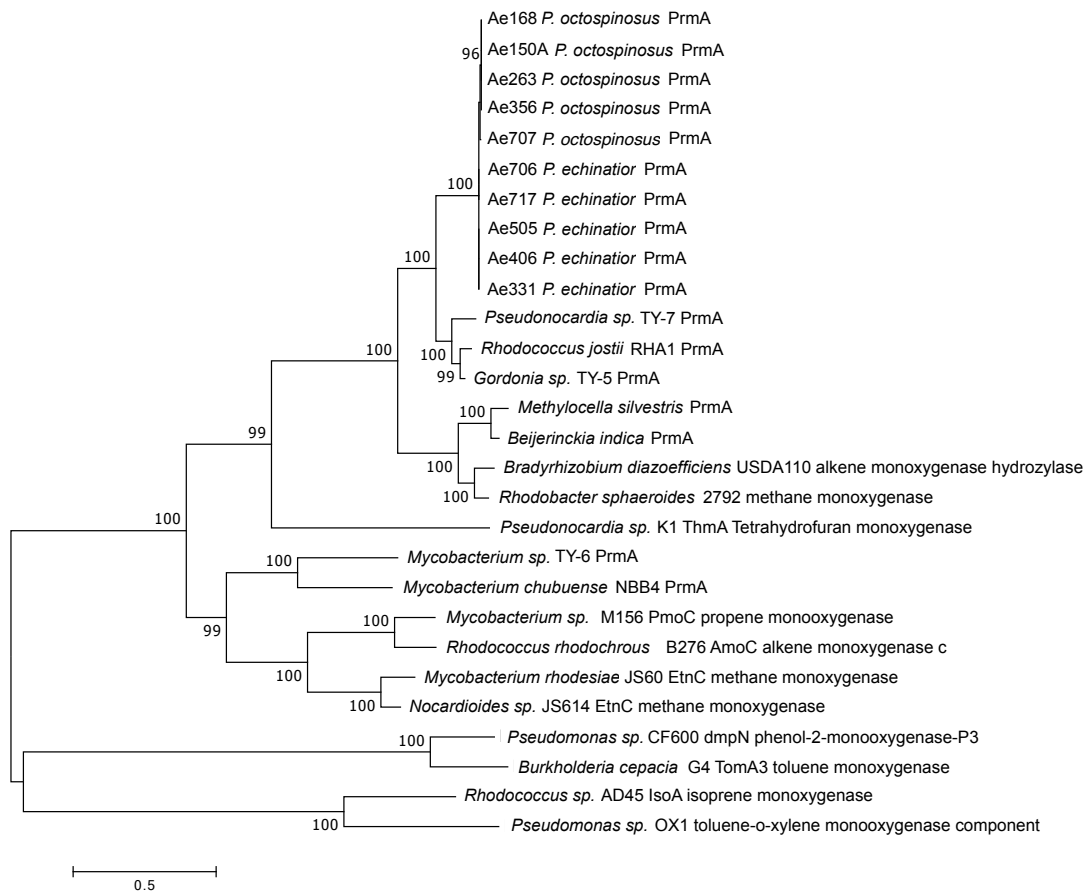


Figure 2.19 Phylogenetic analysis of the PrmA protein encoded by *Pseudonocardia octospinosus* and *Pseudonocardia echinator* isolates. Amino acid sequences were aligned to published PrmA amino acid sequences, as well as to sequences encoding other alkane monooxygenases. The tree was constructed using a Maximum Likelihood method. Values on branches represent Bootstrap values. The scale bar represents amino acid substitutions per site.

2.5 Discussion

This chapter set out to test some of the key assumptions of the screening model for microbiome formation in leafcutter ants. One of the expectations of the model is that a high level of nutrients is being transferred between the ant host and its cuticular microbiome, in order to make antibiotic production affordable, and to set up a highly competitive environment in which bacteria produce antibiotics in the fight for resources (Archetti et al 2011, Scheuring and Yu 2012).

RNA stable isotope probing experiments strongly suggested that ants were transferring a carbon-based resource to their cuticular microbiome. This was evidenced by the fact that RNA derived from cuticular actinobacterial genera, shifted to higher buoyant densities under the ^{13}C treatment after ultracentrifugation, suggesting metabolism of the heavy isotope. Labelled metabolites are assumed to have come via the ant host, rather than directly from the ^{13}C glucose water, since ants supplied with a fluorescently labelled glucose diet did not appear to spread the solution onto their laterocervical plates. Additionally, preliminary IRMS experiments suggested that surface-washed ants were capable of internalising a significant amount of the ^{13}C obtained from their glucose diet; this quantity would have further increased in the SIP feeding experiments as the glucose was increased from 5% (in IRMS measurements) to 20% in the diet used in SIP experiments. *Wolbachia* RNA also showed buoyant density shifts under the ^{13}C treatment. *Wolbachia* are vertically-transmitted intracellular parasites that occur within the tissues of many insect species, and can be found in high abundance in the thoracic muscles of *Acromyrmex* leafcutter ants (Andersen et al 2012). Since it was impossible to remove all thoracic tissue from the underside of laterocervical plates before extracting RNA, it is likely that *Wolbachia* occur in samples as a by-product of the dissection process. However, the fact that they are heavily labelled with ^{13}C is further evidence that resources were being internalised and processed by the ants, since *Wolbachia* do not exist on the external surface of the laterocervical plates (Andersen et al 2012).

Ant-derived resources appeared to be largely public since the RNA of many of the cuticular actinobacterial genera demonstrated buoyant density shifts under the ^{13}C diet. This included bacteria such as *Streptomyces*, which are thought to be horizontally acquired. Additionally, none of the genera present on the laterocervical plates dominated the heaviest of the fractions from the ^{13}C treatment, suggesting that the resources were not privately available, for example to the vertically-transmitted *Pseudonocardia* strain. This is consistent with the screening model for microbiome recruitment; publicly available host resources are predicted to set up a competitive environment on the cuticle and drive interference competition between species (Archetti et al 2011, Scheuring and Yu 2012).

Given more time and resources, an additional way to confirm and track the transfer of ^{13}C labelled resources from the gland-associated crypts on the ant, to the microbial groups that metabolise them, would be to employ a high resolution secondary ion mass spectrometry imaging (NanoSIMS) approach, combined with fluorescent *in situ* hybridisation (FISH), to directly visualise the assimilation of stable isotopes by different bacterial groups (Musat et al 2016). This technique is very sensitive to changes in molecular mass and has been used previously to track the bacterial metabolism of compounds labelled with heavy isotopes secreted by the mouse intestinal mucosa (Berry et al 2013). In the study, NanoSIMS was used to track a stable isotope label from the mouse cecum to the gut lumen, after which phylogenetically distinct FISH probes were used to determine the relative isotopic content of individual cells belonging to different bacterial families (Berry et al 2013). This technique has also been used to study the level and locality of carbon and nitrogen fixation by symbionts in a variety of systems, including termites and cockroaches (Musat et al 2016).

Although the ^{13}C RNA SIP experiment confirmed that resources secreted by ants were carbon-based, it did not allow further identification of the substrate being used by cuticular bacteria. Therefore, the results from total RNA sequencing of laterocervical plate samples were probed to identify metabolic pathways that were highly expressed by *Pseudonocardia* on the ant surface. Surprisingly, genes involved in propane degradation were very highly expressed by both *P. echinator* and *P. octospinosus* on the laterocervical plates. This included a gene cluster with significant homology to *prmABCD*, which encodes a soluble dinuclear-iron-containing monooxygenase known to be capable of converting propane to 2-propanol (Kotani et al 2003, Kotani et al 2006), as well as an NAD⁺ dependent secondary alcohol dehydrogenase similar to that used to convert 2-propanol to acetone (Kotani et al 2003).

It is uncertain why the *prmabcd* cluster and associated genes should be so highly expressed on the ant surface. The cluster was also expressed to a lesser degree on GYM agar plates suggesting that it may, to some extent, be constitutively active. It is possible that the expression of propane degradation genes is not part of an adaptation to living on the ant host. A recent phylogenetic analysis of all known *Pseudonocardia*

strains, found that environmental isolates of *Pseudonocardia* (from soil and plants), frequently appeared within clades containing attine-associated strains, and in some cases were almost identical at the sequence level (Mueller et al 2008, Mueller et al 2010). This finding suggests that *Pseudonocardia* strains may be frequently acquired and switched from the soil environment, which contradicts a model of strict vertical transmission and coevolution with the ant host (Mueller et al 2010). In soil environments, traits such as propane degradation could be highly adaptive and may not have been lost in strains that have only recently become associated with the ant cuticle.

However, since the oxidation of alkanes and the production of associated proteins is relatively costly (Timmis 2010), one might expect that this gene cluster would be down-regulated on the ant if gene products were not being actively used. Instead, the genes are amongst the most highly expressed on the ant laterocervical plates. An alternative hypothesis is that the gene cluster is being used to degrade a substrate present on the ant surface. Although the amino acid sequences of the PrmABCD proteins showed significant identity to those encoded by strains that oxidise propane, the coupling protein and the small sub-unit of the hydroxylase enzyme showed less than 60% and 70% identity, respectively. It is possible that the ant-associated strains have a different substrate specificity to that of propane oxidisers, given that *Acromyrmex* ants have not been documented to produce propane. Ants secrete a wide-range of long-chain hydrocarbons onto their epicuticle and several insect pathogenic fungi have evolved to degrade these molecules through the use of alkane monooxygenases called P450 enzymes (Martin and Drijfhout 2009, Pedrini et al 2013). Similar to propane monooxygenases, these degrade alkanes through terminal oxidation, before further oxidation of the resulting alcohol and alkane products, and entry of fatty acids to the beta-oxidation pathway (Pedrini et al 2013). It is possible that *Pseudonocardia* also make use of cuticular hydrocarbons, although extensive experimentation, including testing the use of different long-chain hydrocarbons as sole energy and carbon sources, qRT-PCR of the *prmABCD* gene cluster on the different substrates, and characterisation of the proteins involved, would be needed to support this hypothesis.

There are several additional emerging techniques that could be applied in order to help identify the host-derived substrates being supplied to the cuticular microbiome. This includes coupling SIP and NanoSIMS-FISH techniques (discussed above), with visualisation techniques such as Raman microspectroscopy (Wang et al 2016). The latter technology creates a chemical fingerprint of a molecule or system, and can be used to identify compounds that have incorporated heavy isotopes, since labelled compounds undergo a specific spectral shift (Wang et al 2016). Techniques such as matrix-assisted laser desorption/ionisation time-of-flight (MALDI-TOF) imaging mass spectrometry could also be applied in a similar way and have been used previously to image the distribution of an antifungal compound over the surface of *A. echinator* ants (Schoenian et al 2011).

In addition to nutrients provision, the screening model also predicts that a competitive environment on the ant cuticle should promote the production of antimicrobials by cuticular microbes, thus indirectly resulting in host protection (Scheuring and Yu 2012). The recruitment of antibiotic-producing bacteria is additionally primed by the presence of the vertically-transmitted *Pseudonocardia* bacteria, which take up niche space at the outset of microbiome formation and which also produce antibiotics (Scheuring and Yu 2012). Thus, other bacteria must also produce antibiotics (and resist *Pseudonocardia*-produced antibiotics) to be competitive in the ant niche (Scheuring and Yu 2012).

RNA sequencing experiments demonstrated that the most highly expressed biosynthetic gene clusters by both *P. octospinosus* and *P. echinator* were those involved in coping with stressful environmental conditions. For example, both ectoine and carotenoid terpene molecules were highly expressed by both species, *in situ* on the ant and *in vitro* on agar medium. The ant cuticle is likely to be a relatively harsh environment for bacterial growth (Kaltenpoth 2009), particularly as the epicuticle is extremely hydrophobic (Pedrini et al 2013), meaning that the risk of desiccation may be high. Additionally, bacterial growth occurs very densely on the laterocervical plates of the propleura which may also lead to osmotic stress. This is also likely to have been the case on the agar plates since bacteria were growing in dense, confluent lawns. The production of terpene molecules may additionally help to protect against superoxide

antimicrobials that might be produced during interspecific competition (Gershenson and Dudareva 2007).

Interestingly, the biosynthetic gene cluster predicted to encode the antifungal compound nystatin was barely expressed in samples taken from laterocervical plates or from bacteria growing on agar for both *Pseudonocardia* species. This is surprising, particularly for agar samples, since strong antifungal activity was demonstrated against *E. weberi* on the same type of agar medium. This suggests that the nystatin cluster is tightly regulated and may only be switched on in the presence of a pathogen, or competitor cues. Microbial co-culture is a well-established technique to turn on cryptic natural product gene clusters (Bertrand et al 2014, Scherlach and Hertweck 2009, van der Meij et al 2017) and since RNA samples were taken from confluent lawns of *Pseudonocardia* on plates (albeit at the same growth stage as those used in bioassays) fungal cues were absent under this scenario. In the ant system, individuals were sampled from healthy colonies that had no obvious signs of *Escovopsis* infection. Therefore, here too, the necessary chemical cues to induce antifungal production may have been absent. In addition, RNA was sampled from mature worker ants that spend more of their time outside of the fungal garden, where antifungal production may be less important. It would be interesting to see if the nystatin cluster was upregulated in younger (“callow”) worker ants that spend the majority of their time within the nest and thus in contact with the fungal cultivar.

However, it is also possible that the nystatin cluster may not be fully functional. In a comparison of *P. echinator* and *P. octospinosus* BGCs, Holmes et al (2016) noted that the nystatin cluster was often disparately arranged; genes were located in two separate regions and in some cases were missing PKS modules. This was the case for almost all *P. octospinosus* isolates and also one isolate of *P. echinator*. A disparity in the genetic arrangements of BGCs has been reported for several other symbiotic bacteria, and can suggest the acquisition of sub-clusters and chemical diversity via horizontal gene transfer (Lopera et al 2017, Miller et al 2017). For example, a group of natural products called gerumycins, isolated from the symbionts of *Apterostigma* and *Trachymyrmex* ants (Sit et al 2015) are arranged such that parts of the cluster are found on plasmids or separate genomic islands in some strains, although all produce

the same end compound (Sit et al 2015). However, another possible cause of fragmentation is that the nystatin cluster is in the process of degrading; fragmentation of BGCs may represent a loss of selective pressure, perhaps due to another, more effective, antifungal compound taking precedence, or because of an increased importance of ant prophylactic behaviours and antimicrobial secretions. This could in turn lead to a weakening of protein function and eventual loss over time (Lopera et al 2017).

In comparison to nystatin, two bacteriocins were the most highly expressed unique BGCs in both *P. octospinosus* and *P. echinator*. They also both appeared to be more highly expressed in the ant cuticle samples relative to samples from agar plates, although further replicates and controls would be needed to confirm this. Bacteriocins are thought to play a major role in mediating interference competition between species, by acting as antimicrobials and quorum sensing inhibitors, particularly under stressful conditions such as nutrient depletion and overcrowding both of which may be present on the ant cuticle (Chikindas et al 2018, Riley and Gordon 1999). The presence of bacteriocins on the ant laterocervical plate is consistent with the screening model, since bacteria are predicted to produce antimicrobials as a by-product of competition for the resources provided in this region of the ant, in an otherwise nutrient-limited niche (Scheuring and Yu 2012). In the future, techniques such as imaging mass spectrometry (Esquenazi et al 2008, Watrous et al 2011, Watrous and Dorrestein 2011) may yield further information about the distribution of antimicrobial compounds over the ant cuticle.

In conclusion, experiments in Chapter 2 show that *A. echinator* leafcutter ants do secrete a public, carbon-based substrate to feed their cuticular microbiome and that the vertically transmitted bacterial mutualist strains express antibacterial biosynthetic gene clusters that encode molecules such as terpenes and bacteriocins, both *in vitro* and *in vivo* on the ant cuticle. Such compounds may enable them to compete for the host-derived resources *in vivo* and potentially suppress bacterial infections. Genes encoding other natural products that provide protection against osmotic pressures and the antimicrobials of other strains are also expressed by the *Pseudonocardia* mutualist. However, it appears that antifungal compounds, if functional, may be more tightly

regulated. An extension of the experiments in this chapter to ants that are in constant contact with the fungal garden or that have been exposed to an *Escovopsis weberi* infection, may yield greater insight into the cues that regulate the expression of antifungal biosynthetic gene clusters.

Chapter 3 **Characterisation of *Streptomyces* species isolated from the roots of *Arabidopsis thaliana* plants**

3.1 Introduction

3.1.1 The plant root microbiome

The vast majority of eukaryotes, including plants, interact extensively with a diverse community of microorganisms. In plants, interactions particularly emerge at the interface between the plant roots and the soil environment, whereby bacteria from the soil abundantly colonise the soil layer, known as the “rhizosphere”, that is immediately surrounding and influenced by the plant root system (Berg et al 2014, Gaiero et al 2013, Hiltner 1904, Philippot et al 2013). Many microbial species are also capable of attaching to the root surface (a region called “the rhizoplane”) and a smaller subset of the soil community can additionally enter the plant root tissue (Berg and Smalla 2009, Berg et al 2014, Gaiero et al 2013). The latter group of microorganisms are adapted to survive within the inter or intracellular spaces within the plant roots, which are collectively known as the “endophytic compartment” (Berg and Smalla 2009, Berg et al 2014, Gaiero et al 2013).

Advances in next generation sequencing have enabled the characterisation of plant root microbiomes and have demonstrated that several factors may influence the composition of the rhizosphere and endophytic microbial communities. This includes abiotic factors such as geography, climate and soil characteristics, which ultimately define the microbial composition of the soil community and therefore the species that are available as an inoculum to the plant host (Berg and Smalla 2009, Bulgarelli et al 2012, Gaiero et al 2013). However, in addition, plant host genotype has also been shown to have a profound influence on the root microbiome, such that different plant species, as well as different cultivars or mutant lines of the same plant species, are associated with different microbial communities (Bressan et al 2009, Bulgarelli et al 2012, Bulgarelli et al 2015, Haichar et al 2008, Lundberg et al 2012). Conversely, individuals of the same plant species often appear to recruit the same broad microbial taxa to their root microbiomes, regardless of host environment, suggesting that plant mechanisms exist that enable the selection of a subset of the soil community (Gaiero

et al 2013). For example, two separate studies of the *Arabidopsis thaliana* root microbiome demonstrated that both the rhizosphere and root compartment were consistently dominated by Proteobacteria and Actinobacteria, and that particular bacterial families were driving the enrichment of these phyla in the endosphere (Bulgarelli et al 2012, Lundberg et al 2012). The enrichment of Actinobacteria was predominantly driven by the presence of the family Streptomycetaceae (Bulgarelli et al 2012, Lundberg et al 2012). These patterns emerged despite different soil types, isolation and sequencing techniques being used in the two different studies, suggesting the presence of a core *Arabidopsis* microbiome (Bulgarelli et al 2012, Lundberg et al 2012). Several factors, such as the specific root architecture of different plant genotypes, as well differences in the composition of root exudates (which can serve as a nutrients source, or inhibit particular bacterial strains), are thought to contribute to the specific recruitment seen within a plant species and drive the variation in microbiome composition between species (Badri and Vivanco 2009, Haichar et al 2008, Philippot et al 2013).

3.1.2 *Streptomyces* in the plant root microbiome

The genus *Streptomyces* has been shown to be consistently enriched in the root microbiomes of a variety of different plant species. This includes different ecotypes of *Arabidopsis thaliana* (Bodenhausen et al 2013, Bulgarelli et al 2012, Lundberg et al 2012), as well as important crop species such as potatoes (Weinert et al 2011), rice (Edwards et al 2015), wheat (Liu et al 2017b) and oilseed rape (Haichar et al 2008). The consistent enrichment of this genus suggests that host plants may be selecting streptomycetes due to particular host beneficial traits and/or that *Streptomyces* species are more competitive than other taxa when colonising the plant root microbiome.

Several traits are required for microorganisms to be able to colonise the rhizosphere and plant root microbiome. Firstly, microbes are required to be able to move or grow chemotactically towards the rhizosphere and the root surface (Liu et al 2017a). Here, they must be able to survive in the presence of antimicrobials secreted by the plant roots and also successfully outcompete other microbial species for carbon-rich resources, for example by producing antagonistic compounds, or via a rapid growth

rate (Gaiero et al 2013, Liu et al 2017a). In order to become endophytic, strains must also have mechanisms to invade and survive within the plant root tissue and simultaneously evade or resist the plant immune system (Gaiero et al 2013, Liu et al 2017a).

The evolution of the first true streptomycetes occurred approximately 450 million years ago and is thought to have been largely stimulated by the transition of plants onto land, approximately 550 million years ago (Chater 2006). The emergence of land plants is thought to have driven the evolution of saprotrophic organisms that could break down plant material and thus, make use of the nutrients locked away in complex molecules such as cellulose and xylan (Chater 2006, Strobel 2003). This may have additionally driven the evolution of mycelial organisms like *Streptomyces* species, since filamentous growth could allow attachment and penetration into living or dead plant material (Chater 2006). Some of these organisms are likely to have evolved an endophytic lifestyle whereby they could invade and reside within the intra or intercellular spaces within plant tissue, which in some cases could have resulted in the evolution of plant-microbe mutualisms (Strobel 2003).

A combination of eGFP tagging, confocal laser scanning microscopy (CLSM) and scanning electron microscopy (SEM) enable the visualisation of interactions between *Streptomyces* and plant roots (Chen et al 2016, Coombs and Franco 2003, Korttemaa et al 1997, Tokala et al 2002, van der Meij et al 2018). For example, the strain *S. lydicus* WYEC 108, which is the bioactive ingredient of the commercial biofungicide Actinovate®, appears to colonise the inner surface layers of nodules on the roots of pea plants (*Pisum sativum*) and exists here as both mycelia and spore chains (Tokala et al 2002). *Streptomyces* species have also been shown to colonise the embryo and endosperm of germinating wheat seeds, when inoculated as a spore preparation onto the seed surface (Coombs and Franco 2003). The exact mode of entry of *Streptomyces* into roots is still uncertain, although it is thought that their filamentous growth may facilitate access into sites of wounding, as well as via openings at the base of root hairs and lateral roots, which in the latter case span the outer layers of the root tissue giving access to the plant root cortex and vascular tissue (Liu et al 2017a, Seipke et al 2012b). In support of this, two *Streptomyces* isolates that were able to colonise both the

rhizoplane and the root cortex of lettuce seedlings were found to be particularly prevalent on, or in close proximity to, root hairs and lateral roots (Chen et al 2016). *Streptomyces* are also capable of producing an array of cellulolytic and hydrolytic enzymes which may allow them to force entry into the plant, by breaking down the epidermal cell walls and middle lamellae between plant cells (Viaene et al 2016).

The abundance of *Streptomyces* in soil environments, their capability to subsist on low levels of a wide range of carbon sources, as well as their ability to produce a diverse array of antimicrobial secondary metabolites, may all contribute to their competitiveness in the plant root niche (Kaltenpoth 2009, Seipke et al 2012b). Thus, millions of years of coevolution with plants may explain why *Streptomyces* are often abundant in the rhizosphere and roots of different plant species, and may also have been a key factor in driving the evolution of many aspects of their growth and metabolism (Chater 2006).

3.1.3 The role of *Streptomyces* in plant protection

Streptomyces-plant interactions are gaining increasing interest due to the observation that *Streptomyces* can provide their plant host with protection against infection by parasites and pathogens. Perhaps some of the best known examples of microbe-mediated defense against soil-borne pathogens are disease suppressive soils, in which plants are protected from infection due to the antagonistic activities of microbial species found within the soil and rhizosphere community (Weller et al 2002). The mechanisms underpinning suppressive soils are not well understood however, Actinobacteria, and particularly *Streptomyces* species, are often enriched in these soils suggesting that they may contribute to antagonism against pathogens (Cha et al 2016, Chappelle et al 2016, Inderbitzin et al 2018, Kinkel et al 2012, Mendes et al 2011). For example, *Streptomyces* species are a major component of light-coloured *Sphagnum* peat in Finland, which is suppressive against a range of soil-borne pathogens, including *Rhizoctania solani* and *Fusarium spp.*, both of which infect a wide range of cereal and horticultural crop species (Tahvonen 1982, Weller et al 2002). *Streptomyces griseoviridis* was later isolated from this soil and used to formulate the broad-spectrum commercial biofungicide Mycostop® (Lahdenperä et al 1991).

Streptomyces species can inhibit phytopathogens through a variety of direct and indirect mechanisms. Directly, strains can inhibit the growth of pathogens via the production of antimicrobial compounds. On a few occasions, a combination of metagenomics, strain isolation, genome sequencing and genome mining, have enabled the isolation of bioactive species and their corresponding secondary metabolites. For example, the strain *Streptomyces* S4-7, isolated from a Korean soil that suppresses *Fusarium* wilt disease, was found to encode 35 biosynthetic gene clusters for producing putative antimicrobial agents (Cha et al 2016). A novel thiopeptide was purified and shown to have potent inhibitory activity against fungal cell wall biogenesis in *Fusarium*, suggesting natural products such as this may be contributing to the disease suppressive nature of the original soil (Cha et al 2016). Other studies have isolated *Streptomyces* species from a range of different environments that show bioactivity against both fungal and bacterial phytopathogens (Law et al 2017, Newitt et al 2019, Viaene et al 2016). Importantly, some of these strains have also been shown to be active *in vivo* under greenhouse or field conditions (e.g. Bonaldi et al 2015, Cao et al 2004, Chen et al 2016, Sarwar et al 2019, Wu et al 2019, Yuan and Crawford 1995).

In addition to soluble antimicrobials, many *Streptomyces* species are also prolific producers of Volatile Organic Compounds (VOCs) (Cordovez et al 2015). These are characteristically small compounds with low molecular weights and high vapour pressures, meaning that they can easily diffuse through water and gas-filled pores in soil (Mendes et al 2013, Wheatley 2002). VOCs have a diverse range of functions *in vitro*, including antimicrobial activity against phytopathogens (Chapelle et al 2016, Cordovez et al 2015, Mendes et al 2011, Wan et al 2008, Wang et al 2013a). *Streptomyces* species additionally encode an enormous variety of secreted enzymes that have a diverse range of extracellular activities including the direct inhibition of pathogens (Chater et al 2010). This includes the production of enzymes called chitinases, which degrade the biomolecule chitin, an abundant component of fungal cell walls (Chater et al 2010, Schrempf 2001). Chitinases isolated from *Streptomyces* species have been shown to inhibit a range of phytopathogenic fungi both *in vitro* and *in vivo*, including economically important genera such as *Fusarium*, *Pythium*,

Magnaporthe and *Rhizoctania* (Gomes et al 2000, Hoster et al 2005, Itoh et al 2003, Joo 2005, Mahadevan and Crawford 1997, Quecine et al 2008).

Streptomyces can also indirectly inhibit the growth of pathogens in the plant microbiome and surrounding soil. This can occur via competitive exclusion, whereby strains take-up niche space and resources, therefore preventing pathogens from colonising the plant root system (Archetti et al 2011, Viaene et al 2016). This is not mutually exclusive from direct antagonism since antimicrobials may be produced as a by-product of interference competition. However, endophytic *Streptomyces* strains can also provide host protection indirectly through the activation of host resistance pathways (Conn et al 2008, Kurth et al 2014, Lugtenberg and Kamilova 2009, Van Wees et al 2008, Viaene et al 2016). In this case, *Streptomyces* are recognized as mildly intrusive by the plant host, leading to the activation of phytohormone defense signaling pathways, including those involving jasmonic acid (JA), ethylene (ET) and salicylic acid (SA). Streptomycete colonisation also causes an upregulation of pathogenesis-related (PR) genes that are involved in systemic acquired resistance (SAR) and are normally activated by biotrophic pathogens (Conn et al 2008, Kurth et al 2014, Lugtenberg and Kamilova 2009). Activation of the plant immune system by microbes, such as *Streptomyces* species, is known as induced systemic resistance (ISR) and leads to an accelerated and elevated response to pathogenic attack (Kurth et al 2014, Lugtenberg and Kamilova 2009).

3.1.4 Potential applications of plant-protective *Streptomyces* species

The ability of *Streptomyces* isolates to protect plant hosts against infection through the production of potent antimicrobial agents, suggests that plant-associated *Streptomyces* strains may act as a substantial resource for unearthing novel antibacterial and antifungal compounds. These may be useful against human pathogens in the clinic, particularly as coevolutionary relationships between *Streptomyces*, plants and phytopathogens may yield secondary metabolites with novel structures and activities that could be used to target multi-drug resistant pathogenic species (Chevrette et al 2019, Seipke et al 2012b). Additionally, since only a handful of *Streptomyces* species (approximately 10 out over 500 characterised strains) are known to be phytopathogenic, but many colonise plant roots, there is strong potential to

develop the most protective strains as plant biocontrol agents (Seipke et al 2012b, Viaene et al 2016). These may act as a good alternative to environmentally damaging and toxic chemical pesticides, particularly as *Streptomyces* species are naturally abundant in soils. Additionally, as *Streptomyces* species are spore-formers, they can remain viable under unfavorable conditions for long periods of time and could be added as dried coatings to seeds (van der Meij et al 2017). This gives them an advantage over other genera that are typically investigated for their biocontrol capabilities, such as *Pseudomonas*, which have to be applied as live cultures and are far less tolerant to desiccation and long-term storage (Coombs et al 2004, O'Callaghan 2016). Indeed, several *Streptomyces* species are already marketed as biocontrol agents, for example *S. griseoviridis* K61 and *S. lydicus* WYEC 108, are the major bioactive components of the commercial biofungicides Mycostop® and Actinovate®, respectively (Lahdenperä et al 1991, Yuan and Crawford 1995). Additionally, several purified streptomycete metabolites, including polyoxin D, streptomycin and kasugamycin are marketed as sprays to eliminate foliar fungal pathogens (Rey and Dumas 2017).

3.1.5 Wheat take-all fungus

Despite *Streptomyces* species gathering increasing interest from a biocontrol point of view, there are still only a handful of studies investigating the potential of these strains to inhibit some of the most detrimental pathogens of economically important cereal crop species, for example wheat and rice. Wheat take-all disease is caused by the fungal pathogen *Gaeumannomyces graminis* var. *tritici*, and is regarded as one of the most important and economically damaging cereal crop pathogens worldwide (Cook 2003, Coombs et al 2004, Kwak and Weller 2013). The fungus can colonise the roots of several different species in the plant family Poaceae, including wheat, barley and rye, whereby infections lead to symptoms such as stunted growth, black lesions on roots and stems, nutrient deficiency, and eventual plant death (Cook 2003, Kwak and Weller 2013). The fungus can survive saprotrophically on dead plant material in soil, which serves as an inoculum for the next wheat crop (Cook 2003). *G. graminis* is a particularly problematic phytopathogen as it can survive under a wide range of precipitation regimes, temperatures and pH conditions (Kwak and Weller 2013). There are currently no wheat cultivars that are resistant to the pathogen, and chemical pesticides are

either very costly, inconsistent, or toxic to humans and the environment (Cook 2003, Kwak and Weller 2013). Presently, the disease is best managed by crop-rotation although this is not always economically viable (Cook 2003, Kwak and Weller 2013). Alternatively, farmers rely on the spontaneous emergence of a phenomenon known as take-all decline, whereby yields recover slightly after several years of monoculture (Cook 2003, Kwak and Weller 2013).

Take-all decline is primarily thought to have a microbial basis with several studies having identified an abundance of bioactive *Pseudomonas fluorescens* in take-all suppressive soils (Kwak and Weller 2013). However, *Pseudomonas* species only colonise the very early stages of wheat growth, before being out-competed by other bacterial species and they are also sensitive to desiccation, making them unsuitable for low precipitation environments (Coombs et al 2004). Only a handful of studies have investigated the potential for *Streptomyces* species to inhibit wheat take-all, however, these have isolated strains that demonstrate bioactivity both *in vitro* and *in vivo* (Chamberlain and Crawford 1999, Coombs et al 2004). For example, spores of a streptomycete strain isolated from healthy cereal crops, were shown to significantly reduce wheat infection in field soils infested with the take-all fungus; this may have been aided by the ability of these strains to colonise the endophytic compartment of wheat roots (Coombs and Franco 2003, Franco et al 2007). As mentioned above, *Streptomyces* species are both saprotrophic and spore-formers and therefore may be helpful in eliminating the take-all fungus that persists in soil between crop cycles. Additionally, they could also be used under low precipitation regimes and may be particularly advantageous because they are known to colonise the mature roots of cereal crops, making them a more persistent form of biocontrol and a possible alternative to *Pseudomonas* species (Coombs et al 2004, Newitt et al 2019, van der Meij et al 2017).

3.1.6 Plant growth promoting traits

In addition to bioactivity, *Streptomyces* species have also been noted for their plant-growth-promoting (PGP) effects, both in the model plant species *Arabidopsis thaliana* (Cordovez et al 2015, Lin and Xu 2013), but also in several crop species such as peas, tomatoes, wheat and rice (Anwar et al 2016, Gopalakrishnan et al 2014, Palaniyandi et

al 2014, Patel et al 2018, Yuan and Crawford 1995). *Streptomyces* strains that carry both plant-protective and PGP traits would make highly desirable plant biocontrol agents. The mechanisms underlying PGP are not always clear, however they are beginning to be established through the use of *in vitro* assays, metagenomic studies and the generation of bacterial mutants.

Several endophytic *Streptomyces* strains are known to produce phytohormones which can have a direct impact on plant growth. For example, numerous isolates have been shown to produce the compound auxin, or its precursor indole-3 acetic acid (IAA), which promotes the growth of primary roots, root hairs and lateral roots, increasing the host plant's access to growth-limiting nutrients (Anwar et al 2016, Gopalakrishnan et al 2014, Lin and Xu 2013, Manulis et al 1994). In addition to influencing root growth, *Streptomyces* strains can also increase access to limited nutrients through the solubilisation of phosphate and through the chelation of metal ions (Viaene et al 2016). Phosphorous is the second most important growth-limiting nutrient for plants after nitrogen; the vast majority of phosphorous is present as inorganic phosphate or organophosphate (soil phytate) in the environment, both of which are insoluble and unavailable for uptake by plant roots (Sharma et al 2013). Plant-growth-promoting bacteria can release phosphate from inorganic phosphate through the production of organic acids, which acidify soils. Similarly, organophosphate can be solubilised from organic matter in soil through the production of enzymes, such as non-specific acid phosphatases and phytases (Sharma et al 2013). Several *Streptomyces* strains have been identified that can solubilise phosphorous, particularly through the production of organic acids (Jog et al 2014). In addition, many strains produce siderophores which chelate metal ions, particularly iron, which can contribute to phosphate solubilisation, and additionally help to alleviate iron-deficiency in the plant host (Anwar et al 2016, Liu et al 2017a, Rungin et al 2012a, Sharma et al 2013).

Another trait that is known to be associated with PGP is the activity of the bacterially-encoded enzyme, 1-aminocyclopropane-1-carboxylate (ACC) deaminase (Glick 2014). This enzyme converts the compound ACC into ammonia and 2-oxobutanoate, which can be used as a source of nitrogen by many different bacterial species. ACC is also the precursor to the plant phytohormone ethylene which is involved in many plant

developmental processes, as well the plant stress response (Glick 2014). Reducing plant ethylene levels can increase plant growth by removing its inhibitory effect on root and shoot development (Shaharoon et al 2006). In addition, a high level of ACC deaminase activity can reduce plant stress under conditions such as drought or high salinity, by preventing the excessive production of ethylene, which might otherwise lead to the onset of senescence and leaf abscission (Glick 2014, Yang et al 2009). ACC deaminase-producing bacteria, including *Streptomyces* species, have been shown to enhance plant host tolerance to a wide variety of environmental stressors including flooding, drought, salinity and heavy metal pollution (Glick 2014, Palaniyandi et al 2014, Yang et al 2009).

3.2 Aims

Several *Streptomyces* isolates have been shown to encode traits that can result in PGP and stress-tolerance, and others have the ability to protect plants of interest against disease through the production of antimicrobials or activation of ISR. An ideal biocontrol agent would carry a combination of all of these traits. The current challenge is to identify the most useful strains, or combination of strains, but also to ensure that these isolates are effective and competitive under natural conditions. This will require extensive isolation and detailed characterisation of strains from various plant root systems and *in vivo* studies of their colonisation dynamics.

The aim of this chapter was to isolate a range of *Streptomyces* species from the *Arabidopsis thaliana* root microbiome and extensively characterise their potential to produce secondary metabolites against several pathogenic indicator species. Since there is also increasing interest in probing microbiomes for novel antimicrobial agents for the clinic, isolates were tested against a range of human pathogenic indicator strains, including clinical isolates of *Escherichia coli* and *Candida albicans*, as well as a multidrug resistant fungus, *Lomentospora prolificans*, currently associated with a 90% mortality rate in humans (Pellon et al 2018). Isolates were also tested for their ability to inhibit the growth of plant pathogens. Wheat take-all fungus was of particular interest, given that only a few studies have investigated the potential for *Streptomyces* to produce antifungals that inhibit this fungus, despite the economic importance of wheat crops worldwide. Since strains that can both protect plants and

promote plant growth are desirable, isolates were also characterised for their potential to enhance plant biomass. The characterisation of strains in this chapter enabled colonisation assays to be carried out in Chapter 5, to determine plant host factors that shape the acquisition of microbial species from their environment.

3.3 Materials and Methods

3.3.1 Plant growth and isolation of *Streptomyces* endophytes

Wild-type *A. thaliana* Col-0 seeds (Table 3.1) were sterilised by washing in 70% (v/v) ethanol for 2 minutes, 20% (v/v) sodium hypochlorite for 2 minutes, then five times in sterile water. Individual seeds were sown into pots of sieved Levington F2 seed and modular compost before being placed at 4°C for 24 hours. Seeds were then grown for 4 weeks under a photoperiod of 12 hours light/ 12 hours dark, at 22°C. Plants were then taken aseptically from pots and roots tapped firmly to remove as much adhering soil as possible. Root material was then placed into sterile, Silwett L-77 amended Phosphate Buffered Saline (PBS-S, Table 3.2) buffer for 30 minutes on a shaking platform. Roots were then placed into fresh PBS-S and washed for 30 minutes before any remaining soil particles were removed with sterile tweezers. Cleaned roots were transferred to 25 ml of fresh PBS-S and sonicated for 20 minutes in a sonicating water bath to remove any remaining material still attached to the root (as in Bulgarelli et al 2012). The roots were then crushed in sterile 10% (v/v) glycerol and serial dilutions were spread onto either soya flour mannitol (SFM) agar, starch casein agar, or minimal salts agar containing sodium citrate (Table 3.2). Plates were incubated at 30°C for up to 14 days. Colonies resembling streptomycetes were re-streaked onto SFM agar (Table 3.2). Their taxonomic identity was confirmed via amplification of the 16S rRNA gene using colony PCR with the universal primers PRM341F and MPRK806R (Table 3.3). PCR products were then ran on a 1% agarose gel with 5% ethidium bromide and bands of approximately 465 base pairs were excised and purified using the QIA quick gel extraction kit (QIAGEN), according to the manufacturers protocol. The PCR products were sequenced by Eurofins Genomics, Germany, and the resulting sequences were analysed using BLASTn. Confirmed *Streptomyces* strains (Table 3.1) were maintained on soya flour mannitol (SFM) agar (strains N1, N2, M2, M3 and *S. coelicolor* M145), maltose-yeast extract-malt extract (MYM) agar (strain L2), oatmeal agar (strain MG) or

ISP2 agar (*S. lydicus* strains). For media recipes see Table 3.2. Spore stocks were made as described previously (in Kieser et al 2000 and section 2.3.3.1).

Table 3.1 Species and strains used in plant microbiome experiments

Species/strain name	Description	Origin
<i>Streptomyces</i> L2	Wild-type	This study
<i>Streptomyces</i> M2	Wild-type	This study
<i>Streptomyces</i> M3	Wild-type	This study
<i>Streptomyces</i> N1	Wild-type	This study
<i>Streptomyces</i> N2	Wild-type	This study
<i>Streptomyces</i> MG	Wild-type	This study
<i>Streptomyces lydicus</i> ATCC25470	Wild-type	American Type Culture Collection
<i>Streptomyces lydicus</i> ATCC31975	Wild-type	American Type Culture Collection
<i>Streptomyces lydicus</i> Actinovate	Wild-type	Isolated from Actinovate™ by Elaine Patrick, UEA
<i>Streptomyces coelicolor</i> M145	Wild-type	John Innes Centre, Norwich, UK
<i>Bacillus subtilis</i>	Wild-type, strain 168	Gift from Nicola Stanley-Wall, University of Dundee
Methicillin resistant <i>Staphylococcus aureus</i>	Clinical isolate	Norfolk and Norwich University Hospital (UK)
<i>Escherichia coli</i> K12	Wild-type	Lab stock, UEA
<i>Pseudomonas syringae</i> DC3000	Wild-type	John Innes Centre, Norwich, UK
<i>Candida albicans</i>	Clinical isolate	Gift from Neil Gow, University of Exeter

<i>Lomentospora prolificans</i>	Environmental isolate	American Type Culture Collection
<i>Gaeumannomyces graminis</i> var. <i>tritici</i>	Environmental isolate	John Innes Centre, Norwich, UK
<i>Arabidopsis thaliana</i> Col-0	Wild-type, ecotype Col-0	Lab stock, UEA
<i>Triticum aestivum</i>	Wild-type, variety Paragon	John Innes Centre, Norwich, UK

Table 3.2 Growth media used for experiments involving plant-associated streptomycetes. All components were from Sigma Aldrich unless otherwise stated.

Media	Component	g L ⁻¹ dH ₂ O
Soya flour mannitol (SFM) agar (Kieser et al 2000)	Soy flour	20
	Mannitol	20
	Agar	20
Starch casein agar (Kuester and Williams 1964)	KNO ₃	2
	K ₂ HPO ₄	2
	MgSO ₄ ·7H ₂ O	0.05
	CaCO ₃	0.02
	FeSO ₄ ·7H ₂ O	0.01
	Casein	0.3
	NaCl	2
	Agar	18
Minimal salts (MS) medium with sodium citrate (Lebeis et al 2015)	Soluble starch	10
	NH ₄ SO ₄	2
	K ₂ HPO ₄	14
	KH ₂ PO ₄	6
	Sodium citrate	1
	MgSO ₄	0.2
Agar	15	

Maltose-yeast extract-malt extract (MYM) agar	Maltose	4
	Yeast Extract	4
	Malt Extract	10
	Agar	18
ISP2 Agar	Yeast Extract	4
	Maltose	10
	D-glucose	4
	Agar	20
Tryptone soy broth (TSB)	Tryptone Soy Broth (Oxoid)	30
Oatmeal agar	Ground oats	20
	Agar	20
Potato glucose agar (PGA)	PGA (Sigma Aldrich)	39
Lysogeny broth (LB)	Tryptone	10
	NaCl	10
	Yeast extract	5
	Glucose (only for growth of <i>P. syringae</i>)	1
Dworkins and Foster medium	(NH ₄) ₂ SO ₄	2
	KH ₂ PO ₄	4
	Na ₂ HPO ₄	6
	MgSO ₄ .7H ₂ O	0.2
	FeSO ₄ .H ₂ O	0.001
	H ₃ BO ₄	0.0001
	MnSO ₄	0.0001
	ZnSO ₄	0.0007
	CuSO ₄	0.0005
	MoO ₃	10
	Agar	20
2xYT	Bacto-tryptone	16
	Yeast extract	10
	NaCl	5
Murashige and Skoog (MSk) Agar	Murashige and Skoog salts (Duchefa Biochemie, Harlem, Netherlands)	4.43

	Sucrose	10 or 0
	Agar	8 or 15
Yeast Peptone Dextrose (YPD) Agar	Yeast Extract	10
	Bactopeptone	40
	Glucose	15
	Agar	15
Silwett L-77 amended	NaH ₂ PO ₄ .H ₂ O	6.33
Phosphate Buffered Saline (PBS-S)	Na ₂ HPO ₄ .H ₂ O	16.5
	200 µl Silwet L-77 added after autoclaving	

Table 3.3 Components and thermocycler conditions for amplification of the bacterial 16S rRNA gene using colony PCR.

Component	Volume (µl)
BioMix™ red (Bioline)	12.5
dH ₂ O	9
Forward primer, PRM341F 5'-CCTACGGGAGGCAGCAG-3' (Yu et al 2005)	0.5
Reverse primer, MPRK806R 5'-GGACTACHVGGGTWTCTAAT-3' (Yu et al 2005)	0.5
A single bacterial colony heated in 50% DMSO at 55°C for 45 minutes	2.5
PCR thermocycler reaction steps	
1. 95°C for 1 min	
2. 30 x cycles of 95°C for 15 secs; 55°C for 15 secs, 72°C for 15 secs	
3. 72°C for 2 mins	

3.3.2 Whole genome sequencing and analysis

3.3.2.1 DNA extraction for whole genome sequencing

For whole genome sequencing, DNA was extracted using an established “salting out” protocol (Kieser et al 2000). Briefly, spores of *Streptomyces* isolates were inoculated into flasks containing 50 ml of tryptone soy broth (TSB, Table 3.2) and sterile metal

springs. Cultures were incubated at 30°C, shaking at 180 rpm, for 5 days. Cell material was then pelleted by centrifuging at 4000 rpm for 10 minutes. Pellets were then resuspended in 10 ml of SET buffer (75 mM NaCl, 25 mM EDTA pH 8, 20 mM Tris-HCl pH 7.5) containing 1 mg ml⁻¹ of lysozyme, 40 µg ml⁻¹ achromopeptidase and 30 µg ml⁻¹ RNaseA, before incubating for 1 hour at 37°C. Proteinase K (0.5 mg ml⁻¹) and 600 µl of 1% sodium dodecyl sulfate (SDS) were then added to the solution, before incubating at 55°C for 2 hours. After incubation, 2 ml of 5 M NaCl was added, along with 5 ml of chloroform. The solution was then mixed continuously for 30 minutes, before centrifuging for 15 minutes at 4000 rpm. The top layer of supernatant was placed into a fresh tube on ice before adding a 0.6 volume of isopropanol and spooling the DNA onto a glass rod. After several minutes of spooling, the glass pipette was dipped into 6 ml of ice cold 70% ethanol before being air-dried. Once dry, 500 µl of sterile dH₂O was used to gently wash the DNA into a 1.5 ml microcentrifuge tube. DNA was left at 4°C overnight to resuspend, before being transferred to -20°C for storage. The quality of DNA was assessed using a nanodrop spectrophotometer and the DNA concentration was established using a Qubit™ fluorometer with the DNA broad sensitivity assay kit (Invitrogen™).

High quality genome sequences were obtained for newly-isolated *Streptomyces* strains N1, N2, M2, M3, and L2, as well as three strains of *Streptomyces lydicus*; one *S. lydicus* strain was isolated from the commercial plant growth-promoting product Actinovate® and two additional *S. lydicus* strains (ATCC25470 and ATCC31975) were obtained from the American Type Culture Collection (Table 3.1). Both the sequencing (using PacBio RSII sequencing technology) and genome assembly, were carried out at the Earlham Institute, Norwich, UK, (as described in Holmes et al 2018). All sequences were uploaded to GenBank upon receipt.

3.3.2.2 Analysis of whole genome sequences

The automated Multi-Locus Species Tree (autoMLST) server (Alanjary et al 2019) was used to phylogenetically classify the newly-isolated streptomycete strains L2, M2, M3, N1 and N2. Genomes were uploaded to the server, which performs a multi-locus sequence analysis against a curated genome database from NCBI, to produce high resolution species trees, as well as average nucleotide identity scores for isolates

compared to sequenced strains (Alanjary et al 2019). AutoMLST automates the process of gene selection for multi-locus comparison by screening for gene homologues using the tool HMMER and essential gene models (Alanjary et al 2019, Finn et al 2011). It also automates the process of finding reference genomes for tree assembly and the *de novo* construction of maximum-likelihood trees (Alanjary et al 2019). The antiSMASH 4.0 server (Blin et al 2017) was used to predict the presence of Biosynthetic Gene Clusters (BGCs) in genome sequences, and genomes were additionally annotated using RAST (Aziz et al 2008, Weber et al 2015). Amino acid sequences were uploaded to the KEGG Automatic Annotation Server (KAAS) for the functional annotation of genes and metabolic pathway mapping. KAAS assigns K numbers to genes via BLAST comparisons against a manually curated KEGG GENES database (Moriya et al 2007). K numbers then act as unique identifiers in the KEGG Orthology (KO) database which classifies genes by molecular function into pathway categories (Kanehisa et al 2016a).

3.3.3 Screening *Streptomyces* isolates for antifungal and antibacterial activity

3.3.3.1 Bioassays on agar plates

Streptomyces spores (4 µl of a 10⁶ spores ml⁻¹ stock) were pipetted onto the centre of agar plates and incubated at 30°C for 7 days, before adding pathogenic indicator strains. The indicator strains *Candida albicans*, *Bacillus subtilis*, a clinical isolate of Methicillin Resistant *Staphylococcus aureus* (MRSA), *Escherichia coli* and *Pseudomonas syringae* DC3000 (Table 3.1) were grown overnight in 10 ml of LB (Table 3.2). These were sub-cultured 1 in 20 (v/v) for a further 4 hours at 30°C. Cultures were then used to inoculate 100 ml of molten LB (0.5% agar), 3 ml of which was used to overlay agar plates with growing *Streptomyces* colonies. Plates were incubated for 48 hours at 30°C, and bioactivity was indicated by a clear halo around the *Streptomyces* colony. For bioassays using the fungal strains *Lomentospora prolificans* or *Gaeumannomyces graminis* (Table 3.1), *Streptomyces* species were grown for 7 days at which point a plug of the fungus (growing on potato glucose agar (Table 3.2) was placed at the edge of the agar plate. Plates were incubated at 25°C for up to 14 days to assess inhibition of fungal growth. Bioassays against *B. subtilis*, MRSA, *E. coli*, *P. syringae* and *C. albicans* were carried out on SFM, MS, ISP2, oatmeal and MYM agar for each *Streptomyces*

strain (Table 3.2). Bioassays against *L. prolificans* and *G. graminis* were carried out on PGA medium (Table 3.2).

3.3.3.2 *In vivo* bioassays against wheat take-all fungus

In order to assess whether the *Streptomyces* isolate N2 (Table 3.1), which exhibited particularly potent antifungal activity, could provide wheat plants with protection against *Gaeumannomyces graminis* (Table 3.1) infection *in vivo*, experiments were carried out using wheat seeds that were inoculated with the N2 strain. Seeds of *Triticum aestivum* (var. Paragon) (Table 3.1) were sterilized by placing them in 70% EtOH for 2 mins followed by 3% NaOCl for 10 minutes. Seeds were then rinsed five times in sterile dH₂O, before placing them into a solution of 10⁷ spores ml⁻¹ of the *Streptomyces* N2. Spores had been pregerminated in 2xYT (Table 3.2) at 50°C for 10 minutes. Seeds were incubated in the spore preparation (on a rotating shaker) for 2 hours, before being allowed to dry in a petri dish under sterile conditions. As a control, sterile seeds were incubated in 2xYT without spores.

In the first experiment, two incubated wheat seeds were placed onto a 10 cm square plate of Murashige and Skoog agar (1.5% (w/v) agar, 0% (w/v) sucrose; Table 3.2), on either side of a plug of the *G. graminis* fungus, which was placed in the centre of the agar plate. Plugs were taken from an actively growing plate of *G. graminis* on PGA agar (Table 3.2). There were three replicate plates of each treatment; N2-coated seeds, or sterile seeds as a control. Plates were incubated for 5 days at room temperature after which inhibition of *G. graminis* was indicated by a zone of clearing around the wheat seeds.

In the second experiment, 25 ml of sterile vermiculite (soaked in water over night, drained and then autoclaved) was placed into the bottom of a 50 ml falcon tube. Five plugs of *G. graminis*, actively growing on PGA (Table 3.2), or uninoculated PGA plugs as a control, were placed on top of this layer, before being covered with a further 10 ml of vermiculite. Five wheat seeds (soaked in either N2 spores or uninoculated 2xYT, as described above) were then placed on top of this vermiculite layer, before the addition of a further 10 ml of vermiculite. Falcons were then sealed with parafilm and incubated at 25°C for 3 weeks, under a 12 hour light/ 12 hour dark photoperiod. There

were five replicates falcons (each containing five replicate seeds) of each of the following combinations: PGA plugs with N2-coated seeds (wheat/*Streptomyces* control); *G. graminis* plugs with N2-coated seeds (wheat/*Streptomyces*/fungus treatment); PGA plugs with uninoculated seeds (wheat control); *G. graminis* plugs with uninoculated seeds (wheat/fungus treatment). After three weeks of incubation, plants were taken from falcons and adhering vermiculite was removed from the roots by rinsing thoroughly with water. Infection severity was scored on a scale of 0-8, using the infection scoring system defined in Figure 3.1. Differences in infection score between treatments were analysed in R 3.2.3 (R Core Team 2017), using a Kruskal-Wallis test, coupled with a post-hoc Dunn's multiple comparison test.

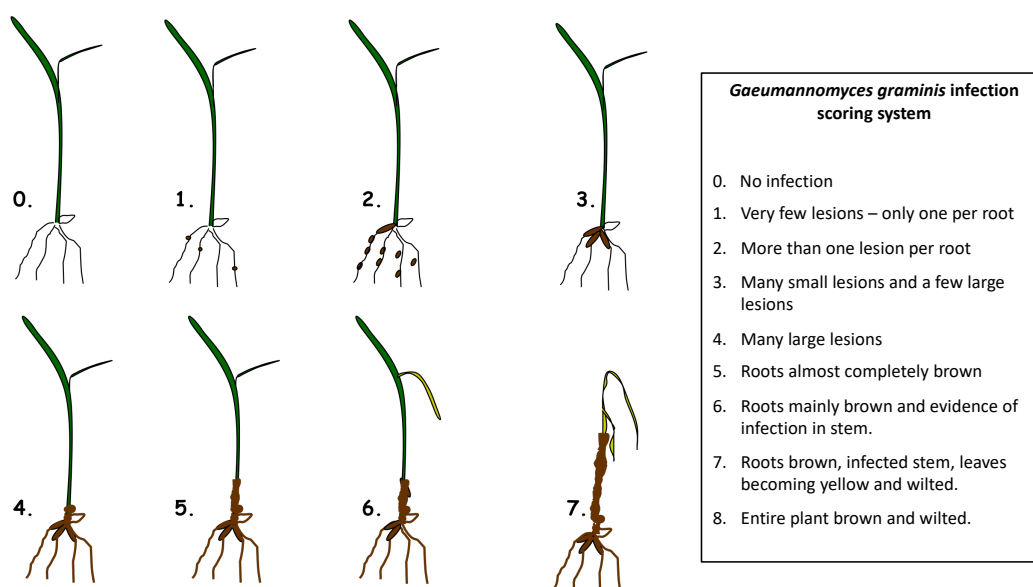


Figure 3.1 System for scoring wheat take-all (*G. graminis*) infection severity.

3.3.4 Characterisation of N2 antifungal compounds

3.3.4.1 Bioassays using filipin

Streptomyces isolate N2 (Table 3.1) contained a biosynthetic gene cluster in which 100% of genes showed significant sequence homology to a cluster encoding the potent antifungal compound filipin. To test whether filipin could be responsible for the strong antifungal effect of N2, bioassays were set up using a dilution series of a commercial

filipin standard. The standard was a filipin complex from *Streptomyces filipinensis* (Sigma Aldrich); this contains 8 isomeric components, with filipin III as the major component. The standard was dissolved in methanol and added to agar media, to generate concentrations of 0, 1, 2.5, 5 and 10 mg L⁻¹ of filipin, respectively. The fungal pathogens *Gaeumannomyces graminis*, *Lomentospora prolificans* and *Candida albicans* were then streaked onto three replicate plates of each concentration (PGA medium was used for *G. graminis* and *L. prolificans* assays, and LB agar was used for assays using *C. albicans*, Table 3.2). For both *G. graminis* and *L. prolificans*, plates were incubated at room temperature for 14 days, and for assays using *C. albicans*, plates were placed at 30°C for 3 days. Inhibition by filipin was indicated by an absence of growth on the agar plate.

3.3.4.2 Isolation of antimicrobial compounds from agar plates

Biochemical extractions were carried out in order to identify whether filipin was being produced by the streptomycete strain N2 (Table 3.1) on different types of agar media. N2 was grown as a confluent lawn on 6 plates each of SFM, ISP2 and oat agar (Table 3.2). Plates were incubated at 30°C for 10 days to allow for sporulation. Agar plates of each type of media were then sliced into small pieces using a sterile razor blade. The pieces from three of the plates of the same type of media were then pooled together, before being added to an equal volume (approximately 75 ml for 3 plates) of methanol. The remaining three plates for each media type were added to an equal volume of ethyl acetate (both methanol and ethyl acetate were HPLC grade, Sigma Aldrich). These mixtures were then left to stand for 2 hours, before filtering the solvent off into a glass vial (the remaining agar was discarded). The solvent was then removed under a vacuum, before re-dissolving the remaining crude solid in 1.5 ml of the same solvent used for the extraction (either methanol or ethyl acetate).

In order to confirm that the agar plate extractions had captured compounds with antimicrobial activity, disc-diffusion bioassays were set up against the fungal indicator strain *Candida albicans* and the Gram-negative bacterium *E. coli* (Table 3.1). Both strains were grown overnight in 10 ml of LB broth (Table 3.2) at 30°C and 200 rpm. Cultures were then diluted 1 in 20 (v/v) into 10 ml of LB and grown for another 4 hours. The 10 ml sub-culture was added to 50 ml of soft LB (0.5% agar), poured into 10

cm square plates and allowed to set. Meanwhile, 6 mm sterile filter paper discs (Whatman) were inoculated with 40 µl of each individual extract; this was either a methanol extract from N2 growing on oat, ISP2 or SFM agar plates, or an ethyl acetate extract from N2 growing on the same types of media. 40 µl of methanol or ethyl acetate were also added to one disc per plate as a solvent control. Additionally, 40 µl of nystatin (5 mg ml⁻¹) was added to discs as a positive control. Once dry, discs were placed onto plates, 3 cm apart. There were nine discs in total per plate; the 6 different extracts, 2 solvent controls and the nystatin positive control. Plates were then incubated at 30°C overnight. Inhibition of the indicator strain was evidenced by a zone of clearing around the disc.

3.3.4.3 Detection of the filipin complex using UPLC-MS and the purification of other compounds

In order to determine whether filipin could be detected in extracts that demonstrated antifungal activity, methanol extracts were compared to a commercial filipin standard (described in 3.3.4.1) using an ultra-performance liquid chromatographer-tandem mass spectrometer (UPLC-MS). UPLC-MS measurements were performed with guidance from Dr Sibyl Batey (John Innes Centre) according to a modified version of an established protocol (detailed in Heine et al 2018), using a Nexera X2 liquid chromatograph (LC-30AD) system (Shimadzu) connected to an autosampler (SIL-30AC), a Prominence column oven (CTO-20AC) and a Prominence photo diode array detector (SPD-M20A). The UPLC System was connected to a LCMS-IT-TOF Liquid Chromatograph mass spectrometer (Shimadzu). A Kinetex® 1.7 µm C18 100 Å, 100 × 2.1 mm column (Phenomenex) was used for chromatographic separation and the column oven temperature was set to 30°C. The mobile phase was a mixture of solvent A (0.1% formic acid in water) and solvent B (methanol). A gradient was run with the following ratios of solvent A and B: solvent A/B in a ratio of 50/50 (v/v) for the initial condition; hold at a 50/50 ratio for 1.0 min; run a linear gradient up to a 10/90 ratio within 3.0 mins, hold for 3.0 mins; linear gradient up to 0/100 within 1.0 min, hold for 1.00 min; linear gradient down to 100/0 within 0.5 min, hold at 0/100 for 1.0 min; returned to 50/50 within 0.5 min, hold at 50/50 for 3.0 mins. MS spectra were acquired within a mass range of m/z 200–1700. The following parameters were used for MS analysis: temperature of the curved desolvation line 250°C; temperature of the heat block

300°C; nebulizer gas flow 1.2 L min⁻¹; the collision-induced dissociation energy was set to 50%. The instrument was calibrated using sodium trifluoroacetate cluster ions according to the manufacturer's instructions. The commercial filipin standard was used for the analysis at a concentration of 1 mg ml⁻¹, as well as a 1 in 10 (v/v) dilution of the methanol extracts from SFM, oat and ISP2 agar plates. The assignment of filipin-like compounds from UPLC-MS data is based on comparisons to the standard as well as published masses and knowledge of the filipin cluster.

Further purification and the structural elucidation of compounds present in *Streptomyces* N2 extracts (grown on SFM agar, Table 3.2) was carried out by Johannes Rassbach at the John Innes Centre. Disc-diffusion bioassays were used to test purified extracts of fungichromin, 14-hydroxy(iso)chainin and actinomycin for bioactivity against both *C. albicans* and *E. coli*; these were carried out as described in 3.3.4.2. Purified compounds were also tested for their ability to inhibit the wheat take-all fungus *G. graminis* (Table 3.1), whereby sterile 6 mm filter discs (Whatman) were inoculated with 40 µl of each compound (in methanol). Discs were allowed to dry before being placed onto PGA agar plates (Table 3.2) 2 cm away from an actively growing plug of *G. graminis*. Plates were left to grow at room temperature for 5 days before imaging. Three technical replicates were run for one purified extract each of fungichromin, 14-hydroxy(iso)chainin and actinomycin.

3.3.5 Plant growth promotion assays

3.3.5.1 The effect of *Streptomyces* species on the *in vitro* growth of *A. thaliana*

A. thaliana Col-0 seeds (Table 3.1) were sterilised as described in 3.3.1 and plated onto MSk medium (1% (w/v) sucrose and 0.8% (w/v) agar; Table 3.2). These were left at 4°C in the dark for 24 hours before being placed, vertically, under a photoperiod of 12 hours light/ 12 hours dark, at 22°C for 10 days. Seedlings were then transferred to square agar plates containing MSk agar (1.5% (w/v) agar, 0% (w/v) sucrose; Table 3.2) and allowed to equilibrate, vertically, overnight at 22°C. 1 µl of *Streptomyces* spores (10⁶ spores ml⁻¹) was added to the top of the root system of each seedling and allowed to dry. 16 replicate seedlings were inoculated per *Streptomyces* strain (all six newly-isolated *Streptomyces* isolates, three *S. lydicus* strains and *S. coelicolor* M145; Table

3.1). 10% (v/v) glycerol was added to control seedlings. Plates were grown vertically for 16 days, before measuring total plant biomass (dry weight). The biomass of plants inoculated with different strains were compared via ANOVA and Tukey's Honestly Significant Difference (HSD) tests; biomass was log-transformed to normalise residuals.

3.3.5.2 The effect of *Streptomyces* species on the *in vivo* growth of *A. thaliana*

A. thaliana Col-0 seeds (Table 3.1) were sterilised as described in 3.3.1, before placing them into a solution containing a mixture of spores from the streptomycete isolates M3, M2 and L2 (Table 3.1), all of which demonstrated *in vitro* plant-growth-promotion. The solution contained 10^3 spores ml^{-1} of each isolate (10^9 spores ml^{-1} in total) and the mixture was pregerminated in 2xYT (Table 3.2) at 50°C for 10 minutes. Seeds were incubated in the spore preparation (on a rotating shaker) for 2 hours, before being transferred to pots containing sieved Levington F2 seed and modular compost. As a control, sterile seeds were incubated in 2xYT without spores. An additional 1 ml of the pregerminated spore mix (or uninoculated 2xYT) was pipetted into the soil surrounding the seed. Pots were then placed at 4°C for 48 hours and grown for 6 weeks under a photoperiod of 12 hours light/ 12 hours dark, at 22°C. There were 5 replicate pots in each treatment (inoculated or uninoculated seeds) and the experiment was run twice using different spore stocks as the inoculum. After 6 weeks of growth, plants were taken from pots and cleaned according to the methods described in 3.3.1. The plants were then dried in an oven at 50°C for 6 hours, before total dry weight was calculated. Differences in biomass were analysed using a linear mixed effects model with treatment (sterile or inoculated seeds) as a fixed effect and experimental run (one or two) as a random effect. The model was built using the package lme4 in R 3.2.3 (R Core Team 2017). Models with and without treatment as a fixed effect were compared using likelihood ratio tests.

3.3.5.3 *In vitro* tests for IAA production

Streptomyces isolates N1, N2, M3, L2, M2 and MG were grown on cellophane membranes covering YPD agar plates (Table 3.2) supplemented with 5 mM tryptophan. After 7 days, cellophane membranes with bacterial biomass were removed and plates were flooded with Salkowski reagent (2% 0.5 M FeCl_3 in 35%

perchloric acid) (as in Bric et al 1991). A red colour indicated that IAA had leached into the medium.

3.3.5.4 *In vitro* test for ACC production

To test for the use of 1-aminocyclopropane-1-carboxylic acid (ACC) as a sole nitrogen source, strains were streaked onto Dworkin and Foster medium (Table 3.2) in which 0.2% (w/v) NH_4SO_4 or 0.051% (w/v) ACC was added as a sole nitrogen source, or no nitrogen source as a control. Plates were left for 10 days at 30°C before imaging.

3.4 Results

3.4.1 Isolation and genome sequencing of *Streptomyces* from the roots of *Arabidopsis thaliana*

3.4.1.1 Isolation of root-associated *Streptomyces* species

Six new *Streptomyces* strains (Table 3.1) were isolated from the roots of *Arabidopsis thaliana* plants growing in Levington F2 Seed and Modular compost, using a range of different isolation media. All strains appeared morphologically different from one another when growing on agar plates (Figure 3.2). The isolates N1, N2, M2 and M3 all grew well and sporulated on SFM agar. The strains L2 and MG grew poorly on most types of agar media, but their growth increased and they sporulated on MYM and oatmeal agar, respectively, enabling them to be spore stocked.

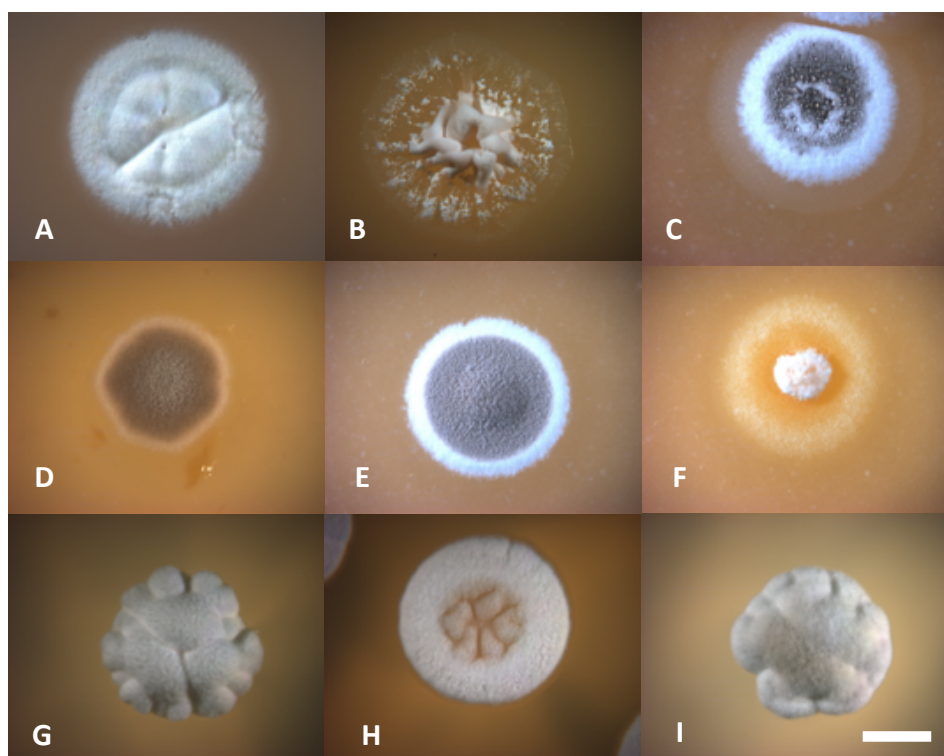


Figure 3.2 Images of *Streptomyces* isolates **A)** L2, **B)** M2, **C)** M3, **D)** MG, **E)** N1, **F)** N2, **G)** Actinovate, **H)** *Streptomyces lydicus* 25470, **I)** *Streptomyces lydicus* 31975. Strains L2, M2, M3, N1 and N2 were grown on SFM. MG was grown on oat agar. *S. lydicus* 25470, *S. lydicus* 31975 and Actinovate were grown on ISP2 agar. Images were taken after 5 days of growth at 30°C. Scale bar = 2.5 mm.

3.4.1.2 Whole genome sequencing of isolates

High quality genome sequences were generated for all novel *Streptomyces* isolates, excluding MG which did not grow well enough on solid agar, or in liquid culture. Additionally, three strains of *Streptomyces lydicus*, including two ATCC strains and one strain that was isolated from the biocontrol and growth-promoting product Actinovate®, were also genome sequenced. All of the resulting genomes were very similar in terms of overall size and content (Table 3.4) and do not show any significant reductions compared to the genomes of other *Streptomyces* isolates, such as that of the model soil-dwelling strain *S. coelicolor*, which has a genome size of 8,667,507 base pairs and encodes 7825 genes (Bentley et al 2002).

Table 3.4 Genome features of plant-associated *Streptomyces* strains sequenced for this study, including their GenBank Accession numbers, their genome size in base pairs (bp) and the total number of open reading frames (ORFs), tRNAs and rRNAs. Biosynthetic gene clusters (BGCs) were predicted using AntiSMASH 4.0.

Strain	Accession number	Genome size (bp)	ORFs	tRNAs	rRNAs	BGCs
L2	QBDT00000000	8,073,926	7079	68	18	32
M2	CP028834	8,718,751	8026	72	18	24
M3	QANR00000000	8,304,843	7561	74	18	28
N1	QBDS00000000	7,207,104	6239	65	21	22
N2	CP038719	8,428,700	7401	69	21	35
Actinovate	RDTC00000000	9,139,876	7989	67	21	36
ATCC25470	RDTD00000000	7,935,716	7084	65	21	26
ATCC31975	RDTE00000000	9,244,118	8128	66	21	34

Genomes of the five newly-isolated and sequenced strains were uploaded to the automated multi-locus species tree (autoMLST) server (Alanjary et al 2019) to enable their phylogenetic classification. The strain N1 has an average nucleotide identity (ANI) of 98.7% to *Streptomyces albidoflavus* as well as several other closely-related species, indicating that it is highly likely to be a member of this clade (Table 3.5). Strain N2 has an ANI of 97.6% to *Streptomyces griseofuscus*, suggesting that it is closely-related to this species (Table 3.5). The highest ANI values for strains L2, M2 and M3, are 88.3%, 94.7% and 91.1%, respectively (Table 3.5); this is below the 95% threshold ANI that is generally believed to be indicative of being of the same species (Jain et al 2018, Konstantinidis and Tiedje 2005), suggesting that these strains may be novel streptomycetes.

Table 3.5 Results of multi-locus sequence analyses of genome-sequenced isolates. Analyses were conducted using the autoMLST server (Alanjary et al 2019). The strain with the highest average nucleotide identity (ANI) to each isolate is displayed, along with the ANI value calculated by the pipeline.

Isolate	Strain with highest ANI	ANI
L2	<i>Streptomyces bungoensis</i>	88.3%
M2	<i>Streptomyces sp.</i> HBG00200	94.7%
M3	<i>Streptomyces pratensis</i>	91.1%
N1	<i>Streptomyces albidoflavus</i>	98.7%
N2	<i>Streptomyces griseofuscus</i>	97.6%

3.4.1.3 The identification of biosynthetic gene clusters

AntiSMASH 4.0 (Blin et al 2017) was used to predict the presence of biosynthetic gene clusters (BGCs) within the genomes of all sequenced root-associated *Streptomyces* isolates (Table 3.4, Figure 3.3). All strains carried a diverse range of BGCs, including those known to produce compounds with antimicrobial activities such as polyketide synthases (PKS), non-ribosomal peptide synthases (NRPS), as well as clusters encoding terpenes and bacteriocins (Figure 3.3). Such compounds may play an important role during interference competition within the plant root and the rhizosphere, allowing *Streptomyces* species access to host-derived resources and niche space. They may also, in turn, provide benefits to the plant host by suppressing the growth of pathogenic organisms.

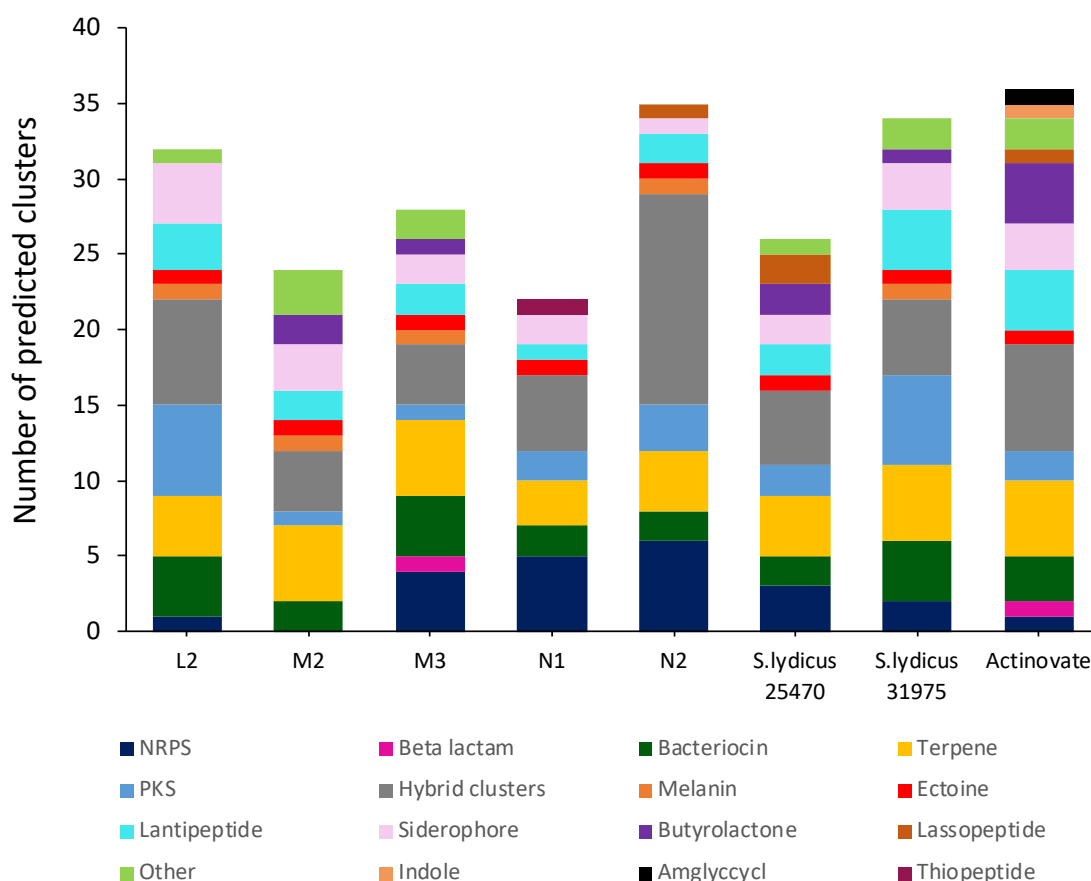


Figure 3.3 Biosynthetic gene cluster (BGC) predictions for genome-sequenced *Streptomyces* isolates. BGCs were predicted by AntiSMASH 4.0. NRPS= Non-Ribosomal Peptide Synthase, PKS= Polyketide Synthase. Hybrid clusters are those in which two clusters were called together as the same cluster e.g. a PKS-NRPS cluster.

All strains also encoded BGCs predicted to produce siderophores (Figure 3.3). These are molecules that chelate metal ions, particularly iron, from the surrounding environment. In the soil and rhizosphere, these can act to scavenge free iron from the soil, release iron from humic and fulvic acids present in organic matter, as well as to mobilise iron from minerals present in solid phase (Carvalhais et al 2013b, Liu et al 2017a). This process generates soluble complexes that can then be taken up by plants (Carvalhais et al 2013b, Liu et al 2017a). The presence of microbes in the soil has been shown to be an important contributor to plant iron uptake and growth (Carvalhais et al 2013b, Rungin et al 2012b). Siderophores may also help microorganisms to compete in the soil, rhizosphere and endosphere, with the added benefit that chelation of ions

may act to exclude pathogen populations that are also competing for iron (Liu et al 2017a).

Only two predicted BGCs were shared between all strains; these were gene clusters encoding the compound ectoine, a compatible solute produced by many microorganisms to combat osmotic stressors (Czech et al 2018), and hopene, a triterpenoid that has a stabilising effect on cytoplasmic membranes and is produced by a range of Gram-positive and Gram-negative bacteria (Siedenburg and Jendrossek 2011). Strain N2 and Actinovate have the greatest number of predicted BGCs, with 35 and 36 gene clusters called by AntiSMASH, respectively. Several of these clusters were called as hybrid clusters (for example PKS-NRPS clusters), possibly further increasing the biosynthetic potential of these strains (Figure 3.3). Many of the clusters predicted for N2 and Actinovate had a very low percentage of genes with homology to known secondary metabolite clusters, however N2 was predicted to encode 9 clusters with over 80% of genes showing sequence homology to known clusters (see Table S3.1 in supplementary information for N2 antiSMASH output). In addition to ectoine (100% similarity) and hopene (92% similarity), this included a T1PKS-NRPS cluster with similarity to 100% of the genes that encode the polyene antifungal filipin. Other clusters with over 80% sequence homology included the antimicrobial compounds actinomycin and albaflavenone, a protective pigment called melanin, a T2PKS-T1PKS spore pigment, an odorous NRPS-terpene cluster likely to be geosmin and a siderophore with similarity to desferrioxamine B.

3.4.2 The bioactivity of plant-associated *Streptomyces* isolates

3.4.2.1 *In vitro* bioactivity of root-associated *Streptomyces* isolates

In order to establish whether biosynthetic potential translated into the ability of root-associated *Streptomyces* isolates to produce antimicrobial compounds *in vitro*, bioassay screens were carried out for each isolate against a range of pathogenic indicator strains. Indicator strains included the Gram-positive bacterial species *Bacillus subtilis* and a clinical isolate of methicillin resistant *Staphylococcus aureus* (MRSA) (Table 3.1). *Escherichia coli* and the plant pathogen, *Pseudomonas syringae* DC3000, were used as Gram-negative indicator strains (Table 3.1). Streptomycete isolates were

additionally tested against the human fungal pathogens *Candida albicans* and *Lomentospora prolificans*, as well as the take-all fungus *Gaeumannomyces graminis* var. *tritici* which is a major root pathogen of wheat plants (Table 3.1). Bioassays were completed on a range of different media types, in order to establish whether antimicrobial production could be switched on under a variety of different growth conditions (Table 3.6, see Table 3.2 for media recipes).

Table 3.6 Bioactivity screens of plant-associated *Streptomyces* species. Each *Streptomyces* species (purple, top) was tested against a range of different pathogenic indicator species (blue column, down). Screens were conducted on a range of different media (see Table 3.2 for media recipes). Green squares indicate inhibition of the indicator strain by the given streptomycete, red indicates no inhibition.

Pathogen strain	Media	Streptomycete strain								
		N1	N2	M3	M2	L2	MG	<i>S. lydicus</i> 25470	<i>S. lydicus</i> 31975	Actinovate
<i>Bacillus subtilis</i>	SFM									
	MS									
	ISP2									
	Oatmeal									
	MYM									
Methicillin-resistant <i>Staphylococcus aureus</i>	SFM									
	MS									
	ISP2									
	Oatmeal									
	MYM									
<i>Escherichia coli</i>	SFM									
	MS									
	ISP2									
	Oatmeal									
	MYM									
<i>Pseudomonas syringae</i> DC3000	SFM									
	MS									
	ISP2									
	Oatmeal									
	MYM									
<i>Candida albicans</i>	SFM									
	MS									
	ISP2									
	PGA									
	MYM									
<i>Gaeumannomyces graminis</i>	PGA									
<i>Lomentospora prolificans</i>	PGA									

The level of bioactivity shown *in vitro* was highly variable across different strains and for the same strain on different media (Table 3.6). Several of the isolates showed very low levels of activity, for example N1 and L2 only inhibited *Bacillus subtilis* on minimal

salts medium (MS). Additionally, M2 only inhibited *P. syringae* on SFM and MS medium. Interestingly, this low level of activity did not always seem to correlate with the number of BGCs encoded in the genome of each strain; although N1 had the lowest number of predicted BGCs of all isolates (22 clusters in total), L2 had a relatively high number of BGCs (32 predicted clusters) many of which may have been switched off under the test conditions used.

The strain M3 demonstrated bioactivity against Gram-positive bacterium *B. subtilis* and the Gram-negative bacterium *P. syringae* on several different types of media (Table 3.6). The strain MG also exhibited moderate levels of bioactivity including against Gram-positive bacteria (*B. subtilis* and MRSA) as well as against the fungus *G. graminis* (Table 3.6). In comparison, the three *S. lydicus* strains (ATCC 25470, ATCC 31975 and Actinovate) showed a much greater level of activity, demonstrating both anti-Gram-positive and antifungal activity; all three strains inhibited *B. subtilis* and MRSA, as well as the fungal pathogens *C. albicans*, *G. graminis* and *L. prolificans*, all on a range of different media types (Table 3.6). However, the isolate N2 showed the greatest level of bioactivity and was able to inhibit all tested bacterial and fungal pathogenic strains on most types of media (Table 3.6, Figure 3.4). This included Gram-negative *E. coli* on oatmeal agar, which all other isolates failed to inhibit. Finding bacterial strains that have activity against Gram-negative bacteria is particularly rare, as the outer membrane of these bacteria prevents antimicrobials from entering the cell; those that are able to cross this barrier are often effectively removed by efflux pumps (Fischbach and Walsh 2009).

A detailed investigation of the antiSMASH output for N2 (Figure 3.3 and see Table S3.1) did not reveal any BGCs that had significant levels of homology to clusters particularly well-known for their anti-Gram-negative activity. It is possible that the cluster predicted to encode an actinomycin-like compound was contributing to this activity, since actinomycin compounds are known to be generally toxic (Katz 1967). It is also likely that the compound responsible is different to that exhibiting antifungal activity, since antifungal activity occurred broadly on most types of media, whereas the inhibition of *E. coli* by N2 was restricted to oatmeal agar. Due to its ability to inhibit a

wide range of pathogens including wheat take-all fungus (Table 3.6, Figure 3.4), N2 was taken forward for further *in vivo* and biochemical analysis.

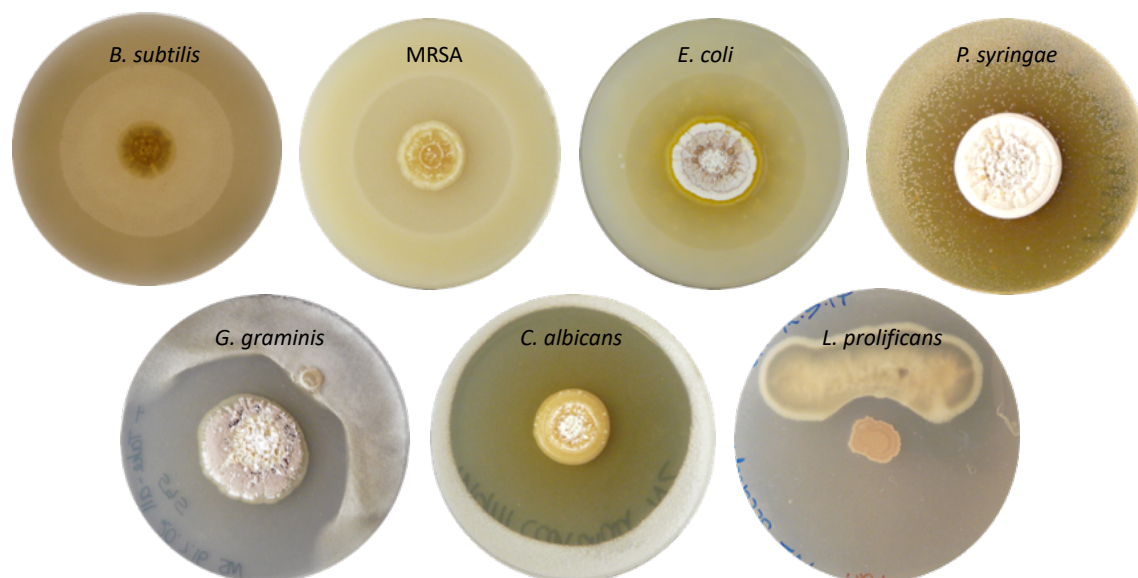


Figure 3.4 The bioactivity of *Streptomyces* strain N2. N2 (in the centre of plates) was able to inhibit the growth of Gram-positive bacteria (*B. subtilis* and MRSA, both shown on SFM); Gram-negative bacteria (*E. coli* and *P. syringae*, shown on oat agar and MYM agar, respectively); and fungal organisms (*C. albicans* shown on MYM, and *G. graminis* and *L. prolificans* both shown on PGA medium).

3.4.2.2 *In vivo* bioactivity of *Streptomyces* N2 against wheat take-all fungus

Streptomyces N2 demonstrated strong antifungal activity against the wheat take-all fungus (*G. graminis*) *in vitro* (Figure 3.4). In order to test whether the observed antifungal activity could extend to protecting wheat plants against *G. graminis* in an *in vivo* system, wheat seeds were inoculated with N2 spores and grown next to a central plug of *G. graminis* on agar plates (Figure 3.5). After 5 days, seeds had germinated and roots had begun to emerge. On control plates, *G. graminis* grew outwards across the agar plate towards the uninoculated wheat seedlings (Figure 3.5 A). However, where seeds had been inoculated with a spore preparation of N2, *G. graminis* was inhibited from growing over the seed and emerging roots, indicated by a zone of inhibition around the wheat seeds (Figure 3.5 B). This suggested that N2 spores had successfully germinated on the wheat seed surface, despite having been dried down, and that the

streptomycete was producing antifungals which were then diffusing across the agar plate.

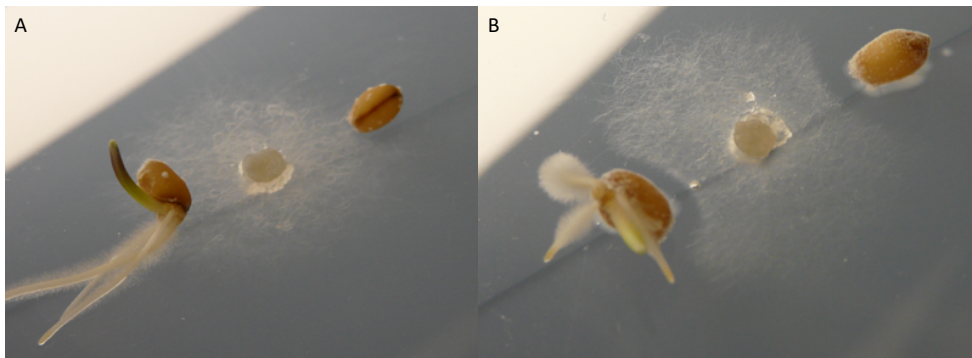


Figure 3.5 The inhibition of *G. graminis* by seed-coatings of *Streptomyces* strain N2. Germinating wheat seeds are either **A)** sterile or **B)** inoculated with a spore preparation of the streptomycete isolate N2, growing next to a plug of *G. graminis*. *G. graminis* is prevented from growing towards inoculated seeds, as demonstrated by the zone of inhibition.

Although promising, using the agar plate method to test for the inhibition of take-all infection is limited, since seedlings can only grow in plates over a short period of time before becoming too large. Therefore it is impossible to score infection in older wheat plants using this system. In addition, agar medium is a poor representation of the true environmental conditions in which wheat plants grow, since plant roots would normally be surrounded by a growth medium (such as soil) as well as the infecting fungal pathogen. Therefore, to further test the potential of the *Streptomyces* strain N2 to act as a biocontrol strain against *G. graminis in vivo*, wheat seeds were soaked in N2 spores, allowed to dry, and then grown in sterile vermiculite (artificial soil) containing *G. graminis* mycelia.

After 3 weeks of growth at 25°C, wheat plants that had germinated and grown from un-inoculated seeds in the presence of the *G. graminis* fungus (N = 25) showed extensive and severe levels of take-all infection, with an average infection score of 7.24 ± 0.26 SE (Figure 3.6, see Figure 3.1 for scoring system). Most of the plants in this treatment group exhibited infected roots, stems and leaves, which all appeared senescent and brown (Figure 3.7). However, there was a significant effect of plant

treatment group on infection score (Kruskal-Wallis test $H_{DF=3} = 83.41$, $P = <0.001$). Plants that had grown from seeds coated in N2 spores ($N = 25$), demonstrated a significant decrease in average infection severity to 5.47 ± 0.59 , compared to plants grown from uninoculated seeds in the presence of take-all (Figure 3.6, Dunn's test between inoculated and sterile wheat grown with *G. graminis*: $P = 0.023$). For most of these plants, the roots had also gone almost completely brown and there was some evidence of stem infection. However, in many cases the leaves remained green for plants under this treatment, suggesting that, although N2 did not eliminate take-all infection it did contribute to a slower progression of the fungal disease phenotype (Figure 3.7). Plants that had emerged from seeds that were either sterile or coated in N2 spores, but had grown in the absence of the *G. graminis* fungus appeared to be significantly more healthy. These plants had green leaves and healthy roots in which there was an absence of any brown lesions (Figure 3.7).

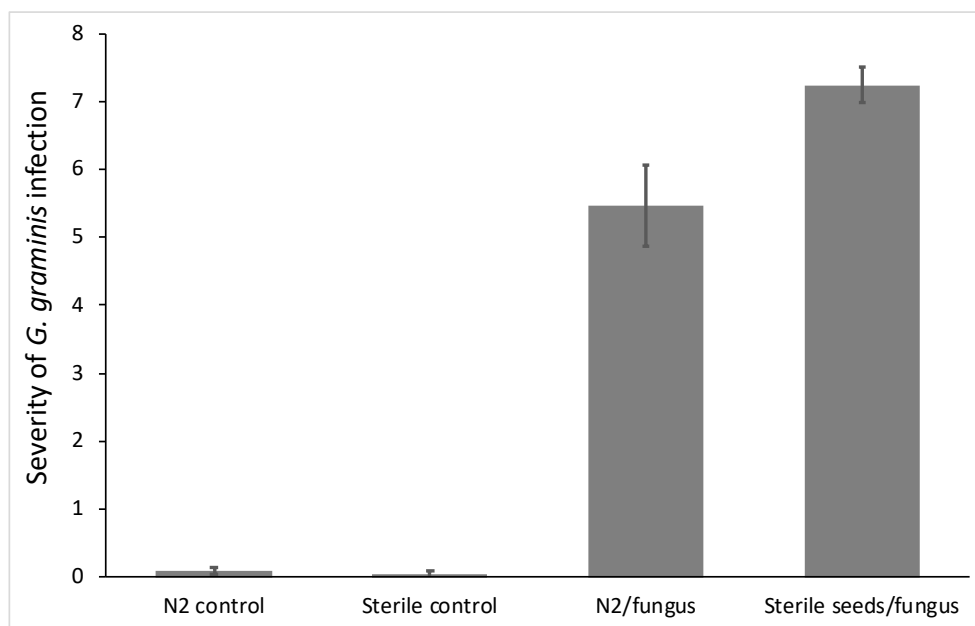


Figure 3.6 The effect of *Streptomyces* strain N2 on wheat plant infection severity by *G. graminis*. Infections were scored after three weeks of growth (scored according to Figure 3.1). N2 control= seeds coated in N2 spores/no *G. graminis*; Sterile control= sterile seeds/no *G. graminis*; N2/fungus= seeds coated in N2 spores grown in the presence of *G. graminis*; Sterile seeds/fungus= sterile seeds grown in the presence of *G. graminis*. $N=25$ plants per treatment group, error bars represent standard errors.



Figure 3.7 Images of *in vivo* bioassays against *G. graminis*. Wheat plants were grown **A)** from sterile seeds in the presence of *G. graminis*, **B)** from seeds inoculated with N2 spores, in the presence of *G. graminis* **C)** from sterile seeds, no *G. graminis* **D)** from seeds coated with N2 spores, no *G. graminis*.

3.4.3 Isolation and characterisation of antimicrobials from *Streptomyces* N2

3.4.3.1 Filipin-like compounds as a potential antifungal candidates

To further identify the source of antifungal activity exhibited by *Streptomyces* strain N2, antiSMASH outputs for this strain were investigated in more detail. As discussed in section 3.4.1.3 the genome of N2 is predicted to encode 35 BGCs (Figure 3.3), although many of these have a low percentage sequence homology to known antimicrobial compounds (Table S3.1, supplementary information). However, one cluster, predicted to be a hybrid cluster containing a polyketide synthase and a non-ribosomal peptide synthase (PKS-NRPS), was identified that demonstrated sequence similarity to 100% of the genes required to make the potent antifungal compound filipin. Filipin is a non-glycosylated polyene macrolide antifungal, known to be produced by the

streptomycete species *S. filipinensis*, *S. avermitilis*, *S. miharaensis* and strain FG26 isolated from the cuticles of *Allomerus* trap ants (Gao et al 2014, Payero et al 2015). Polyene macrolides are a large family of polyketides that bind to ergosterol in fungal cell membranes, altering their permeability and eventually leading to fungal cell death (Kong et al 2013). Filipin is usually produced as a complex of related compounds (filipin I-IV) with each component varying in the number of post-polyketide hydroxyl functions that are introduced to a 28-membered macrolide ring by two cytochrome P450 monooxygenases (Payero et al 2015) (Figure 3.8). To make filipin II, filipin I is hydroxylated at C-26. Filipin III, the major component found in nature, is then produced from filipin II through the hydroxylation of C-1' (Figure 3.8). Filipin IV is the epimer of filipin III (Payero et al 2015).

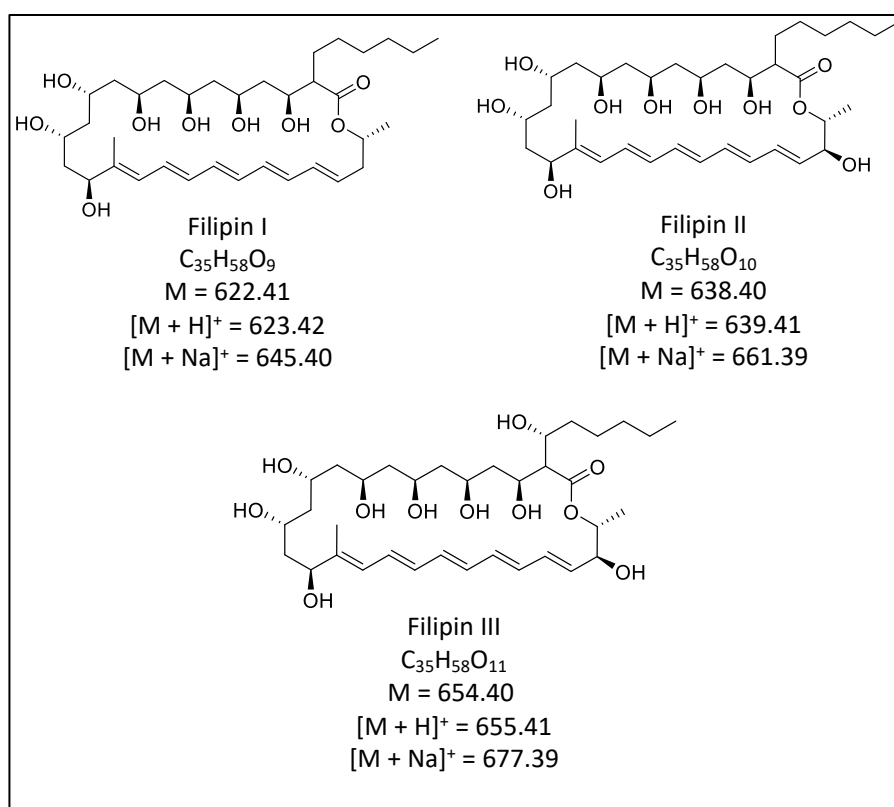


Figure 3.8 The chemical structures of different members of the filipin complex (filipin I, filipin II and filipin III), along with the molecular mass (M) of each component, and the masses of their hydrogen ([M+H]⁺) and sodium ([M+Na]⁺) adducts, respectively.

The BGCs predicted to encode filipin in the genomes of N2 and *S. avermitilis* both encode 13 proteins which include 6 polyketide synthase (PKS) genes, 5 oxioeductase genes and 2 regulatory genes (Figure 3.9). BLASTp analysis demonstrated that the proteins encoded by N2 demonstrated high levels of homology to those encoded by *S. avermitilis*, with percentage identities ranging from 80-93% (Table 3.7) and coverage being 99-100% .

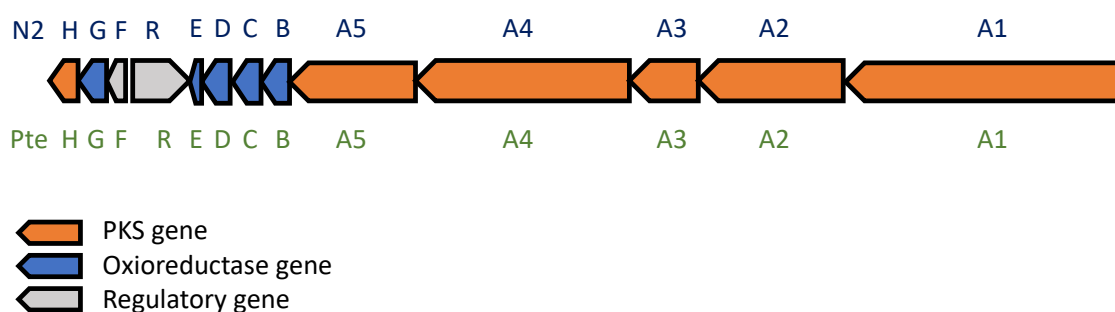


Figure 3.9 The structure of the gene cluster encoding filipin in *Streptomyces* N2 (blue letters, top) and *S. avermitilis* (Pte proteins in green, bottom). The clusters both encode 13 proteins.

Table 3.7 The percentage identity of protein sequences encoded by genes found in the N2 filipin gene cluster, compared to proteins encoded by the filipin cluster of *S. avermitilis*, as determined by BLASTp analysis (see Figure 3.9 for cluster organisation).

N2 Protein	<i>S. avermitilis</i> protein	Percentage identity (%)	Proposed function
A1	PteA1	85	Polyketide synthase
A2	PteA2	87	Polyketide synthase
A3	PteA3	85	Polyketide synthase
A4	PteA4	86	Polyketide synthase
A5	PteA5	86	Polyketide synthase
B	PteB	93	Putative dehydrogenase
C	PteC	93	Cytochrome P450 hydroxylase
D	PteD	89	Cytochrome P450 hydroxylase
E	PteE	84	Ferredoxin
R	PteR	80	DnRI/RedD/AfsR-family transcriptional regulator
F	PteF	89	LuxR family transcriptional regulator
G	PteG	90	Putative oxidase
H	PteH	83	Thioesterase

In order to test whether the compound filipin could inhibit the same fungal strains that are inhibited by N2 *in vitro*, agar plates were made containing a dilution series of a commercial filipin standard (Sigma Aldrich). The growth of *Lomentospora prolificans* was completely inhibited by the presence of 2.5 mg L⁻¹ of filipin in plates (Figure 3.10). The wheat take-all fungus *G. graminis*, began to be inhibited at 5 mg L⁻¹, and was almost completely prevented at 10 mg L⁻¹, whereby the fungus only appeared to proliferate on the plug of PGA used as an inoculum (Figure 3.10). *Candida albicans* was also inhibited by 5 mg L⁻¹ of filipin (Figure 3.10). The minimum inhibitory concentration (MIC) values observed for these strains are all above previously reported MICs for filipin III against *Candida utilis* and *Saccharomyces cerevisiae* which were 0.3 mg L⁻¹ and

0.4 mg L⁻¹, respectively (Payero et al 2015). However, it is possible that N2 produces a more potent version of filipin, or it is produced in combination with other antifungals.

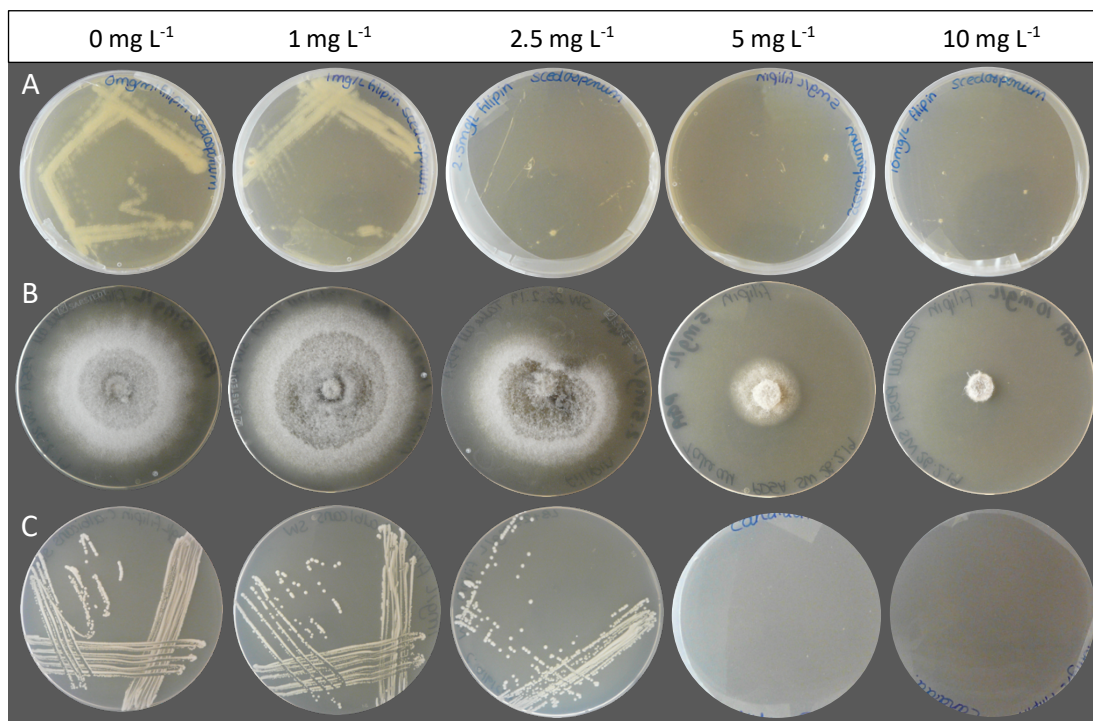


Figure 3.10 The minimum inhibitory concentration (MIC) of a filipin standard against **A)** *Lomentospora prolificans* **B)** *Gaeumannomyces graminis* and **C)** *Candida albicans*. Concentrations of filipin are shown along the top. Assays A and B were carried out on PGA medium, C was carried out on LB medium.

3.4.3.2 Isolation of antifungal compounds

To further investigate whether N2 was producing filipin *in vitro*, and the possible structure of this compound, chemical extractions were made from plates of N2 growing on SFM, oat or ISP2 agar; these three media types induce antifungal activity in N2 *in vitro* (Table 3.6). Separate extractions were carried out using the solvents methanol and ethyl acetate, respectively. In order to confirm that solvents had successfully isolated compounds with antifungal activity, extracts were used in disc-diffusion bioassays against *C. albicans*. All extracts, from both types of solvents and from all three types of media, showed strong antifungal activity, as indicated by zones of clearing around inoculated discs (Figure 3.11). Interestingly, none of the extracts

inhibited *E. coli* (Figure 3.11) suggesting that extractions had not captured the compounds responsible for the anti-Gram-negative activity that was observed for N2 *in vitro* (Table 3.6, Figure 3.4).

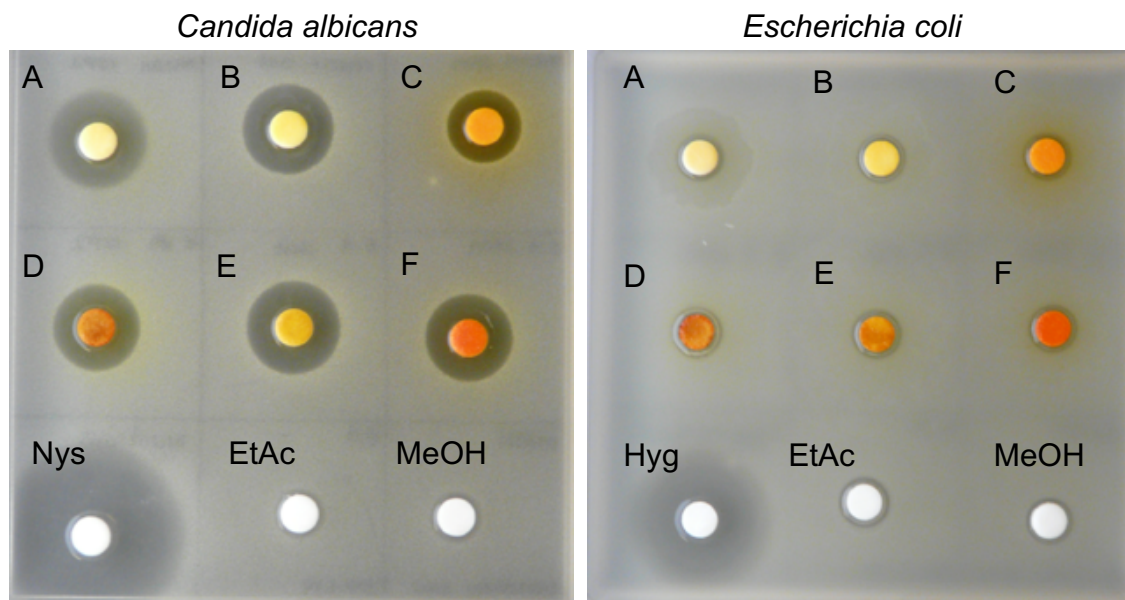


Figure 3.11 Disc-diffusion bioassays using extracts from *Streptomyces* strain N2. Extracts were tested against *Candida albicans* (left) and *Escherichia coli* (right). Discs were soaked in either methanol (top row) or ethyl acetate (middle row) extracts from N2 growing on ISP2 (A and D), oat agar (B and E) or SFM (C and F) medium, respectively. Nystatin (Nys) or hygromycin (Hyg) were used as a positive controls and ethyl acetate (EtAc) and methanol (MeOH) were inoculated as negative controls.

To confirm whether the antifungal activity of extracts from N2 might be linked to the production of filipin, LC-MS analysis was used to compare the composition of extracts to a commercial filipin standard. Analysis of the commercial standard, revealed the presence of several peaks, consistent with filipin being a complex of different compounds. The major peak had a mass-to-charge ratio (m/z) of 677.39 (Figure 3.12) which is consistent with the accurate mass of filipin III (calculated from $C_{35}H_{58}O_{11}$ [$M + Na$] $^+$ as 677.39, Figure 3.8); this was the major component of the standard as reported by the manufacturer (Sigma Aldrich). There was also a prominent peak with an m/z of 661.39 (Figure 3.12) which corresponded to the accurate mass of filipin II (calculated from $C_{35}H_{58}O_{10}$ [$M + Na$] $^+$ as 661.39, Figure 3.8). In addition to these major peaks, there

were also several smaller peaks present with m/z values of 659.37, 675.38 and 693.38 (Figure 3.12). The peaks with masses 659.37 and 675.38 were predicted to be filipin II and filipin III, respectively, both with an additional carbon-carbon double bond. The very small peak at 693.38 is predicted to be a hydroxylated version of filipin III (filipin III $[M + Na]^+$ plus the mass of one oxygen molecule).

All of the extracts from N2 grown on the different types of agar media (oat, SFM or ISP2) had peaks present within the range of retention times shown by the filipin standard (between 2.6 and 3.8 minutes, Figure 3.12). Extracts from N2 grown on oat and SFM agar media both showed peaks with m/z values of 663.41 and 677.38, consistent with these representing the sodium adducts of filipin II (plus two hydrogen molecules) and filipin III, respectively (Figure 3.8, Figure 3.12). However, the major peak in all extracts (N2 grown on oat, SFM and ISP2 agar media) had an m/z value of 693.38 $[M + Na]^+$ (Figure 3.12), which is consistent with a hydroxylated form of filipin III. As discussed in the above paragraph, a very small amount of this compound was detected in the standard, however this was present at a much lower abundance, with filipin III being the dominant compound. In contrast, the hydroxylated form was the dominant peak in N2 extracts. As with the standard, all major peaks from the N2 extracts had a “three finger” UV absorbance trace at 338 nm which is typical of polyene compounds such as filipin (Figure 3.13).

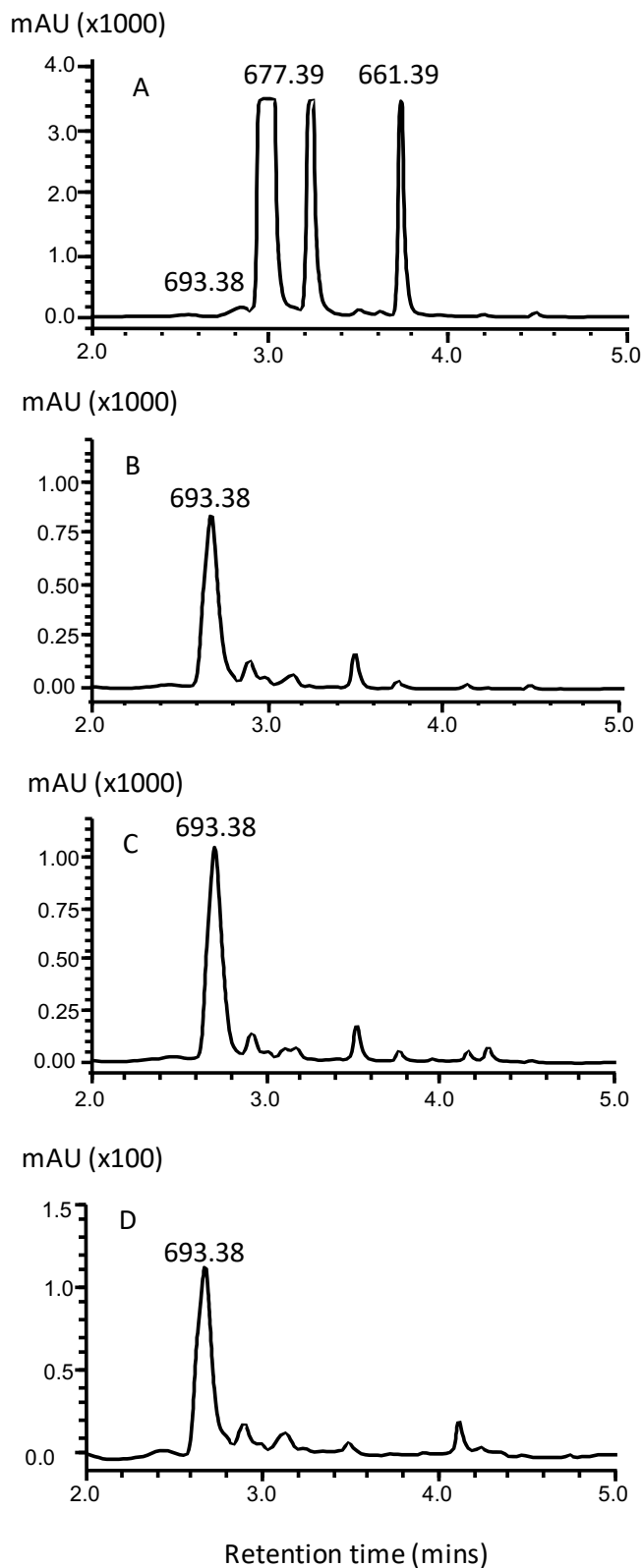


Figure 3.12 Mass spectra from UPLC-MS analysis of N2 extracts. Spectra were generated from **A)** the commercial filipin standard (Sigma Aldrich) or methanol extracts obtained from N2 growing on **B)** SFM **C)** oat or **D)** ISP2 agar medium. Numbers written above peaks represent mass-to-charge (m/z) ratios. The y-axis is in milli-absorbance (mAU) units.

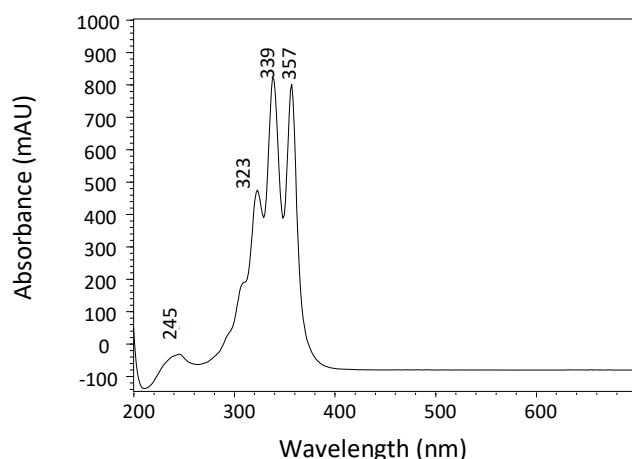


Figure 3.13 A representative UV absorbance trace (in units of milli-absorbance, mAU) for the major peak (mass 693.38 [M+Na]⁺) in methanol extracts made from N2 growing on oat agar. A similar “three finger” conformation was seen for the major peaks arising in extracts taken from N2 growing on ISP2 and SFM medium.

In section 3.4.1.2, autoMLST analysis suggested that N2 had significant sequence homology to the species *Streptomyces griseofuscus* (Table 3.5). Species in the same clade as *S. griseofuscus*, are known to produce the compound fungichromin (also called pentacyclin) which has the same mass (an m/z of 693 [M + Na]⁺, exact mass of 670) as the hydroxylated form of filipin found to be dominant in extracts of N2 (Cope and Johnson 1958, Shih et al 2003, Shimizu et al 2004, Xiong et al 2012). As such, fungichromin has an identical chemical structure to filipin III, apart from the presence of an additional hydroxyl group at C-14 (Figure 3.14) (Cope and Johnson 1958). NMR analysis carried out by Johannes Rassbach (John Innes Centre, Norwich) demonstrated that the compound produced by *Streptomyces* N2 that has a mass of 693 [M + Na]⁺, has the same chemical structure as fungichromin (Figure 3.14). The conversion of filipin III to fungichromin is thought to occur via the action of an additional cytochrome P450 enzyme located upstream of the first PKS gene in the filipin cluster (Zhou et al 2019). As mentioned, the hydroxylation of filipin I and filipin II occurs via the action of two P450 enzymes (PteC and PteD) which are encoded within the filipin BGC (Figure 3.9). It is possible that one of these enzymes is more promiscuous in strain N2 than in other filipin-producing strains, meaning that the enzyme is capable of hydroxylating multiple carbon residues, resulting in a greater prevalence of the hydroxylated form of filipin III. However, since the filipin cluster forms part of a hybrid PKS-NRPS BGC in N2

(Figure 3.15), it is also possible that the hydroxylation of filipin III is catalysed by another enzyme situated in the NRPS part of the cluster. Indeed, the NRPS encodes two additional P450 enzymes that could be responsible for this (Figure 3.15). One of these additional enzymes is located directly upstream of the first filipin PKS gene and is in the same position as a cytochrome P450 enzyme, identified in *Streptomyces* S816, which has been shown to be able to convert filipin III to fungichromin *in vitro* (Zhou et al 2019).

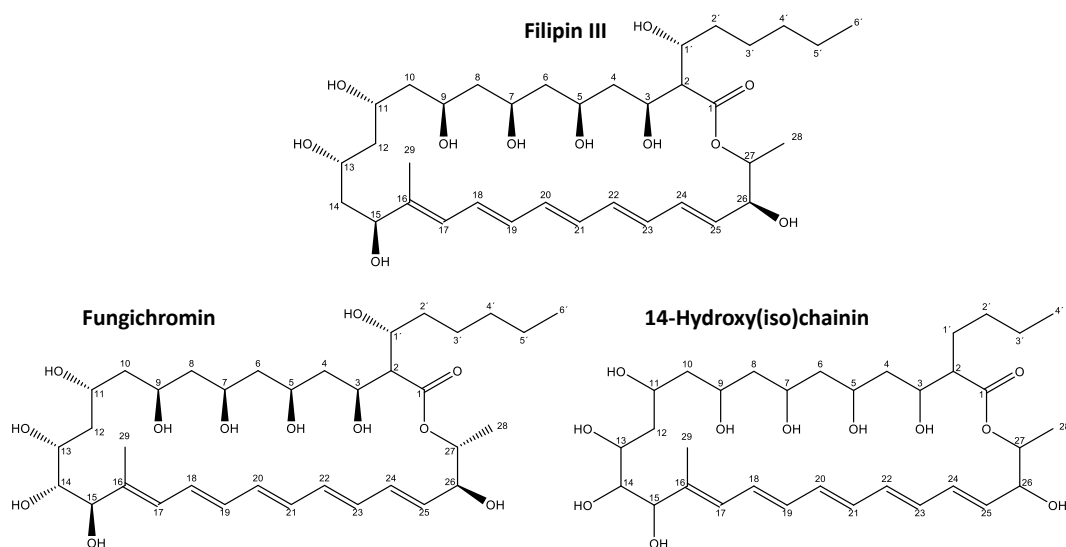


Figure 3.14 The structures of filipin III, fungichromin and 14-hydroxy(iso)chainin that were purified from *Streptomyces* N2 extracts (purification and structural elucidation was carried out by Johannes Rassbach, John Innes Centre).

responsible for the antifungal activity exhibited by N2 against wheat take-all, potentially in combination with lower quantities of filipin that are also produced by N2. This compound may reduce the MIC values against fungal pathogens, compared to those observed for the commercial filipin standard (Figure 3.10). However, since many polyene compounds are light-sensitive and generally unstable at room temperature it is possible that fungichromin degraded too rapidly in bioassay experiments against *G. graminis* for antifungal activity to be observed. Further controls will be needed to see whether this is the case. Future work will include purifying greater quantities of the filipin-like compounds produced by N2 and quantitatively testing their stability and antifungal activities against take-all fungus both *in vitro* and *in vivo*. Interestingly, none of the isolated compounds (fungichromin, 14-hydroxy(iso)chainin or actinomycin) inhibited the growth of *E. coli* to a greater extent than a methanol control (Figure 3.16), suggesting that another compound is likely to be responsible for the anti-Gram-negative activity observed for N2 (Figure 3.4, Table 3.6). Further extractions with different solvents may enable this compound to be isolated.

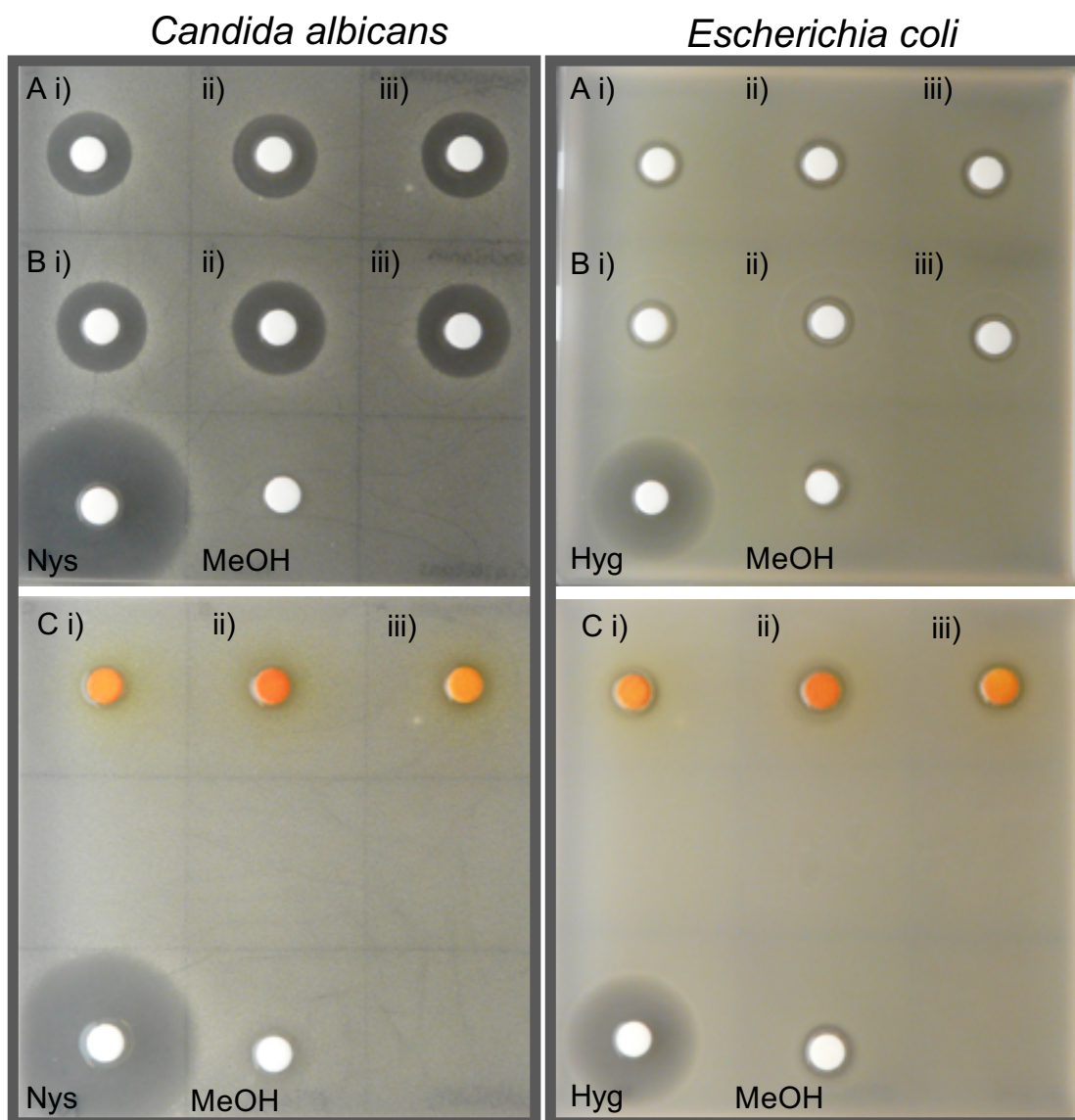


Figure 3.16 Disc-diffusion bioassays using compounds purified from *Streptomyces* strain N2 against *Candida albicans* and *Escherichia coli*. Discs were soaked in purified extracts of either **A**) fungichromin, **B**) 14-hydroxy(iso)chainin or **C**) actinomycin. N=3 (i-iii) technical replicates of each extract. Nystatin (Nys) or hygromycin (Hyg) were used as a positive controls and methanol (MeOH) was used as a negative control.

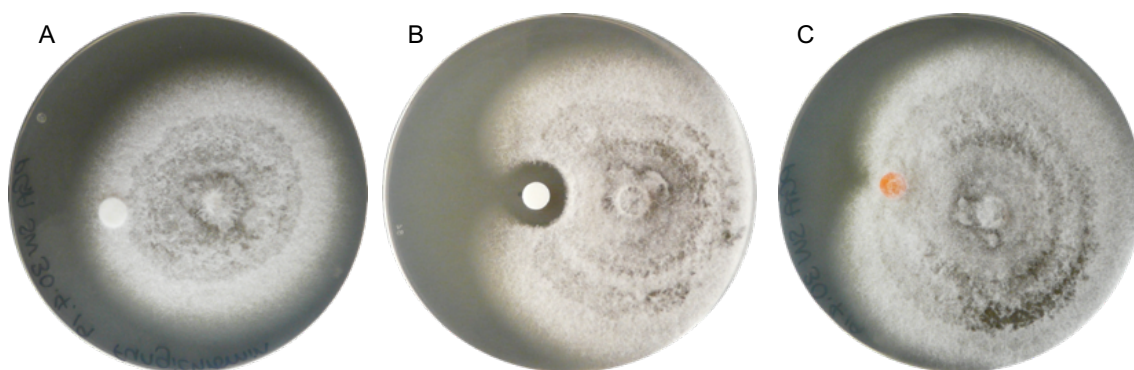


Figure 3.17 Disc-diffusion bioassays using compounds purified from *Streptomyces* strain N2 against *G. graminis*. Discs were soaked in purified extracts of either **A)** fungichromin, **B)** 14-hydroxy(iso)chainin or **C)** actinomycin. Antifungal activity is indicated by a zone of clearing around the disc.

3.4.4 The impact of *Streptomyces* isolates on plant growth

There are several studies showing that, in addition to producing antimicrobials, *Streptomyces* species can contribute to an increase in plant biomass. In order to test whether *Streptomyces* isolates could increase the growth of *Arabidopsis thaliana*, both *in vitro* and *in vivo* plant growth promotion assays were carried out in agar plates and soil, respectively.

3.4.5 The impact of *Streptomyces* isolates on plant biomass *in vitro*

To investigate whether the *Streptomyces* isolates could promote plant growth *in vitro*, pre-germinated *Streptomyces* spores were added to the roots of newly-germinated *Arabidopsis thaliana* seedlings. The inoculation of roots with different isolates had a significant effect on total plant dry weight (Figure 3.18, ANOVA test on log-transformed biomass: $F_{(10,165)} = 23.62$, $P < 0.001$). The endophyte strains L2, M2 and M3 all significantly increased plant biomass compared to sterile control plants (Figure 3.18 and Figure 3.19, $P < 0.05$ in a Tukey's HSD tests). However, not all strains promoted plant growth; application of *Streptomyces* strains N1 (Figure 3.19) and N2 significantly reduced the growth of *A. thaliana* (Figure 3.18, $P < 0.05$ in Tukey's HSD tests) and in some cases resulted in a senescence phenotype with leaf browning. It is possible that some of the BGCs in the genomes of these strains may encode novel herbicidal compounds, or that some of the other natural products produced by isolates N1 and

N2 are phytotoxic when expressed at high concentrations. For example, filipin-like compounds (produced by strain N2) are known to bind to and sequester sterols in the plasma membranes of fungal and mammalian cells and a small number of studies have shown that these compounds can also bind to phytosterols in plant cell membranes (Bonneau et al 2010, Grebe et al 2003, Moeller and Mudd 1982). At high concentrations, this can reduce root tip growth and eventually induce plant cell mortality (Bonneau et al 2010).

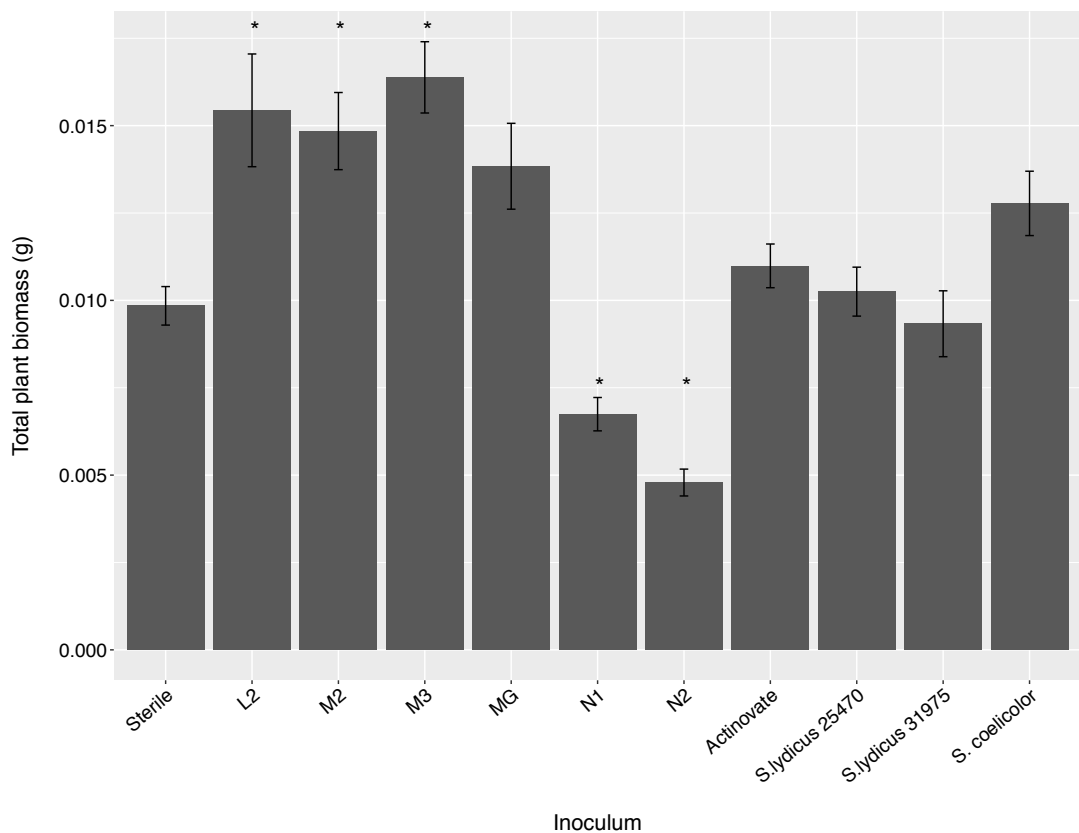


Figure 3.18 The average biomass of *Arabidopsis thaliana* plants growing on agar plates, following inoculation with different *Streptomyces* isolates. Biomass (dry weight in grams) was measured 16 days after inoculation. Sterile plants were grown as a control. N= 16 plants per treatment. Error bars represent standard errors. * represents treatments in which biomass was significantly different from the sterile control ($P < 0.05$ in a Tukey Kramer HSD test).



Figure 3.19 Plant growth phenotypes following inoculation with different streptomycete strains. *Arabidopsis thaliana* plants were either sterile (left), or inoculated with the *Streptomyces* isolates N1 (middle) or M3 (right). Images were taken 16 days after inoculation. Scale bar = 1 cm.

3.4.6 The impact of a mixture of *Streptomyces* isolates on plant biomass *in vivo*

In order to establish whether the growth promoting properties of the strains L2, M2 and M3 observed *in vitro* (Figure 3.18) could be further extended to growth promotion *in vivo*, *Arabidopsis* seeds were incubated with a spore preparation containing an equal ratio of the three strains. Seeds were then sown into compost and the biomass of plants was measured after six weeks of growth. Total plant dry weight appeared to increase, although with some variability, in plants inoculated with a combination of M2, M3 and L2, compared to those that had germinated from sterile seeds (Figure 3.20 and Figure 3.21). Likelihood ratio tests comparing linear mixed effects models with or without treatment (sterile or inoculated seeds) as a fixed effect (experimental run was controlled for as a random effect), confirmed that the inoculation of seeds with a mixture of streptomycete strains significantly increased plant biomass ($\chi^2(1)=7.37$, $P < 0.01$) from an average of $26.26 \text{ mg} \pm 4.79$ (SE) to an average of $45.22 \text{ mg} \pm 4.97$.

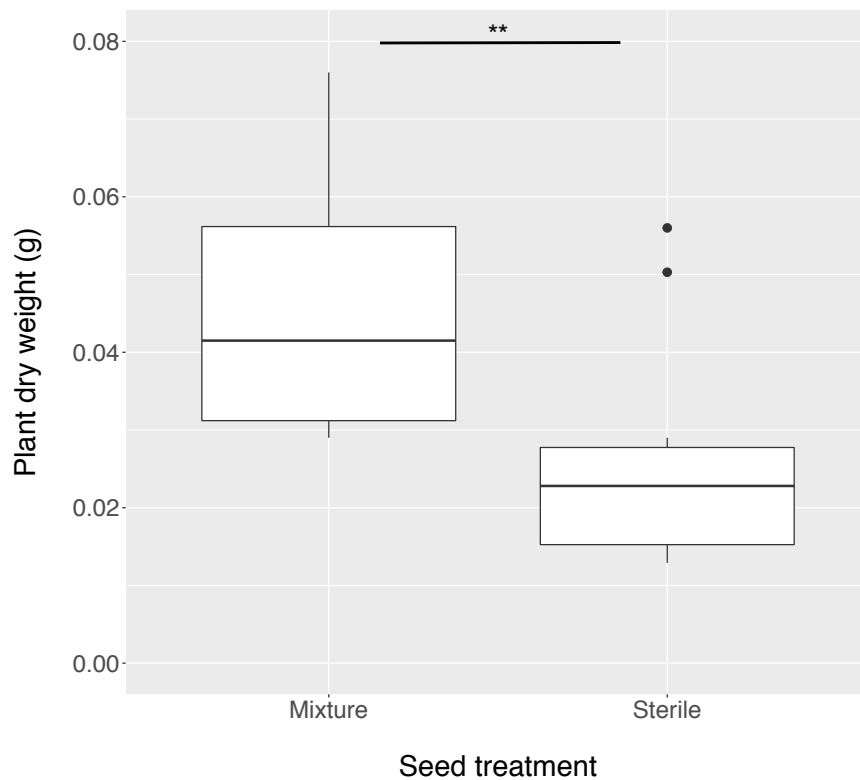


Figure 3.20 Total dry weight of *Arabidopsis thaliana* plants grown in Levington compost from seeds inoculated with a mixture of L2, M2 and M3 *Streptomyces* spores. Dry weight is shown in grams. Sterile seeds were grown as a control. The experiment was run twice with $n = 5$ replicate plants per treatment, per experiment. ** represents a significant difference ($P < 0.01$) between treatments based on likelihood ratio tests.

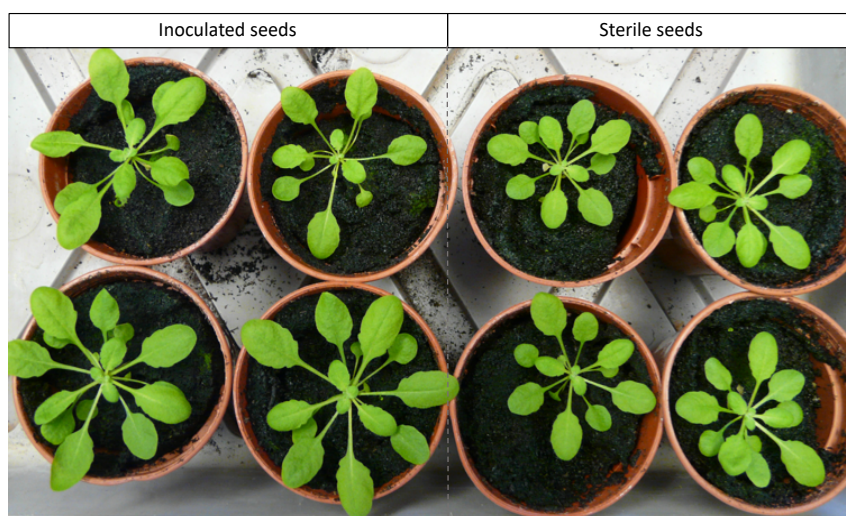


Figure 3.21 Plant growth promotion by a mixture of *Streptomyces* strains. *Arabidopsis thaliana* plants were grown from seeds inoculated with a mixture of L2, M2 and M3 *Streptomyces* spores (left), or from sterile seeds (right).

3.4.7 Production of plant-growth-promoting compounds

Streptomyces are known to produce several compounds that may contribute to an increase in plant biomass. For example, several strains are known to produce plant phytohormones including the compound indole-3-acetic acid (IAA) which is a precursor to the phytohormone auxin and can contribute to shoot and root growth (Remans et al 2006). In order to establish whether the genome-sequenced isolates in this study had the potential to produce IAA, genome sequences were annotated using the KEGG Automated Annotation Server (KAAS). Annotated genomes were then submitted for KEGG pathway analysis, which revealed all genomes carried genes encoding proteins involved in some of the pathways that are known to produce IAA (Table 3.8). For example, all strains have genes encoding key proteins involved in the indole-3-acetamide (IAM) pathway (Table 3.8), whereby tryptophan is converted to IAM via a tryptophan 2-monooxygenase enzyme (KEGG reaction R00679). IAM is then further converted to IAA through the action of an amidase enzyme (KEGG reaction R03096). The strain Actinovate also possessed genes with significant homology to enzymes involved in the tryptamine (TAM) pathway (Table 3.8), which converts tryptophan to tryptamine and then to IAA via an amine oxidase enzyme (R02173) and an acetaldehyde oxidase enzyme (R02681), respectively. Several other strains also had two out of the three enzymes in the TAM pathway, required to convert tryptamine to IAA (Table 3.8).

Table 3.8 The presence and absence of genes encoding enzymes involved in plant growth promotion pathways in sequenced *Streptomyces* isolates.

Green indicates the presence of the enzyme in a given isolate, red indicates the absence of the enzyme.

Pathway	Enzyme	KO number	Kegg Reaction	Reaction	<i>Streptomyces</i> strain									
					MG	M2	M3	N1	N2	L2	S.lydicus 25470	S.lydicus 31975	Actinovate	
IAA biosynthesis: IpyA pathway	Tryptophan aminotransferase	K14265	R00684	Tryptophan -> Indole-3-pyruvate	Red	Red	Red	Red	Red	Red	Red	Red	Red	Red
	Indole-3-pyruvate decarboxylase	K04103	R01974	Indole-3-pyruvate -> Indole-3-acetaldehyde	Red	Red	Red	Red	Red	Red	Red	Red	Red	Red
	Acetaldehyde oxidase/dehydrogenase	K11817/K00128	R02681/R02678	Indole-3-acetaldehyde -> Indole-3-acetic acid	Green	Green	Green	Green	Green	Green	Green	Green	Green	Green
IAA biosynthesis: IAM pathway	Tryptophan 2-monooxygenase (IaaM)	K00466	R00679	Tryptophan -> Indole 3-acetamide	Green	Green	Green	Green	Green	Green	Green	Green	Green	Green
	IAM hydrolase (IaaH)	K01426/K21801	R03096	indole 3-acetamide -> Indole 3-acetic acid	Green	Green	Green	Green	Green	Green	Green	Green	Green	Green
IAA biosynthesis: IAN pathway	Nitrilase	K01501	R03093	3-Indoleacetonitril -> Indole 3-acetic acid	Red	Red	Red	Red	Red	Red	Red	Red	Red	Red
IAA biosynthesis: TAM pathway	Tryptophan decarboxylase	K01593	R00685	Tryptophan -> Tryptamine	Red	Red	Red	Red	Red	Red	Green	Red	Green	Green
	(Mono or di) Amine oxidase	K00274/K11182	R02173	Tryptamine -> indole-3-acetaldehyde	Green	Green	Red	Green	Red	Green	Red	Green	Green	Green
	Acetaldehyde oxidase/dehydrogenase	K11817/K00128	R02681/R02678	Indole-3-acetaldehyde -> Indole-3-acetic acid	Green	Green	Green	Green	Green	Green	Green	Green	Green	Green
ACC degradation	1-aminocyclopropane-1-carboxylic acid (ACC) deaminase	K01505	R00997	1-aminocyclopropane-1-carboxylate + H2O -> 2-oxobutanoate + ammonia	Green	Green	Green	Green	Green	Green	Green	Green	Green	Green

In order to test whether strains were able to make IAA-related compounds *in vitro*, colorimetric assays were carried out, whereby newly-isolated *Streptomyces* strains were grown on cellophane discs covering agar plates. Cellophanes (and bacterial biomass) were then removed and plates were flooded with Salkowski reagent (as in Bric et al 1991) which qualitatively suggested that strains had the ability to make IAA, since a red colour was observed on the plates (Figure 3.22). Further biochemical analysis, for example mass spectrometry analysis of extracts compared to an auxin standard, would be needed to further confirm that the strains were indeed producing the IAA compound.

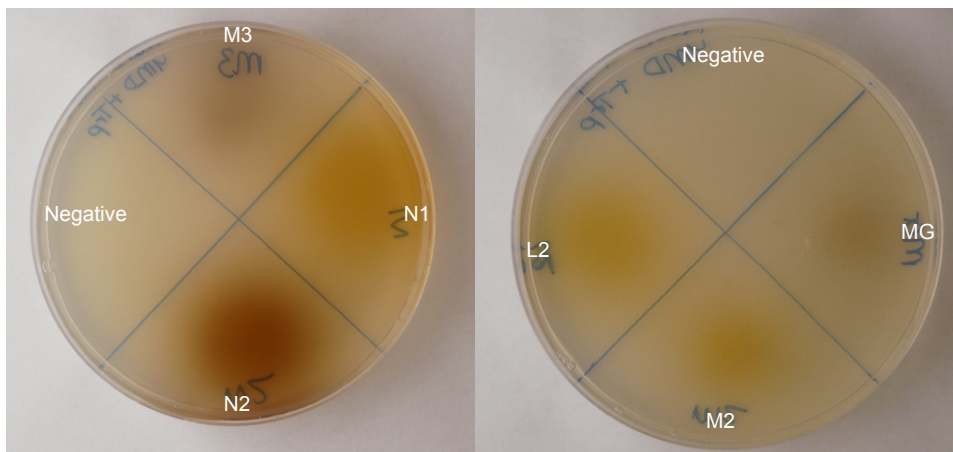


Figure 3.22 The *in vitro* production of IAA by *Streptomyces* isolates. Assays were carried out for *Streptomyces* strains M3, N1, N2, MG, M2 and L2. Isolates were grown on cellophanes covering YMD agar supplemented with 5 mM tryptophan for 7 days. Cellophanes were removed and plates were flooded with Salkowski reagent. A red/pink colour indicates IAA has leached into the media. Negative = no colony was grown on this part of the cellophane.

In addition to IAA, the genomes of all streptomycete isolates possess up to two copies of genes encoding the enzyme aminocyclopropane-1-carboxylate (ACC) deaminase (Table 3.8). This cleaves ACC, the direct precursor to the plant phytohormone ethylene, into ammonia and 2-oxobutanoate, (Kegg reaction: R00997). Bacteria can use the products of this reaction as a nitrogen source (Glick 2014). It was demonstrated that, *in vitro*, all tested isolates were capable of utilising ACC as a sole

nitrogen source when added to minimal medium (Figure 3.23). Interestingly, a query of the ActinoBlast database (Chandra and Chater 2014) demonstrated that the ACC deaminase enzyme is relatively common in *Streptomyces* species, but absent from many other Actinobacterial genera. Actinoblast is a database curated from reciprocal BLASTp best hits between the genomes of *S. coelicolor* A3(2) and more than 100 other actinobacterial genomes and can be used to gain an understanding of the distribution of genes across the phylum (Chandra and Chater 2014).

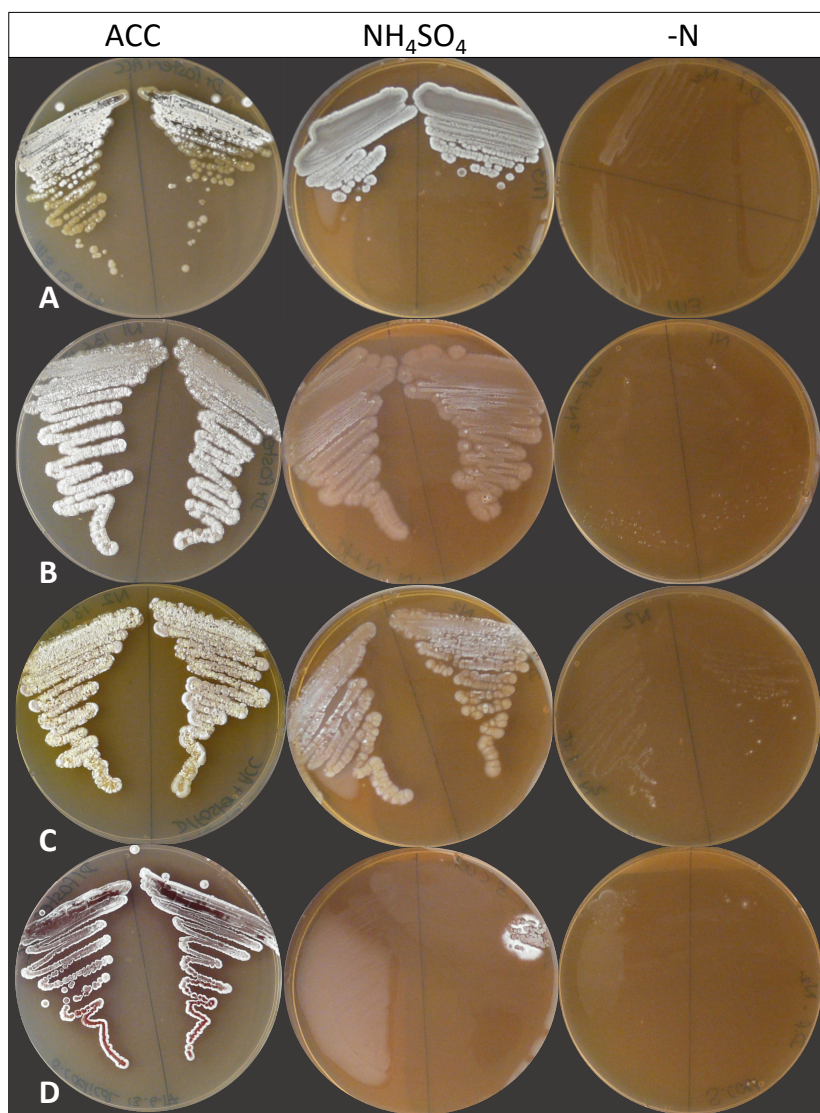


Figure 3.23 The use of ACC as a sole nitrogen source. *Streptomyces* strains **A)** M3, **B)** N1, **C)** N2 or **D)** *Streptomyces coelicolor*, were grown on Dworkin and Foster medium containing either 1-aminocyclopropane-1-carboxylic acid (ACC) or NH₄(SO)₄ as a sole nitrogen source, or no nitrogen (-N) as a control.

3.5 Discussion

This chapter set out to isolate *Streptomyces* species from the root microbiome of *Arabidopsis thaliana* and characterise them in terms of their genomic potential to produce antimicrobial and plant-growth-promoting agents. This was then followed by an investigation into whether this potential translated into an ability to produce compounds *in vitro* and to promote plant fitness *in vivo*. Experiments with newly-isolated *Streptomyces* strains were carried out alongside *Streptomyces lydicus* species that are associated with the biocontrol and the plant-growth-promoting agent Actinovate®, as well as the model species *S. coelicolor* M145.

Genome sequencing of the plant-associated *Streptomyces* isolates, followed by biosynthetic analysis, revealed that each of the strains was predicted to encode a wealth of biosynthetic gene clusters (BGCs), many of which showed homology to compounds commonly associated with interspecific competition, such as bacteriocins, polyketide synthases and non-ribosomal peptide synthases. These may provide species with a competitive advantage in the rhizosphere and endosphere, but might also contribute to host plant protection due to their antimicrobial activities. However, when tested *in vitro*, there was large variation in the ability of different strains to inhibit different pathogenic species, regardless of the number of BGCs encoded, and antimicrobial activities were highly dependent on the type of medium used as a growth substrate. As whole genome sequencing has become more accessible it has become clear that this is a commonly observed phenomenon; many actinomycetes are predicted to encode an abundance of antimicrobial BGCs, but the vast majority of these remain “silent” under laboratory conditions (Bentley et al 2002, Chater 2016, van der Meij et al 2017). Antimicrobial production is considered to be a metabolically expensive process since BGCs can stretch across tens of kilobases in a genome and the construction and transportation of resulting products can require a large amount of energy (van der Meij et al 2017). Therefore, antibiotic production tends to be a tightly regulated process that is intimately tied to the abiotic and biotic conditions of the surrounding environment and to the ecological conditions in which strains evolved (Seipke et al 2012b, van der Meij et al 2017). *Streptomyces* have a huge diversity of regulatory, sensory and transport proteins all allowing them to monitor and respond

to changes in their external environment (van der Meij et al 2017). Such ecological dependence is one of the reasons why many antibiotics are not seen to be expressed *in vitro*, but can sometimes be switched on by altering media components, as was seen for the strains isolated in this chapter. However, in addition to changing between commonly used media types, it is likely that the real challenge is to replicate conditions found in the strain's native environment, in this case the plant root microbiome, in order to induce antimicrobial production.

The plant root microbiome is a highly competitive environment, in which there are likely to be many different chemical cues coming from a variety of different sources, including components of the soil, other competing organisms, as well as the host plant in the form of carbon-rich and organically diverse root exudates (Adnani et al 2017, van der Meij et al 2017). Co-culture with other species aims to replicate the competitive conditions observed in natural environments and has seen some success in switching on silent clusters in various fungi and bacteria (Adnani et al 2017, Bertrand et al 2014, Onaka et al 2011, Wang et al 2013b). Genera such *Pseudomonas* were abundantly isolated from the compost used for growing *Arabidopsis* plants in this chapter and it is possible that co-culture with competitors such as these may elicit antimicrobial production in *Streptomyces* strains.

Host plant cues may also be involved in modulating the production of antimicrobials in root-associated microbial strains. Plants exude up to 20-40% of photosynthetically fixed carbon out of their roots (Haichar et al 2016, Whipps 1990), and these exudates contains a whole range of amino acids, organic acids, carbohydrates and fatty acids, many of which can serve as nutrients, or as antimicrobials (Badri and Vivanco 2009, Badri et al 2013, Chaparro et al 2013, Chaparro et al 2014). Several studies have implicated the role of plant phytohormones in switching on antimicrobial BGCs. For example, the precursor to auxin, IAA, stimulates aerial hyphae formation in some *Streptomyces* strains and can also upregulate antibiotic production by plant-associated *Streptomyces* species, as well as other rhizobacteria *in vitro* (Daddaoua et al 2018, Matsukawa et al 2007, van der Meij et al 2018). Root exudation is a dynamic process and exudate components shift with plant age and abiotic stressors (Badri and Vivanco 2009, Badri et al 2013, Chaparro et al 2013, Chaparro et al 2014). Interestingly,

pathogenic infection can also alter root exudation (Lanoue et al 2010, Yuan et al 2018). It has been postulated that such changes may represent a “cry for help” from the plant host, causing shifts in microbiome composition but also potentially leading to the upregulation of antagonistic compounds by beneficial, protective species (Lebeis et al 2015, van der Meij et al 2017, Yuan et al 2018). For example, changes in barley root exudates infected with *Pythium* have been shown to upregulate antimicrobial production by the biocontrol strain *Pseudomonas fluorescens* (Jousset et al 2011). Thus, growth media containing a combination of different root exudates, particularly those upregulated in response to pathogenic infection, may switch on antimicrobial production in root-associated *Streptomyces* isolates. It was interesting to note that several isolates, particularly MG, grew poorly on many types of media; this perhaps indicates that some of the isolates are primarily adapted and finely-tuned to growth conditions present within the root niche. Thus, understanding conditions in the endophytic compartment, as well as plant-microbe regulatory networks, may be a crucial next step for unlocking the biosynthetic potential of strains isolated from the root microbiome as well as for improving the functionality of biocontrol agents *in vivo*. Additionally, it will also be important to test all strains for their ability to inhibit plant pathogens *in vivo*, since strains that produce a low diversity of antimicrobial secondary metabolites may still protect the plant host via activation of the plant immune system (ISR) or by competitive exclusion (Kurth et al 2014). Indeed, a study that screened over 50 *Streptomyces* strains for their ability to inhibit the growth of *Phytophthora* species, demonstrated that *in vitro* antagonism was a poor predictor of the ability of strains to protect alfalfa and soybean seedlings *in vivo* (Xiao et al 2002). Instead, the ability of strains to increase plant biomass upon inoculation was a stronger predictor of disease outcomes (Xiao et al 2002). Thus, there is also a need to develop better proxies that represent the ability of strains to elicit the host defense response and provide protection *in situ*.

Although there was variability in secondary metabolite production by strains *in vitro*, some of the isolates demonstrated very potent antimicrobial activity against a wide range of pathogenic indicator strains. This included inhibition of the multi-drug resistant fungal pathogen *Lomentospora prolificans* and the Gram-negative pathogen *Escherichia coli*, both of which are normally very difficult to target with antimicrobials

(Fischbach and Walsh 2009, Pellon et al 2018). Increasingly, systems in which many species interact (such as in microbiomes), and particularly those in which there are beneficial partnerships between hosts and protective microorganisms, are being shown to be a key source of novel antimicrobials with unique activities (Adnani et al 2017, Chevrette et al 2019, Kaltenpoth 2009, Seipke et al 2012b). Since microbial symbionts continuously interact with their host organism and must also compete with other microbial species in order to take advantage of the host niche, selective pressures and coevolutionary dynamics may result in a continuous supply of novel compounds (Adnani et al 2017). Such compounds may also be less toxic to eukaryotic organisms, if they originally evolved as a result of a symbiotic partnership with a eukaryotic host (Adnani et al 2017). Since many of the BGCs predicted by antiSMASH analysis showed low percentage homology to known BGCs it is possible that some of the isolates from this chapter encode novel compounds. In particular, the genome of N2 did not contain any clusters that would obviously result in the inhibition of Gram-negative bacteria and none of the purified compounds from this strain, including generally toxic molecules like actinomycin, were bioactive against *E. coli* despite N2 inhibiting this species *in vitro*. Attempts to isolate the compound responsible using methanol and ethyl acetate extractions were unsuccessful, possibly because these were unsuitable solvents.

The *Streptomyces* strain N2, showed particularly broad-spectrum antimicrobial activity and demonstrated antifungal activity against *L. prolificans*, *C. albicans* and the wheat take-all fungus, *G. graminis*. This antifungal activity partially extended to the inhibition of wheat take-all disease *in vivo* with a significant reduction in infection severity of wheat plants grown from seeds inoculated with N2 spores. However, infection was only reduced in aerial parts of the plant and appeared to have been slowed rather than eliminated completely. A disadvantage of the assay was that it was conducted in sterile vermiculite, a silicate mineral commonly used as a soil substitute or aeration additive, which provides very limited levels of organic nutrients. Thus, N2 proliferation and antimicrobial production may have been reduced in this environment. It is possible that in soil, an enhanced availability of organic nutrients and the presence of many competing organisms could have driven greater antimicrobial production. Organic matter has previously been shown to modulate the success of some biocontrol agents

by sustaining their growth (Hoitink and Boehm 1999). However, it is also possible that biocontrol would have been further reduced in soil if the strain was outcompeted by other rapidly-growing soil microbes. In order to understand these dynamics, it will be crucial to conduct further assays in field soils to assess whether strains can protect plant hosts under meaningful environmental conditions. Additionally, different seed application techniques can influence the viability of strains and their subsequent proliferation on the seed surface and in the rhizosphere (O'Callaghan 2016, Spadaro and Gullino 2005). Thus, the mode of application of biocontrol strains could also alter their antibiotic-producing potential *in situ*.

In addition to the use of a soil growth medium, a combination of streptomycete isolates may have further enhanced the reduction in take-all infection severity observed in wheat plants. It is increasingly being shown that compatible biocontrol strains can have synergistic effects on plant protection (de Boer et al 2003, Ezziyyani et al 2007, O'Callaghan 2016). For example, a combination of strains of *Pseudomonas putida* was able to greatly reduce the severity of wilt disease caused by *Fusarium oxysporum*, because one strain produced siderophores that competed with the pathogen for iron, which in turn increased the efficacy of induced systemic resistance brought about by the second strain (de Boer et al 2003). Co-inoculation is also advantageous since it increases the range of environmental conditions under which a seed treatment is likely to be active and different strains could produce multiple bioactive compounds that have differing modes of action against the same pathogenic organism; this may help to reduce the potential for the evolution of pathogen resistance (O'Callaghan 2016, Spadaro and Gullino 2005). Multiple compounds could also target many soil-borne pathogens simultaneously (O'Callaghan 2016, Spadaro and Gullino 2005).

An analysis of the N2 genome suggested that it may produce the antifungal compound filipin and further biochemical and structural analysis confirmed that it was indeed producing filipin-like compounds. This included the compound fungichromin, also called pentamycin, which shares the same 28-membered polyene macrolide ring present in filipin III but with an additional hydroxyl group at the C-14 position. The additional hydroxyl group is potentially derived from a P450 monooxygenase enzyme

located in an adjacent NRPS cluster. Additionally, the compound 14-hydroxy(iso)chainin was also isolated from N2 extracts which shares the same structure as fungichromin but carries a shorter sidechain. Fungichromin was first described in the 1950's (Cope and Johnson 1958, Umezawa et al 1958) and is widely used as a fungicidal drug to treat infectious vaginitis in humans (Frey Tirri et al 2010, Kranzler et al 2015, Xiong et al 2012). However, several plant-associated streptomycete strains also produce this compound including those isolated from *Rhododendron* and *Protea* species (Human et al 2016, Shimizu et al 2004). Additionally, fungichromin isolated from the putative species *S. padanus* (which is part of the same clade to which N2 belongs) has been shown to reduce the severity of damping-off disease caused by *Rhizoctonia solani* in cabbage and ginseng plants (Shih et al 2003, Van Minh et al 2017).

Interestingly, although the fungichromin (purified from N2) was found to be active against *C. albicans* it did not show activity against the wheat Take-all fungus *in vitro*, whereas 14-hydroxy(iso)chainin (also isolated from N2) was able to inhibit the growth of both strains. It is possible that the modified structure of 14-hydroxy(iso)chainin makes it more active against wheat take-all, however, as polyene macrolides can be relatively unstable in solution, it is also conceivable that fungichromin degraded over the 5 day period used for wheat take-all bioassays, resulting in an absence of antifungal activity. Thus, a deeper investigation into the stability of these compounds will be required before differences in their specificity can be accurately evaluated. However, the fact that 14-hydroxy(iso)chainin remained stable enough to inhibit the wheat take-all fungus over the same period suggests it may be a more promising candidate for biocontrol. As mentioned, the compound 14-hydroxy(iso)chainin has only been identified in a single precursor-directed biosynthesis experiment in which *Streptomyces cellulosa* was provided with structural analogues of oleic acid (a required precursor for fungichromin production); this initiated the production of compounds that were similar to fungichromin, but that had altered side chains, including isochainin and derivatives such as 14-hydroxy(iso)chainin (Li et al 1989). Thus, expression of the same BGC appears to be able to produce multiple variants of the same bioactive compound depending on the substrates available and each derivative may have different stabilities and activities that could be exploited for

biocontrol purposes. This phenomenon is widespread in nature and may have evolved to generate chemical diversity and increase the chances of inhibitory activity against competitors at a low cost (Fischbach and Clardy 2007). In addition to the diversity of compounds produced by N2, the low toxicity that has been reported for fungichromin against both mammalian and plant cells (Xiong et al 2012) suggests that N2 may be a good candidate for providing protection against wheat take-all if antifungal production can be enhanced *in situ*, potentially in combination with other streptomycetes .

An ideal experiment to confirm the role of filipin-based compounds in contributing to the antifungal activity of N2, and to determine whether other BGCs were also responsible for this activity, would have been to delete the filipin gene cluster in N2 and re-run the bioassay experiments. Attempts were made to do this using CRISPR/Cas9 technology as well as by use of a suicide vector. However, despite generating two complete pCRISPomyces-2 plasmids with two different guide RNAs, as well as a complete suicide vector containing the flanking regions of the filipin cluster, conjugations between *E. coli* carrying these plasmids and N2 were unsuccessful. Previous experiments with N2 have suggested that this strain may have a very low conjugation efficiency (only two successful exconjugants were made when transforming N2 with an eGFP carrying plasmid). Extensive attempts to increase conjugation efficiency were made, for example by altering MgCl₂ and CaCl₂ ratios in conjugation plates, altering N2 spore concentrations, as well as the pre-germination conditions and conjugation media. However, despite these attempts, no successful filipin deletion mutant could be made. In the future, protoplast transformation could be used as an alternative tool to introduce plasmids into N2.

In addition to the production of antimicrobial agents, several of the newly-isolated plant-associated *Streptomyces* strains significantly enhanced the growth of *Arabidopsis thaliana* plants *in vitro*. In comparison, *S. lydicus* strains, which contribute to the biocontrol and plant-growth-promoting agent Actinovate[®], did not have any effect on plant growth. The most promising strains M2, M3 and L2 were also able to promote plant biomass *in vivo* when added in combination. Analysis of the genomes of these strains suggested that they carry several genes associated with plant-growth-promotion, for example those involved in the production of IAA and ACC deaminase.

However, further biochemical and genetic analysis would be needed to confirm the role of these genes in plant-growth-promotion.

Plant-growth-promotion was not universal, however, as two isolates (N1 and N2) significantly reduced the growth of *A. thaliana* seedlings *in vitro*. BGC analysis of the *Streptomyces* strain N2 suggested that this strain had the potential to produce the compound actinomycin, which is generally toxic to eukaryotic cells, as it interferes with mRNA synthesis during transcription and thus, could have contributed to the observed plant phenotype (Katz 1967). N2 was also shown to produce low levels of filipin *in vitro*, which is known to target sterols in plasma cell membranes and can result in the lysis of mammalian and fungal cells (Behnke et al 1984, Bonneau et al 2010, Payero et al 2015). Several studies have also shown that filipin can bind to phytosterols present in the plasma cell membranes of plants (Bonneau et al 2010, Grebe et al 2003, Moeller and Mudd 1982); at high concentrations this can result in cell mortality and inhibition of root hair growth (Bonneau et al 2010). However, at sub-lethal concentrations, filipin can trigger changes to plasma membrane viscosity that results in the activation of signaling pathways involved in the controlled production of ROS by tobacco plant cells; such changes to membrane structure are thought to be important in allowing the plant to sense and respond to changes in its surrounding environment (Bonneau et al 2010). Interestingly, although N2 appeared to inhibit the growth of *Arabidopsis thaliana* *in vitro*, it was not observed to have the same effect on wheat during *in vivo* bioassay experiments. Thus, the beneficial or detrimental effects of strains may be specific to a particular plant host species. However, it is also possible that filipin and other toxic antimicrobials like actinomycin, were only produced at sub-inhibitory concentrations under the conditions used for wheat bioassay experiments, whereas concentrations on agar plates could have resulted in the growth inhibition observed in *A. thaliana* plants. Although beyond the scope of experiments carried out in this Chapter, it would be interesting to establish the true environmental concentrations of antibiotics produced by streptomycetes introduced to the plant root microbiome. Some studies have suggested that antibiotic production actually plays a relatively minor role in suppressing plant pathogens in the plant root niche due to low levels of production or compound concentrations (Hennessy et al 2017, Koch et al 2018). Instead competitive exclusion may be more important for inhibiting the establishment of pathogenic

species (Koch et al 2018). However, given the potential for sub-inhibitory concentrations of antibiotics to influence plant cell signaling (Bonneau et al 2010), it would also be of interest to assess the role that such compounds could play in enhancing plant host resistance to pathogenic infection, for example via inducing systemic activation of the plant immune system.

In conclusion, the experiments reported in this chapter identified several plant-associated *Streptomyces* species that have the biosynthetic potential to produce an array of compounds that may contribute to competence in the rhizosphere and endosphere, as well as plant host growth and protection. The next challenge is to establish the extent to which compounds are expressed in the root microbiome as well as the cues responsible for eliciting antimicrobial production by different *Streptomyces* isolates *in situ*. This will help to establish the role that *Streptomyces* secondary metabolites can play in reducing pathogen infection under variable conditions *in vivo* and will ultimately provide information for the development of more consistent biocontrol strategies. In order to develop efficient biocontrol strains, it will also be necessary to determine plant host factors that influence the establishment of microbial species within the plant root microbiome and the competitiveness of introduced strains. The role of root exudates in directing plant root microbiome formation will be examined in Chapters 4 and 5.

Chapter 4 The role of root exudates in plant root microbiome establishment

4.1 Introduction

The plant root microbiome is a complex and diverse ecosystem consisting of a dynamic community of microorganisms. However, as discussed in Chapter 3, there is often a high level of consistency in the composition of the root microbiome across members of the same plant species. This includes the species *Arabidopsis thaliana*, in which particular families of Proteobacteria and Actinobacteria are found to be enriched in the roots compared to the surrounding bulk soil, regardless of the soil type used as a growth medium (Bodenhause et al 2013, Bulgarelli et al 2012, Lundberg et al 2012). Distinct microbiome assemblages have also been noted across a wide range of other cultivated and uncultivated plant species (Costa et al 2006, Dias et al 2012, Edwards et al 2015, Garbeva et al 2008, Haichar et al 2008, Philippot et al 2013). The consistent association between plant hosts of a particular genotype and specific microbial taxa, strongly suggests that the plant host can influence the establishment of its own microbiome and that selection mechanisms exist which enable the host to filter microbial species from the surrounding soil. Understanding these mechanisms in greater detail is of interest, as these could be exploited to enhance the number of beneficial microbial species present within the plant root microbiome and therefore promote traits such crop growth and protection against disease (Dessaux et al 2016).

4.1.1 Vertical transmission

As discussed in Chapter 1, various host organisms vertically transmit beneficial microbial species between generations, either through the germline or via the inoculation of sterile offspring, in order to ensure the colonisation of certain bacterial strains and provide them with a competitive advantage in the host niche (Foster et al 2017, Marsh et al 2014). A growing number of studies are investigating the role of plant seeds in the vertical transmission of the root and rhizosphere microbiome. Diverse communities of microorganisms have been isolated from the seeds of a variety of different plants species and in some cases these communities appear to be consistent across members of the same host species (Philippot et al 2013, Shahzad et

al 2018). Certain members of the seed microbiome have also been found to colonise the plant rhizosphere following germination, suggesting that they may contribute to the fitness of the adult plant (Bergna et al 2018, Johnston-Monje and Raizada 2011). However, other studies have demonstrated a high rate of turn-over, or inconsistency in the seed microbiome across generations (Philippot et al 2013, Shahzad et al 2018). Thus, the relative importance of vertical transmission for plant root microbiome establishment, versus the horizontal acquisition of bacteria from the soil, still remains unclear (Philippot et al 2013, Shahzad et al 2018). Additionally, since both endophytic and rhizosphere-associated bacterial communities are known to change significantly with factors such as plant age, abiotic conditions and biotic stressors, it is highly likely that additional mechanisms, other than vertical transmission, also play a role in directing the dynamic establishment of the plant root microbiome (Chaparro et al 2014, Haichar et al 2012, Lanoue et al 2010).

4.1.2 The role of plant root exudates

One proposed mechanism by which plants can selectively acquire particular groups of bacteria from the soil is via the secretion of carbon-based compounds. Plants are predicted to exude 20-40% of their photosynthetically fixed carbon into the soil via their roots (Badri and Vivanco 2009, Haichar et al 2016, Hiltner 1904). This leads to the so-called “rhizosphere effect”, first noted by Hiltner in 1904, which describes the increase in microbial abundance and activity found in the vicinity of plant roots. Root exudates contain a wide variety of different compounds including sugars, sugar alcohols, amino acids, organic acids and fatty acids, all of which could act as specific chemoattractant molecules, or as an energy source, for particular microbial taxa (Badri and Vivanco 2009, Badri et al 2013). Different plant species are known to produce different types of root exudate and this, in turn, is likely to influence microbiome composition, since different classes of root exudate likely recruit microorganisms with specific metabolic or chemotactic capabilities (Badri and Vivanco 2009, Haichar et al 2008(Badri and Vivanco 2009, Haichar et al 2008).

Several studies have purified root exudates from *Arabidopsis thaliana* and found that the concentrations of particular groups of compound tend to correlate with the abundances of certain bacterial genera (Badri et al 2013, Chaparro et al 2013,

Chaparro et al 2014). For example, the application of individual fractions of *A. thaliana* root exudates to soil demonstrated that sugars can act as general attractants for a broad range of microbes, whereas phenolic compounds, including organic acids, fatty acids and a range of amino acids, positively correlated with the abundances of particular bacterial taxa, including species of Actinobacteria, suggesting that these compounds may act as specific substrates or signaling molecules (Badri et al 2013). Additionally, some compounds were found to have opposing effects on different groups of bacteria. For example, the compound gamma-aminobutyric acid (GABA) was found to reduce the abundance of the sub-order Streptomycinae, but promoted the growth of several Proteobacterial genera (Badri et al 2013).

Other studies have used mutant plants in order to demonstrate the relationship between particular chemical pathways, root exudates and microbiome composition (Badri et al 2009, Bressan et al 2009, Carvalhais et al 2015, Huang et al 2019). For example, *A. thaliana* plants carrying mutations in the jasmonate pathway, which is usually activated in response to necrotrophic pathogens and herbivores, showed altered root exudation profiles, including reduced levels of tryptophan and asparagine but increased levels of other compounds such as fructose (Carvalhais et al 2015). These changes resulted in distinct bacterial and archaeal communities associated with mutant plant roots, including an increased abundances of genera such as *Bacillus*, which are known to respond chemotactically to fructose (Carvalhais et al 2015). Similarly, ABC transporter mutants of *A. thaliana* that produce a greater level of phenolic compounds compared to wildtype plants, were associated with greater abundances of beneficial bacteria, including those involved in plant growth promotion (PGP) and nitrogen fixation (Badri et al 2009).

Root exudation is a dynamic process with exudate profiles changing over the course of the plant lifecycle. In *A. thaliana*, sugars and sugar alcohols are found to be present at high abundances during earlier stages of plant development, but are then replaced with a greater abundance of amino acids and phenolics at later developmental stages (Chaparro et al 2013). Accordingly, shifts in the rhizosphere bacterial community have been shown to correspond with these changes, for example, Actinobacteria increase in abundance between seedling and vegetative stages, in line with an increase in the

level of phenolic compounds (Chaparro et al 2014). There is additional evidence that changes in root exudation could modulate the functionality of the plant root microbiome, independent of causing shifts in community composition, by altering the expression of particular bacterial genes over the course of development. For example, studies of *A. thaliana* have shown that bacteria that are capable of producing antagonistic compounds, such as *Streptomyces* species, are more transcriptionally active during later developmental stages, which may result in the suppression of pathogens or the induction of the plant immune system, enabling plants to remain healthy during flowering and seed development (Chaparro et al 2014). Changes to root exudation may additionally encourage the expression of antagonistic molecules indirectly, by driving interference competition between microbial species in the rhizosphere and endosphere (Viaene et al 2016).

In addition to changes brought about through plant development, root exudation has also been shown to respond to pathogenic infection. Several studies on barley and *A. thaliana* plants, have indicated that root exudate profiles change in response to foliar and soil-borne pathogens which, in turn, leads to changes in the rhizosphere and endophytic bacterial community composition (Jousset et al 2011, Lanoue et al 2010, Yuan et al 2018). For example, a study on *A. thaliana* showed that foliar infection with the pathogen *Pseudomonas syringae* resulted in an increased exudation of amino acids and long chain organic acids from plant roots and a concurrent change in the structure of the rhizosphere microbiome (Yuan et al 2018). Adding purified root exudates from infected plants to soil led to similar changes in microbial community composition and could also induce disease suppressiveness, suggesting that plants might recruit beneficial microbes upon attack, to better defend against pathogenic infection (Yuan et al 2018). A similar role as a “cry for help” molecule has been suggested for the compound salicylic acid; mutant plants that over-produce this plant defence phytohormone recruit different types of bacteria to their root microbiome, including greater abundances of *Streptomyces* bacteria that are presumed to aid the plant by producing antimicrobial compounds (Lebeis et al 2015, but see Chapter 5).

4.1.3 Determining the use of root exudates by bacteria in the plant root microbiome

Most of the studies described above have been carried out using root exudates that have been purified from plants grown in a sterile system, or have used correlation analyses to implicate the role of certain microbial taxa in using root exudates. However, the role of exudates in enhancing microbial biomass and recruiting certain species can be complex; whereas certain microbial taxa will use root exudates directly as a growth substrate, others will benefit indirectly by using the secondary products of the primary utilisers of root exudates. Another group of microbes will benefit from the contribution that root exudates can make towards activating the breakdown of soil organic matter (SOM), making it easier to use as a nutrients source in the vicinity of plant roots (Haichar et al 2008, Haichar et al 2016). Further techniques have been developed that enable the direct detection of root exudate metabolism by microbial groups *in vivo*. This includes the use of nucleic acid Stable Isotope Probing (SIP) experiments which enable isotopically labelled metabolites (e.g. those labelled with the heavy isotope of carbon, ^{13}C) to be tracked from the host organism to the nucleic acids of bacteria in the microbiome that metabolise host-derived resources (Dumont and Murrell 2005, Dunford and Neufeld 2010, Haichar et al 2016, Neufeld et al 2007, Radajewski et al 2000). In plants, this works by introducing $^{13}\text{CO}_2$ into sealed growth chambers, which is then fixed via photosynthesis into carbon-based metabolites (Figure 4.1). Labelled metabolites are then exuded out of the plant roots and are available to bacteria in the endosphere and rhizosphere. Bacteria that grow and divide using these resources will incorporate the ^{13}C isotope into nucleic acids. ^{13}C labelled nucleic acids extracted from the endosphere or rhizosphere can then be separated from those that are unlabeled (^{12}C) via density gradient ultracentrifugation (Figure 4.1). Following the fractionation of density gradients, community profiling of the labelled nucleic acids can enable the identification of bacteria that directly metabolise host-derived resources.

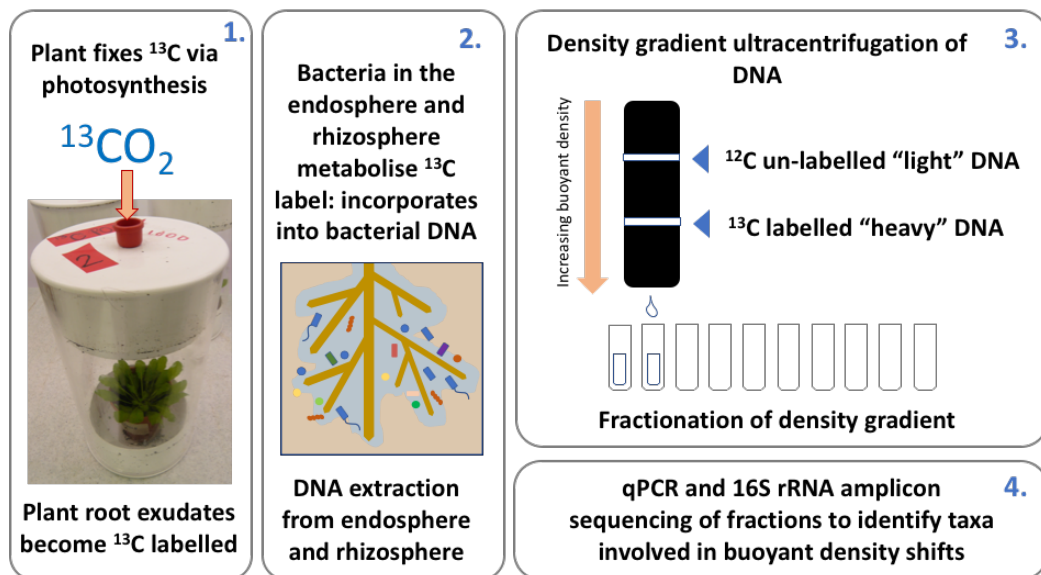


Figure 4.1 A schematic showing the steps involved in DNA Stable Isotope Probing (DNA-SIP) experiments, to establish the identity of bacteria responsible for metabolising root exudates in the rhizosphere and endosphere of plant roots.

SIP has been used in a variety of plant species to determine which microbial taxa (bacterial, archaeal or fungal taxa) are responsible for utilising plant root exudates (Table 4.1). Such studies have demonstrated that a subset of the microbial species present in the plant rhizosphere are able to utilise root exudates, whilst the remaining taxa are likely to make use of unlabeled soil organic matter that is activated by root exudation. This community of root exudate metabolisers can also be dynamic over time, differs between plant host species and can also change dramatically when mutant plants with different root exudate profiles are compared to wildtype plants (Bressan et al 2009, Haichar et al 2008, Haichar et al 2012, Hannula et al 2012). Many older SIP studies have used either Terminal Restriction Fragment Length Polymorphism (T-RFLP) or Denaturing Gradient Gel Electrophoresis (DGGE) of 16S rRNA gene amplicons, to profile the differences between bacterial communities responsible for metabolising root exudates. However, more recent studies on wheat, rice and oil seed rape (Table 4.1) have used 16S rRNA gene amplicon sequencing to determine all of the microbial taxa metabolising root exudates at greater resolution. Studies on wheat and oil seed rape have both shown that Actinobacteria were active metabolisers of root exudates in the rhizosphere, with the genus *Streptomyces* being active at all soil depths in the wheat system (Gkarmiri et al 2017, Uksa et al 2017).

Table 4.1 A summary of published Stable Isotope Probing (SIP) experiments investigating the microbial metabolisers of plant root exudates.

Plant species	Compartment	Nucleic acid	Profiling technique	Key findings	Reference
Grassland	Bulk soil and rhizosphere	RNA	DGGE	Microbial uptake of ^{13}C from plant exudates was low, except under continuously wetted treatments. Methods required optimisation.	(Griffiths et al 2004)
Grassland	Rhizosphere	RNA	DGGE	Bacterial, archaeal and fungal communities involved in the metabolism of exudates were more complex in limed versus un-limed soils, probably due to differences in the amount of exudation under different conditions.	(Rangel-Castro et al 2005)
Grassland	Rhizosphere	DNA	16S rRNA gene amplicon sequencing using Illumina MiSeq technology.	Plant nutrient availability and nutrient use strategy shapes the active microbiota involved in root exudate assimilation and SOM degradation.	(Guyonnet et al 2018)
Rice	Rhizosphere and bulk soil	RNA	Archaeal T-RFLP from RNA and sequencing of 16S rRNA clone libraries	^{13}C was incorporated into archaeal RNA in soil surrounding rice roots; plant-derived carbon was suggested to play a key role in archaeal CH_4 production in anoxic rice soils.	(Lu and Conrad 2005)
Rice	Endosphere and rhizosphere	RNA	Bacterial T-RFLP from RNA and sequencing of 16S rRNA clone libraries	Alpha- and Beta- Proteobacteria as well as Firmicutes were dominant in rice roots. Proteobacteria were the most active in assimilating root exudates.	(Lu et al 2006)

Rice	Roots and rhizosphere	RNA	454-sequencing amplicon sequencing of 16S rRNA gene	Proteobacteria and Verrucomicrobia were the most highly labelled. Different bacterial groups were labelled in the root and rhizosphere. A greater proportion of OTUs were labelled in the roots versus the rhizosphere.	(Hernandez et al 2015)
Potato	Rhizosphere	RNA	Fungal T-RFLP	Ascomycete, glomeromycete and basidiomycete fungi all accumulated labelled carbon. Fungal communities using root exudates were different in genetically modified potato varieties.	(Hannula et al 2012)
Potato	Rhizosphere	RNA	DGGE and sequencing of 16S rRNA clone libraries	Different potato cultivars were associated with different active bacterial genera metabolising root exudates.	(Dias et al 2013)
Wheat	Rhizosphere	DNA	454 amplicon sequencing of the 16S rRNA gene.	Root exudates were predominantly metabolised by Actinobacteria and Proteobacteria. Soil fertilisation reduced the use of root exudates by Actinobacteria.	(Ai et al 2015)
Wheat	Rhizosphere	DNA	16S rRNA gene amplicon sequencing using Illumina MiSeq technology.	Different bacterial communities use plant-derived resources in the rhizosphere of wheat at different soil depths. Proteobacteria were important in the topsoil, whereas Firmicutes and Bacteroidetes were active in the subsoil rhizosphere. <i>Streptomyces</i> were ¹³ C enriched at all depths.	(Uksa et al 2017)

Wheat	Rhizosphere	DNA	DGGE	Different bacterial phyla were metabolising root exudates in the rhizosphere of the four different plant species. Root exudates also activated communities involved in the degradation of SOM.	(Haichar et al 2008)
Maize					
Rape					
Barrel Clover					
Oil seed rape	Roots and rhizosphere	RNA	454-pyrosequencing of 16S and 18S rRNA genes.	Root and rhizosphere communities of bacteria and fungi differed. Planctomycetes and Actinobacteria were enriched in ¹³ C fractions of rhizosphere samples. Bacteroides were more active in roots.	(Gkarmiri et al 2017)
<i>Arabidopsis thaliana</i>	Rhizosphere	DNA	DGGE coupled with sequencing of enriched bands	Transgenic plants that produce exogenous glucosinolates were associated with different active bacterial communities versus wildtype plants . Alphaproteobacteria were predominantly affected.	(Bressan et al 2009)
<i>Arabidopsis thaliana</i>	Rhizosphere	DNA and mRNA	DGGE analysis of taxon-specific 16S rRNA gene fragments, followed by sequencing of specific bands.	Bacterial taxa responsible for metabolising root exudates changed over time in the rhizosphere. Certain genera of Proteobacteria and Firmicutes were using exudates.	(Haichar et al 2012)

4.1.4 Stable isotope probing experiments involving *Arabidopsis thaliana*

Two stable isotope probing experiments have investigated the metabolism of root exudates by microbial communities in the rhizosphere of *A. thaliana* (Table 4.1). The first study extracted DNA from the rhizosphere of ¹³C labelled plants at 3 different developmental time points (Haichar et al 2012). DGGE was then used to profile the microbial communities present in the heavy (labelled) and light fractions of DNA samples. DGGE enables profiling of the bacterial community in a sample by separating PCR amplified fragments of the 16S rRNA gene on a gel. Gels contain a linearly increasing gradient of denaturant which separates fragments of the same length based on sequence variation, as different bases alter the melting properties of different fragments (Muyzer et al 1993). The study found that bands present in heavy fractions on the gel were different during later developmental time points, suggesting that different bacterial taxa were metabolising root exudates at later stages of plant development, although these were not taxonomically identified (Haichar et al 2012). Group-specific primers, coupled with DGGE were then used to investigate the role of Alpha-, Beta- and Gamma- Proteobacteria, as well as Firmicutes in metabolising root exudates at the latest developmental time point, which showed that particular genera had greater access to root exudates than others (Haichar et al 2012). However, a comprehensive analysis of the total bacterial community was not carried out.

The second study used SIP to investigate whether microbial populations involved in the degradation of root exudates in the rhizosphere were altered in transgenic *A. thaliana* plants producing exogenous glucosinolates, relative to wild-type plants (Bressan et al 2009). Glucosinolates are compounds specific to several species of brassicaceous plants and can be hydrolysed by the plant to produce biocidal compounds. DGGE analysis of SIP fractions showed that plant genotype significantly altered the active microbial populations found in the rhizosphere, and group-specific primers for Alpha-, Beta- and Gamma- Proteobacteria as well as Acidobacteria, archaea and fungi were used to investigate changes for these specific groups (Bressan et al 2009).

In both of the stable isotope probing experiments involving *A. thaliana*, taxon-specific primers (coupled with DGGE analysis) were used to investigate the use of root exudates by particular microbial groups (Bressan et al 2009, Haichar et al 2012). However, neither of the studies investigated the role of Actinobacteria in the metabolism of root exudates, despite this phylum (and particularly the genus *Streptomyces*) having been reported as an abundant and important member of the rhizosphere and root compartments of several plant species, including *A. thaliana* (Bulgarelli et al 2012, Lundberg et al 2012, Viaene et al 2016). Additionally, the vast majority of plant SIP experiments have focused on microbial communities found in the rhizosphere, with little attention having been paid to the activity of microorganisms residing within the plant root tissue as endophytes (Table 4.1). However, similar to bacteria in the plant rhizosphere, endophytic bacteria can make large contributions to plant fitness by producing compounds that enhance plant growth and/or protect against disease (Brader et al 2014, Franco et al 2007, Liu et al 2017a). Endophytes may have a particularly large influence on plant fitness because they are in closer proximity to their plant host. Thus, these bacteria are receiving an increased level of interest from a biocontrol and plant-growth-promotion point of view (Franco et al 2007, Gaiero et al 2013, Strobel 2003). As a result, a more comprehensive analysis of the total bacterial community involved in utilising plant-derived metabolites in both the rhizosphere and endosphere of *A. thaliana* would be beneficial, as it would yield important information regarding the factors that influence the establishment, functionality and activity of the different bacterial taxa present within these two compartments.

4.2 Aims

Understanding the role of root exudates versus soil organic matter in recruiting certain microbial species to the root microbiome and in maintaining a diverse, beneficial root-associated microbial community could improve the development and efficacy of microbial-based PGP and biocontrol technologies. For example, this knowledge may help to direct plant breeding programmes towards developing plants that produce particular root exudate profiles (Dessaux et al 2016). It could also improve the development of microbial inoculation techniques that increase the competitiveness of beneficial microbial species in the plant root niche (Ryan et al 2009). Actinobacteria

are gaining increasing levels of interest as agents to promote plant fitness (Schrey and Tarkka 2008, Viaene et al 2016), and results presented in Chapter 3 demonstrated that *Streptomyces* species isolated from the *A. thaliana* root microbiome can both promote plant growth and protect against disease. However, previous SIP experiments have not investigated whether *Streptomyces* can use root exudates in the root microbiome of *A. thaliana*.

The aim of this chapter was to build on pre-existing SIP experiments by carrying out an extensive evaluation of the microbial species involved in the metabolism of root exudates both in the rhizosphere and endosphere of *A. thaliana*. This was achieved by carrying out a DNA-SIP experiment, whereby plants were grown under $^{13}\text{CO}_2$ or $^{12}\text{CO}_2$ conditions for 21 days. Heavy (labelled) and light (unlabelled) DNA in samples from the endosphere and rhizosphere were then separated via density gradient ultracentrifugation and 16S rRNA gene amplicon sequencing was carried out on the different fractions (Figure 4.1). Amplicon sequencing enabled the evaluation of all taxa as root exudate metabolisers, including the genus *Streptomyces*. Root exudates that had been purified from *A. thaliana* plants were also tested as a sole carbon and nitrogen source for *Streptomyces* strains isolated in Chapter 3. *A. thaliana* was used in experiments, since there are currently no studies detailing the use of root exudates by microbes associated with the endophytic compartment of the roots of this species and *Streptomyces* have not been previously investigated in this system despite having been noted to be highly abundant in the root and rhizosphere of this plant species (Bulgarelli et al 2012, Lundberg et al 2012). Additionally, using *A. thaliana* tied in with work carried out in Chapter 3, as well as experiments in Chapter 5 which investigated the role of salicylic acid in recruiting *Streptomyces* to plant roots by making use of mutant lines of *A. thaliana* plants.

4.3 Materials and Methods

4.3.1 DNA Stable Isotope Probing

4.3.1.1 Plant growth and ^{13}C labelling

^{13}C DNA-SIP was carried out in order to establish which bacteria in the rhizosphere and endosphere of *Arabidopsis thaliana* were metabolising root exudates (Figure 4.1). All

reagents used in these experiments are from Sigma Aldrich, unless otherwise stated. *A. thaliana* Col-0 seeds (Table 3.1) were sterilised by washing in 70% (v/v) ethanol for 2 minutes, 20% (v/v) sodium hypochlorite for 2 minutes, then five times in sterile water. Individual seeds were then sown singly in pots containing 100 ml sieved Levington F2 seed and modular compost, soaked with dH₂O. Pots were placed in the dark at 4°C for 48 hours, before being transferred to short day growth conditions (a photoperiod of 8 hours light and 16 hours dark) at 22°C for 32 days. Each plant was then placed into an air-tight, transparent 1.9 L cylindrical tube. Three plants were exposed to 1000 parts per million volume (ppmv) of ¹²CO₂ and three plants were exposed to 1000 ppmv of ¹³CO₂ (99%, Cambridge isotopes, Massachusetts, USA). Three additional unplanted controls containing only Levington F2 compost were also exposed to 1000 ppmv of ¹³CO₂ to control for autotrophic fixation of ¹³CO₂ by soil microbes. CO₂ was introduced manually to growth tubes using a needle and syringe which was inserted into an inlet located in the lids of the air-tight cylinders (Figure 4.1). Injections took place every 20 minutes over the course of the 8 hour light period and labelling was carried out over a period of 21 days (ending 53 days after germination when plants were still in the vegetative stage). The rate of plant CO₂ uptake was determined every 4 days; this enabled the volume of CO₂ to be added at each 20 minute interval to be calculated, in order to maintain the concentration at 1000 ppmv within tubes. CO₂ concentrations were measured using an Agilent 7890A gas chromatography instrument with a flame ionisation detector and a Poropak Q (6ft x 1/8") HP plotQ column (30 m x 0.530 mm, 40 µm film) with a nickel catalyst and a helium carrier gas. The instrument was run with the following settings: injector temperature 250°C, detector temperature 300°C, column temperature 115°C and oven temperature 50°C. The injection volume was 100 µl and the run time was 5 mins, with CO₂ having a retention time of 3.4 mins. Peak areas were compared to a standard curve to convert them to CO₂ concentrations in ppmv. Standards of known CO₂ concentration were prepared in 120 ml serum vials that had been flushed with an 80%/20% nitrogen/oxygen mixture (Brin's Oxygen Company, Ltd., UK) prior to the introduction of CO₂. The volume of CO₂ to be added at each 20 minute interval could then be calculated using the formula:

$$\text{Volume of CO}_2 \text{ to inject (ml)} = ((1000 \text{ ppmv} - \text{the measured ppmv})/1000) * 1.9 \text{ L}$$

At the end of the light period each day, tube lids were removed to prevent the build-up of respiratory CO₂ during the dark period. Just before the next light period, tubes were flushed with the 80%/20% nitrogen/oxygen mix to remove any residual CO₂ before replacing the lids and beginning the first injection of 1.9 ml of CO₂.

4.3.1.2 Sampling the soil, root and rhizosphere compartments

At the end of the CO₂ labelling experiment samples of the soil, rhizosphere and endophytic compartments were taken from pots for analysis. Samples (500 mg) of root-free “bulk soil” were collected from each of the planted and unplanted pots; samples were snap-frozen in liquid nitrogen and stored at - 80°C. For the planted pots, roots were tapped firmly to remove all soil, apart from the particles adhering firmly to the root surface; the remaining soil was defined as the rhizosphere fraction. To collect this, roots were placed into 25 ml of sterile, Silwett L-77 amended Phosphate Buffered Saline (PBS-S, see Table 3.2) and were washed on a shaking platform at top speed for 30 minutes before transferring to 25 ml of fresh PBS-S. Used PBS-S from the first washing stage was centrifuged at 4000 rpm for 15 minutes and the supernatant was removed. The resulting pellet (the rhizosphere sample) was snap-frozen and then stored at - 80°C. The roots were then shaken in fresh PBS-S for a further 30 minutes before removing any remaining soil particles with sterile tweezers. The cleaned roots were then transferred to fresh PBS-S and sonicated for 20 minutes in a sonicating water bath to remove any remaining material from the root surface (as in Bulgarelli et al 2012). The root (“endophytic”) sample for each plant was then snap frozen and stored at - 80°C. The endophytic sample consisted of bacteria within the roots and those very firmly attached to the root surface (the “rhizoplane”). A modified version of the manufacturer’s protocol for the FastDNA™ SPIN Kit for Soil (MP Biomedicals) was used to extract DNA from soil, rhizosphere, and root samples. Modifications included pre-homogenisation of the root material by grinding in a mortar and pestle with liquid nitrogen before addition of lysis buffer, an extended incubation time for samples (10 minutes) in the DNA matrix buffer, and elution in 150 µl of sterile water. DNA yields were quantified using a Qubit fluorimeter combined with a Qubit™ dsDNA High Sensitivity (HS) or Broad Range (BR) Assay kit (Invitrogen™) depending on the expected concentration.

4.3.1.3 Density gradient ultracentrifugation and fractionation of DNA

In order to separate ^{13}C labelled DNA (belonging to metabolisers of root exudates), from ^{12}C DNA, DNA samples from the rhizosphere and roots of planted pots as well as from the soil of unplanted pots, underwent density gradient separation according to an established protocol (as detailed in Neufeld et al 2007). Briefly, a 7.163 M cesium chloride (CsCl) solution was made, which had a measured density of 1.858 g ml^{-1} . Gradient buffer (GB: 0.1 M Tris, 0.1 M KCl, 1mM EDTA) and DNA were then mixed together and added to 4.8 ml of the CsCl solution. The total volume of the GB/DNA mixture to add to the CsCl solution depends upon the initial CsCl stock solution density and should result in a solution with an approximate density of 1.725 g ml^{-1} to give optimal separation of DNA. The volume of GB/DNA to add was quantified using the following calculation (from Neufeld et al 2007):

$$\text{Combined GB/DNA volume} = (\text{CsCl stock density} - 1.725\text{ g ml}^{-1}) \times 4.8\text{ ml CsCl} \times 1.52$$

For each of the replicate rhizosphere samples from both the $^{12}\text{CO}_2$ and $^{13}\text{CO}_2$ incubated plants, $1.5\text{ }\mu\text{g}$ of DNA was loaded into the GB and added to the CsCl solution. For the three unplanted soil sample replicates, $1\text{ }\mu\text{g}$ of DNA was used. For the three root samples from each of the different planted treatments ($^{12}\text{CO}_2$ and $^{13}\text{CO}_2$) it was necessary to combine replicates as the low DNA yields from each sample did not meet the minimum DNA yield requirement for ultracentrifugation ($0.5\text{ }\mu\text{g}$) on their own. Thus, $0.2\text{ }\mu\text{g}$ of DNA of each of the three replicates was pooled per $^{12}\text{CO}_2$ and $^{13}\text{CO}_2$ treatment and the final $0.6\text{ }\mu\text{g}$ was loaded into the GB and CsCl solution.

The refractive index (R.I, measured as the temperature adjusted RI in nD-TC) of each complete gradient solution was checked using a refractometer (Reichert Analytical Instruments, NY, USA) which had been calibrated with nuclease free water. Gradient buffer (if the nD-TC was too high) or CsCl solution (if the nD-TC was too low) was added in order to achieve an nD-TC value of 1.4038 (this approximates a density of 1.725 g ml^{-1}); this was done to normalise the density of solutions between samples. Once solutions were complete they were loaded into polyallomer quickseal centrifuge tubes (Beckman Coulter) and heat-sealed. Tubes were then placed into a vti 65.2 rotor (Beckman Coulter), balancing them to within 10 mg. The rotor was then loaded into a

Beckman Optima XL-100K ultracentrifuge and set to run at 20°C and 44,100 rpm for a minimum of 36 hours. A vacuum was applied during the run and breaks were not used for deceleration to ensure that the gradient remained intact at the end of the run.

After ultracentrifugation, each sample underwent gradient fractionation. For this, a 0.6 mm sterile needle was attached to the tubing of a peristaltic pump (cleaned with dH₂O before use) and pierced into the top of the ultracentrifuge tube, which was held in place by a clamp stand. The bottom of the centrifuge tube was then pierced swiftly with a sterile needle and dH₂O was pumped into the centrifuge tube at a rate of 450 µl per minute, displacing the gradient into 1.5 ml microcentrifuge tubes that were placed beneath the clamp stand. Tubes were exchanged every minute until the water had fully displaced the gradient solution, resulting in approximately 12 x 450 µl fractions being collected in total. The RI of 60 µl of each fraction was measured to confirm successful gradient formation. DNA was then precipitated by adding 4 µl of linear polyacrylamide (Invitrogen™) and 2 volumes of PEG-NaCl solution (30% PEG 6000, 1.6 M NaCl) to each fraction, before leaving them overnight at 4°C. DNA was then pelleted by centrifuging at 13,000 rpm for 30 minutes and the supernatant was removed. The pellet was then washed in 500 µl 70% EtOH, before centrifuging again at 13000 rpm for 10 minutes. The resulting pellet was then air-dried and resuspended in 30 µl sterile dH₂O. Fractions were then stored at - 20°C before use as a template in qPCR and PCR reactions.

4.3.1.4 16S rRNA gene amplification and DGGE analysis of fractions

In order to qualitatively analyse the distribution of the 16S rRNA gene across fractions, DGGE was carried out for samples under the different labelling treatments. For DGGE, the 16S rRNA gene was amplified from each fraction using PCR (Table 4.2, using BioMix™ red) with the DGGE primers 341F-GC and 518R (Table 4.3). The forward primer introduces a GC clamp to the 5' end of products which further modifies the melting properties of fragments and allows for greater resolution (Muyzer et al 1993).

Table 4.2 Components and thermocycler conditions for the amplification of the 16S rRNA gene using PCR.

Component	Volume (μ l)
BioMix™ red (containing BIOTAQ™ DNA polymerase, Bioline) or 2 x Ultra mix (containing Ultra DNA polymerase, PCR BIO)	10
dH ₂ O	9
Forward Primer	0.5
Reverse Primer	0.5
Sample DNA	5
PCR thermocycler reaction steps for DGGE primers 341F-GC/518R	
1. 95°C for 5 mins 2. 30 x cycles of 95°C for 1 min, 65°C 1 min, 72°C 1 min 3. 72°C for 10 mins	
PCR thermocycler reaction steps for all other experiments	
1. 95°C for 1 min 2. 30 x cycles of 95°C for 15 secs; 55°C for 15 secs, 72°C for 15 secs 3. 72°C for 2 mins	

Table 4.3 Primers used in stable isotope probing experiments.

Primer	Sequence	Reference
341F-GC	5'-CGCCCGCCGCGCGGGCGGGCGGGCGGG GGCACGGGGGGCCTACGGGAGGCAGCAG-3'	(Muyzer et al 1993)
518R	5'-ATTACCGCGGCTGCTGG-3'	
PRK341F	5'-CCTACGGGAGGCAGCAG-3'	(Yu et al 2005)
MPRK806R	5'-GGACTACHVGGGTWTCTAAT-3'	

An 8% polyacrylamide denaturing gel with a linear denaturant gradient of 40-80% (2.8 M urea/16% formamide, to 5.6M urea/32% formamide) was made along with a top loading gel of 0% denaturant (Table 4.4). For each sample, 5 μ l of PCR product from each fraction was loaded consecutively into each well of the gel. The gel was then

loaded into an electrophoresis tank filled with 1 x Tris acetate EDTA (TAE) buffer (242 g Tris base, 57.1 ml acetic acid, 100 ml 0.5 M EDTA pH 8.0). Electrophoresis was run at 0.2 Amps, 75 Volts and 60°C for 16 hours. Gels were then stained for one hour in the dark, using a solution of 400 ml 1 x TAE buffer with 4 µl of SYBR Gold Nucleic Acid Gel stain (Invitrogen™). Gels were then washed twice with dH₂O and imaged using a Bio-Rad Gel Doc XR imager. Bands of interest that were enriched in heavy fractions were sliced from the gel using a sterile scalpel blade and placed into a microcentrifuge tube containing 50 µl of sterile dH₂O. Tubes were then vortexed vigorously, before spinning down briefly. The supernatant was then used as a template in a PCR reaction (Table 4.2, using BioMix™ red) to amplify the 16S rRNA gene, using the primers PRK341F, 518R (Table 4.3). PCR products were then purified from a 1% agarose gel using the Qiagen™ MinElute gel extraction kit. Products were sent for sequencing at Eurofins Genomics (Germany) and the taxonomic identity of bands was confirmed using BLASTn.

Table 4.4 Components of an 8% polyacrylamide denaturing gel, with a linear denaturant gradient of 40-80% (2.8 M urea/16% formamide, to 5.6M urea/32% formamide). APS and TEMED are added to the solution just before the gel is cast.

Gel component	40% denaturing solution	80% denaturing solution	Top loading gel
40% (w/v) Bis-Acrylamide (37:5:1) (ml)	20	20	0.75
50 x TAE buffer (ml)	2	2	0.1
Formamide (ml)	16	32	-
Urea (g)	16.8	33.6	-
dH ₂ O (ml)	To 100 ml	To 100 ml	4.1
Added just before casting the gel:			
10% (w/v) Ammonium Persulfate (APS) (µl)	135 per 20 ml	135 µl per 20 ml	50
Tetramethylethylenediamine (TEMED) (µl)	13.5 per 20 ml	13.5 µl per 20 ml	5

4.3.1.5 Analysis of the 16S rRNA gene copy number across fractions using qPCR

To further identify fractions containing heavy (^{13}C) and light (^{12}C) DNA for each sample, 16S rRNA gene copy number was quantified across fractions using qPCR. Reactions were carried out in 25 μl volumes. 1 μl of template DNA (either sample DNA or standard DNA), or dH_2O as a control, was added to 24 μl of reaction mix containing 12.5 μl of 2x Sybr Green Jumpstart Taq Ready-mix (Sigma Aldrich), 0.125 μl of each of the primers PRK341F and MPRK806R (Table 4.3), 4 μl of 25 mM MgCl_2 , 0.25 μl of 20 μg μl^{-1} Bovine Serum Albumin (BSA, Roche), and 7 μl dH_2O . Sample DNA, standards (a dilution series of the target 16S rRNA gene at known molecular quantities), and negative controls were quantified in duplicate. Reactions were run under the following conditions: 96°C for 10 mins; 40 cycles of 96°C for 30 sec, 52°C for 30 sec, and 72°C for 1 min; 96°C for 15 sec; 100 cycles at 75°C-95°C for 10 secs, ramping 0.2°C per cycle. Reactions were performed in 96-well plates (Bio-Rad). The threshold cycle (C_T) for each sample was then converted to target molecule number by comparing to C_T values of a dilution series of target DNA standards.

4.3.2 16S rRNA gene amplicon sequencing of fractions

Following quantification of 16S rRNA gene copy number in each fraction using qPCR and DGGE, fractions spanning the peaks in copy number were identified. Equal quantities of each of these fractions were combined to create a labelled “heavy” (H) and unlabelled “light” (L) fraction for each sample, respectively. For the rhizosphere, there were three replicate H and L fractions for each of the ^{12}C and ^{13}C treatments (deriving from the three replicate pots under each labelling treatment). For the endosphere, there was only one replicate H and L fraction for each of the ^{12}C and ^{13}C treatments, however, as mentioned in section 4.3.1.3, these were made up of a pool of the DNA from the three replicate pots which was combined at the ultracentrifugation step. For the ^{13}C unplanted control, three replicate H fractions were submitted for sequencing along with one pooled L fraction (produced by combining equal volumes of each L fraction from the three replicate soil samples). A pooled L fraction was submitted due to sequencing cost constraints, but this could be justified because light fractions appeared highly reproducible on DGGE gels.

For each H and L fraction, the 16S rRNA gene was amplified by PCR using the universal primers PRK341F and MPRK806R; these amplify the V3 and V4 variable region of the 16S rRNA gene (Table 4.3). PCR was performed using an Ultra DNA polymerase according to the protocol defined in Table 4.2. The 16S rRNA gene was also amplified from three replicate unfractionated DNA samples of the bulk soil, rhizosphere and roots of *A. thaliana* grown under the $^{12}\text{CO}_2$ treatment, in order to provide information about the complete bacterial communities in each of these compartments. The resulting PCR products were purified using the Qiagen™ MinElute gel extraction kit and submitted for 16S rRNA gene amplicon sequencing using Illumina MiSeq technology at Mr DNA (Molecular Research LP), Shallowater, Texas, USA. Sequence data was then processed at Mr DNA using their custom pipeline (Dowd et al 2008a, Dowd et al 2008b). As part of this pipeline, paired-end sequences were merged, barcodes were trimmed, and sequences of less than 150 bp and/or with ambiguous base calls were removed. The resulting sequences were denoised, and OTUs were assigned by clustering at 97% similarity. Chimeras were removed, and OTUs were assigned taxonomies using BLASTn against a curated database from GreenGenes, RDP II, and NCBI (DeSantis et al 2006). Plastid-like sequences were removed from the analysis.

Upon receipt of the 16S rRNA gene sequencing data from Mr DNA, further processing and statistical analyses were carried out using R 3.2.3 (R Core Team 2017), using the packages tidyr and reshape (for manipulating data-frames), ggplot2 and gplots (for plotting graphs and heatmaps, respectively), vegan (for calculating Bray-Curtis dissimilarities, conducting principle coordinate and PERMANOVA analyses, and for generating heatmaps) and ellipse (for plotting principle coordinate analyses). All 16S rRNA gene amplicon sequencing data for this experiment was submitted to the European Nucleotide Archive public database under the study accession number PRJEB30923.

4.3.3 Investigating root exudates as a sole carbon source

Seeds of *A. thaliana* Col-0 (Table 3.1) were sterilised (as above) and plated onto Murashige and Skoog (MSK) agar (Table 3.2, 0.5% agar, 1% sucrose). Plates were placed at 4°C for 24 hours before being grown vertically under a photoperiod of 12

hours light/12 hours dark, for 7 days at 22°C. Seedlings were then transferred to 12 well plates containing 3 ml of liquid MSk (Table 3.2, 0% sucrose) in each well and were then grown for 10 days, before being transferred to new wells containing 3 ml of sterile water. The roots of each plant were rinsed with sterile water before being transferred. After 5 days of growth in water, plant material was removed and the liquid from each well was collected, filter sterilised and added to sterile agarose (0.8% w/v). This was then melted to make solid growth medium plates. Spores of the *Streptomyces* isolates L2, N1, N2, M3, M2, MG, *S. lydicus* 25470, *S. lydicus* 31975, *S. lydicus* Actinovate and *S. coelicolor* (Table 3.1) were streaked individually onto plates and incubated for 7 days at 30°C. Agarose/water (0.8% w/v) plates were used as a control.

4.4 Results

4.4.1 Bacterial communities in the soil, rhizosphere and roots associated with *Arabidopsis thaliana* plants

4.4.1.1 The total bacterial community

In order to assess the composition of bacterial communities associated with the soil, rhizosphere and root compartments of *A. thaliana* plants grown in compost, triplicate unfractionated DNA samples from each of these compartments underwent 16S rRNA gene amplicon sequencing and analysis. To compare the overall bacterial community composition in the different compartments, a Bray-Curtis (BC) dissimilarity matrix was calculated based on the relative abundances of genera or phyla present in each sample. A principle coordinate analysis (PCoA) of BC dissimilarities showed that the three compartments separated spatially from one another on ordination plots, at both phylum and genus taxonomic levels, suggesting that each compartment had a different bacterial community composition (Figure 4.2). A Permutational Multivariate Analysis of Variance (PERMANOVA) test on the BC dissimilarity matrices confirmed that compartment had a statistically significant effect on the bacterial community composition at both taxonomic levels (Phylum PERMANOVA: permutations=999, $R^2=0.94$, $P=0.006$. Genus PERMANOVA: permutations=999, $R^2=0.87$, $P=0.002$).

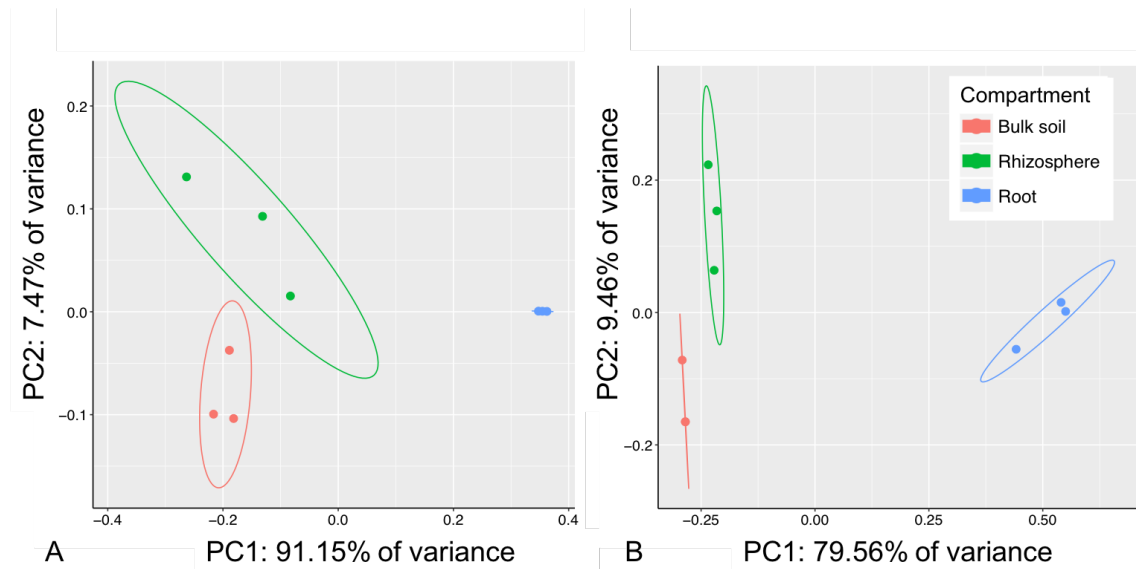


Figure 4.2 Principle coordinate analyses of Bray-Curtis dissimilarities between the bulk soil, rhizosphere and root-associated communities of *Arabidopsis thaliana* (n= 3 samples per compartment). Significant dissimilarities between compartments were observed at the **A**) phylum (PERMANOVA, $R^2= 0.94$, $P < 0.01$) and **B**) genus (PERMANOVA, $R^2= 0.87$, $P < 0.01$) taxonomic level. Principle component 1 explains A) 91.15% and B) 79.56% of the variance in Bray-Curtis dissimilarities between compartments. Ellipses represent 95% confidence intervals.

Significant differences between soil, rhizosphere and root-associated bacterial communities have been reported in numerous other studies involving many different plant species and distinct soil types (Bulgarelli et al 2012, Bulgarelli et al 2015, Edwards et al 2015, Lundberg et al 2012). This includes several studies conducted on the soil, rhizosphere and root microbiome of *Arabidopsis thaliana* plants (Bulgarelli et al 2012, Lundberg et al 2012). Collectively, these observations suggest that different microbial taxa are adapted to live in each of the different compartments, and that the plant host may have a significant influence on the composition of the root-associated and rhizosphere bacterial communities (Berg and Smalla 2009, Liu et al 2017a). However, it should also be noted that several studies on *A. thaliana* have suggested that this species has a relatively small “rhizosphere effect” compared to other plants, meaning that there is a weaker differentiation in terms of microenvironment and community composition between the rhizosphere and bulk soil, than there is between these two compartments and the endophytic niche (Bulgarelli et al 2015, Schlaeppli et al 2014).

Results of sequencing analysis in this chapter appear to be in agreement with these findings; although all compartments separated from one another following a PCoA analysis, the soil and rhizosphere compartments appeared to be more similar to one another (they were closer together on the PC1 axis of ordination plots) than the root compartment was to either of these two compartments (Figure 4.2).

The relative abundances of the majority of phyla were reduced in the root compartment compared to the rhizosphere and the soil environment suggesting that only a small proportion of the total soil community was either adapted to reside in the root niche or had a competitive advantage when colonising this environment (Figure 4.3). An exception to this was the phylum Proteobacteria, which was significantly enriched in the root compartment compared to the bulk soil and rhizosphere compartments ($P < 0.05$ in Dunn's multiple comparison tests between root and rhizosphere and root and soil compartments, with adjusted P values). The relative abundance of Proteobacteria increased to 91.22% ($\pm 0.74\%$ standard deviation) of the root-associated community, compared to 38.85% ($\pm 9.80\%$) of the rhizosphere and 35.46% ($\pm 1.97\%$) of the soil community, respectively (Figure 4.3). This phylum dominated the root compartment, with Actinobacteria, Bacteroidetes and Firmicutes being the next most abundant taxa in the root niche, making up 2.87% ($\pm 0.88\%$), 2.08% ($\pm 0.55\%$) and 0.55% ($\pm 0.15\%$), respectively (Figure 4.3). The weak rhizosphere effect of *A. thaliana* was further evidenced by the fact that, although there were small differences, most phyla identified in this study showed very similar abundances between the rhizosphere and soil compartments (Figure 4.3).

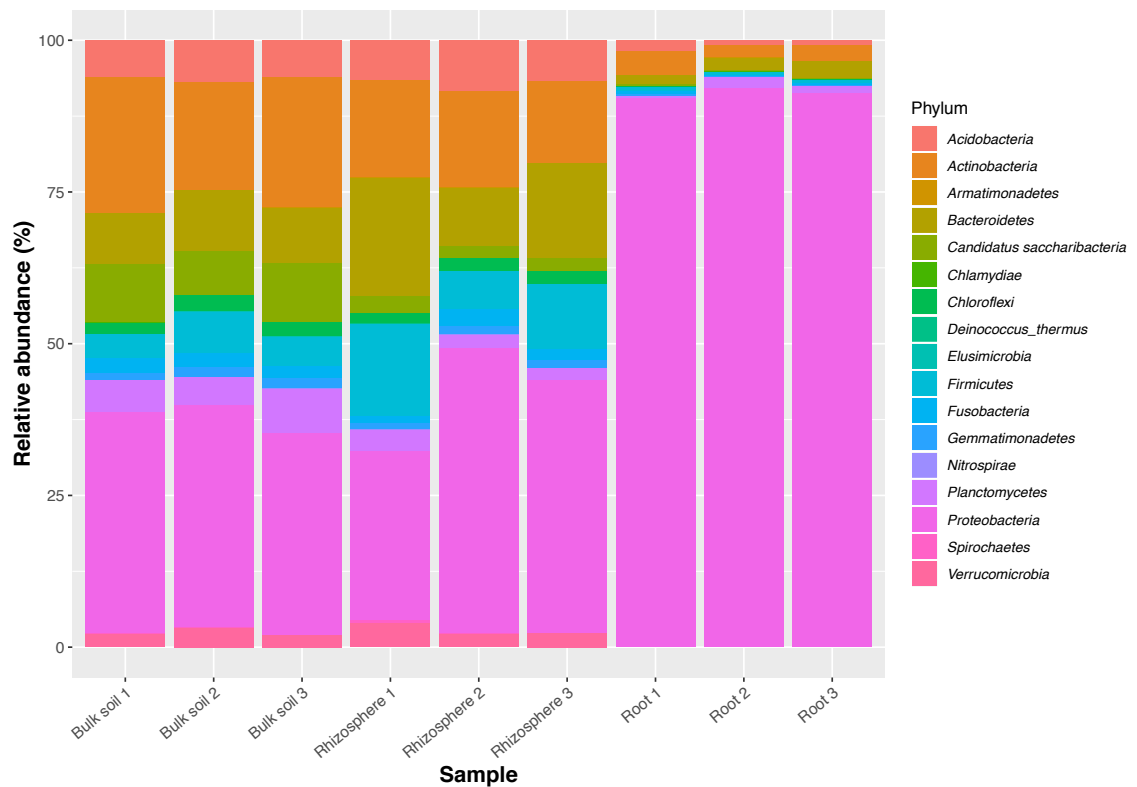


Figure 4.3 The relative abundance (%) of bacterial phyla in samples from the bulk soil, rhizosphere and root compartments of *Arabidopsis thaliana* grown in compost (n=3 replicate samples per compartment).

Looking within phyla, particular taxa showed individual patterns of change across the three different compartments. For example, certain families of Proteobacteria were enriched in the root microbiome, whilst others were only present at very low abundances (Figure 4.4). Enriched families included those such as the Pseudomonadaceae and Rhizobiaceae, both of which are well-known colonisers of plant roots, including those of *A. thaliana*, and are also known to contribute to plant fitness for example via pathogen protection and PGP (Garrido-Oter et al 2018, Mercado-Blanco and Bakker 2007, Preston 2004, Zhao et al 2017). Individual families also showed similar abundances in rhizosphere and soil samples, which is again consistent with a weak rhizosphere effect in *A. thaliana* (Figure 4.4).

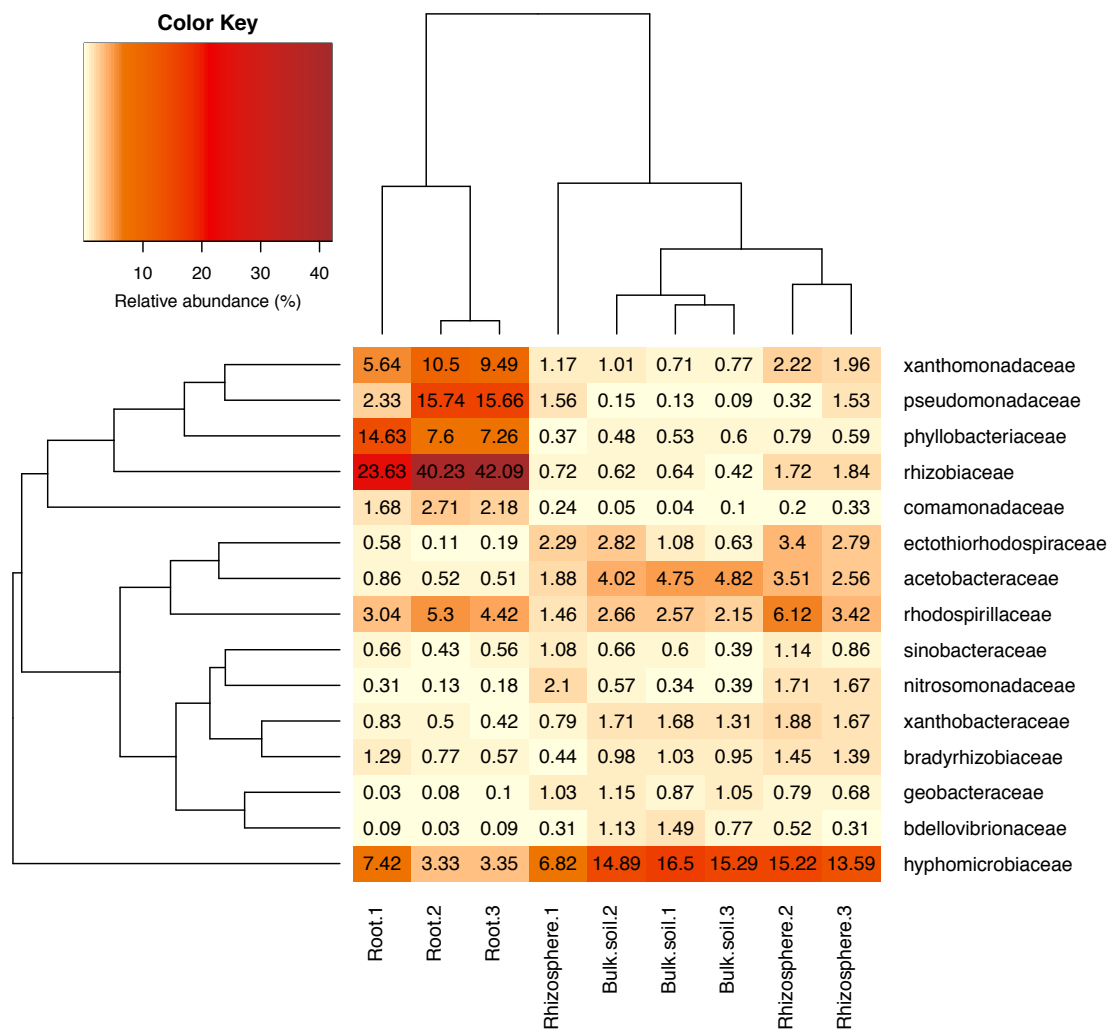


Figure 4.4 The relative abundance (%) of families of Proteobacteria across the soil, rhizosphere and root compartment of *A. thaliana* plants. Only genera that had a maximum relative abundance of greater than 1% across all three compartments are shown. N = 3 replicate plant pots. Clustering is based on Bray-Curtis dissimilarities. Light yellow to brown represents an increasing relative abundance (%).

4.4.1.2 Actinobacteria in the root, rhizosphere and bulk soil compartments

The actinobacterial portion of the soil, rhizosphere and root bacterial communities was found to be dominated by the family Streptomycetaceae, which made up an average of 10.33% ($\pm 1.87\%$ standard deviation) of the total bacterial community present in bulk soil samples, 5.62% ($\pm 1.10\%$) of the rhizosphere community and 1.12% ($\pm 0.50\%$) of the endophytic community (Figure 4.5). In comparison, Actinobacteria as a whole made up 20.60% ($\pm 2.41\%$), 15.15% ($\pm 1.47\%$) and 2.87% ($\pm 0.88\%$) of these compartments, respectively (Figure 4.5). Although the Streptomycetaceae were not

enriched in either the rhizosphere or root compartments relative to the surrounding bulk soil (Figure 4.5), its dominance is in agreement with other studies that have shown that this family tends to drive the presence of Actinobacteria in the *A. thaliana* rhizosphere and root microbiome as well as in the microbiomes of other plant species (Bulgarelli et al 2012, Edwards et al 2015, Lundberg et al 2012, Weinert et al 2011). Most other families of Actinobacteria were only present at very low abundances in the root compartment of *A. thaliana*, although some families, such as the Micromonosporaceae and Nocardiaceae, were found to be enriched in the rhizosphere compared to the surrounding soil but were then reduced again in the root compartment (Figure 4.5). This suggests that barriers may have prevented the entry of these bacteria into the root compartment, or that species were less competitive in the root niche than they were in the rhizosphere.

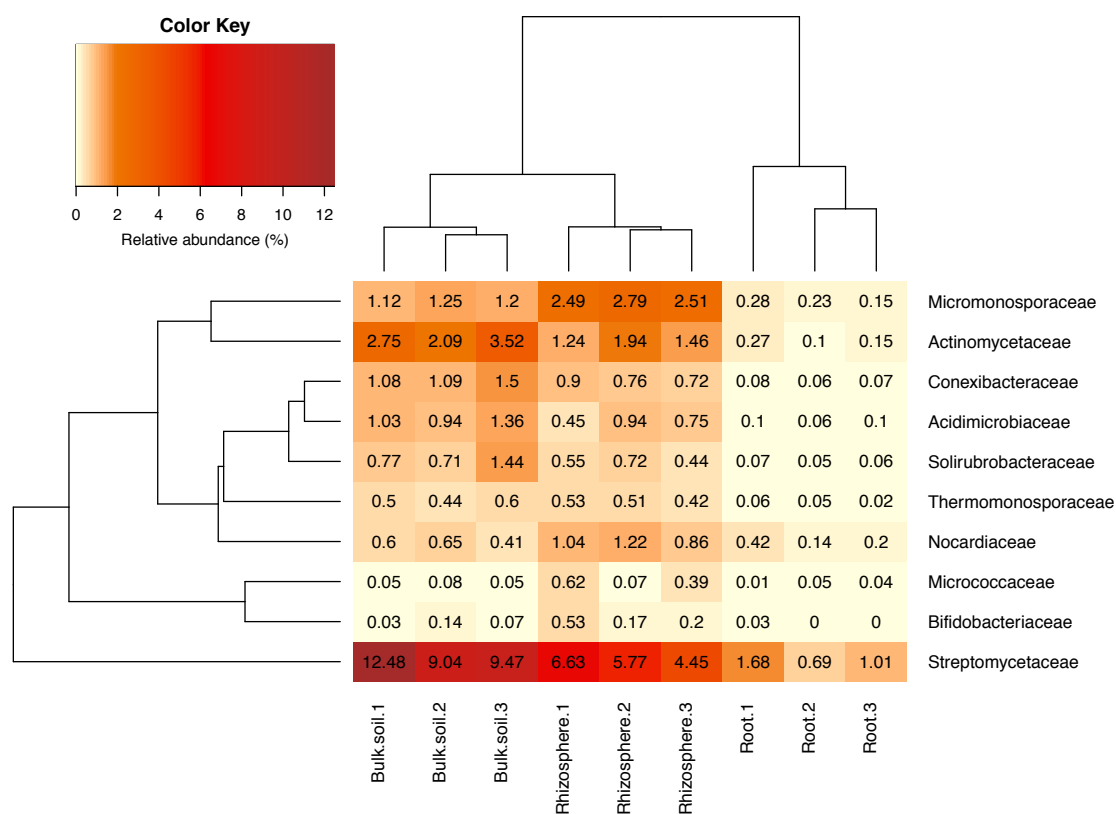


Figure 4.5 The relative abundance (%) of actinobacterial families in the soil, rhizosphere and root compartment of *A. thaliana* plants. N = 3 replicate plants in individual pots. Streptomycetaceae was the most abundant family of Actinobacteria in all three compartments. Clustering is based on Bray-Curtis dissimilarities. Light yellow to brown represents increasing relative abundance.

4.4.2 Stable Isotope Probing to assess bacterial metabolism of *Arabidopsis thaliana* root exudates

In order to identify whether root exudates may be promoting the growth of certain bacteria within the roots and rhizosphere of *A. thaliana*, ^{13}C DNA SIP was used to track the utilisation of host-derived resources by bacteria in the plant rhizosphere and root-associated microbiome. Plants were grown in sealed growth chambers for 21 days under a short-day photoperiod (8 hours light) in the presence of 1000 ppmv of either $^{13}\text{CO}_2$ or $^{12}\text{CO}_2$ ($n=3$ plants per treatment) (Figure 4.1). Unplanted pots were also incubated with $^{13}\text{CO}_2$ to control for the possibility of autotrophic fixation of the $^{13}\text{CO}_2$ by soil bacteria. Given the relatively short time frame of CO_2 exposure, the ^{13}C that was fixed by plants during photosynthesis, was expected to mainly be incorporated into carbon-based metabolites, rather than into plant cell wall material. Bacteria that incorporate ^{13}C into their DNA are therefore likely to be feeding on plant metabolites exuded from the roots, or directly metabolising $^{13}\text{CO}_2$ autotrophically, rather than degrading complex plant cell wall components.

4.4.2.1 Fraction selection

After 21 days, total DNA was extracted from the rhizosphere and endosphere compartments of the $^{12}\text{CO}_2$ or $^{13}\text{CO}_2$ incubated plants, as well from soil in unplanted control pots. Labelled “heavy” (^{13}C) and unlabelled “light” (^{12}C) DNA were then separated via density gradient ultracentrifugation (Neufeld et al 2007). The gradient for each sample was then fractionated into approximately twelve different fractions (Figure 4.1). Fractions were analysed to confirm shifts in bacterial DNA to higher buoyant density fractions under the $^{13}\text{CO}_2$ treatment, which is indicative of metabolism of the heavy ^{13}C isotope. Denaturing gradient gel electrophoresis (DGGE) was carried out as a preliminary step to identify shifts in the DNA of particular bacterial taxa. DGGE enables 16S rRNA gene sequences of the same length to be separated on a denaturing gel, based on the fact that nucleotide differences lead to different sequence “melting” properties in response to a denaturant; sequences that melt more quickly (for example those with a high AT content) will migrate shorter distances down the gel (Muyzer et al 1993). A comparison of DGGE banding patterns suggested that there were a number of taxonomic groups that had shifted to fractions of higher buoyant densities under the ^{13}C treatment, when compared to banding patterns under the ^{12}C treatment (Figure

4.6). Bands that were enriched in the heaviest fractions of the $^{13}\text{CO}_2$ samples compared to the lighter fractions, were also absent from fractions of equivalent buoyant densities in samples from the $^{12}\text{CO}_2$ treatment ($^{13}\text{CO}_2\text{H}$ versus $^{12}\text{CO}_2\text{H}$ in Figure 4.6). This suggested that particular 16S rRNA gene fragments (representative of particular taxa) had shifted to higher buoyant densities due to the metabolism of ^{13}C and not due to an innate property of that taxon's genome making the DNA heavier, such as a very high GC content. Sequences of two of the bands that showed the greatest level of enrichment in heavy fractions were identified as *Pseudomonas* species (Figure 4.6). *Pseudomonas* species have been previously shown to play an important role in the rhizosphere of several different plant species and are likely to be able to feed on root exudates (Haichar et al 2012, Mark et al 2005, Preston 2004).

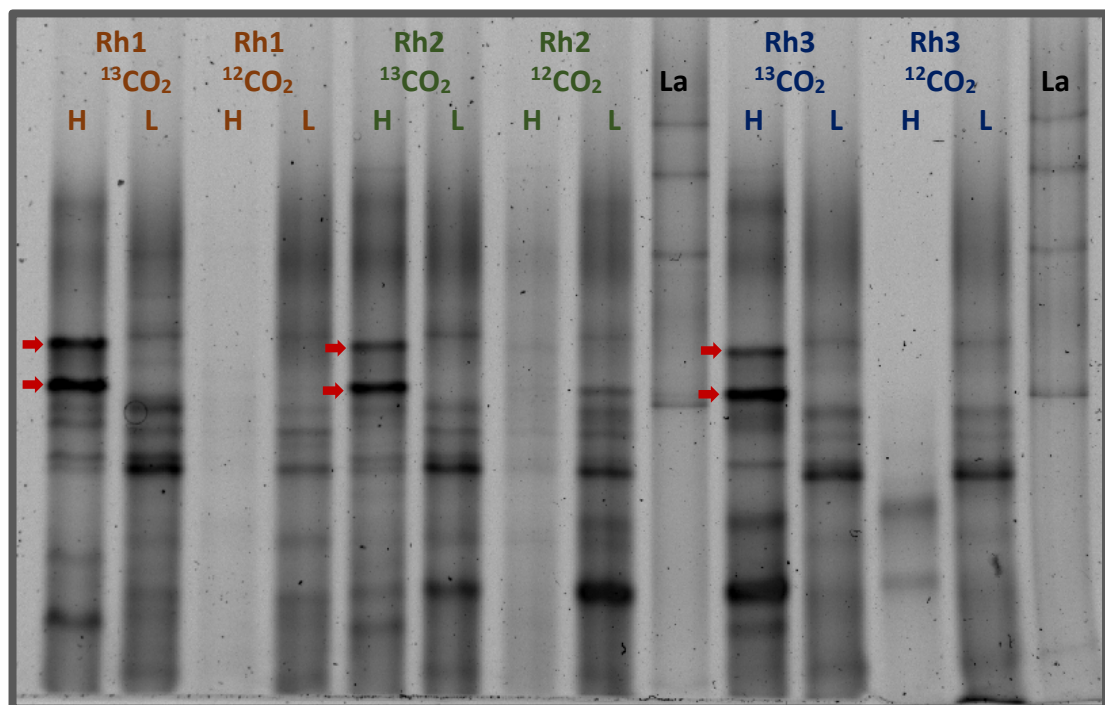


Figure 4.6 A denaturing gradient gel electrophoresis (DGGE) profile of 16S rRNA genes amplified from rhizosphere SIP fractions. Representative heavy (H) and light (L) buoyant density DNA fractions are shown; these were from *A. thaliana* plants incubated under $^{13}\text{CO}_2$ or $^{12}\text{CO}_2$ conditions for 21 days (n=3 plants per CO_2 treatment: Rh1-3). Bands represent different taxonomic groups. Red arrows indicate where bands were successfully sequenced and identified as *Pseudomonas*. La= ladder.

DGGE profiles of 16S rRNA genes fragments amplified from fractions of root samples showed similar patterns to the rhizosphere, in that certain bands (including those identified as *Pseudomonas*) were enriched in heavier fractions of $^{13}\text{CO}_2$ incubated samples, compared to both the lighter fractions of the same sample and also the heavier fractions of the $^{12}\text{CO}_2$ incubated samples (Figure 4.7, A). Conversely, very few bands had shifted to higher buoyant density fractions of soil samples taken from unplanted pots (Figure 4.7, B) and the vast majority of 16S rRNA gene fragments appeared to remain in lighter fractions, suggesting that only a small proportion of the soil community were capable of fixing the $^{13}\text{CO}_2$ directly. Therefore, the majority of bands that are enriched in ^{13}CH fractions of rhizosphere and endosphere samples, are likely to be taxa that have metabolised host root exudates, rather than autotrophs.

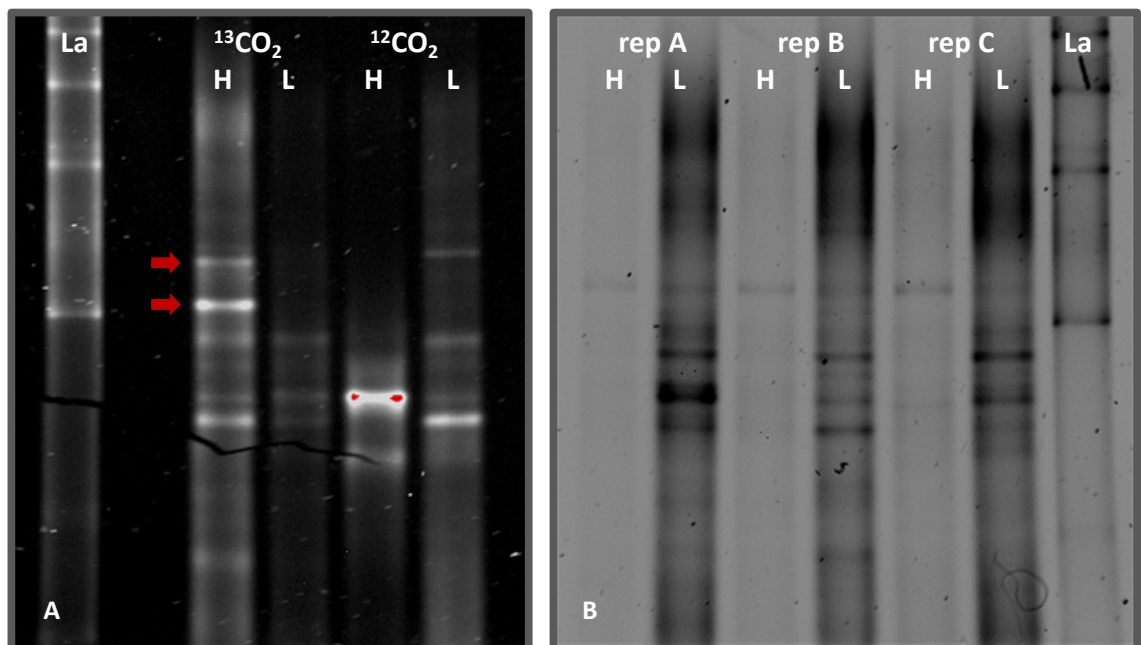


Figure 4.7 A denaturing gradient gel electrophoresis (DGGE) profile of 16S rRNA genes amplified from **A)** root fractions and **B)** unplanted soil samples. Representative heavy (H) and light (L) buoyant density fractions of root DNA samples are from *A. thaliana* plants incubated under either $^{13}\text{CO}_2$ or $^{12}\text{CO}_2$ conditions for 21 days (DNA samples from n=3 replicate plants were pooled for each CO_2 treatment). Unplanted soil samples (n=3, rep A-C) were incubated under $^{13}\text{CO}_2$ for 21 days. Bands represent different taxonomic groups. Red arrows indicate where bands were successfully sequenced and identified as *Pseudomonas*. La= ladder.

In order to further confirm that labelling had occurred and that bacterial DNA had shifted to higher buoyant densities under the $^{13}\text{CO}_2$ treatment, qPCR was carried out to quantify the 16S rRNA gene copy number occurring across fractions of both root (Figure 4.8) and rhizosphere (supplementary information, Figure S5.1) samples. In all cases, peaks in 16S rRNA gene copy number had shifted to higher buoyant densities under the $^{13}\text{CO}_2$ incubation, particularly in the root-associated samples (Figure 4.8). This information, coupled with the DGGE analysis, enabled the identification of representative “heavy” and “light” fractions (at high and low buoyant densities, respectively) that encompassed the peaks in 16S rRNA under the two different CO_2 treatments (Figure 4.8 and S4.1, Table 4.5); these were then submitted for 16S rRNA gene amplicon sequencing, to further identify the taxa responsible for buoyant density shifts.

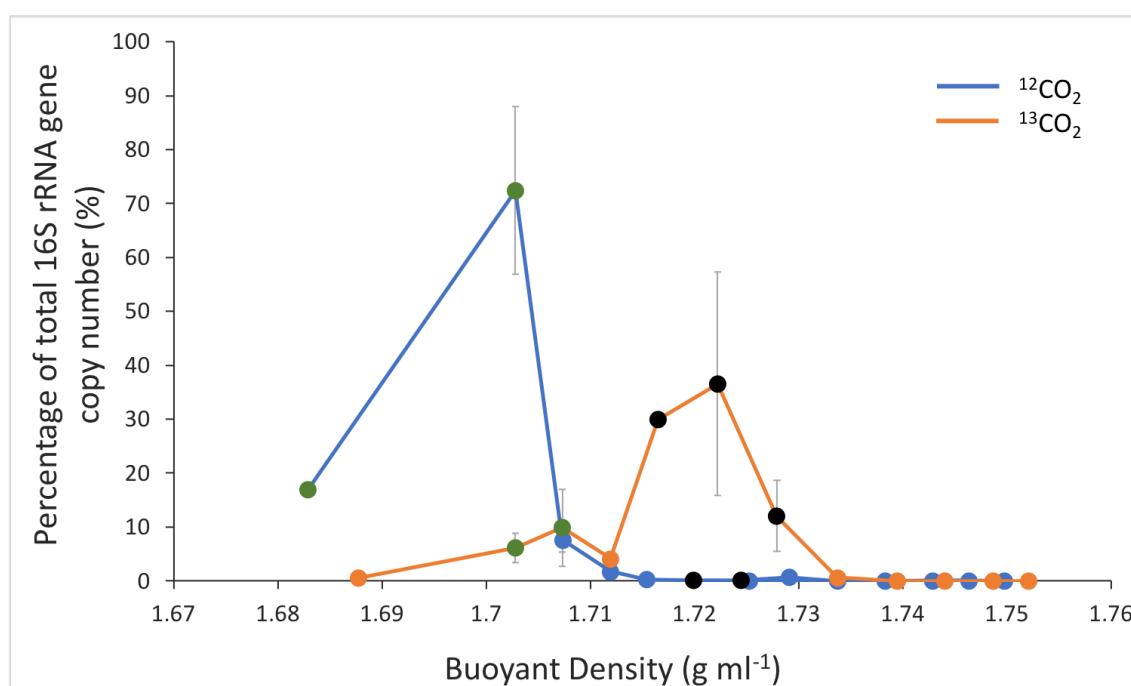


Figure 4.8 16S rRNA gene copy number across buoyant density fractions of DNA isolated from root samples of *A. thaliana* plants incubated under either $^{12}\text{CO}_2$ (blue) or $^{13}\text{CO}_2$ (orange) conditions. Copy number is shown as a percentage of total copy number per sample. N=2 replicate measurements on the same fraction. Bars represent standard errors. Green and black dots represent the “light” and “heavy” fractions, respectively, that were pooled in each treatment and submitted for 16S rRNA gene amplicon sequencing.

Table 4.5 Heavy (H) and Light (L) fractions of DNA selected for 16S rRNA gene amplicon sequencing, following density gradient ultracentrifugation, DGGE and qPCR analysis. Fractions were chosen for root and rhizosphere samples incubated under either $^{12}\text{CO}_2$ (12) or $^{13}\text{CO}_2$ (13) conditions, as well as for $^{13}\text{CO}_2$ (13) incubated unplanted controls. 13L fractions for unplanted soils were pooled before sequencing.

Origin of fractions	Fraction classification	Pooled fractions	Fraction density range (g ml ⁻¹)
Pooled root sample	12H	8, 9	1.7199 - 1.7245
	12L	12, 13	1.6829 - 1.7028
	13H	10, 11	1.7165 - 1.7279
	13L	6, 7, 8	1.7028 - 1.7073
Rhizosphere sample 1	12H	9, 10	1.7211 - 1.7234
	12L	13, 14	1.6993 - 1.7096
	13H	7, 8	1.7188 - 1.7234
	13L	10, 11	1.7050 - 1.7085
Rhizosphere sample 2	12H	7, 8	1.7222 - 1.7268
	12L	10, 11	1.7073 - 1.7119
	13H	7, 8	1.7211 - 1.7268
	13L	10, 11	1.7050 - 1.7108
Rhizosphere sample 3	12H	7, 8	1.7188 - 1.7234
	12L	10, 11	1.6970 - 1.7073
	13H	7, 8	1.7176 - 1.7234
	13 L	10, 11	1.6883 - 1.7050
Unplanted soil sample 1	13H	6, 7	1.7222-1.7279
	13L	11, 12	1.6627 - 1.7050
Unplanted soil sample 2	13H	6, 7	1.7211 - 1.7257
	13L	9, 10	1.6962 - 1.7108
Unplanted soil sample 3	13H	6,7	1.7222 - 1.7279
	13L	10, 11	1.6959 - 1.7108

Heavy (H) and light (L) fractions were submitted from each of the three replicate rhizosphere samples taken from $^{12}\text{CO}_2$ and $^{13}\text{CO}_2$ incubated plants (Table 4.5). One replicate H and one replicate L fraction was submitted for each of the $^{13}\text{CO}_2$ and $^{12}\text{CO}_2$ incubated root samples; these fractions each resulted from pooled DNA taken from the three replicate plant samples (DNA was combined prior to ultracentrifugation due to low DNA yields) (Table 4.5). For the $^{13}\text{CO}_2$ incubated, unplanted soil controls, three replicate H fractions along with one pooled L fraction (produced by combining equal volumes of each L fraction from the three replicate soil samples) were submitted for sequencing.

4.4.2.2 16S rRNA gene amplicon sequencing of density gradient fractions

In order to get a preliminary overview of the effect of different CO_2 treatments on the bacterial community composition in fractions from rhizosphere samples, a principle coordinates analysis was carried out using a Bray-Curtis dissimilarity matrix calculated from the relative abundances of genera present in each of the different rhizosphere fractions (^{13}CH , ^{13}CL , ^{12}CH , ^{12}CL , Table 4.5, $n=3$ replicate fractions each). The analysis suggested that fractions had a differing community composition at the genus level, since they separated spatially from one another on an ordination plot (Figure 4.9). A PERMANOVA analysis confirmed that fraction type had a significant effect on the community composition (permutations=999, $R^2=0.80$, $P < 0.01$). In particular, the ^{12}CH and the ^{13}CH fractions appeared to be widely separate from one another, as well as from the ^{12}CL and ^{13}CL fractions (Figure 4.9). This implied that the incorporation of the ^{13}C label into microbial DNA had altered the composition of heavy fractions. In contrast, the ^{12}CL and ^{13}CL fractions appeared more similar to one another and had overlapping confidence intervals (Figure 4.9). This is most likely due to the fact that different genera, as well as species within the same genus, may have differing metabolic characteristics, with only a subset being capable of metabolising root exudates, or using root exudates as their preferred carbon source. Due to limitations of sequencing depth, resolution was not high enough to investigate species-level changes in buoyant density. Reduced differences between the two light fractions could also have been due to an incomplete level of labelling of bacterial communities, either due to a low level of labelled exudates dissipating into the rhizosphere (due to the small rhizosphere effect of *A. thaliana*), or due to a slow metabolism of root exudates

by some microbial taxa in the rhizosphere. This would mean that genera that are capable of metabolising root exudates are present in both the ^{13}CL and ^{13}CH fractions (rather than shifting completely to the ^{13}CH fraction), making the ^{13}CL and ^{12}CL fractions more similar.

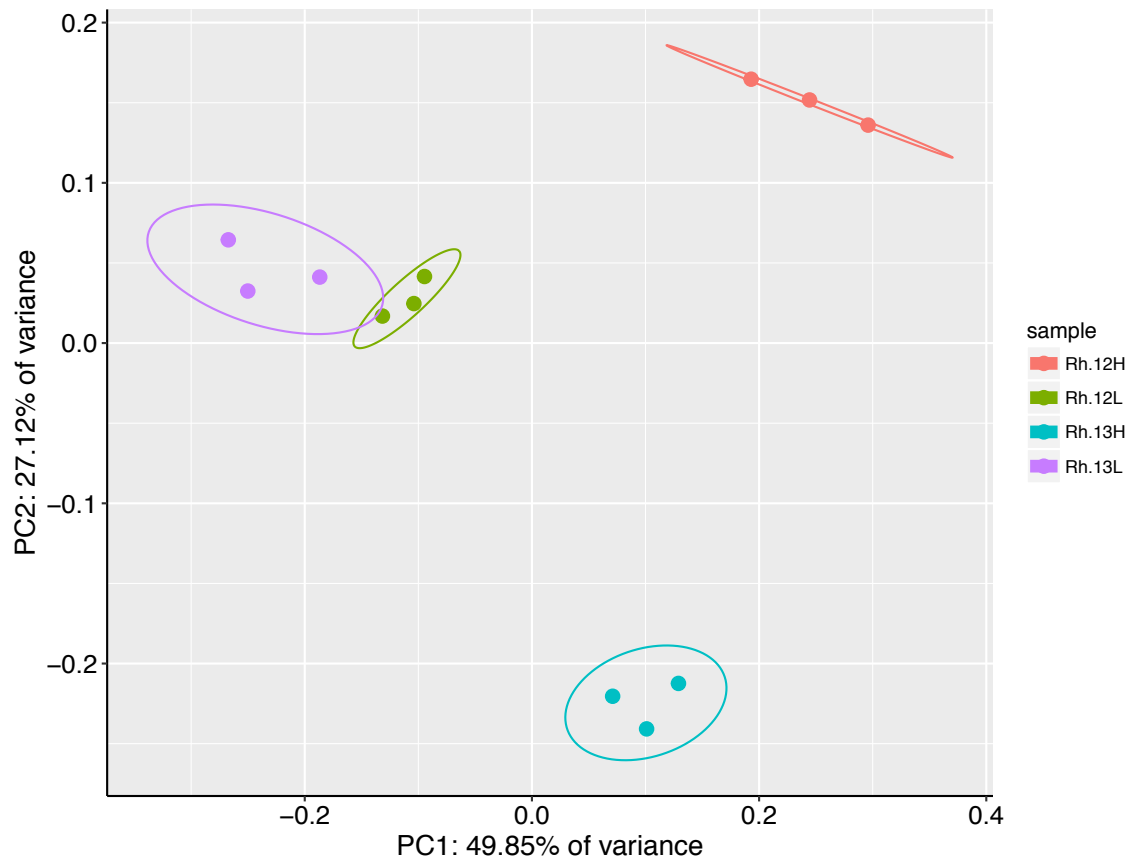


Figure 4.9 Results of a principle coordinates analysis of Bray-Curtis dissimilarities between bacterial genera present in the heavy (H) and light (L) buoyant density fractions of rhizosphere samples. Samples were taken from plants incubated under either $^{12}\text{CO}_2$ (12L, 12H) or $^{13}\text{CO}_2$ (13L, 13H) treatments (n= 3 replicate plants under each treatment). Principle Component 1 and 2 explain 49.85% and 27.12% of the variance in Bray-Curtis dissimilarities, respectively, between fraction types. Ellipses represent 95% confidence intervals.

In order to determine which bacterial taxa were responsible for metabolising root exudates, 16S rRNA gene amplicon sequencing data for representative heavy and light fractions from $^{12}\text{CO}_2$ and $^{13}\text{CO}_2$ incubated plants (Table 4.5) were compared at the

genus level. For the rhizosphere and endophytic samples, bacterial genera were defined as metabolisers of root exudates if they showed at least a two-fold increase in relative abundance in the heavy fraction of $^{13}\text{CO}_2$ plants (^{13}CH) compared to both the $^{13}\text{CO}_2$ light fraction (^{13}CL) and $^{12}\text{CO}_2$ heavy fraction (^{12}CH), respectively. Importantly, the abundance of these bacteria was also less than two-fold greater in the heavy versus the light fractions of $^{13}\text{CO}_2$ unplanted controls, meaning that they were not likely to be autotrophically fixing CO_2 .

A comparison of the relative abundances of particular genera in the H and L fractions of rhizosphere and endosphere samples with fractions from unplanted controls, identified several genera as possible candidates involved in the direct fixation of $^{13}\text{CO}_2$; these were not only enriched in the ^{13}CH fractions of rhizosphere and endosphere samples, but were also enriched in the ^{13}CH fraction of the unplanted controls (Table 4.6). For example, this included the genus *Bacteroides* which is known to carry out direct carbon fixation during carbohydrate fermentation (Caldwell et al 1969, Fischbach and Sonnenburg 2011). Candidate autotrophs were removed from lists of taxa enriched in the heavy fractions of the endosphere and rhizosphere samples, in order to conservatively control for direct carbon fixation.

Following sorting of the data and the removal of autotrophic candidates, 28 genera showed an average of two-fold (or more) enrichment in the ^{13}CH fraction of rhizosphere samples (Table 4.6). The majority of these taxa were in the phylum Proteobacteria (24 out of 28 genera), with only one representative each from the phyla Chloroflexi (*Levilinea*), Firmicutes (*Pelotomaculum*), Cyanobacteria (*Chroococcidiopsis*), and the Planctomycetes (*Pirellula*). The most enriched genus was *Pseudomonas*, which demonstrated a 64-fold enrichment in relative abundance between the ^{13}CH (8.63% average relative abundance \pm 3.33% SE) and ^{13}CL (0.13% \pm 0.01% SE) fractions and a 23-fold enrichment between the ^{13}CH fraction compared to the ^{12}CH control fraction (0.37% \pm 0.06% SE) (Figure 4.10).

Table 4.6 Summary of SIP results displaying a list of genera that were identified as candidate autotrophs in either the rhizosphere or endosphere, as well as the genera (and their associated phyla) that were identified to be metabolising root exudates in the rhizosphere or endosphere (or both, shown in red).

Autotrophic genera		Metabolisers of root exudates in the rhizosphere		Metabolisers of root exudates in the endosphere	
Rhizosphere	Endosphere	Phylum	Genus	Phylum	Genus
<i>Bacteroides</i>	<i>Amaricoccus</i>	Proteobacteria	<i>Ensifer</i>	Proteobacteria	<i>Sphingobium</i>
<i>Bordetella</i>	<i>Bacteroides</i>	Proteobacteria	<i>Sideroxydans</i>	Actinobacteria	<i>Jatrophihabitans</i>
<i>Brevundimonas</i>	<i>Bordetella</i>	Proteobacteria	<i>Pseudomonas</i>	Proteobacteria	<i>Novosphingobium</i>
<i>Candidatus nitrotoga</i>	<i>Brevundimonas</i>	Proteobacteria	<i>Sinorhizobium</i>	Proteobacteria	<i>Methyloferula</i>
<i>Candidimonas</i>	<i>Candidatus nitrotoga</i>	Proteobacteria	<i>Telluria</i>	Proteobacteria	<i>Sinorhizobium</i>
<i>Delftia</i>	<i>Frateuria</i>	Proteobacteria	<i>Herbaspirillum</i>	Proteobacteria	<i>Shinella</i>
<i>Frateuria</i>	<i>Geobacter</i>	Proteobacteria	<i>Shinella</i>	Proteobacteria	<i>Pseudomonas</i>
<i>Hirschia</i>	<i>Heliobacterium</i>	Proteobacteria	<i>Limnobacter</i>	Proteobacteria	<i>Acidovorax</i>
<i>Methylibium</i>	<i>Hirschia</i>	Proteobacteria	<i>Massilia</i>	Proteobacteria	<i>Ensifer</i>
<i>Methylobacterium</i>	<i>Longilinea</i>	Proteobacteria	<i>Azohydromonas</i>	Proteobacteria	<i>Rhizobium</i>
<i>Nitrospira</i>	<i>Luteimonas</i>	Proteobacteria	<i>Sphingopyxis</i>	Proteobacteria	<i>Agrobacterium</i>
<i>Paracoccus</i>	<i>Magnetospirillum</i>	Proteobacteria	<i>Chelatococcus</i>	Planctomycetes	<i>Blastopirellula</i>
<i>Prochlorococcus</i>	<i>Methylibium</i>	Proteobacteria	<i>Aquicola</i>	Proteobacteria	<i>Azospirillum</i>
<i>Sterolibacterium</i>	<i>Methylobacterium</i>	Chloroflexi	<i>Levilinea</i>	Proteobacteria	<i>Sphingopyxis</i>
<i>Woodsholea</i>	<i>Methyloversatilis</i>	Proteobacteria	<i>Altererythrobacter</i>	Proteobacteria	<i>Roseomonas</i>
	<i>Nannocystis</i>	Proteobacteria	<i>Hyphomicrobium</i>	Proteobacteria	<i>Lacibacterium</i>
	<i>Paracoccus</i>	Proteobacteria	<i>Methylocella</i>	Proteobacteria	<i>Pseudoxanthomonas</i>
	<i>Prosthecomicrobium</i>	Proteobacteria	<i>Pseudoxanthomonas</i>	Proteobacteria	<i>Rhodanobacter</i>
	<i>Rhodocista</i>	Cyanobacteria	<i>Chroococcidiopsis</i>	Planctomycetes	<i>Pirellula</i>
	<i>Thermoleophilum</i>	Proteobacteria	<i>Rhizobium</i>	Proteobacteria	<i>Telluria</i>
	<i>Woodsholea</i>	Proteobacteria	<i>Duganella</i>	Proteobacteria	<i>Massilia</i>
		Proteobacteria	<i>Asticcacaulis</i>	Proteobacteria	<i>Thermomonas</i>
		Proteobacteria	<i>Solimonas</i>	Chloroflexi	<i>Chloroflexus</i>
		Proteobacteria	<i>Thermomonas</i>	Firmicutes	<i>Chelativorans</i>
		Proteobacteria	<i>Acidovorax</i>	Planctomycetes	<i>Gemmata</i>
		Planctomycetes	<i>Pirellula</i>	Proteobacteria	<i>Aquicola</i>
		Proteobacteria	<i>Aetherobacter</i>	Proteobacteria	<i>Limimonas</i>
		Firmicutes	<i>Pelotomaculum</i>		

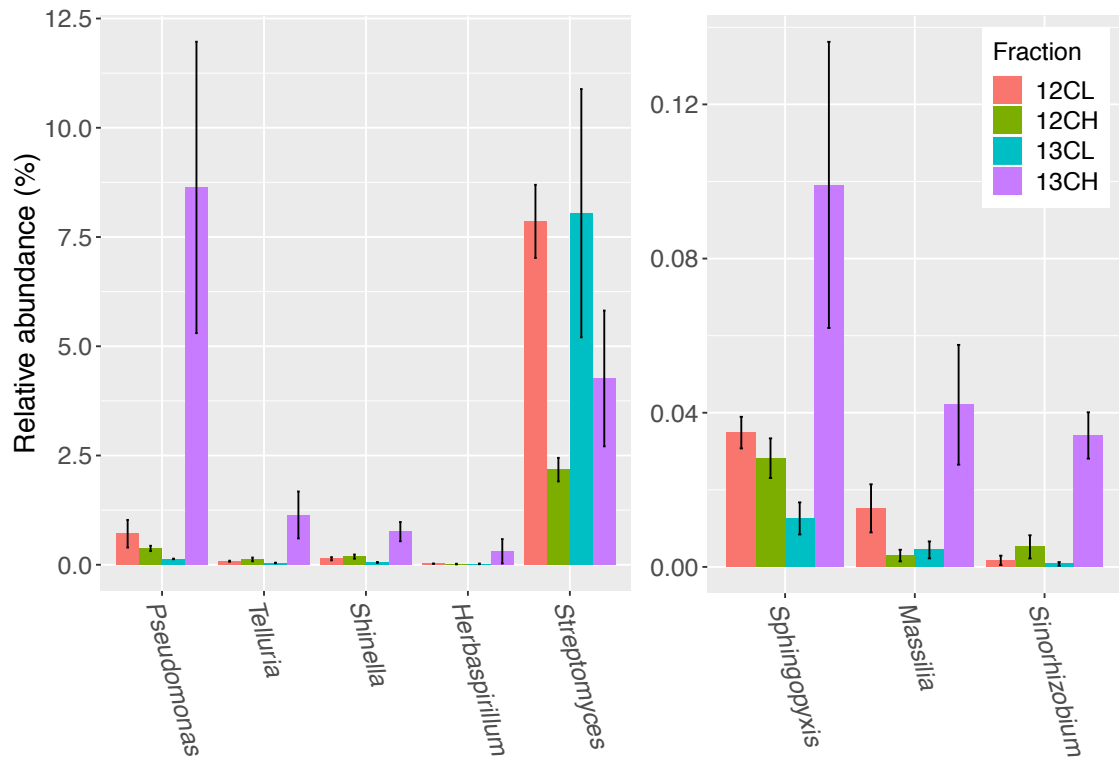


Figure 4.10 Seven bacterial genera in the rhizosphere compartment of *A. thaliana* plants whose relative abundance demonstrated the greatest overall enrichment in the ^{13}CH fraction relative to the ^{12}CH fraction due to the metabolism of ^{13}C labelled root exudates. *Streptomyces* were not enriched, but are included for comparison. 12CL/13CL and 12CH/13CH stand for buoyant density fractions representing the light (L) and heavy (H) fractions of DNA from $^{12}\text{CO}_2$ (12C) or $^{13}\text{CO}_2$ (13C) incubated plants, respectively. N= 3 replicate plants. Bars represent $\pm\text{SE}$.

In comparison to rhizosphere samples, a total of 27 genera demonstrated enrichment in the ^{13}CH fraction of the endophytic compartment relative to the ^{12}CH and ^{13}CL fractions. Here, the majority of root exudate metabolisers were also Proteobacteria (21 genera in total), with three other genera belonging to the phylum Planctomycetes (*Blastopirellula*, *Pirellula* and *Gemmata*), one to the Firmicutes (*Clostridium*), one to the Chloroflexi (*Chloroflexus*), and one to the Actinobacteria (*Jatrophihabitans*) (Table 4.6). Several of the non-proteobacterial genera identified as root exudate metabolisers are known to be associated with plant roots, including species of *Jatrophihabitans* which are known to exist endophytically (Alcaraz et al 2018, Gong et al 2016,

Madhaiyan et al 2013). The most abundant genus in the ^{13}CH fraction of the endophytic samples was the proteobacterial genus *Shinella*, which demonstrated a 38-fold enrichment between the ^{13}CH (26.42% relative abundance) and ^{13}CL (0.68% relative abundance) fractions and a 23-fold enrichment between the ^{13}CH and the ^{12}CH control fractions (1.14%) (Figure 4.11). *Shinella* is a member of the family Rhizobioaceae and members of this genus have previously been isolated from the root nodules of leguminous plants in which they are capable of fixing nitrogen (An et al 2006, Lin et al 2008). In terms of fold change, however, *Pseudomonas* was the genus that was most enriched in ^{13}C heavy fractions from the endophytic compartment, with a 26-fold increase in abundance between ^{13}CH (15.64% relative abundance) and ^{12}CH (0.61% relative abundance) fractions of $^{13}\text{CO}_2$ incubated plants (Figure 4.11). Out of the 28 genera that were found to be metabolising exudates in the root compartment, 15 genera only metabolised root exudates in the endosphere and not in the rhizosphere. Conversely, 16 out of 29 genera were found to be metabolising exudates in the rhizosphere but not the endosphere. The remaining 13 genera were enriched in the heavy fractions of both the endophytic and rhizosphere compartments, suggesting that they are able to survive and make use of plant metabolites in both niches (Table 4.6).

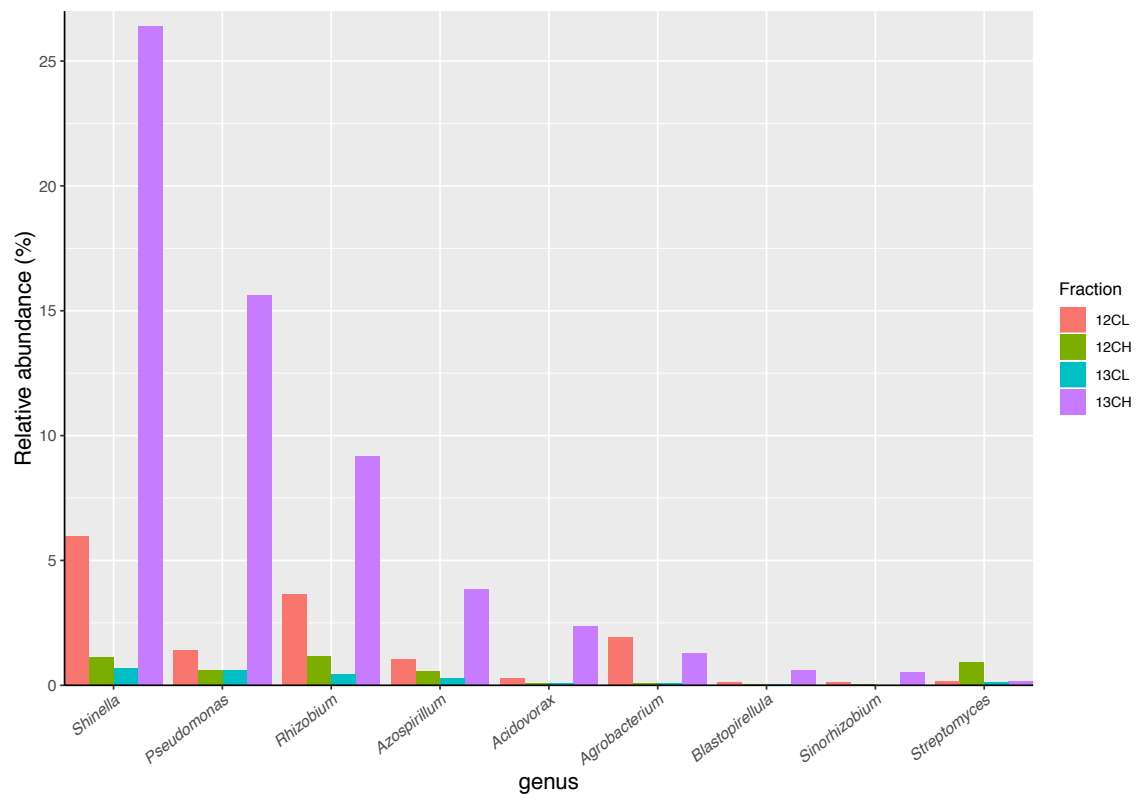


Figure 4.11 Eight bacterial genera isolated from the endophytic compartment of *A. thaliana*, whose relative abundance demonstrated the greatest overall enrichment in the ^{13}CH fraction relative to the ^{12}CH fraction due to the metabolism of ^{13}C labelled root exudates. In comparison, the genus *Streptomyces* did not demonstrate enrichment between these fractions suggesting they did not metabolise labelled root exudates. $^{12}\text{CL}/^{13}\text{CL}$ and $^{12}\text{CH}/^{13}\text{CH}$ = buoyant density fractions representing the light/unlabelled (L) and heavy/labelled (H) fractions of DNA from $^{12}\text{CO}_2$ (^{12}C) or $^{13}\text{CO}_2$ (^{13}C) incubated plants respectively. Each fraction represents a pooled sample from N=3 plants.

Surprisingly, although one actinobacterial genus (*Jatrophihabitans*) was found to be labelled in the endophytic compartment, there was no enrichment of *Streptomyces* bacteria in the ^{13}CH fractions of either the rhizosphere or endosphere, despite being the most dominant member of the phylum Actinobacteria in both compartments (Figure 4.5, Figure 4.10, Figure 4.11). Taken together, these data suggest that *Streptomyces* bacteria were outcompeted for the use of root exudates by unicellular bacteria, particularly Proteobacteria, under the conditions used in this experiment. In the current study, Proteobacteria were very abundant in the unfractionated soil (35%

average relative abundance), rhizosphere (39 %) and endophytic compartment (91%), compared to Actinobacteria (present at 20 %, 15% and 3% in the soil, rhizosphere and root compartments, respectively) (Figure 4.3) and were therefore likely to have the upper hand during competition (Scheuring and Yu 2012). This particularly likely to have been the case in the endophytic compartments in which *Streptomyces* only made up 1.12% (\pm 0.50%) of the total community. Accordingly, genera that were found to be metabolising the greatest amount of exudates in the root compartment were also found to be the most enriched in the endophytic compartment compared to the surrounding soil (Figure 4.12).

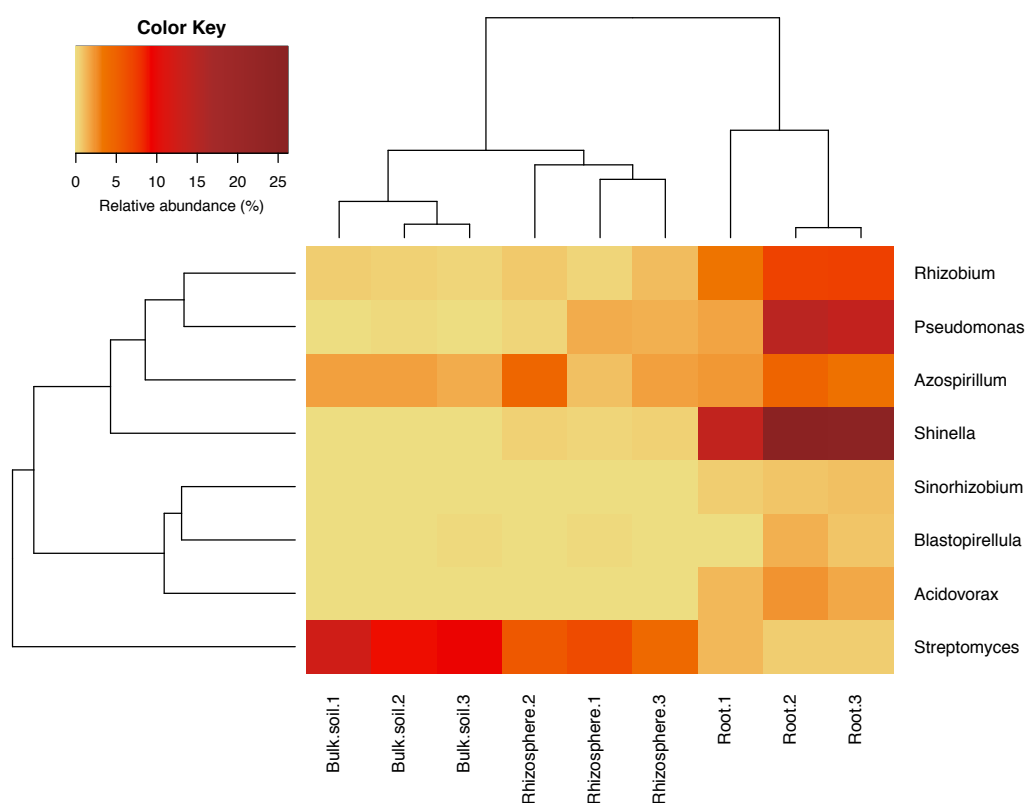


Figure 4.12 The abundance of the eight bacterial genera metabolising the greatest quantities of labelled exudates in the endophytic compartment of *A. thaliana* (determined by ratios of abundance in ^{13}CH to ^{12}CH fractions). Their relative abundances (%) are shown across the bulk soil, rhizosphere and root compartments (light yellow to brown indicates increasing relative abundance). $N = 3$ replicate plants in individual pots. *Streptomyces* species were not metabolising root exudates, nor were they enriched in the endophytic compartment, but are shown for comparison. Clustering represents Bray-Curtis dissimilarities.

4.4.3 The use of root exudates as a sole carbon and nitrogen source

A. thaliana plants are known to exude a wide range of compounds into the surrounding soil medium (Badri et al 2013, Chaparro et al 2013). However, the DNA-SIP experiment suggested that *Streptomyces* species were not feeding on these root exudates in compost-grown plants (Figure 4.10, Figure 4.11). To test whether streptomycetes could use root exudates when grown in monoculture *in vitro*, root exudates were collected from hydroponically-grown, wild-type *A. thaliana* plants and used as a growth medium for several different *Streptomyces* strains that had previously been isolated from *A. thaliana* roots (see Chapter 3, Table 3.1). Isolates were grown on agarose plates containing water only, or agarose plus sterile root exudates. None of the strains grew on agarose alone, but all grew on agarose plates containing root exudates, suggesting that strains were capable of utilising root exudates in the absence of other microbial competition (Figure 4.13).

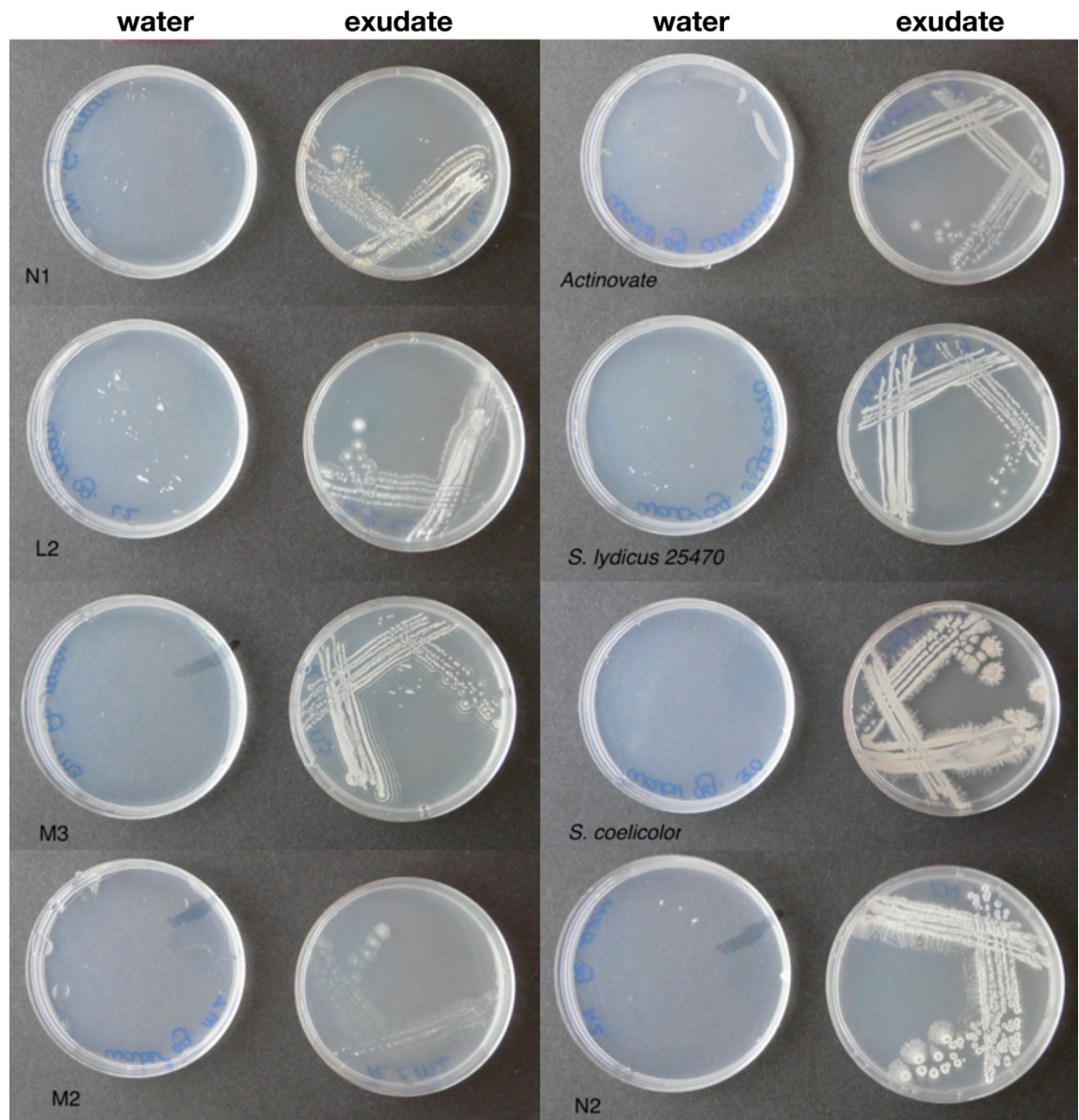


Figure 4.13 The growth of *Streptomyces* isolates on purified root exudates. *Streptomyces* strains were grown on agarose dissolved in sterile water, or agarose dissolved in filter-sterilised *A. thaliana* root exudates. Strains M2, M3, N1, N2, and L2 are endophytes isolated from *A. thaliana* roots. The other strains are the ATCC strain *S. lydicus* 25470, *S. lydicus* isolated from Actinovate and the model laboratory strain *Streptomyces coelicolor*.

4.5 Discussion

The aim of this chapter was to fully characterise the bacterial community composition of the *A. thaliana* root and rhizosphere microbiomes, as well as to establish the capacity for different bacterial taxa to metabolise plant root exudates in these two

different compartments. The role of *Streptomyces* bacteria in the root microbiome was of particular interest because of their potential as biocontrol and plant growth-promoting agents.

The results of 16S rRNA gene amplicon sequencing of unfractionated samples from the soil, rhizosphere and roots of *A. thaliana* plants, were in agreement with the findings of previous studies that have shown that *A. thaliana* is associated with a relatively stable and consistent bacterial community, whereby the phyla Proteobacteria and Actinobacteria are found to be abundant in the rhizosphere and root compartments (Bodenhausen et al 2013, Bulgarelli et al 2012, Lundberg et al 2012). In the experiments carried out in this chapter, Proteobacteria were found to dominate the plant-associated bacterial community and were particularly enriched in the plant root samples, relative to the rhizosphere and soil compartments. Additionally, although Actinobacteria were not enriched in roots, or in the rhizosphere compartment compared to the soil, this was the second most abundant phylum in all three compartments. The phylum was also found to be dominated by the family Streptomycetaceae, which is in agreement with the results of other studies that have shown that the presence of Actinobacteria in the microbiome of *A. thaliana* is driven by the abundance of *Streptomyces* species (Bulgarelli et al 2012, Lundberg et al 2012).

DNA-SIP was used to identify which bacteria were feeding on plant root exudates in the rhizosphere and endosphere compartments of *A. thaliana*. This is the first report, to our knowledge, of DNA-SIP being used to investigate the endosphere of *A. thaliana* roots. Therefore, although a pooled sample of replicates was used to generate root-associated fractions, this is an advance on other SIP experiments that have only investigated bacterial metabolism in the rhizosphere (Bressan et al 2009, Haichar et al 2012). Additionally, the experiments in this Chapter investigated the metabolic capabilities of the total bacterial community in the microbiome of *A. thaliana* by using 16S rRNA gene amplicon sequencing to analyse light and heavy fractions. Previous SIP experiments that have used *A. thaliana* (Table 4.1) have restricted their analysis to members of the phyla Proteobacteria and Firmicutes, by using DNA-SIP combined with taxon-specific primers and DGGE (Bressan et al 2009, Haichar et al 2012).

The results of the DNA-SIP experiment, combined with previous published reports on the chemistry of *A. thaliana* root exudates, suggest that exudates are a rich and public food resource and play a key role in root microbiome establishment (Badri et al 2013, Chaparro et al 2013, Haichar et al 2012). Root exudates are known to contain a diverse range of metabolites including sugars, amino acids, and phenolic compounds many of which can be used as carbon sources by a wide variety of bacterial taxa (Badri and Vivanco 2009, Badri et al 2013, Chaparro et al 2013). Proteobacterial genera were found to be particularly enriched with ^{13}C , in both the rhizosphere and endosphere samples of *A. thaliana* plants in the DNA-SIP experiment. Many of these genera have been previously noted for their positive influence on plant fitness and were also found to be enriched in abundance in the endophytic compartment, suggesting that root exudates may enable beneficial bacteria to establish within the plant root microbiome. For example, the genus *Pseudomonas* was highly enriched in the heavy fractions of ^{13}C and was also abundant in plant root samples; this genus is well-known for producing many different bioactive and growth-promoting molecules (Glick et al 1997, Hernández-León et al 2015, Mercado-Blanco et al 2016, Raza et al 2016). Additionally, genera in the clade Rhizobia, such as *Rhizobium* and *Sinorhizobium*, were also heavily labelled and have previously been shown to have a positive influence on root development and plant biomass when in association with *A. thaliana* plants (Zhao et al 2017). It is likely that root exudates are, in part, responsible for stabilising the apparent mutualisms that exist between these beneficial bacteria and the plant host, through a combination of the Partner Fidelity Feedback and Competitive Screening models discussed in Chapter 1 (Archetti et al 2011, Foster and Wenseleers 2006, Scheuring and Yu 2012, Weyl et al 2010). Bacterial colonies that release growth-promoting factors or bioactive molecules exploit a widespread pre-adaptation in plants to proliferate root biomass in soils that are rich in nutrients or free from disease. In return, plant roots release nutritional resources for bacteria, via root exudates, which promote local colony growth. Exudates are also likely to fuel interference competition amongst microbes, during which the most abundant or fast-growing strains are predicted to have an advantage (Scheuring and Yu 2012); in the SIP experiment, proteobacterial genera were present in the greatest abundances. Interference competition amongst bacteria typically manifests as competitive exclusion by taking up niche space, plus the

secretion of antibacterial and antifungal compounds, both of which may indirectly benefit the plant by excluding pathogenic species.

Interestingly streptomycetes, the main focus of this chapter, did not feed off root exudates in the SIP experiment despite being able to grow on purified root exudates *in vitro* in the absence of other microbial competition. *Streptomyces* species were present in the endosphere and rhizosphere of *A. thaliana*, suggesting that their preferred substrates might have been absent from root exudates at the time of labelling, or that they were largely out-competed by the more abundant, fast-growing proteobacterial genera for plant-derived resources. Proteobacteria are dominant in the rhizosphere of many different plant species and have previously been noted as metabolisers of root exudates (Ai et al 2015, Haichar et al 2008, Haichar et al 2012, Zhalnina et al 2018). Many members of this phylum are also thought to be “r-strategists” that have the ability to thrive and rapidly proliferate in fluctuating environments where resources are highly abundant, such as in the rhizosphere and root-associated microbiome (Philippot et al 2013). On the other hand, species of *Streptomyces* typically exhibit slower growth and are competitive in environments in which resource availability is limited, such as in the bulk soil (van der Meij et al 2017). Thus, it is possible that Proteobacteria were able to rapidly proliferate around and within plant roots and therefore outcompete the slower growing actinomycetes, particularly those that were already present at lower abundances. Altering the ratio of relative abundances of phyla in the starting soil inoculum may have resulted in different competitive outcomes (Scheuring and Yu 2012).

Given their diverse metabolic capabilities, it is likely that streptomycetes are able to persist at low abundances by feeding on more complex organic polymers under conditions of high competition. *Streptomyces* are effective saprophytes that are known to produce a huge array of extracellular enzymes to break down complex and insoluble biopolymers in their surrounding environment that are unavailable to other bacterial taxa (Chater et al 2010). Therefore, this genus may have predominantly fed off older, plant-originated organic material such as root cells and mucilage that were sloughed off before ¹³C labelling commenced, or on similar matter present in the compost growth medium; these resources would have contained a much lower level of labelled

¹³C. As *A. thaliana* appears to exhibit a relatively small rhizosphere effect compared to other plant species (Bulgarelli et al 2015, Schlaeppi et al 2014) complex polymers may have been more readily available in the rhizosphere than exudates, particularly given the fact that compost contains a relatively high level of organic matter. A small rhizosphere effect was supported by the data in this chapter which showed an incomplete level of rhizosphere labelling and a low differentiation between the soil and rhizosphere microbial communities.

Using compost as a plant growth medium may have additionally had an effect on the carbon-use preferences of streptomycetes in the SIP experiment. This is because the chemical composition of soils can alter plant-microbe interactions. Indeed, long-term fertilisation regimes have been shown to reduce the dependence of bacteria on plant-derived carbon (Ai et al 2015). In a ¹³C SIP study on the wheat rhizosphere, Actinobacteria were less enriched with ¹³C when plants were grown in soils treated with a high levels of inorganic fertilisers (nitrogen, phosphorous and potassium- NPK), with a corresponding increase in the dependence of Proteobacteria on root exudates (Ai et al 2015). This was suggested to be because NPK altered root exudate profiles and carbon-use-efficiency by these bacteria (Ai et al 2015). Organic fertilisation also reduced the diversity of bacteria feeding on root exudates to a few taxa, potentially by altering exudate regimes, but also by offering increased SOM as an alternative carbon source (Ai et al 2015). Levington F2 Seed and Modular Compost is supplemented with NPK and is likely to contain greater levels of organic matter than some agricultural soils. It would be interesting to see if changing the soil growth medium to one with lower levels of NPK and SOM resulted in a greater dependence on root exudates by actinobacterial genera.

As mentioned, the composition of plant root exudates are known to fluctuate considerably over the plant life cycle and in response to abiotic and biotic stressors. Accordingly, the abundance of particular microbial taxa has been shown to correlate with these changes, suggesting some specificity in exudate usage (Chaparro et al 2013, Chaparro et al 2014, Haichar et al 2008, Zhalnina et al 2018). Therefore, it is also possible that the preferred substrates of *Streptomyces* and other Actinobacterial genera were absent from root exudates at the time of sampling. Studies that have

sampled at different stages of plant development have demonstrated that the microbial community metabolising root exudates shifts between seedling, vegetative and flowering stages (Chaparro et al 2013, Haichar et al 2012, Zhalnina et al 2018). Thus, an interesting extension to the experiment carried out in this Chapter would be to carry out a time-course SIP experiment whereby samples are taken at different points over the *A. thaliana* lifecycle, or from plants that have been exposed to pathogenic or abiotic stress. Metabolomics could also be used to unpick which carbon sources are preferentially used by *Streptomyces* species, given that they can grow *in vitro* on raw root exudates. Such experiments have been used to investigate root exudate usage by bacteria in the root microbiome of the grass species *Avena barbata*; a comparison of the chemical composition of raw root exudates versus spent root exudates that were used as a bacterial growth medium, revealed that many of the bacterial species that abundantly colonised roots had a preference for metabolising aromatic organic acids (Zhalnina et al 2018). Similar methods could be used to establish whether exudates used by streptomycetes are those that are widely available under normal growth conditions, or are only upregulated when plants are exposed to certain conditions.

It is important to note here that *Streptomyces* bacteria are also spore-formers and thus may enter a dormant phase in their lifecycle under unfavourable conditions (Flärdh and Buttner 2009, van der Meij et al 2017). Accordingly, *Streptomyces* species have been reported to be predominantly present as spores in natural soils, only germinating and developing into vegetative mycelium during periods of time, or in pockets of soil, in which particular nutrients become more readily available (Goodfellow and Williams 1983, Lloyd 1969, Wellington et al 1990). As such, streptomycetes may have been detectable via their DNA, but dormant, under conditions of high competition in the root, rhizosphere and soil whilst plants were being pulse-labelled with $^{13}\text{CO}_2$. Indeed, *Streptomyces* have been observed to sporulate within the tissue of pea plant nodules shortly after inoculation (Tokala et al 2002). An RNA versus DNA-SIP approach may have given a better indication of the transcriptionally active bacterial community present in the roots and rhizosphere of *A. thaliana* plants (Dumont and Murrell 2005, Haichar et al 2016). Since RNA has a higher turnover rate than DNA, RNA-SIP may also have identified whether *Streptomyces*

actively metabolise root exudates, but only incorporate a low level of ^{13}C into DNA because of an extremely slow growth rate (Haichar et al 2008).

In conclusion, the experiments in this Chapter have shown that the root exudates of *A. thaliana* can be metabolised by a wide variety of genera, including those that are known to be beneficial to plant host fitness. Thus, root exudates are likely to play a key role in recruiting beneficial bacteria from the soil and in maintaining mutualistic relationships within the plant root microbiome. However, factors such as the initial abundance of taxa in the soil growth medium, bacterial growth strategies, as well as edaphic factors such as pH, soil organic matter and the levels of inorganic nutrients, may all determine the outcomes of competition for plant-derived resources *in situ*. As such, *Streptomyces* species were not observed to be using root exudates *in vivo*, despite being able to use these as a sole energy source *in vitro*. Future experiments that focus on understanding the variability of root exudation and bacterial resource-use preferences may help to understand how the abundance of genera like *Streptomyces* could be altered in the rhizosphere and root microbiome to better promote plant host fitness and disease protection. Finally, although easily manipulated, *A. thaliana* does not act as a good model for all agriculturally relevant crop species. Therefore, it would be interesting to extend studies on root exudate metabolism under variable conditions to economically important plant species, such as wheat, that would be the direct target of streptomycete biocontrol and growth-promoting agents in agriculture. Additionally, bacteria do not interact with plants in isolation from other microorganisms in the soil and so, in the future, it will also be important to investigate the role of other taxa including archaeal, fungal and protist communities in using root exudates, to gain a more complete understanding of the competitive dynamics unfolding within the plant root microbiome.

Chapter 5 **Salicylic acid as a modulator of root colonisation by** *Streptomyces*

5.1 Introduction

Pressures from a rising world population require that crop production is massively increased over the coming years to ensure global food security. This could either occur via the development of methods to enhance plant growth, or by reducing crop losses caused by pests and diseases (Beddington 2010, Godfray et al 2010). However, an increase in food production needs to occur within the limits of land availability and in a way that causes minimal damage to the surrounding ecosystem. Biocontrol and plant-growth-promoting (PGP) bacterial strains that improve crop health and yield, could act as sustainable alternatives to chemical pesticides and fertilisers, which can cause extensive pollution and damage to non-target species (Pimentel et al 1993). However, many biocontrol agents, such as those that are streptomycete-based (including Actinovate® and Mycostop®), can be highly inconsistent in their ability to suppress disease and promote plant growth under varying field conditions or in the presence of different plant host species (Ryan et al 2009, Tahvonon et al 1995, Zhang et al 2011). There are several reasons for this, including poor colonisation efficiency due to a lack of competitiveness in plant roots and the rhizosphere niche (Dessaux et al 2016, Quiza et al 2015, Ryan et al 2009). Additionally strains may not express plant beneficial traits under all environmental scenarios or be viable under field conditions (Ryan et al 2009, van der Meij et al 2017).

Deciphering the chemical cues that have evolved to mediate plant-microbe interactions and to enable beneficial species of bacteria to establish within the plant root microbiome under natural conditions, could lead to the development of methods that enhance the efficacy of biocontrol agents and enable us to engineer beneficial plant root microbiomes (Quiza et al 2015, Ryan et al 2009). For example, an understanding of the plant host factors that influence microbial colonisation could be used to optimise microbial delivery systems that ensure microbial functionality and competitiveness within the root niche (Dessaux et al 2016, Quiza et al 2015, Ryan et al 2009). Such knowledge could also facilitate the generation of plants with particular

root exudate or root architecture profiles that enhance the recruitment of beneficial microbes, but simultaneously exclude pathogenic species (Dessaux et al 2016, Quiza et al 2015, Ryan et al 2009).

As discussed in Chapters 3 and 4, the selection of the plant root microbiome is generally accepted to be a non-random process, with numerous studies showing distinctive patterns of microbial colonisation within and across plant host species (Berg and Smalla 2009, Bulgarelli et al 2012, Fitzpatrick et al 2018, Lundberg et al 2012, Schlaeppi et al 2014). Specific selection mechanisms have likely evolved to enable plants to limit their interactions to beneficial microorganisms (Badri and Vivanco 2009, Bais et al 2006, Foster et al 2017). Plants exude 20-40% of their photosynthetically fixed carbon from their roots into the surrounding soil and the diverse range of compounds contained in this exudate have the potential to act as chemoattractants, metabolic substrates or inhibitors for a broad range of microbial species (Badri and Vivanco 2009, Bais et al 2006, Haichar et al 2016). Exudates are also likely to mediate interference competition between microbial species in the soil and potentially drive such interactions towards outcomes that are beneficial to the plant host (Badri and Vivanco 2009, Bais et al 2006). Thus, in combination with other factors, such as the starting soil inoculum and abiotic factors, root exudates are likely to play a key role in directing the assembly of a beneficial plant root microbiome (Berg and Smalla 2009). However, in many cases, the specific trophic or chemotactic links between specific plant root exudates and bacterial species have not yet been established.

Perhaps one of the best-characterised examples of a plant-microbe interaction that is understood in detail at the chemical level, is the relationship between leguminous plants and specific bacterial species of nitrogen-fixing rhizobia (Bais et al 2006, Liu and Murray 2016). Flavonoid compounds released by plants induce rhizobial chemotaxis towards the plant roots, as well as the expression of *nod* genes encoded by specific rhizobial strains (Bais et al 2006, Liu and Murray 2016). The expression of *nod* genes results in the synthesis of Nod factor molecules, which are chemically modified such that the nod factors produced by a particular rhizobial species will be unique and thus, will only be recognised by the correct host plant species (Bais et al 2006, Liu and

Murray 2016). Symbiosis, in the form of nodulation, is only initiated once these different layers of recognition have been established.

In addition to the recruitment of rhizobia to the root microbiome, specific root exudates are also thought to be involved in enabling the establishment of the protective PGP species, *Bacillus subtilis* FB17, in the root microbiome of *A. thaliana* (Rudrappa et al 2008). Root secretion of the tricarboxylic acid intermediate, malic acid, enables *B. subtilis* to be selectively recruited under conditions of foliar infection (Rudrappa et al 2008). Leaf infections by the pathogen *Pseudomonas syringae* have been shown to enhance the secretion of malic acid from *A. thaliana* roots which, in turn, initiates the chemotaxis of *B. subtilis* towards *A. thaliana* and the subsequent biofilm formation by this bacterial species on plant roots (Rudrappa et al 2008). Furthermore, colonisation by *B. subtilis* has been shown to induce systemic resistance in the plant host which reduces the severity of *P. syringae* infections (Rudrappa et al 2008).

The examples described above, represent rare cases in which the chemical basis of the interactions between plants and bacterial species are relatively well-defined. For the vast majority of other microbial species that are consistently found to colonise the rhizosphere and endosphere of particular plant species, these relationships are far less clear. However, as discussed in Chapter 4, the abundance of certain types of root exudate have been shown to correlate with the abundance of certain microbial taxa. In particular, phenolic compounds released from plant roots, including a range fatty acids, amino acids and organic acids, have been shown to correlate positively with the abundances of several microbial groups, including the phylum Actinobacteria (Badri et al 2009, Badri et al 2013, Chaparro et al 2013, Chaparro et al 2014, Zhalnina et al 2018). A large diversity of phenolic compounds are released by plant roots including plant defence phytohormones such as jasmonic acid (JA) and salicylic acid (SA), which have been implicated to play a role in plant microbiome assembly under a range of different conditions and in several different plant species.

5.1.1 Plant defense phytohormones

As sessile organisms, plants have evolved finely tuned pathways that enable them to perceive and adapt to changes in their environment, including colonisation by both pathogenic and beneficial microorganisms (Pieterse et al 2012). Plant defense phytohormones play a key role in modulating such response pathways. In particular, SA and JA are involved in directing the plant immune response which, when activated, leads to the production of antimicrobial compounds, as well as the onset of ROS production and localised cell death to restrict the spread of pathogenic invasion (Carvalhais et al 2017, Clarke et al 2000, Pieterse et al 2014). In general, SA tends to be biosynthesised in response to biotrophic pathogens, that are detected via evolutionarily conserved pathogen (or microbial) associated molecular patterns (PAMPs or MAMPs), and that feed on the contents of live cells (Pieterse et al 2012, Quiza et al 2015). An accumulation of SA locally can also result in the emergence of longer-lasting resistance to pathogens in distal, uninfected parts of the plant; this phenomenon is known as systemic acquired resistance (SAR) (Pieterse et al 2012). In contrast, the phytohormone JA generally tends to be activated in response to damage brought about by herbivorous insects and necrotrophic pathogens, the latter of which tend to destroy host cells before feeding on their contents (Pieterse et al 2012). The gaseous plant hormone ethylene can also act synergistically with JA to regulate the plant immune response (Pieterse et al 2012). Beneficial microbes are thought to have evolved mechanisms to avoid or attenuate the plant host immune response, but may also activate an enhanced level of disease resistance systemically away from the site of colonisation via a process known as induced systemic resistance (ISR) (Pieterse et al 2014). This enables plants to respond more rapidly to pathogenic attack (Pieterse et al 2014). In addition to this, there are now several lines of evidence to suggest that the production of plant phytohormones can, in turn, have a significant role in directing the recruitment of beneficial microbial species to the plant root microbiome.

5.1.2 The role of phytohormones in directing plant root microbiome establishment

Several studies have shown that the exogenous activation of defense signaling pathways can influence the diversity and composition of the plant root microbiome. For example, the exogenous application of methyljasmonate (MeJA) to plants induces JA signaling and has been shown to have a significant influence on the community

composition of the *A. thaliana* rhizosphere (Carvalhais et al 2013b, Carvalhais et al 2017). In particular, bacteria that have are known to be involved in plant defence, including *Bacillus* species, were shown to be significantly enriched in JA-induced *A. thaliana* plants, relative to untreated controls (Carvalhais et al 2013a, Carvalhais et al 2017). This suggests that plants may release defense phytohormones as a “cry for help” that aims to recruit defensive microorganisms from the soil (Carvalhais et al 2017). Similar experiments have been conducted on wheat, whereby the exogenous application of MeJA has been shown to reduce bacterial diversity and alter the community composition associated with the root endophytic compartment, compared to that of untreated plants (Liu et al 2017b). The abundance of several *Streptomyces* OTUs was observed to change in this system, with some increasing in induced plants, whilst others were present at lower abundances (Liu et al 2017b).

Other studies have made use of mutant plant lines that have been engineered to produce or accumulate altered levels of plant defense phytohormones, to investigate the role of these compounds in directing plant root microbiome establishment. For example, *A. thaliana* plants carrying disruptions in two major branches of the JA signaling pathway were shown to have significantly altered plant root exudate profiles, with reduced quantities of the compounds asparagine, ornithine and tryptophan, but increased levels of fructose (Carvalhais et al 2015). This, in turn, led to distinct archaeal and bacterial communities being present in the rhizosphere of mutant lines compared to wild-type plants (Carvalhais et al 2015). In particular, the study found a greater abundance of genera such as *Streptomyces* and *Bacillus* in plants that were producing lower levels of JA (Carvalhais et al 2015). Similarly, the roots of tobacco plants (*Nicotiana attenuate*) deficient in ethylene biosynthesis have been shown to be associated with a distinct community of culturable bacterial species versus wild-type plants (Long et al 2010).

Of particular note is a study by Lebeis et al (2015) which investigated the root-associated and rhizosphere microbiome of *A. thaliana* plants that had been engineered to either constitutively express SA biosynthesis genes (*cpr5* plants), or accumulate lower levels of SA (including *sid2-2* and *pad4* plants). The study demonstrated that the microbiome of mutant lines significantly differed from wild-type plants, with a

complementary enrichment or depletion of certain bacterial families depending on whether plants produced more or less SA relative to wild-type plants. To test the results of these experiments, which suggested a specific role of SA in recruiting or inhibiting bacterial colonisers, simple, synthetic communities (syncomms) of bacteria (containing 38 species from representative bacterial families) were established and added to the growth medium of sterile plants. 16S rRNA gene amplicon sequencing demonstrated that several of the syncomm bacterial species were enriched in the roots of mutant plants that were not able to accumulate SA, suggesting that SA normally inhibited their colonisation. On the other hand, when SA was exogenously applied to leaves or soil (to induce SA production) three isolates became particularly enriched in the root-associated microbiome of *A. thaliana* including one species in the phylum Bacteroidetes (a species of *Flavobacterium*), and two species in the phylum Actinobacteria (one *Terracoccus* species and one *Streptomyces* species). The enriched streptomycete isolate, *Streptomyces* species 303, was additionally reported to be able to use SA as a sole carbon source and its genome encodes orthologues of known SA degrading enzymes. The results from syncomm experiments, combined with those from plants grown in a complex soil medium, led the authors to suggest that phytohormones play a major role in regulating the composition of the plant root microbiome and SA, in particular, may be directly important for attracting and acting as a substrate for species, like *Streptomyces* sp. 303, during pathogen attack (Lebeis et al 2015).

5.1.3 Heterogeneity in the results of phytohormone studies

Although the study by Lebeis et al (2015) demonstrated that plant genotype can have a large influence on the composition of the plant root microbiome, the direct role of SA in driving these differences is still not clearly defined. For example, despite observing extensive differences between the root microbiomes of the different *A. thaliana* genotypes grown in soil, only three isolates, including one species of streptomycete, were shown to be specifically enriched in plants exogenously exposed to SA, out of the 38 strains used as an inoculum in the syncomm experiments. Additionally, in soil experiments, half of the bacterial families observed to be depleted in mutants that accumulated lower levels of SA were not consistently depleted across all mutants with the same SA phenotype, suggesting that the relationship between

plant genotype and microbiome assembly is complex and that other factors are likely to be involved. It should also be noted that when testing *Streptomyces* sp. 303 for the use of SA as a sole carbon source, the supplementary methods of Lebeis et al (2015) state that sodium citrate was also added to minimal medium which could serve as an additional carbon source for streptomycetes. SA metabolism has been noted previously in a streptomycete species isolated from soil (*Streptomyces* sp. strain WA46) whereby a new pathway for salicylate degradation was identified involving salicylyl-CoA and gentisate as intermediates (Ishiyama et al 2004). Thus, it is not impossible that *Streptomyces* sp. 303 isolated by Lebeis et al (2015) is capable of metabolising SA. However, further experimentation is required to establish how widespread responsiveness to SA is amongst *Streptomyces* species isolated from the root microbiome of *A. thaliana* and whether direct responsiveness to SA is the cause of altered root colonisation in plants with disrupted phytohormone signaling pathways.

It should also be noted that although several studies have demonstrated an association between the levels of plant phytohormones (particularly JA and SA) and the microbial communities associated with plants roots, there are other studies that demonstrate contradictory results. For example, several studies have suggested that JA and SA signaling pathways can have a significant impact on the composition of the *A. thaliana* root microbiome, but another study that used both mutant lines and the exogenous application of these two phytohormones, suggested that they had minimal effects on the rhizosphere community and differences in plant morphology and development between mutant lines played a greater role in influencing bacterial root colonisation (Doornbos et al 2011). Additionally, studies on tobacco (*Nicotiana attenuate*) demonstrated that bacterial community composition was largely unaltered between control plants and those impaired in their capacity to make JA. This result was consistent across soil type, plant tissue type and developmental stage (Santhanam et al 2014, Santhanam et al 2015). Additionally, bacterial strains isolated from tobacco roots did not demonstrate colonisation specificity when inoculated onto plants of different genotypes *in vitro* (Santhanam et al 2015). Factors such as the local soil conditions, plant tissue type (leaf, stem or roots) and plant cell wall characteristics were thought to play a greater role in directing microbiome establishment, rather than

the levels of phytohormone compounds (Santhanam et al 2015). Thus, the direct effects of phytohormones on the microbiome still remain unclear.

5.2 Aims

Deciphering the chemical cues that recruit microorganisms to plant roots may enable the development of more efficient biocontrol strategies (Quiza et al 2015). The experiments in this chapter aimed to further investigate the results set out by Lebeis et al (2015) by testing the ability of *Streptomyces* species to colonise the roots of *A. thaliana* lines that either constitutively expressed SA biosynthesis genes (*cpr5* plants), or were deficient in their ability to produce or accumulate SA (*sid2-2* and *pad4* plants), compared to wild-type *A. thaliana* plants. A range of *Streptomyces* strains were also tested for their ability to respond to SA *in vitro* and/or *in vivo* in soil microcosms. This included strains that were isolated from the roots of *A. thaliana* plants (see Chapter 3), the model streptomycete *S. coelicolor* M145 as well as three strains of *S. lydicus*; one of these was isolated from the biocontrol formulation Actinovate® and the other two were *S. lydicus* endophytes taken from a culture collection.

5.3 Materials and Methods

5.3.1 Generating eGFP-labelled *Streptomyces* strains

In order to generate marked streptomycete strains, the plasmid pIJ8660/eGFP (Table 5.1) was conjugated into both *Streptomyces coelicolor* M145 and *Streptomyces* isolate M3 (see Table 3.1 for strain information). The plasmid pIJ8660/eGFP contains an optimised eGFP gene under the control of the constitutive, high-level *ermE** promoter as well as an *aac* apramycin resistance marker (Table 5.1). The plasmid was used to transform the non-methylating *E. coli* donor strain, ET12567 (pUZ8002) (Table 5.1) via electroporation; successful transformants (henceforth called ET cells) were then identified via growth on plates containing 25 µg ml⁻¹ chloramphenicol, 50 µg ml⁻¹ kanamycin and 50 µg ml⁻¹ apramycin. For conjugations, ET cells were grown overnight in 10 ml of LB medium (Table 3.2) supplemented with 25 µg ml⁻¹ chloramphenicol, 50 µg ml⁻¹ kanamycin and 50 µg ml⁻¹ apramycin. Cultures were grown at 37°C, shaking at 250 rpm. Cells were then sub-cultured 1 in 20 (v/v) into a further 10 ml of LB medium, supplemented with the three antibiotics (as described above), and were grown at 37°C

for approximately 4 hours, shaking at 250 rpm. The ET cell culture was then pelleted by centrifuging at 4000 rpm for 3 minutes and resuspended in 10 ml of ice-cold LB medium. Pelleting and resuspension steps were then repeated a further two times to wash the cells, before resuspending the cell pellet in 1 ml of LB medium. Meanwhile, 50 μ l of spores (from stocks containing 10^7 spores ml^{-1}) of either *S. coelicolor* M145 or *Streptomyces* strain M3 (Table 3.1) were added to 500 μ l of 2xYT (Table 3.2) and heated at 50°C for 10 minutes to synchronise germination. 500 μ l of the washed ET cells were then added to the pre-germinated spores. The mixture was centrifuged for 2 minutes at 13'000 rpm before resuspending the pellet to a volume of 100 μ l. 10^0 , 10^{-1} and 10^{-2} dilutions were then plated onto SFM agar (Table 3.2) containing 10 mM MgCl_2 and 50 $\mu\text{g ml}^{-1}$ apramycin. Plates were then incubated for up to 7 days at 30°C. Exconjugants were selected by growth on 50 $\mu\text{g ml}^{-1}$ of apramycin.

Table 5.1 Strains and plasmids used for work described in Chapter 5. Vector resistance markers are denoted as *aac^R* for apramycin resistance, *kan^R* for kanamycin resistance and *cmI^R* for chloramphenicol resistance.

Strain/plasmid	Description	Reference
pIJ8660/eGFP	Contains an optimised eGFP gene under the control of the constitutive <i>ermE*</i> promoter; <i>aac^R</i>	Sun et al (1999). Promoter introduced by Dr. Neil Holmes, UEA.
ET12567 (pUZ8002)	Non-methylating donar strain of <i>E. coli</i> (<i>kan^R</i> and <i>cmI^R</i>). Contains an RK2 derivative plasmid (puZ8002) with a defective oriT, which supplies transfer functions to oriT-containing plasmids. Used for conjugations into <i>Streptomyces</i> strains.	(Paget et al 1999)
<i>Streptomyces</i> M3-eGFP	<i>Streptomyces</i> M3 containing pIJ8660/eGFP; <i>aac^R</i> .	This study

<i>Streptomyces coelicolor</i> M145-eGFP	<i>Streptomyces coelicolor</i> M145 containing pIJ8660/eGFP; <i>aac^R</i> .	This study
<i>Arabidopsis thaliana</i> ecotype Col-0	Wild type, ecotype Col-0.	Lab seed stock
<i>Arabidopsis thaliana cpr5</i>	Genotype <i>cpr5</i> in a Col-0 genetic background, gene code At5g64930. Constitutive expression of PR genes and high levels of SA due to the deletion of the <i>CPR5</i> gene.	National <i>Arabidopsis</i> Stock Centre (NASC).
<i>Arabidopsis thaliana sid2-2</i>	Genotype <i>sid2-2</i> in a Col-0 genetic background, gene code At1g74710. Deficient in induction of SA accumulation.	National <i>Arabidopsis</i> Stock Centre (NASC).
<i>Arabidopsis thaliana pad4</i>	Genotype <i>pad4-1</i> in a Col-0 genetic background, gene code At3g52430. Phytoalexin deficient and deficient in SA accumulation.	National <i>Arabidopsis</i> Stock Centre (NASC).

5.3.2 Root colonisation by *Streptomyces* isolates

5.3.2.1 Plant growth and inoculation of *Streptomyces* isolates

In order to test whether plant genotypes with altered levels of SA production or accumulation affected the ability of *Streptomyces* strains to colonise plant roots, a re-isolation technique was developed using apramycin-marked streptomycetes. Seeds of wild-type *A. thaliana* Col-0, *cpr5*, *pad4*, and *sid2-2* plants were obtained from the Nottingham *Arabidopsis* Stock Centre (NASC, Table 5.1). Seeds were sterilised by washing in 70% ethanol for 2 minutes, followed by 20% NaOCl for 2 minutes. Seeds were then rinsed five times in sterile dH₂O, before being placed into 500 µl solutions of 2xYT (Table 3.2) containing pre-germinated spores (10⁶ spores ml⁻¹) of either *S. coelicolor* M145-eGFP or *Streptomyces* strain M3-eGFP (Table 5.1). Spores were pre-germinated in the 2xYT at 50°C for 10 minutes before the seeds were added. Sterile seeds were also added to uninoculated 2xYT as a control. Seeds were incubated in their respective solutions for 90 minutes on a rotating shaker before being transferred

to pots of sieved Levington F2 seed and modular compost, soaked with dH₂O. A further 1 ml of pre-germinated spores of the same strain (or 2xYT for the control) was pipetted into the soil to a depth of approximately 2 cm below the seed. Pots were then incubated at 4°C for 48 hours, before being grown for 5 weeks under a photoperiod of 12 hours light/ 12 hours dark at 22°C. Six replicate plants were grown for each plant genotype inoculated with each streptomycete strain.

5.3.2.2 Quantifying *Streptomyces* root colonisation

After 5 weeks of growth in the presence or absence of apramycin-marked strains, plants were removed from pots. Roots were removed aseptically and cleaned as detailed in Chapter 3, section 3.3.1, which is also the same protocol used by Lebeis et al (2015) for root colonisation experiments. This eliminated all bacteria apart from those living within the roots (endophytes), or those that were very firmly attached to the root surface (the “rhizoplane”). Cleaned roots were weighed, then crushed in 1 ml of sterile 10% (v/v) glycerol, using a pestle and mortar. 100 µl of the homogenate was then plated onto three replicate SFM agar plates containing 50 µg ml⁻¹ apramycin, allowing for the selective re-isolation of inoculated, aac^R-marked strains. Plates also contained 5 µg ml⁻¹ nystatin and 100 µg ml⁻¹ cyclohexamide to inhibit fungal growth. Agar plates were incubated at 30°C for 5 days, after which Colony Forming Units (CFU) of the inoculated apramycin-resistant streptomycete strains were counted. CFU counts were converted to CFU per gram of root tissue; these values were then log-transformed to normalise residuals, before using ANOVA and Tukey's Honestly Significant Difference (HSD) tests to analyse results. Statistical tests were conducted using R 3.2.3 (R Core Team 2017).

5.3.3 Testing for use of salicylic acid as a sole carbon source by streptomycetes

In order to test whether *Streptomyces* strains could use SA as a sole carbon source, streptomycete strains L2, M2, M3, N1, N2, and the *S. lydicus* strains 25470, 31975 and Actinovate (Table 3.1) were streaked onto minimal medium agarose plates (Table 5.2). *S. coelicolor* M145 was not tested as it can use agarose as a sole carbon source (Stanier 1942, Temuujin et al 2012). Plates were supplemented with either 0.5 mM SA (as in Lebeis et al 2015), 3.875 mM sodium citrate (to replicate concentrations in minimal

media used by Lebeis et al 2015) or each of the strain's preferred carbon source as a positive control. Preferred carbon sources were 5 g L⁻¹ of mannitol for strains N2 and M2; 5 g L⁻¹ maltose for strains M3, N1, *S. lydicus* 25470 and Actinovate; 5 g L⁻¹ sucrose for L2; or 10 g L⁻¹ glucose for *S. lydicus* 31975. Plates with no carbon source were used as a control. Three replicate plates were carried out for each strain on each carbon source. All plates were incubated for seven days at 30°C before imaging. Strains were also streaked onto minimal medium plates with agar as the gelling agent instead of agarose, with either 3.875 mM sodium citrate as the sole carbon source, or no carbon source as a control, to test whether these conditions (which replicate those used by Lebeis et al, 2015) could also support bacterial growth.

Table 5.2 Minimal medium recipe used for experiments in Chapter 5. All components were from Sigma Aldrich.

Media name	Ingredient	g L ⁻¹ dH ₂ O
Minimal medium (Kieser et al 2000)	NH ₄ SO ₄	1
	KH ₂ PO ₄	0.5
	MgSO ₄ .7H ₂ O	0.2
	FeSO ₄ .7H ₂ O	0.01
	Agarose or	6
	Agar	15
	Trace elements	200 µl after autoclaving
	Optional carbon source:	
	Mannitol or	5
	Maltose or	5
Sucrose or	5	
Glucose or	10	
SA or	0.069	
Sodium citrate	1	
Trace element solution (Kieser et al 2000)	ZnCl ₂	0.04
	FeCl ₃ .6H ₂ O	0.2
	CuCl ₂ .2H ₂ O	0.01
	MnCl ₂ .4H ₂ O	0.01
	Na ₂ B ₄ O ₇ .10H ₂ O	0.01
	(NH ₄) ₆ Mo ₇ O ₂₄ .4H ₂ O	0.01

5.3.4 Screening for salicylic acid metabolism genes in the genomes of *Streptomyces* isolates

To identify whether isolates carried homologues to known salicylic acid (SA) degradation genes, all experimentally verified pathways involving SA (or salicylate) degradation were identified using the MetaCyc database (<http://www.metacyc.org/>). Amino acid sequences of characterised genes involved in each of the five pathways were then retrieved from UniProt (Table 5.3). Protein sequences were used to perform BLASTp searches against the predicted open reading frames (ORFs) for each genome-sequenced streptomycete strain. These were N1, N2, M2, M3, L2, *S. lydicus* 25470, *S. lydicus* 31975 and *S. lydicus* Actinovate (see Chapter 3, sections 3.3.2 and 3.4.1, for information regarding genome sequencing) as well as the published genome sequence of *S. coelicolor* (taxid:100226, Bentley et al 2002). The results of the best hit (% identity and % query coverage) are reported.

Table 5.3 Proteins involved in SA degradation pathways. Amino acid sequences were used for BLASTp analysis against predicted ORFs in the genomes of sequenced *Streptomyces* isolates. All experimentally verified proteins involved in SA (or salicylate) degradation were identified using the MetaCyc database (<http://www.metacyc.org/>).

Pathway	Gene	UniProt ID	EC number	Organism	Notes
Salicylate degradation I	<i>salA</i>	Q0VH44	1.14.13.1	<i>Pseudomonas reinekei</i>	One step reaction: different versions of the same enzyme.
	<i>nahW</i>	Q9ZI64	1.14.13.1	<i>Pseudomonas stutzeri</i> AN10	
	<i>nahG</i>	P23262	1.14.13.1	<i>Pseudomonas putida</i> PpG7	
Salicylate degradation II	<i>nagG</i>	O52379	1.14.13.172	<i>Ralstonia sp.</i> U2	One step reaction: different versions of the same enzyme.
	<i>nagH</i>	O52380	1.14.13.172	<i>Ralstonia sp.</i> U2	
	<i>sdC</i>	POCT50	4.1.1.90	<i>Trichosporon moniliiforme</i>	One step reaction. For

Salicylate degradation III	<i>bsdD</i>	C0H3U9	4.1.1.91	<i>Bacillus subtilis</i>	<i>Bacillus subtilis</i> , three subunits of the same enzyme are encoded in an operon.
	<i>bsdC</i>	P94405	4.1.1.91	<i>Bacillus subtilis</i>	
	<i>bsdB</i>	P94404	4.1.1.91	<i>Bacillus subtilis</i>	
Salicylate degradation IVa	<i>sdgA</i>	Q7X279	No EC number	<i>Streptomyces sp.</i> WA46	Five step reaction. All genes are encoded in an operon, with <i>sdgD</i> catalysing two reactions.
Salicylate degradation IVb	<i>sdgB</i>	Q7X280	No EC number	<i>Streptomyces sp.</i> WA46	
Salicylate degradation IVc	<i>sdgC</i>	Q7X281	No EC number	<i>Streptomyces sp.</i> WA46	
Salicylate degradation IVd	<i>sdgD</i>	Q7X284	1.13.11.4	<i>Streptomyces sp.</i> WA46	
Salicylate degradation V	AY323 951	Q67FT0	1.13.11.-	<i>Pseudaminobacter salicylatoxidans</i> BN12	One step reaction.

5.3.5 Salicylic acid chemoattraction assays

In order to test whether SA might act as a chemoattractant for *Streptomyces* species, 4 μl of *Streptomyces* spores (10^6 spores ml^{-1}) were pipetted onto the centre of SFM agar plates (Table 3.2) and 40 μl of either 1 mM or 0.5 mM filter-sterilised SA was inoculated onto 6 mm filter paper discs (Whatman) and allowed to dry. Discs were then added to one side of the agar plate, 2 cm away from the streptomycete spores. SA solutions were prepared by diluting a 100 mM stock solution to a 1 mM or 0.5 mM SA solution in PBS (Table 3.2). The 100 mM stock solution was made by dissolving 0.138 g of SA (Sigma Aldrich) in 2 ml of 100% DMSO before making the solution up to 10 ml with PBS. Thus, the resulting 1 mM and 0.5 mM solutions had a final concentration of 0.2% and 0.1% DMSO, respectively. To check that any observations were not due to the effects of DMSO, control plates were also run alongside the SA experiment, in which discs were soaked in 40 μl of a 0.2% DMSO solution (in PBS), equivalent to the final concentration of DMSO in the 1 mM SA solution. Spores of the strains L2, M2, M3, MG, N1, N2, *S. coelicolor* M145 and *S. lydicus* Actinovate (Table 3.1) were tested for chemotactic responses. Three replicate plates for each strain

under each condition (1 mM SA, 0.5 mM SA, DMSO control), were incubated for seven days at 30°C before imaging.

5.3.6 The effect of salicylic acid on *Streptomyces* in soil microcosms

To test whether the SA exuded by plant roots could be altering the competitive ability of streptomycetes in soil, Levington F2 seed and modular compost (4 ml) was placed into each compartment of a 12-well plate. Soil was soaked with 0.5 ml of sterile dH₂O or 0.5 mM SA. Each well was then inoculated with 10⁷ spores ml⁻¹ of either *S. coelicolor* M145-eGFP or *Streptomyces* M3-eGFP (Table 5.1), suspended in dH₂O or 0.5 mM SA. Spores of eGFP-tagged M3 or M145 were used so that experiments aligned with results from *in vivo* plant colonisation experiments described in 5.3.2. Wells soaked with SA or dH₂O were left uninoculated as a control. There were nine replicate wells for each of the six treatment groups. Well-plates were then placed under a photoperiod of 12 hours light/ 12 hours dark for 10 days, after which 100 mg of the soil from each well was diluted into 900 µl of water and vortexed. Serial dilutions were plated onto SFM agar plates (Table 3.2) containing 50 µg ml⁻¹ apramycin (for selection of inoculated strains). Plates also contained 10 µg ml⁻¹ nystatin and 100 µg ml⁻¹ cyclohexamide to repress fungal growth. After 5 days, CFU of the *Streptomyces* inoculum were enumerated on the 10⁻² dilution plates. A generalised linear model (GLM) with a negative binomial distribution was then generated, using the package MASS in R 3.2.3 (R Core Team 2017), to model the effect of strain (*S. coelicolor* M145-egfp or M3-egfp), soil treatment (wetting with SA or dH₂O), and their interaction term (strain*treatment) on the number of bacterial CFU returned from soil wells. Likelihood ratio tests were used to establish the significance of terms in the model. A negative binomial model was used because the CFU count data was over-dispersed, whereby the variance was greater than the mean and residual deviances were much higher than the residual degrees of freedom when a Poisson model (conventionally used for count data) was used.

5.4 Results

5.4.1 The effect of plant genotype on plant root colonisation by *Streptomyces* species

To test whether SA can play a role in recruiting streptomycetes to the *A. thaliana* root microbiome, as was previously reported by Lebeis et al (2015), the root colonisation efficiencies of the strains *S. coelicolor* M145 and *Streptomyces* M3 (both marked with an apramycin resistance gene) were compared in wild-type *A. thaliana* Col-0 plants, *cpr5* mutant plants that constitutively produce SA (Bowling et al 1994), and for *pad4* and *sid2-2* plants that are deficient in SA production and accumulation (Jirage et al 1999, Wildermuth et al 2001, Zhou et al 1998). The results confirmed that root colonisation efficiencies (measured by counting apramycin-resistant CFU returned per gram of plant root) were significantly affected by plant genotype, irrespective of the *Streptomyces* strain used as an inoculum; plant genotype had a significant effect on the log-transformed CFU g⁻¹ ($F_{(3,39)} = 6.17$, $P < 0.01$), whereas the strain-genotype interaction term was insignificant ($F_{(3,39)} = 0.51$, $P = 0.68$) in an ANOVA test. Specifically, the colonisation of both M145 and M3 was significantly increased in *cpr5* mutant plants (Figure 5.1) which constitutively express SA genes, compared to the other three genotypes, despite a high level of variability ($P < 0.05$ in all Tukey's HSD tests between *cpr5* and other plant genotypes, for both inoculation treatments). However, there was no significant difference between the CFU g⁻¹ returned from roots of wild-type plants and those of *pad4*, or *sid2-2* plant roots ($P > 0.05$ in Tukey's HSD tests, Figure 5.1). Streptomycetes colonised the roots of these three genotypes at lower abundances and with less variability (Figure 5.1). No streptomycete colonies were returned from plants grown from uninoculated seeds, suggesting that any apramycin-resistant colonies that were re-isolated were those that had been originally inoculated onto seeds and were not present naturally in the soil.

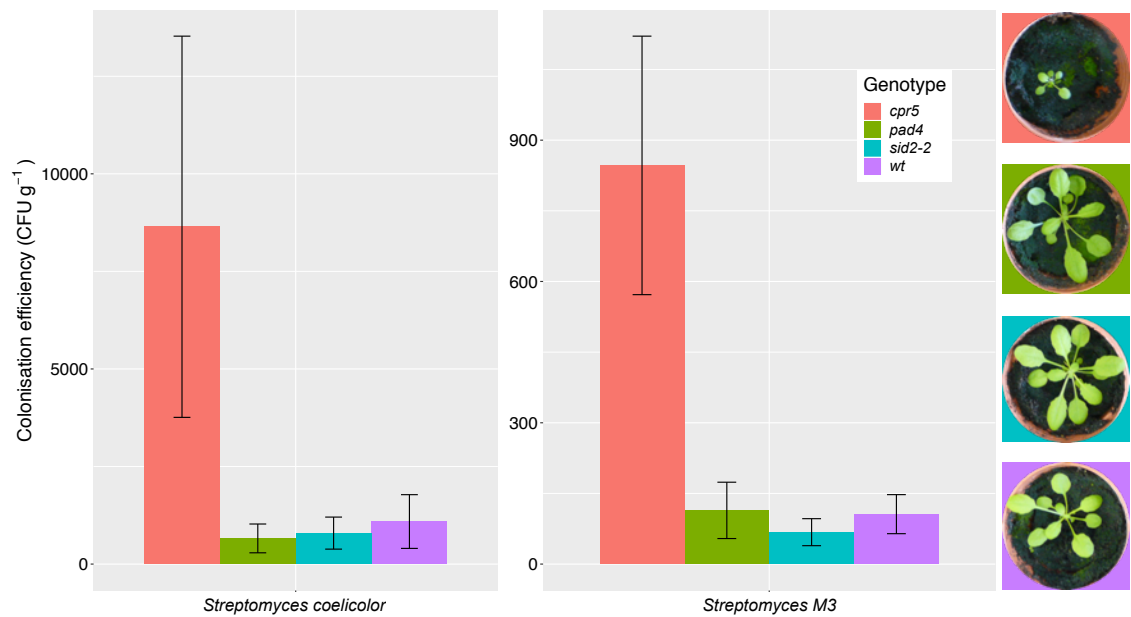


Figure 5.1 Root colonisation efficiency by *Streptomyces* strains *S. coelicolor* M145 and *Streptomyces* strain M3, in *cpr5 A. thaliana* plants (constitutively expressing salicylic acid biosynthesis genes) compared to *pad4* and *sid2-2* lines (deficient in salicylic acid accumulation) and wild-type Col-0 plants. Root colonisation is displayed as the average colony forming units (\pm SE) of each *Streptomyces* strain, per gram of root (CFU g⁻¹), that could be re-isolated from plants 5 weeks after germination. N = 6 plants per treatment. Plant phenotypes are shown for comparison.

It is important to note here, that the CPR5 gene (deleted in *cpr5* plants) is known to have a complex role in regulating plant growth, immunity, and senescence (Jing et al 2007, Jing et al 2008). Interestingly, *cpr5* plants demonstrated weak growth in compost compared to the other plant genotypes (Figure 5.1). This, along with the fact that *sid2-2* and *pad4* plant genotypes did not have an effect on streptomycete colonisation (Figure 5.1) gives rise to the possibility that the observed increase in streptomycete colonisation in *cpr5* plants was due to the complex phenotype of the *cpr5* mutant plants (Jing et al 2007, Jing et al 2008) and not necessarily due to the higher levels of SA produced by these plants.

5.4.2 Salicylic acid as a sole carbon source

In order to test whether streptomycetes isolated from the *A. thaliana* root microbiome were capable of using SA as a sole carbon source, the growth of all genome-sequenced strains (isolated in Chapter 3) was compared on minimal medium agarose plates containing a preferred carbon source, 0.5 mM SA or no carbon source as a control. All of the strains grew on their preferred carbon source, however, unlike the strain *Streptomyces* sp. 303 reported by Lebeis et al (2015), no growth was observed for any of the strains on the minimal medium agarose plates containing SA, or the no carbon control (Figure 5.2). This suggests that SA was not being used as a carbon source by these streptomycetes, including *Streptomyces* strain M3 that had shown increased levels of root colonisation in *cpr5* plants; this indicates that other factors may have led to the increased level of colonisation observed for plants of this genotype.

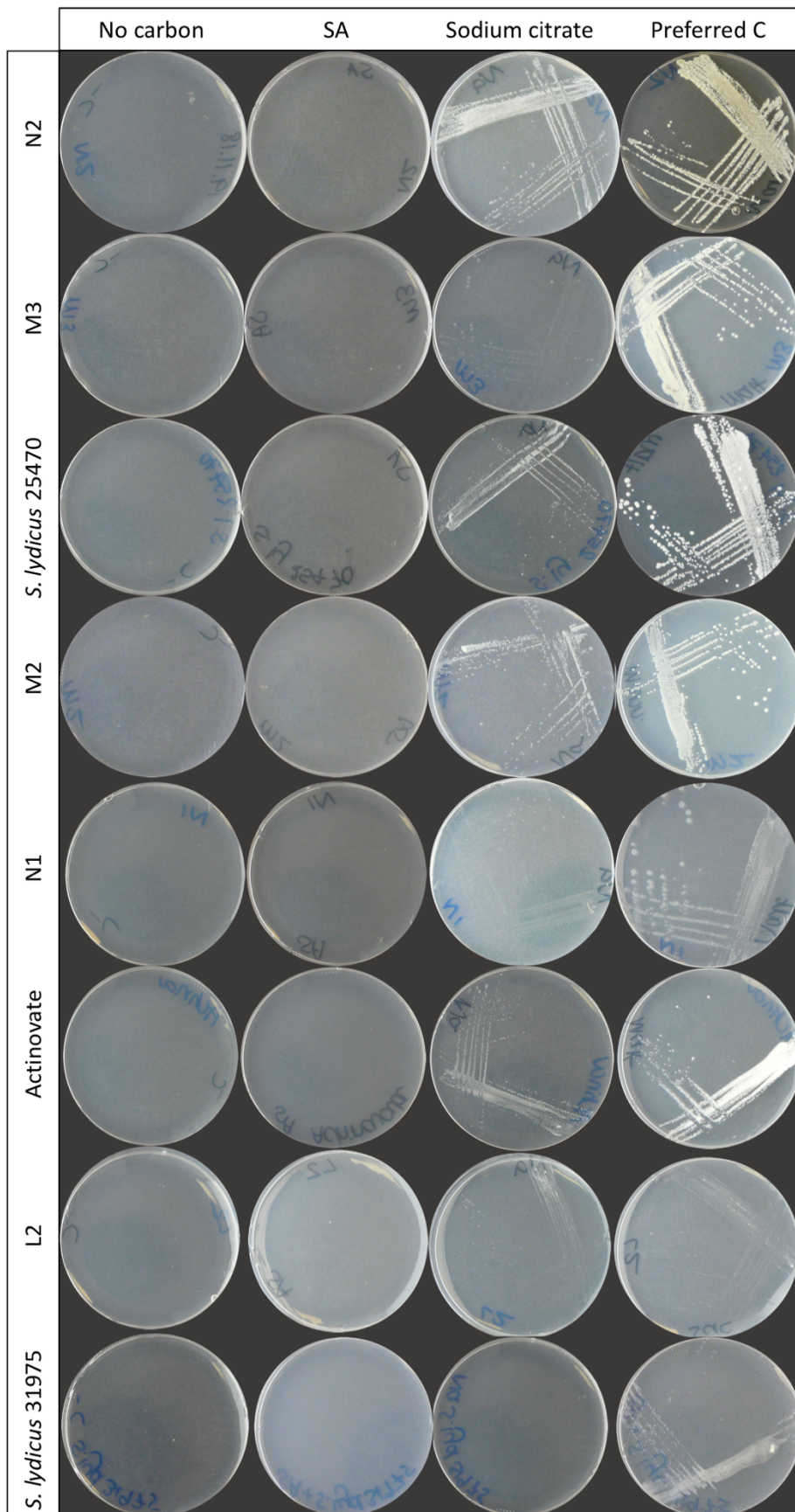


Figure 5.2 Isolate growth on minimal medium agarose plates containing either no carbon source, 0.5 mM salicylic acid (SA), 3.875 mM sodium citrate or a preferred carbon source as a sole carbon sources.

The lack of growth of isolates on SA was additionally supported by the absence of genes involved in known SA degradation pathways in the genomes of all sequenced isolates, as well as in the published genome of *S. coelicolor* (Table 5.3 and Table 5.4). In the majority of cases, there was a very low percentage identity (<40%) and/or percentage coverage between amino acid sequences of strains and the protein sequences of SA degradation enzymes identified in the literature (Table 5.4). Slightly higher percentage identities were identified between the amino acid sequences of strains and the proteins known to be involved in the salicylate degradation IV pathway (Table 5.4). However, this is most likely a phylogenetic artefact, since the amino acid sequences involved in the salicylate degradation IV pathway are derived from another streptomycete species (*Streptomyces sp.* strain WA46, Ishiyama et al 2004), whereas the enzymes in other pathways are derived from genera in more distantly related phyla such as *Bacillus* (Table 5.3). Indeed, although several of the sequenced strains encoded proteins with between 40-50% amino acid sequence identity to the enzymes SdgA and SdgC, which represent a salicylyl-coA ligase and salicylyl-CoA 5-hydroxylase enzyme, respectively (Table 5.4), none of the proteins identified as best hits in any of the *Streptomyces* isolates were annotated as such. For example, proteins that appeared as best hits to SdgA shared a greater level of sequence identity to other ligase proteins that are involved in siderophore and nonribosomal peptide (NRPS) biosynthesis and are likely to be widespread in streptomycetes. Additionally, amino acid sequences that appeared as best hits to SdgC were in fact identified as monooxygenase enzymes. In comparison, the amino acid sequence of the strain *Streptomyces sp.* 303 identified by Lebeis et al (2015) had over 90% sequence identity (with 99-100% coverage) to all enzymes in the salicylate degradation IV pathway and carried the same annotations as proteins in this pathway.

Table 5.4 The results of BLASTp analyses comparing the amino acid sequences of genes involved in known salicylic acid degradation pathways and predicted open reading frames (ORFs) encoded by the genomes of *Streptomyces* isolates N1, N2, M2, M3, L2, *S. lydicus* 31975, *S. lydicus* 25470, *S. lydicus* Actinovate and *S. coelicolor*. Percentage identity and percentage query coverage (in brackets) to the best hit are reported.

Pathway	Gene name	Enzymatic activity	N1	N2	M2	M3	L2	<i>S. lydicus</i> 31975	<i>S. lydicus</i> 25470	Actinovate	<i>S. coelicolor</i> M145
Salicylate degradation I	<i>salA</i>	salicylate 1-hydroxylase	25 (75)	27 (75)	33 (89)	27 (80)	31 (75)	28 (32)	28 (80)	28 (85)	29 (81)
Salicylate degradation I	<i>nahW</i>	salicylate hydroxylase	29 (91)	29 (95)	34 (96)	30 (75)	32 (82)	30 (85)	29 (82)	30 (66)	39 (77)
Salicylate degradation I	<i>nahG</i>	salicylate hydroxylase	30 (54)	28 (80)	33 (95)	26 (88)	32 (83)	28 (90)	27 (83)	26 (83)	31 (89)
Salicylate degradation II	<i>nagG</i>	salicylate-5-hydroxylase	29 (46)	27 (48)	29 (50)	26 (43)	31 (48)	27 (66)	27 (47)	27 (47)	27 (36)
Salicylate degradation II	<i>nagH</i>	salicylate-5-hydroxylase	38 (29)	36 (27)	23 (39)	45 (19)	50 (13)	50 (21)	28 (56)	32 (26)	29 (34)
Salicylate degradation III	<i>sdc</i>	salicylate decarboxylase	22 (84)	25 (73)	29 (96)	21 (92)	29 (18)	24 (54)	28 (86)	25 (48)	24 (89)

Salicylate degradation III	<i>bsdD</i>	salicylate decarboxylase	33 (84)	44 (33)	36 (48)	38 (42)	37 (40)	43 (32)	34 (58)	52 (33)	46 (34)
Salicylate degradation III	<i>bsdC</i>	salicylate decarboxylase	37 (88)	33 (84)	33 (84)	33 (84)	32 (84)	33 (84)	33 (84)	33 (84)	32 (84)
Salicylate degradation III	<i>bsdB</i>	salicylate decarboxylase	30 (28)	34 (90)	32 (90)	34 (88)	34 (90)	32 (92)	32 (97)	32 (93)	35 (88)
Salicylate degradation IVa	<i>sdgA</i>	salicylyl-CoA ligase	50 (96)	47 (96)	33 (92)	48 (97)	31 (91)	32 (88)	32 (89)	47 (96)	50 (96)
Salicylate degradation IVb	<i>sdgB</i>	salicylyl-CoA synthase	31 (75)	33 (96)	33 (97)	32 (83)	32 (97)	33 (97)	34 (97)	33 (97)	33 (97)
Salicylate degradation IVc	<i>sdgC</i>	salicylyl-CoA 5-hydroxylase	26 (44)	42 (76)	44 (80)	39 (80)	42 (80)	41 (81)	40 (81)	42 (81)	42 (81)
Salicylate degradation IVd	<i>sdgD</i>	gentisate 1,2-dioxygenase	30 (21)	58 (95)	30 (38)	29 (24)	26 (43)	29 (24)	34 (89)	34 (89)	27 (31)
Salicylate degradation V	AY3239 51	salicylate 1,2-dioxygenase	39 (8)	57 (69)	27 (55)	30 (11)	29 (21)	41 (7)	30 (64)	31 (60)	29 (21)

The supplementary methods of Lebeis et al (2015) state that the minimal medium agar used to test the isolated strain, *Streptomyces* sp. 303, for the use of 0.5 mM SA as a sole carbon source, additionally contained 1 g L⁻¹ (3.875 mM) of sodium citrate. Sodium citrate is an additional candidate source of carbon and energy and is known to be used as such by many bacterial species, including some streptomycetes (Brocker et al 2009, Shetty et al 2014, Wang et al 2013a). To test whether strains could use sodium citrate in this way, each isolate was grown on agarose containing 3.875 mM sodium citrate (equivalent to concentrations used by Lebeis et al, 2015). Although use of sodium citrate was not universal, several of the strains were able to use it as a sole carbon source (Figure 5.2). This included N2, M2, *S. lydicus* 25470 and *S. lydicus* Actinovate, and to a lesser extent N1, L2 and M3 (Figure 5.2).

Media used by Lebeis et al (2015) also used agar as a gelling agent for solid media. It is important to note that all strains tested for growth on salicylic acid and sodium citrate in this chapter, could also grow on minimal medium plates made up with agar, in the absence of any additional carbon source (Figure 5.3 and Figure S6.1), hence this is why agarose was used in experiments testing carbon usage. Interestingly, this growth was enhanced in the strains M2 and M3, when sodium citrate was also added to the agar plates (Figure 5.3). Agar is known to carry impurities that can support the growth of bacteria, whilst agarose is a purer gelling agent that carries fewer of these contaminants. Thus, although it is possible that the streptomycete isolated by Lebeis et al (2015) is capable of using SA, as it carried orthologues to known SA degradation genes, it could also have been using several other alternative carbon sources in the minimal medium, other than SA, including impurities in agar plates and/or sodium citrate. This should be considered for any future experiments investigating sole carbon usage by streptomycetes.

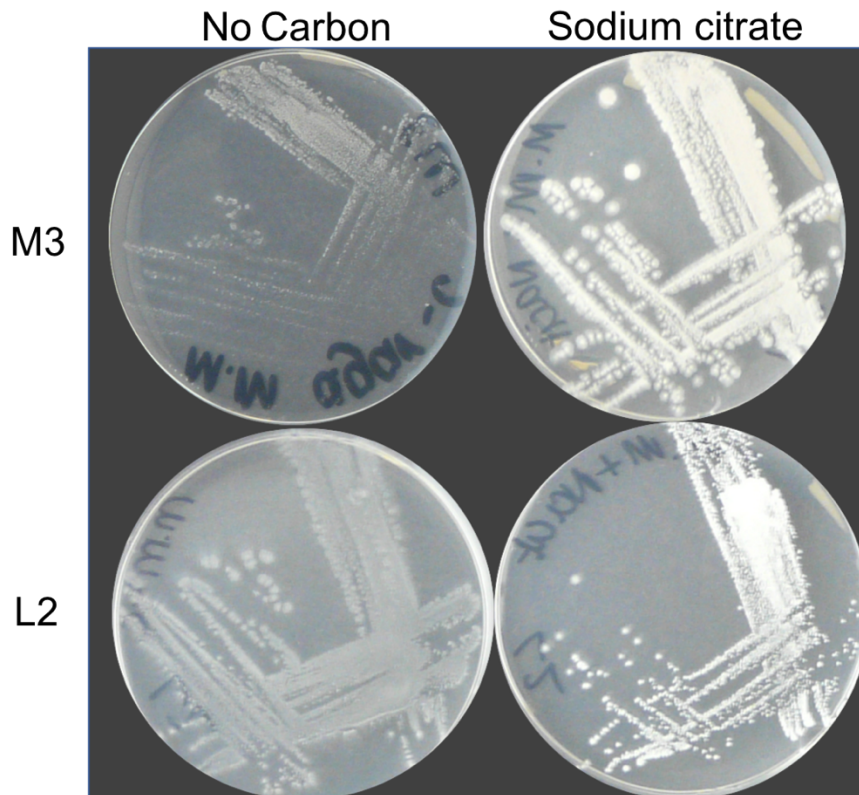


Figure 5.3 The growth of *Streptomyces* strains on minimal medium containing agar as the gelling agent. *Streptomyces* strains M3 (top) and L2 (bottom) were grown with either no carbon source present (left) or 3.875 mM sodium citrate (right) as a sole carbon source.

5.4.3 Salicylic acid as a chemoattractant

Rather than acting as a nutrient source, some root exudates, such as malic acid, may act as chemoattractants that recruit bacteria to the root niche under certain conditions; once there, the bacteria can then compete for alternative abundant carbon sources. In order to test whether SA acts as a chemoattractant to *Streptomyces* species, sequenced streptomycete strains were grown next to filter paper disks soaked in either 0.5 mM SA, 1 mM SA, or the 0.1% (v/v) DMSO solvent control. However, there was no obvious growth towards SA by any of the strains after 10 days, suggesting that it was not being used as a chemoattractant (Figure 5.4). This included the strains *S. coelicolor* M145 and *Streptomyces* strain M3 that had been enriched in the roots of *cpr5* plants during colonisation experiments.

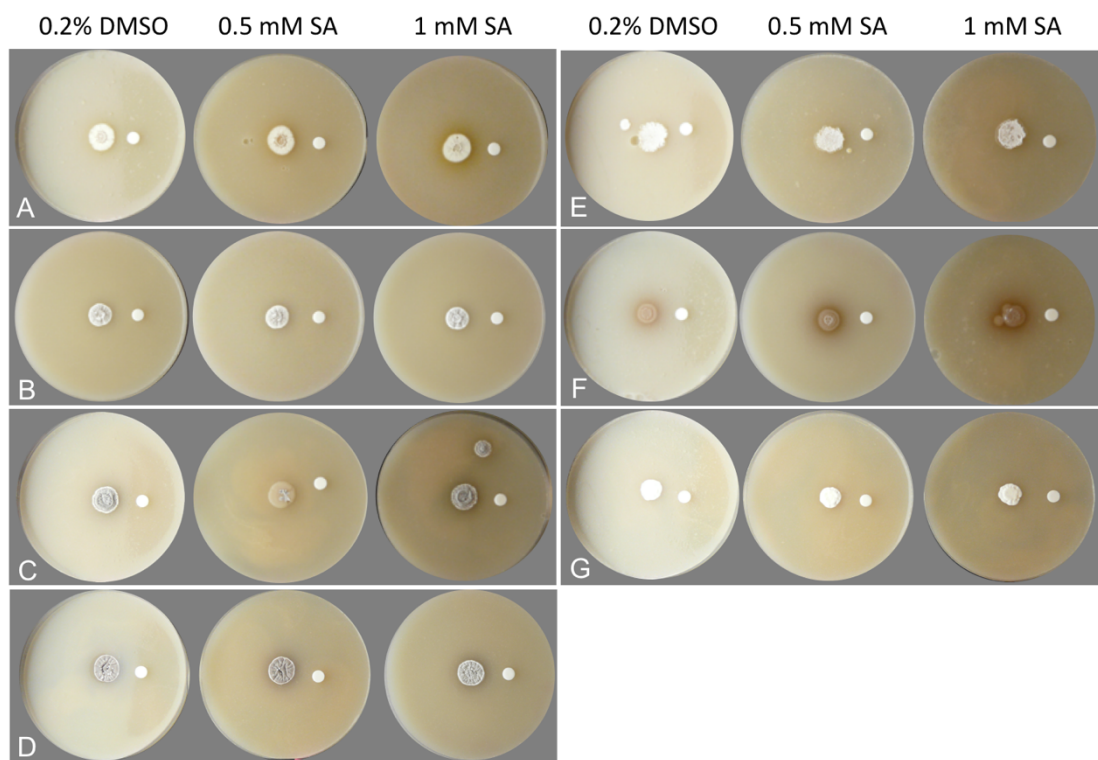


Figure 5.4 Salicylic acid chemoattractant assays . Streptomycete colonies were grown next to disks soaked in 0.1% DMSO (as a control for the SA solvent), 0.5 mM SA or 1 mM SA. Images were taken after 10 days. All assays were carried out on SFM agar media. *Streptomyces* strains **A)** N2, **B)** N1, **C)** M3, **D)** *Streptomyces coelicolor*, **E)** M2, **F)** L2 and **G)** Actinovate were tested for their response to SA.

5.4.4 The effect of salicylic acid on the competitiveness of *Streptomyces* in soil microcosms

It is possible that an increased level of SA entering the soil environment might indirectly benefit streptomycetes by negatively modulating the levels of other rhizobacteria in the soil, as is the case for certain plant allelochemicals (Badri and Vivanco 2009, Huang et al 2019, Neal et al 2012). To test this hypothesis, soil microcosms were established in deep, 12-well plates, which were then wetted with either sterile dH₂O or 0.5 mM SA. Microcosms were inoculated with spores of either *Streptomyces coelicolor* M145-eGFP or *Streptomyces* M3-eGFP and nine replicates of each wetting treatment were run in parallel for each strain. After 10 days, strains were recovered from soil using apramycin selective medium and the resulting colony forming units were counted (Figure 5.5). No colonies were recovered from

uninoculated controls on this medium. A GLM with a negative binomial distribution demonstrated that, overall, there was no significant effect of soil wetting treatment (d.f= 1, $P = 0.07$) on CFU number. The interaction term was also non-significant (d.f= 1, $P = 0.20$), indicating that this absence of effect did not differ between the two inoculated strains (Figure 5.5). This suggested that neither strain had a competitive advantage when greater concentrations of SA were present.

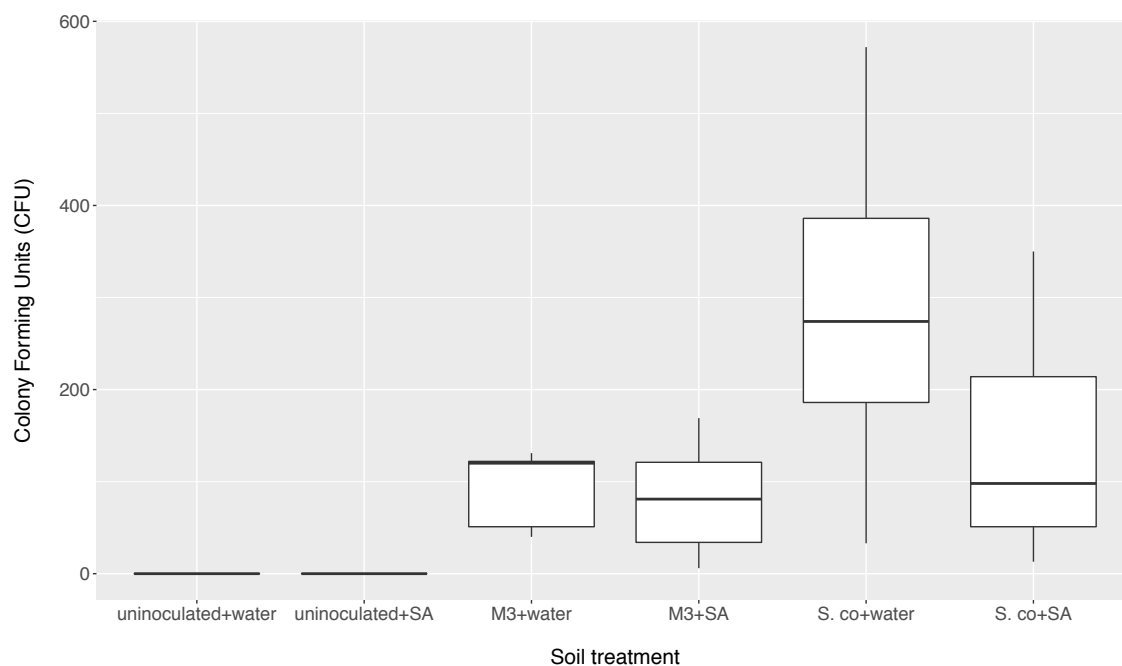


Figure 5.5 The number of colony forming units (CFU) of streptomycete inoculants retrieved from soil microcosms treated with either 0.5 mM salicylic acid (SA) or dH₂O after 10 days. Microcosms were inoculated with spores of either *S. coelicolor* M145-egfp (*S.co*), M3-egfp, or left uninoculated as a control. N = 9 microcosms per treatment.

5.5 Discussion

Previous studies have suggested that phenolic compounds, particularly SA, have a direct effect on microbiome composition and can act as growth substrates that attract genera such as *Streptomyces* species to the roots of *A. thaliana* plants (Lebeis et al 2015). To test whether responsiveness to plant-derived SA extended to other *Streptomyces* species, the strains *S. coelicolor* M145 and *Streptomyces* M3 were tested

for their ability to colonise the roots of *cpr5 A. thaliana* plants that constitutively produce high levels of SA, compared to plants that were deficient in their ability to produce SA (*pad4* and *sid2-2* lines) and wild-type *A. thaliana* Col-0 plants.

Levels of colonisation were observed to be significantly greater for both streptomycete strains in *cpr5* plants, relative to wild-type and SA deficient lines. However, despite this, there was no evidence that these strains could use SA as a sole carbon source, or that they were able to respond chemotactically to SA. The absence of a direct response to SA, either as a substrate or as a chemoattractant, was also observed in seven other streptomycete strains, four of which had been isolated from the roots of *A. thaliana*. The remaining three isolates were endophytic strains of *S. lydicus*, one of which is the active ingredient in the horticultural product Actinovate®. Apart from acting as substrates or chemoattractants, molecules released from plant roots can also alter the root-associated microbiome by modulating competitive outcomes between bacterial species (Badri and Vivanco 2009). For example, triterpenes are suggested to inhibit the colonisation of some bacterial strains within the *A. thaliana* root microbiome whilst promoting the proliferation of others, and benzoxazinoids have a similar impact on the root microbiome of cereal crop species (Huang et al 2019, Neal et al 2012). Therefore, it is possible that SA was able to indirectly enhance streptomycete colonisation by reducing competition from other bacterial species. However, the addition of SA to soil microcosms did not have a significant influence on the abundance of *S. coelicolor* M145 or *Streptomyces* M3, suggesting that the increased levels of colonisation observed in *cpr5* plants by both of these strains was not due to SA increasing their competitiveness in soil.

The results of the minimal media screens, genome analyses, chemoattractant assays and microcosm experiments described in this chapter, all suggest that SA was not having a direct influence on the colonisation of the *Streptomyces* isolates in *cpr5* plants. Interestingly, although colonisation went up for both strains inoculated onto *cpr5* plants, colonisation levels in *sid2-2* and *pad4 A. thaliana* plants were similar to that of wild-type plant roots, suggesting that the loss of SA accumulation did not have any impact on root colonisation. This is potentially because SA is only exuded at very low levels under normal conditions and so loss of SA would not have had a large

impact on bacterial colonisation efficiency. However, given that the streptomycetes did not respond to SA *in vitro*, it is also possible that the *cpr5* mutation has additional impacts on the host plant that could also result in greater levels of streptomycete root colonisation in plants with this genotype, independently from SA levels.

In this chapter, the *A. thaliana cpr5* plants that were grown in compost appeared to have stunted growth relative to the other plant genotypes (wild-type Col-0, *sid2-2* and *pad4* plants). *A. thaliana cpr5* plants carry a deletion of the CPR5 gene which encodes a putative transmembrane protein (Kirik et al 2001). This protein is part of a complex regulatory signaling network and its deletion results in the constitutive activation of SA biosynthesis genes, enabling plants to accumulate high levels of SA (Bowling et al 1994, Clarke et al 2000, Kirik et al 2001). However, apart from elevated phytohormone levels, a large number of other pleiotropic phenotypes have been noted for *cpr5* plants, including stunted root and aerial growth, disrupted cellular organisation, spontaneous cell death, early senescence in young plants, lesions on various tissue types, disrupted cell wall biogenesis, high levels of oxidative stress and an increased production of ROS (Brininstool et al 2008, Gao et al 2011, Jing et al 2007, Jing et al 2008, Kirik et al 2001). Thus, through its involvement in an intricate signaling network, the CPR5 gene is predicted to play a complex role in directing many processes, including normal plant development, cellular redox balance and senescence, in addition to its role in mediating plant defence (Jing et al 2007, Kirik et al 2001). Furthermore, its expression has been found to be ubiquitous throughout *A. thaliana* plants, with similar levels being produced in roots, stems, leaves and flowers (Kirik et al 2001).

The pleiotropic effects of the *cpr5* mutation could have had a profound influence on root microbiome assembly in *A. thaliana* and also may have contributed to the increased, but variable, colonisation of *Streptomyces* isolates observed in *cpr5* plants. For example, an altered cell wall composition, coupled with an increase in spontaneous plant cell death, could have resulted in easier access to plant roots, particularly as *Streptomyces* are thought to enter roots in compromised areas, such as lesions and sites of wounding, by using a combination of filamentous growth and the production of hydrolytic enzymes (Chater 2006, Viaene et al 2016). *Streptomyces* are

also saprotrophic organisms that are specialised to degrade complex biopolymers such as dead and decaying plant cell wall material (Chater et al 2010); thus, the growth of streptomycete inoculants may have been further enhanced in the vicinity of *cpr5* roots that were undergoing early-onset senescence. Microscopic analysis that investigates the behaviour and growth of eGFP-labelled streptomycetes on and within the roots of *cpr5* plants relative to wild-type roots may help to decipher whether this is the case.

In addition to the influence of the *cpr5* mutation on plant development and senescence, the elevated levels of SA present in the *cpr5* mutant plants could have had multiple downstream effects, including the activation of pathways that regulate the abundance of other compounds found in the root exudates of *A. thaliana*. Indeed, several studies have shown that activation of SA and JA signaling pathways can, in turn, have a profound impact on plant cell signaling, with many genes involved in processes such as defense signaling, metabolism and cell transport showing altered levels of expression (Badri et al 2008, Carvalhais et al 2015, Carvalhais et al 2017). In turn, this leads to significantly altered root exudation, with changes in the abundance and transportation of a wide variety of phytochemicals including amino acids, organic acids and sugars (Badri et al 2008, Carvalhais et al 2015, Carvalhais et al 2017). Thus, it is possible that the elevated levels of SA in mutant plants (and/or the other pleiotropic effects of the *cpr5* mutation) resulted in extensive changes to root exudate profiles with other compounds being exuded in greater abundance. These compounds may have attracted *Streptomyces* species to roots or could have altered competitive outcomes in the soil in a way that would not have been seen by adding SA on its own to soil microcosms. Indeed, a previous proteomic study demonstrated that the proteome of *cpr5* root exudates was significantly different to that of wild-type plants, with an elevated abundance of defense-related proteins such as chitinases, glucanases and myrosinases (De-la-Pena et al 2010). The exudates of *cpr5* plants also showed greater levels of antimicrobial activity *in vitro*, whereby they inhibited the growth of several species of *Pseudomonas* (De-la-Pena et al 2010). Thus, elevated SA signaling could have induced changes to root exudates that in turn altered the abundance of competitors in the soil, such as pseudomonads, giving streptomycetes an advantage in the rhizosphere and root niche. In this case, SA indirectly effects the recruitment of bacteria to the root microbiome, however this influence is hard to untangle from the

other pleiotropic phenotypes of the *cpr5* mutation. In the future, metabolomic experiments could be conducted on wildtype and phytohormone mutant plants to decipher which root exudates change in abundance as a result of the *cpr5* mutation. Similar experiments could be conducted using plants that have been induced to produce SA (rather than using *cpr5* mutants), either via the exogenous application of SA, or by the application of elicitors, such as bacterial flagellin peptides (Denoux et al 2008, Mishina and Zeier 2007). This could be coupled with further experiments to determine whether streptomycetes use exudates that are particularly enriched in *cpr5* or activated plants. As mentioned in Chapter 4, similar methodology has recently been used to determine which root exudates are being used by bacteria that respond positively to the growth of the plant species *Avena barbata*; here, a pool of root exudates was used as a growth medium for individual strains, before being compared to complete, uninoculated root exudates via LC-MS (Zhalnina et al 2018). This enabled the identification of compounds that were removed by bacterial growth (Zhalnina et al 2018).

In comparison to the results of this chapter, Lebeis et al (2015) suggested that SA had a direct influence on microbiome recruitment, since the *Streptomyces* strain that was enriched in SA-activated plants was capable of using SA as a sole carbon source. However, Lebeis et al (2015) included agar and sodium citrate in the minimal medium used to test this strain, both of which were shown to support the growth of streptomycete isolates in this chapter, in the absence of any other carbon source. Additionally, it should be noted that other strains that were found to be enriched in SA-producing plants did not universally demonstrate the ability to grow on SA as a sole carbon source, or carry orthologues of genes involved in known pathways of salicylic acid degradation (Lebeis et al 2015). This supports the idea that other factors (that may or may not be linked to SA signaling) could be involved in the recruitment of enriched strains to plant roots.

In conclusion, experiments in this chapter suggest that SA was not directly responsible for enhancing the colonisation of *Streptomyces* species in the microbiome of *cpr5* mutant plants. Instead, the *cpr5* mutation appears to result in a large number of pleiotropic phenotypes spanning plant growth, development, defense and senescence,

all of which could have influenced root exudation, root morphology and microbiome assembly in these plants. Unpicking the role of individual root exudates and establishing the trophic links that exist between plants and bacterial species is complex, particularly as many of the mutations that are used to study the impact of individual root exudates often lead to additional changes to plant physiology that can also influence plant-microbe interactions (Ryan et al 2009). Additionally, root exudation is highly dependent on both abiotic factors (such as edaphic and climatic factors) and biotic factors (including plant genotype, infection status and microbial species present in the soil) meaning that many relationships between plant and microbe may be transient or context dependent. Making sense of the variation in exudate patterns and establishing the links between plants and bacterial species could enable engineering of beneficial plant root microbiomes and improve the consistency of biocontrol agents (Quiza et al 2015). In the future, a more targeted approach may be needed to study the influence of plant root exudates on members of the microbial community, for example by establishing techniques to eliminate or heterologously express genes responsible for single (or a small number of) root exudates (Ryan et al 2009), or by using novel metabolomic tools (Zhalnina et al 2018) combined with labelling and visualisation techniques (Musat et al 2016) to enable the identification of species that are responding to, and metabolising, particular plant-derived compounds.

Chapter 6 General Conclusions

The central aim of this project was to investigate the mechanisms by which hosts can selectively recruit Actinobacteria from their environment in order to assemble a protective microbiome. A better understanding of these mechanisms could enable the manipulation of microbiomes, with the goal of increasing the abundance of beneficial microbial species that interact with the host. It could also improve the efficacy of probiotic treatments and the delivery of bacterial biocontrol strains to increase their colonisation efficiency and competitiveness within the host microbiome.

As discussed, several mechanisms are thought to have evolved that enable a host to direct the assembly of its own microbiome. Firstly, beneficial bacteria can be vertically-transmitted between host generations, giving them preferential access to space and resources within the host niche. Secondly, the host can provide nutrients that either recruit bacteria with particular metabolic traits, or that drive competitive interactions between species in a way that is beneficial to the host. Additionally, the host can also prevent certain species from colonising the microbiome by producing compounds that reduce the competitive ability of these strains. In this work, *Acromyrmex echinatior* leafcutter ants and the plant species *Arabidopsis thaliana* were used as model organisms to investigate some of the hypotheses surrounding the establishment of defensive microbiomes, particularly those in which species of Actinobacteria can protect their host from infection by producing antimicrobial compounds.

The leafcutter ant system is a well-known example of a defensive mutualism, in which vertically transmitted *Pseudonocardia* bacteria and other environmentally-recruited strains, such as *Streptomyces* species, provide the ants' food fungus with protection against infection by producing antimicrobials on the surface of the ant cuticle (Currie 2001, Worsley et al 2018). The competitive screening model has been proposed to explain the dominance of antibiotic-producing Actinobacteria on the ant laterocervical plates and is an amalgamation of the three selection mechanisms listed above (Archetti et al 2011, Scheuring and Yu 2012). The screening model proposes that the ant host sets up a desirable environment by providing nutrients to its cuticular microbiome, however the vertical transmission of *Pseudonocardia* bacteria also makes

the cuticle a demanding environment, as these bacteria compete with other potential microbial colonists (Scheuring and Yu 2012). Interference competition fuels the production of antimicrobial compounds that can, in turn, be used to protect the ants and their fungal gardens against infection, but which also prevent strains that do not produce these molecules from being competitive on the ant cuticle (Scheuring and Yu 2012). In Chapter 2, RNA-SIP experiments demonstrated that leafcutter ants do indeed transmit carbon-based resources to their cuticular microbiome and that these appear to be widely available to Actinobacteria, including *Pseudonocardia* and *Streptomyces* species. RNA sequencing also confirmed that several secondary metabolite biosynthetic gene clusters were expressed by *Pseudonocardia* on the ant cuticle. This included gene clusters that encode bacteriocins, which are often associated with intense bacterial competition, as well as secondary metabolites such as ectoine and carotenoid terpenes, which are used to cope with environmental and biotic stressors. This suggests that bacteria on the ant cuticle are experiencing strong competition for the resources provided by the ant host and that host-directed competition is likely to be a key force in enabling the establishment of an antimicrobial-producing microbiome. However, although several gene clusters involved in the production of antibacterial compounds were expressed by *Pseudonocardia* species on the ant cuticle, this was not the case for gene clusters encoding the biosynthesis of antifungal compounds. Therefore it is likely that microbiome functioning can also be dynamic, with different compounds being produced either in response to pathogenic infection (these cues could come directly from the pathogen or indirectly via the host), or in response to the host environment, for example whether or not ants are in frequent contact with the fungal garden and/or fungal parasites.

Unlike *Pseudonocardia* in the leafcutter ant system, bacteria in most plant root microbiomes are not vertically-transmitted across plant generations. However, similarly to the ant cuticular microbiome, plant root microbiome assembly is not a random process and certain beneficial bacteria, including *Streptomyces* species, appear to be consistently enriched within the roots of particular plant species, relative to the surrounding soil (Berg and Smalla 2009, Bulgarelli et al 2012, Lundberg et al 2012). In experiments reported in this thesis, several *Streptomyces* species were isolated from the roots of *A. thaliana* that demonstrated plant-growth-promoting

effects both *in vitro* and *in vivo*. Additionally, several isolates produced compounds with potent inhibitory activity against important plant pathogens, including the wheat take-all fungus, suggesting that root microbes may act as a useful resource to search for novel biocontrol strains. However, although inhibition of the take-all fungus was observed *in vitro*, pathogen suppression was less efficient *in vivo*. Numerous factors may influence the success and functionality of biocontrol strains including their access to key resources, such as nutrients and space, in the root niche (Ryan et al 2009). Thus, the development of efficient biocontrol strains requires a greater understanding of the factors that influence microbial colonisation of plant roots. Additionally, not all streptomycete isolates conferred benefits to their plant host and so careful screening will be required to identify the best biocontrol agents and establish whether the antimicrobials produced by such strains could also have non-target effects.

As with the ant system, host-derived nutrients, in the form of root exudates, are thought to be, in part, responsible for recruiting bacterial species to plant roots (Badri and Vivanco 2009, Bais et al 2006, Haichar et al 2008). Results of the DNA SIP experiment carried out in Chapter 4 were in agreement with this, as it suggested that the root exudates of *A. thaliana* were a largely public resource that could be utilised by many different bacterial genera. However, Proteobacteria (including beneficial genera such as *Rhizobium* and *Pseudomonas*) were found to be the dominant utilisers of root exudates in the SIP experiment and, despite the observation that *Streptomyces* isolates could utilise purified root exudates *in vitro*, they were out-competed for these resources *in vivo*. This suggests that additional factors, apart from the metabolic capabilities of a species or genus, determine whether they are able to establish within the root niche and gain access to host-derived resources.

Soils can be highly variable in terms of characteristics such as mineral content, quantities of organic matter and pH. Accordingly, the presence and abundance of different microbial species also varies across different soil types (Berg and Smalla 2009). All of these variables are likely to impact upon competitive outcomes between microbes and therefore which species have access to nutrients in the plant root niche. For example, the compost used in DNA SIP experiments contained high levels of organic matter which may have acted as an alternative carbon source for *Streptomyces*

species under conditions of high competition. Additionally, fast-growing proteobacterial species had a greater initial abundance in the soil relative to Actinobacteria, potentially giving them an advantage during competition for root exudates. In the ant system, the vertical transmission of *Pseudonocardia* ensures that they are abundant at the outset of microbiome formation and have the capacity to influence competitive interactions with other microbial species; similarly, increasing the initial abundances of biocontrol agents, for example via plant seed inoculation, may enable them to have a greater chance of establishing and accessing host-derived resources at the outset of plant germination and may also influence the accumulation of other antagonistic species.

The absence of particular types of root exudate under ambient conditions may also prevent the colonisation of different bacterial species. Unpicking the trophic links between plants and microbes could enable the development of bacteria with particular substrate preferences, or plants that over-produce certain types of compound to recruit bacterial species of interest (Dessaux et al 2016, Ryan et al 2009). Salicylic acid (SA) is produced by plants in response to pathogenic attack and a previously published study suggested that this compound is directly responsible for recruiting defensive bacteria, including streptomycetes, to the root microbiome by acting as a growth substrate (Lebeis et al 2015). However, colonisation experiments carried out in Chapter 5 coupled with growth and chemoattraction assays did not support the hypothesis that SA was directly responsible for recruiting bacteria to the root microbiome of *A. thaliana* plants. Instead, mutant plants that over-produce SA are known to demonstrate many other pleiotropic phenotypes, including disrupted plant development, early onset senescence and altered levels of other root exudates (Brininstool et al 2008, De-la-Pena et al 2010, Jing et al 2007), any or all of which could be responsible for altering root microbiome composition. The results of experiments carried out in that chapter suggest that a more targeted approach is needed to unpick the roles of particular root exudates in dynamically recruiting bacteria to the root microbiome, rather than studying mutant plants that have broad-scale effects on plant physiology.

Overall, experiments reported in this thesis suggest that both plants and leafcutter ants are associated with mixed communities of protective bacteria, including species of *Streptomyces*, that produce a range of antimicrobial compounds and that could be exploited for future drug and biocontrol development. The antimicrobials produced by these strains can play an important role in microbial competition and therefore influence the process of microbiome assembly. Additionally, host-derived resources and priority effects can drive competitive interactions in ways that are beneficial to the host. Understanding the chemical cues and resources that are involved in host-microbe interactions may enable us to manipulate microbiomes to our advantage. However, experiments conducted in this thesis have also shown that the factors that affect microbiome assembly and functionality (such as the production of protective, antimicrobial compounds) are likely to be context dependent. A priority for future research will be to understand how abiotic and biotic variability influences microbial competition, as well as host-derived cues and resources, so that we can develop consistent approaches for engineering beneficial host microbiomes.

Bibliography

- Adnani N, Rajski SR, Bugni TS (2017). Symbiosis-inspired approaches to antibiotic discovery. *Nat Prod Rep* **34**: 784-814.
- Ai C, Liang G, Sun J, Wang X, He P, Zhou W *et al* (2015). Reduced dependence of rhizosphere microbiome on plant-derived carbon in 32-year long-term inorganic and organic fertilized soils. *Soil Biol and Biochem* **80**: 70-78.
- Alanjary M, Steinke K, Ziemert N (2019). AutoMLST: an automated web server for generating multi-locus species trees highlighting natural product potential. *Nucleic Acids Res.*
- Alcaraz LD, Peimbert M, Barajas HR, Dorantes-Acosta AE, Bowman JL, Arteaga-Vázquez MA (2018). *Marchantia* liverworts as a proxy to plants' basal microbiomes. *Sci Rep* **8**: 12712.
- Algburi A, Zehm S, Netrobov V, Bren AB, Chistyakov V, Chikindas ML (2017). Subtilosin prevents biofilm formation by inhibiting bacterial quorum sensing. *Probiotics Antimicrob Proteins* **9**: 81-90.
- An DS, Im WT, Yang HC, Lee ST (2006). *Shinella granuli* gen. nov., sp. nov., and proposal of the reclassification of *Zoogloea ramigera* ATCC 19623 as *Shinella zoogloeoides* sp. nov. *Int J Syst Evol Microbiol* **56**: 443-448.
- Anders S, Pyl PT, Huber W (2015). HTSeq- a Python framework to work with high-throughput sequencing data. *Bioinformatics* **31**: 166-169.
- Andersen SB, Boye M, Nash DR, Boomsma JJ (2012). Dynamic *Wolbachia* prevalence in *Acromyrmex* leaf-cutting ants: potential for a nutritional symbiosis. *J Evol Biol* **25**: 1340-1350.
- Andersen SB, Hansen LH, Sapountzis P, Sorensen SJ, Boomsma JJ (2013). Specificity and stability of the *Acromyrmex-Pseudonocardia* symbiosis. *Mol Ecol* **22**: 4307-4321.
- Andersen SB, Yek SH, Nash DR, Boomsma JJ (2015). Interaction specificity between leaf-cutting ants and vertically transmitted *Pseudonocardia* bacteria. *BMC Evol Biol* **15**: 1.
- Anwar S, Ali B, Sajid I (2016). Screening of rhizospheric actinomycetes for various *in-vitro* and *in-vivo* plant growth promoting (PGP) traits and for agroactive compounds. *Front Microbiol* **7**: 1334.
- Apprill A, Marlow HQ, Martindale MQ, Rappe MS (2009). The onset of microbial associations in the coral *Pocillopora meandrina*. *ISME J* **3**: 685-699.
- Archetti M, Ubeda F, Fudenberg D, Green J, Pierce NE, Yu DW (2011). Let the right one in: a microeconomic approach to partner choice in mutualisms. *Am Nat* **177**: 75-85.

- Armitage SA, Broch JF, Marin HF, Nash DR, Boomsma JJ (2011). Immune defense in leaf-cutting ants: a cross-fostering approach. *Evolution* **65**: 1791-1799.
- Aziz RK, Bartels D, Best AA, DeJongh M, Disz T, Edwards RA *et al* (2008). The RAST Server: rapid annotations using subsystems technology. *BMC Genomics* **9**: 75.
- Badri DV, Loyola-Vargas VM, Du J, Stermitz FR, Broeckling CD, Iglesias-Andreu L *et al* (2008). Transcriptome analysis of *Arabidopsis* roots treated with signaling compounds: a focus on signal transduction, metabolic regulation and secretion. *New Phytol* **179**: 209-223.
- Badri DV, Quintana N, El Kassis EG, Kim HK, Choi YH, Sugiyama A *et al* (2009). An ABC transporter mutation alters root exudation of phytochemicals that provoke an overhaul of natural soil microbiota. *Plant Physiology* **151**: 2006-2017.
- Badri DV, Vivanco JM (2009). Regulation and function of root exudates. *Plant, Cell & Environment* **32**: 666-681.
- Badri DV, Chaparro JM, Zhang R, Shen Q, Vivanco JM (2013). Application of natural blends of phytochemicals derived from the root exudates of *Arabidopsis* to the soil reveal that phenolic-related compounds predominantly modulate the soil microbiome. *J Biol Chem* **288**: 4502-4512.
- Bais HP, Weir TL, Perry LG, Gilroy S, Vivanco JM (2006). The role of root exudates in rhizosphere interactions with plants and other organisms. *Annu Rev Plant Biol* **57**: 233-266.
- Barke J, Seipke RF, Gruschow S, Heavens D, Drou N, Bibb MJ *et al* (2010). A mixed community of actinomycetes produce multiple antibiotics for the fungus farming ant *Acromyrmex octospinosus*. *BMC Biol* **8**.
- Barke J, Seipke RF, Yu DW, Hutchings MI (2011). A mutualistic microbiome: How do fungus-growing ants select their antibiotic-producing bacteria? *Commun Integr Biol* **4**: 41-43.
- Beddington J (2010). Food security: contributions from science to a new and greener revolution. *Philos Trans R Soc Lond B Biol Sci* **365**: 61-71.
- Behnke O, Tranum-Jensen J, van Deurs B (1984). Filipin as a cholesterol probe. II. Filipin-cholesterol interaction in red blood cell membranes. *Eur J Cell Biol* **35**: 200-215.
- Bentley SD, Chater KF, Cerdeno-Tarraga AM, Challis GL, Thomson NR, James KD *et al* (2002). Complete genome sequence of the model actinomycete *Streptomyces coelicolor* A3(2). *Nature* **417**: 141-147.
- Berg G (2009). Plant-microbe interactions promoting plant growth and health: perspectives for controlled use of microorganisms in agriculture. *Appl Microbiol Biotechnol* **84**: 11-18.

Berg G, Smalla K (2009). Plant species and soil type cooperatively shape the structure and function of microbial communities in the rhizosphere. *FEMS microbiology ecology* **68**: 1-13.

Berg G, Grube M, Schloter M, Smalla K (2014). Unraveling the plant microbiome: looking back and future perspectives. *Front Microbiol* **5**: 148.

Bergna A, Cernava T, Rändler M, Grosch R, Zachow C, Berg G (2018). Tomato seeds preferably transmit plant beneficial endophytes. *Phytobiomes Journal* **2**: 183-193.

Berry D, Stecher B, Schintlmeister A, Reichert J, Brugiroux S, Wild B *et al* (2013). Host-compound foraging by intestinal microbiota revealed by single-cell stable isotope probing. *Proc Natl Acad Sci U S A* **110**: 4720-4725.

Bertrand S, Bohni N, Schnee S, Schumpp O, Gindro K, Wolfender JL (2014). Metabolite induction via microorganism co-culture: a potential way to enhance chemical diversity for drug discovery. *Biotechnol Adv* **32**: 1180-1204.

Blin K, Wolf T, Chevrette MG, Lu X, Schwalen CJ, Kautsar SA *et al* (2017). AntiSMASH 4.0-improvements in chemistry prediction and gene cluster boundary identification. *Nucleic Acids Res* **45**: W36-W41.

Bodenhausen N, Horton MW, Bergelson J (2013). Bacterial communities associated with the leaves and the roots of *Arabidopsis thaliana*. *PLoS one* **8**: e56329.

Bonaldi M, Chen X, Kunova A, Pizzatti C, Saracchi M, Cortesi P (2015). Colonization of lettuce rhizosphere and roots by tagged *Streptomyces*. *Front Microbiol* **6**: 25.

Bonneau L, Gerbeau-Pissot P, Thomas D, Der C, Lherminier J, Bourque S *et al* (2010). Plasma membrane sterol complexation, generated by filipin, triggers signaling responses in tobacco cells. *Biochim Biophys Acta* **1798**: 2150-2159.

Bouizgarne B, El Hadrami I, Ouhdouch Y (2006). Novel production of isochainin by a strain of *Streptomyces* sp. Isolated from rhizosphere soil of the indigenous moroccan plant *Argania Spinosa* L. *World J Microb Biot* **22**: 423-429.

Bowling SA, Guo A, Cao H, Gordon AS, Klessig DF, Dong X (1994). A mutation in *Arabidopsis* that leads to constitutive expression of systemic acquired resistance. *Plant Cell* **6**: 1845-1857.

Boza G, Worsley SF, Yu DW, Scheuring I (2019). Efficient assembly and long-term stability of defensive microbiomes via private resources and community bistability. *Plos Comput Biol* **15**: e1007109.

Brader G, Compant S, Mitter B, Trognitz F, Sessitsch A (2014). Metabolic potential of endophytic bacteria. *Curr Opin Biotechnol* **27**: 30-37.

- Branstetter MG, Jesovnik A, Sosa-Calvo J, Lloyd MW, Faircloth BC, Brady SG *et al* (2017). Dry habitats were crucibles of domestication in the evolution of agriculture in ants. *Proc Biol Sci* **284**.
- Bressan M, Roncato M-A, Bellvert F, Comte G, el Zahar Haichar F, Achouak W *et al* (2009). Exogenous glucosinolate produced by *Arabidopsis thaliana* has an impact on microbes in the rhizosphere and plant roots. *The ISME journal* **3**: 1243-1257.
- Bric JM, Bostock RM, Silverstone SE (1991). Rapid *in situ* assay for indoleacetic acid production by bacteria immobilized on a nitrocellulose membrane. *Appl Environ Microbiol* **57**: 535-538.
- Brininstool G, Kasili R, Simmons LA, Kirik V, Hulskamp M, Larkin JC (2008). Constitutive Expressor Of Pathogenesis-related Genes5 affects cell wall biogenesis and trichome development. *BMC Plant Biol* **8**: 58.
- Brocker M, Schaffer S, Mack C, Bott M (2009). Citrate utilization by *Corynebacterium glutamicum* is controlled by the CitAB two-component system through positive regulation of the citrate transport genes *citH* and *tctCBA*. *J Bacteriol* **191**: 3869-3880.
- Brucker RM, Bordenstein SR (2012). The roles of host evolutionary relationships (genus: *Nasonia*) and development in structuring microbial communities. *Evolution* **66**: 349-362.
- Buffie CG, Pamer EG (2013). Microbiota-mediated colonization resistance against intestinal pathogens. *Nat Rev Immunol* **13**: 790-801.
- Bulgarelli D, Rott M, Schlaeppi K, van Themaat EVL, Ahmadinejad N, Assenza F *et al* (2012). Revealing structure and assembly cues for *Arabidopsis* root-inhabiting bacterial microbiota. *Nature* **488**: 91-95.
- Bulgarelli D, Garrido-Oter R, Munch PC, Weiman A, Droge J, Pan Y *et al* (2015). Structure and function of the bacterial root microbiota in wild and domesticated barley. *Cell Host Microbe* **17**: 392-403.
- Bursy J, Kuhlmann AU, Pittelkow M, Hartmann H, Jebbar M, Pierik AJ *et al* (2008). Synthesis and uptake of the compatible solutes ectoine and 5-hydroxyectoine by *Streptomyces coelicolor* A3(2) in response to salt and heat stresses. *Appl Environ Microbiol* **74**: 7286-7296.
- Cai T, Cai W, Zhang J, Zheng H, Tsou AM, Xiao L *et al* (2009). Host legume-exuded antimetabolites optimize the symbiotic rhizosphere. *Mol Microbiol* **73**: 507-517.
- Caldwell DR, Keeney M, Van Soest PJ (1969). Effects of carbon dioxide on growth and maltose fermentation by *Bacteroides amylophilus*. *J Bacteriol* **98**: 668-676.
- Camilios-Neto D, Bonato P, Wasseem R, Tadra-Sfeir MZ, Brusamarello-Santos LC, Valdameri G *et al* (2014). Dual RNA-seq transcriptional analysis of wheat roots

colonized by *Azospirillum brasilense* reveals up-regulation of nutrient acquisition and cell cycle genes. *BMC Genomics* **15**: 378.

Cao L, Qiu Z, You J, Tan H, Zhou S (2004). Isolation and characterization of endophytic *Streptomyces* strains from surface-sterilized tomato (*Lycopersicon esculentum*) roots. *Lett Appl Microbiol* **39**: 425-430.

Carvalhais LC, Dennis PG, Badri DV, Tyson GW, Vivanco JM, Schenk PM (2013a). Activation of the jasmonic acid plant defence pathway alters the composition of rhizosphere bacterial communities. *PLoS One* **8**: e56457.

Carvalhais LC, Muzzi F, Tan C-H, Hsien-Choo J, Schenk PM (2013b). Plant growth in *Arabidopsis* is assisted by compost soil-derived microbial communities. *Front Plant Sci* **4**: 235-235.

Carvalhais LC, Dennis PG, Badri DV, Kidd BN, Vivanco JM, Schenk PM (2015). Linking jasmonic acid signaling, root exudates, and rhizosphere microbiomes. *Mol Plant Microbe Interact* **28**: 1049-1058.

Carvalhais LC, Schenk PM, Dennis PG (2017). Jasmonic acid signalling and the plant holobiont. *Curr Opin Microbiol* **37**: 42-47.

Cha JY, Han S, Hong HJ, Cho H, Kim D, Kwon Y *et al* (2016). Microbial and biochemical basis of a *Fusarium* wilt-suppressive soil. *ISME J* **10**: 119-129.

Chamberlain K, Crawford DL (1999). *In vitro* and *in vivo* antagonism of pathogenic turfgrass fungi by *Streptomyces hygroscopicus* strains YCED9 and WYE53. *J Ind Microbiol Biotechnol* **23**: 641-646.

Chan Kwo Chion CK, Askew SE, Leak DJ (2005). Cloning, expression, and site-directed mutagenesis of the propene monooxygenase genes from *Mycobacterium* sp. strain M156. *Appl Environ Microbiol* **71**: 1909-1914.

Chandra G, Chater KF (2014). Developmental biology of *Streptomyces* from the perspective of 100 actinobacterial genome sequences. *FEMS Microbiol Rev* **38**: 345-379.

Chaparro JM, Badri DV, Bakker MG, Sugiyama A, Manter DK, Vivanco JM (2013). Root exudation of phytochemicals in *Arabidopsis* follows specific patterns that are developmentally programmed and correlate with soil microbial functions. *PLoS One* **8**: e55731.

Chaparro JM, Badri DV, Vivanco JM (2014). Rhizosphere microbiome assemblage is affected by plant development. *ISME J* **8**: 790-803.

Chapelle E, Mendes R, Bakker PA, Raaijmakers JM (2016). Fungal invasion of the rhizosphere microbiome. *ISME J* **10**: 265-268.

- Chater KF (2006). *Streptomyces* inside-out: a new perspective on the bacteria that provide us with antibiotics. *Philos Trans R Soc Lond B Biol Sci* **361**: 761-768.
- Chater KF, Biro S, Lee KJ, Palmer T, Schrempf H (2010). The complex extracellular biology of *Streptomyces*. *FEMS Microbiol Rev* **34**: 171-198.
- Chater KF (2016). Recent advances in understanding *Streptomyces*. *F1000Res* **5**: 2795.
- Chen X, Pizzatti C, Bonaldi M, Saracchi M, Erlacher A, Kunova A *et al* (2016). Biological control of lettuce drop and host plant colonization by rhizospheric and endophytic streptomycetes. *Front Microbiol* **7**: 714.
- Chevrette MG, Carlson CM, Ortega HE, Thomas C, Ananiev GE, Barns KJ *et al* (2019). The antimicrobial potential of *Streptomyces* from insect microbiomes. *Nat Commun* **10**: 516.
- Chikindas ML, Weeks R, Drider D, Chistyakov VA, Dicks LM (2018). Functions and emerging applications of bacteriocins. *Curr Opin Biotechnol* **49**: 23-28.
- Clarke JD, Volko SM, Ledford H, Ausubel FM, Dong X (2000). Roles of salicylic acid, jasmonic acid, and ethylene in cpr-induced resistance in *Arabidopsis*. *Plant Cell* **12**: 2175-2190.
- Clay K (2014). Defensive symbiosis: a microbial perspective. *Funct Ecol* **28**: 293-298.
- Coleman NV, Spain JC (2003). Epoxyalkane: coenzyme M transferase in the ethene and vinyl chloride biodegradation pathways of mycobacterium strain JS60. *J Bacteriol* **185**: 5536-5545.
- Coleman NV, Wilson NL, Barry K, Brettin TS, Bruce DC, Copeland A *et al* (2011). Genome Sequence of the ethene- and vinyl chloride-oxidizing actinomycete *Nocardioides* sp. strain JS614. *J Bacteriol* **193**: 3399-3400.
- Conn VM, Walker AR, Franco CM (2008). Endophytic Actinobacteria induce defense pathways in *Arabidopsis thaliana*. *Mol Plant Microbe Interact* **21**: 208-218.
- Cook RJ (2003). Take-all of wheat. *Physiol Mol Plant P* **62**: 73-86.
- Coombs JT, Franco CM (2003). Visualization of an endophytic *Streptomyces* species in wheat seed. *Appl Environ Microbiol* **69**: 4260-4262.
- Coombs JT, Michelsen PP, Franco CMM (2004). Evaluation of endophytic actinobacteria as antagonists of *Gaeumannomyces graminis* var. *tritici* in wheat. *Biol Control* **29**: 359-366.
- Cope AC, Johnson HE (1958). Fungichromin. Determination of the structure of the pentaene chromophore. *J Am Chem Soc* **80**: 1504-1506.

Cordovez V, Carrion VJ, Etalo DW, Mumm R, Zhu H, van Wezel GP *et al* (2015). Diversity and functions of volatile organic compounds produced by *Streptomyces* from a disease-suppressive soil. *Front Microbiol* **6**: 1081.

Costa R, Gotz M, Mrotzek N, Lottmann J, Berg G, Smalla K (2006). Effects of site and plant species on rhizosphere community structure as revealed by molecular analysis of microbial guilds. *FEMS Microbiol Ecol* **56**: 236-249.

Cotter PD, Ross RP, Hill C (2013). Bacteriocins - a viable alternative to antibiotics? *Nat Rev Microbiol* **11**: 95-105.

Crombie AT, Murrell JC (2014). Trace-gas metabolic versatility of the facultative methanotroph *Methylocella silvestris*. *Nature* **510**: 148-151.

Crombie AT, Khawand ME, Rhodius VA, Fengler KA, Miller MC, Whited GM *et al* (2015). Regulation of plasmid-encoded isoprene metabolism in *Rhodococcus*, a representative of an important link in the global isoprene cycle. *Environ Microbiol* **17**: 3314-3329.

Currie C, Bot A, Boomsma JJ (2003). Experimental evidence of a tripartite mutualism: bacteria protect ant fungus gardens from specialized parasites. *Oikos* **101**: 91-102.

Currie CR, Mueller UG, Malloch D (1999a). The agricultural pathology of ant fungus gardens. *Proc Natl Acad Sci U S A* **96**: 7998-8002.

Currie CR, Scott JA, Summerbell RC, Malloch D (1999b). Fungus-growing ants use antibiotic-producing bacteria to control garden parasites. *Nature* **398**: 701-704.

Currie CR (2001). A community of ants, fungi, and bacteria: a multilateral approach to studying symbiosis. *Annu Rev Microbiol* **55**: 357-380.

Currie CR, Stuart AE (2001). Weeding and grooming of pathogens in agriculture by ants. *Proc Biol Sci* **268**: 1033-1039.

Currie CR, Poulsen M, Mendenhall J, Boomsma JJ, Billen J (2006). Coevolved crypts and exocrine glands support mutualistic bacteria in fungus-growing ants. *Science* **311**: 81-83.

Czech L, Hermann L, Stoveken N, Richter AA, Hoppner A, Smits SHJ *et al* (2018). Role of the extremolytes ectoine and hydroxyectoine as stress protectants and nutrients: genetics, phylogenomics, biochemistry, and structural Analysis. *Genes (Basel)* **9**.

Daddaoua A, Matilla MA, Krell T, Chini A, Morel B (2018). An auxin controls bacterial antibiotics production. *Nucleic Acids Res* **46**: 11229-11238.

Das S, Pettersson BMF, Behra PRK, Ramesh M, Dasgupta S, Bhattacharya A *et al* (2015). Characterization of three *Mycobacterium* spp. with potential use in bioremediation by genome sequencing and comparative genomics. *Genome Biol Evol* **7**: 1871-1886.

- Davidson SK, Koropatnick TA, Kossmehl R, Sycuro L, McFall-Ngai MJ (2004). NO means 'yes' in the squid-vibrio symbiosis: nitric oxide (NO) during the initial stages of a beneficial association. *Cell Microbiol* **6**: 1139-1151.
- de Boer M, Bom P, Kindt F, Keurentjes JJ, van der Sluis I, van Loon LC *et al* (2003). Control of *Fusarium* Wilt of radish by combining *Pseudomonas putida* strains that have different disease-suppressive mechanisms. *Phytopathology* **93**: 626-632.
- De Fine Licht HH, Schiott M, Mueller UG, Boomsma JJ (2010). Evolutionary transitions in enzyme activity of ant fungus gardens. *Evolution* **64**: 2055-2069.
- De Fine Licht HH, Boomsma JJ, Tunlid A (2014). Symbiotic adaptations in the fungal cultivar of leaf-cutting ants. *Nat Commun* **5**: 5675.
- de Man TJ, Stajich JE, Kubicek CP, Teiling C, Chenthamara K, Atanasova L *et al* (2016). Small genome of the fungus *Escovopsis weberi*, a specialized disease agent of ant agriculture. *Proc Natl Acad Sci U S A* **113**: 3567-3572.
- De-la-Pena C, Badri DV, Lei Z, Watson BS, Brandao MM, Silva-Filho MC *et al* (2010). Root secretion of defense-related proteins is development-dependent and correlated with flowering time. *J Biol Chem* **285**: 30654-30665.
- Denoux C, Galletti R, Mammarella N, Gopalan S, Werck D, De Lorenzo G *et al* (2008). Activation of defense response pathways by OGs and Flg22 elicitors in *Arabidopsis* seedlings. *Mol Plant* **1**: 423-445.
- DeSantis TZ, Hugenholtz P, Larsen N, Rojas M, Brodie EL, Keller K *et al* (2006). Greengenes, a chimera-checked 16S rRNA gene database and workbench compatible with ARB. *Appl Environ Microbiol* **72**: 5069-5072.
- Dessaux Y, Grandclement C, Faure D (2016). Engineering the rhizosphere. *Trends Plant Sci* **21**: 266-278.
- Dias AC, Dini-Andreote F, Hannula SE, Andreote FD, Pereira ESMC, Salles JF *et al* (2013). Different selective effects on rhizosphere bacteria exerted by genetically modified versus conventional potato lines. *PLoS One* **8**: e67948.
- Dias ACF, Hoogwout EF, Pereira e Silva MdC, Salles JF, van Overbeek LS, van Elsas JD (2012). Potato cultivar type affects the structure of ammonia oxidizer communities in field soil under potato beyond the rhizosphere. *Soil Biol Biochem* **50**: 85-95.
- Doornbos RF, Geraats BP, Kuramae EE, Van Loon LC, Bakker PA (2011). Effects of jasmonic acid, ethylene, and salicylic acid signaling on the rhizosphere bacterial community of *Arabidopsis thaliana*. *Mol Plant Microbe Interact* **24**: 395-407.
- Dowd SE, Callaway TR, Wolcott RD, Sun Y, McKeethan T, Hagevoort RG *et al* (2008a). Evaluation of the bacterial diversity in the feces of cattle using 16S rDNA bacterial tag-encoded FLX amplicon pyrosequencing (bTEFAP). *BMC Microbiol* **8**: 125.

- Dowd SE, Wolcott RD, Sun Y, McKeehan T, Smith E, Rhoads D (2008b). Polymicrobial nature of chronic diabetic foot ulcer biofilm infections determined using bacterial tag encoded FLX amplicon pyrosequencing (bTEFAP). *PLoS One* **3**: e3326.
- Dumont MG, Murrell JC (2005). Stable isotope probing - linking microbial identity to function. *Nat Rev Microbiol* **3**: 499-504.
- Dunford EA, Neufeld JD (2010). DNA stable-isotope probing (DNA-SIP). *J Vis Exp*.
- Edgar RC (2004). MUSCLE: a multiple sequence alignment method with reduced time and space complexity. *BMC Bioinformatics* **5**: 113.
- Edwards J, Johnson C, Santos-Medellin C, Lurie E, Podishetty NK, Bhatnagar S *et al* (2015). Structure, variation, and assembly of the root-associated microbiomes of rice. *Proc Natl Acad Sci U S A* **112**: E911-920.
- Egan S, Harder T, Burke C, Steinberg P, Kjelleberg S, Thomas T (2013). The seaweed holobiont: understanding seaweed-bacteria interactions. *FEMS Microbiol Rev* **37**: 462-476.
- Esquenazi E, Coates C, Simmons L, Gonzalez D, Gerwick WH, Dorrestein PC (2008). Visualizing the spatial distribution of secondary metabolites produced by marine cyanobacteria and sponges via MALDI-TOF imaging. *Mol Biosyst* **4**: 562-570.
- Evans C, Hardin J, Stoebel DM (2018). Selecting between-sample RNA-Seq normalization methods from the perspective of their assumptions. *Brief Bioinform* **19**: 776-792.
- Ezziyyani M, Requena ME, Egea-Gilabert C, Candela ME (2007). Biological control of *Phytophthora* root rot of pepper using *Trichoderma harzianum* and *Streptomyces rochei* in combination. *J Phytopathol* **155**: 342-349.
- Fang FC (2004). Antimicrobial reactive oxygen and nitrogen species: concepts and controversies. *Nat Rev Microbiol* **2**: 820-832.
- Fernandez-Marin H, Zimmerman JK, Rehner SA, Wcislo WT (2006). Active use of the metapleural glands by ants in controlling fungal infection. *Proc Biol Sci* **273**: 1689-1695.
- Fernandez-Marin H, Nash DR, Higginbotham S, Estrada C, van Zweden JS, d'Ettorre P *et al* (2015). Functional role of phenylacetic acid from metapleural gland secretions in controlling fungal pathogens in evolutionarily derived leaf-cutting ants. *Proc Biol Sci* **282**: 20150212.
- Finking R, Marahiel MA (2004). Biosynthesis of Nonribosomal Peptides. *Annu Rev Microbiol* **58**: 453-488.
- Finn RD, Clements J, Eddy SR (2011). HMMER web server: interactive sequence similarity searching. *Nucleic Acids Res* **39**: W29-37.

- Fischbach MA, Clardy J (2007). One pathway, many products. *Nat Chem Biol* **3**: 353-355.
- Fischbach MA, Walsh CT (2009). Antibiotics for emerging pathogens. *Science* **325**: 1089-1093.
- Fischbach MA, Sonnenburg JL (2011). Eating for two: how metabolism establishes interspecies interactions in the gut. *Cell host & microbe* **10**: 336-347.
- Fitzpatrick CR, Copeland J, Wang PW, Guttman DS, Kotanen PM, Johnson MTJ (2018). Assembly and ecological function of the root microbiome across angiosperm plant species. *Proc Natl Acad Sci U S A* **115**: E1157-E1165.
- Flärdh K, Buttner MJ (2009). *Streptomyces* morphogenetics: dissecting differentiation in a filamentous bacterium. *Nat Rev Microbiol* **7**: 36-49.
- Ford SA, King KC (2016). Harnessing the Power of Defensive Microbes: Evolutionary Implications in Nature and Disease Control. *PLoS Pathog* **12**: e1005465.
- Fortunato CS, Huber JA (2016). Coupled RNA-SIP and metatranscriptomics of active chemolithoautotrophic communities at a deep-sea hydrothermal vent. *ISME J* **10**: 1925-1938.
- Foster KR, Wenseleers T (2006). A general model for the evolution of mutualisms. *J Evol Biol* **19**: 1283-1293.
- Foster KR, Schluter J, Coyte KZ, Rakoff-Nahoum S (2017). The evolution of the host microbiome as an ecosystem on a leash. *Nature* **548**: 43-51.
- Franco C, Michelsen P, Percy N, Conn V, Listiana E, Moll S *et al* (2007). Actinobacterial endophytes for improved crop performance. *Australas Plant Pathol* **36**: 524-531.
- Frey Tirri B, Bitzer J, Geudelin B, Drewe J (2010). Safety, tolerability and pharmacokinetics of intravaginal pentamycin. *Chemotherapy* **56**: 190-196.
- Gaiero JR, McCall CA, Thompson KA, Day NJ, Best AS, Dunfield KE (2013). Inside the root microbiome: bacterial root endophytes and plant growth promotion. *Am J Bot* **100**: 1738-1750.
- Gao G, Zhang S, Wang C, Yang X, Wang Y, Su X *et al* (2011). Arabidopsis CPR5 independently regulates seed germination and postgermination arrest of development through LOX pathway and ABA signaling. *PLoS One* **6**: e19406.
- Gao H, Grünschow S, Barke J, Seipke RF, Hill LM, Orivel J *et al* (2014). Filipins: the first antifungal “weed killers” identified from bacteria isolated from the trap-ant. *RSC Advances* **4**: 57267-57270.
- Garbeva P, Van Elsas J, Van Veen J (2008). Rhizosphere microbial community and its response to plant species and soil history. *Plant and soil* **302**: 19-32.

- Garrido-Oter R, Nakano RT, Dombrowski N, Ma KW, AgBiome T, McHardy AC *et al* (2018). Modular traits of the rhizobiales root microbiota and their evolutionary relationship with symbiotic rhizobia. *Cell Host Microbe* **24**: 155-167 e155.
- Gershenzon J, Dudareva N (2007). The function of terpene natural products in the natural world. *Nat Chem Biol* **3**: 408-414.
- Gil-Turnes MS, Hay ME, Fenical W (1989). Symbiotic marine bacteria chemically defend crustacean embryos from a pathogenic fungus. *Science* **246**: 116-118.
- Gil-Turnes MS, Fenical W (1992). Embryos of *Homarus americanus* are protected by epibiotic bacteria. *Biol Bull* **182**: 105-108.
- Gkarmiri K, Mahmood S, Ekblad A, Alstrom S, Hogberg N, Finlay R (2017). Identifying the Active Microbiome Associated with Roots and Rhizosphere Soil of Oilseed Rape. *Appl Environ Microbiol* **83**.
- Glick BR (2014). Bacteria with ACC deaminase can promote plant growth and help to feed the world. *Microbiol Res* **169**: 30-39.
- Godfray HC, Beddington JR, Crute IR, Haddad L, Lawrence D, Muir JF *et al* (2010). Food security: the challenge of feeding 9 billion people. *Science* **327**: 812-818.
- Gomes RC, Semêdo LTAS, Soares RMA, Alviano CS, And LFL, Coelho RRR (2000). Chitinolytic activity of actinomycetes from a cerrado soil and their potential in biocontrol. *Lett Appl Microbiol* **30**: 146-150.
- Gong ZL, Ai MJ, Sun HM, Liu HY, Yu LY, Zhang YQ (2016). *Jatrophihabitans huperziae* sp. nov., an endophytic actinobacterium isolated from surface-sterilized tissue of the medicinal plant *Huperzia serrata* (Thunb.). *Int J Syst Evol Microbiol* **66**: 3972-3977.
- Goodfellow M, Williams ST (1983). Ecology of actinomycetes. *Annu Rev Microbiol* **37**: 189-216.
- Gopalakrishnan S, Vadlamudi S, Bandikinda P, Sathya A, Vijayabharathi R, Rupela O *et al* (2014). Evaluation of *Streptomyces* strains isolated from herbal vermicompost for their plant growth-promotion traits in rice. *Microbiol Res* **169**: 40-48.
- Graf J, Ruby EG (2000). Novel effects of a transposon insertion in the *Vibrio fischeri* glnD gene: defects in iron uptake and symbiotic persistence in addition to nitrogen utilization. *Mol Microbiol* **37**: 168-179.
- Grebe M, Xu J, Mobius W, Ueda T, Nakano A, Geuze HJ *et al* (2003). *Arabidopsis* sterol endocytosis involves actin-mediated trafficking via ARA6-positive early endosomes. *Curr Biol* **13**: 1378-1387.
- Griffiths RI, Manefield M, Ostle N, McNamara N, O'Donnell AG, Bailey MJ *et al* (2004). ¹³C₂ pulse labelling of plants in tandem with stable isotope probing: methodological

considerations for examining microbial function in the rhizosphere. *J Microbiol Methods* **58**: 119-129.

Guyonnet JP, Guillemet M, Dubost A, Simon L, Ortet P, Barakat M *et al* (2018). Plant nutrient resource use strategies shape active rhizosphere microbiota through root exudation. *Front Plant Sci* **9**: 1662.

Haeder S, Wirth R, Herz H, Spiteller D (2009). Candidicin-producing *Streptomyces* support leaf-cutting ants to protect their fungus garden against the pathogenic fungus *Escovopsis*. *Proc Natl Acad Sci USA* **106**: 4742-4746.

Haichar FE, Marol C, Berge O, Rangel-Castro JI, Prosser JI, Balesdent J *et al* (2008). Plant host habitat and root exudates shape soil bacterial community structure. *ISME J* **2**: 1221-1230.

Haichar FEZ, Heulin T, Guyonnet JP, Achouak W (2016). Stable isotope probing of carbon flow in the plant holobiont. *Curr Opin Biotechnol* **41**: 9-13.

Haichar FZ, Roncato MA, Achouak W (2012). Stable isotope probing of bacterial community structure and gene expression in the rhizosphere of *Arabidopsis thaliana*. *FEMS Microbiol Ecol* **81**: 291-302.

Haine ER (2008). Symbiont-mediated protection. *Proc Biol Sci* **275**: 353-361.

Hannula SE, Boschker HT, de Boer W, van Veen JA (2012). ¹³C pulse-labeling assessment of the community structure of active fungi in the rhizosphere of a genetically starch-modified potato (*Solanum tuberosum*) cultivar and its parental isolate. *New Phytol* **194**: 784-799.

Hartmann A, Schmid M, van Tuinen D, Berg G (2009). Plant-driven selection of microbes. *Plant and Soil* **321**: 235-257.

Heine D, Holmes NA, Worsley SF, Santos ACA, Innocent TM, Scherlach K *et al* (2018). Chemical warfare between leafcutter ant symbionts and a co-evolved pathogen. *Nat Commun* **9**: 2208.

Hennessy RC, Glaring MA, Olsson S, Stougaard P (2017). Transcriptomic profiling of microbe-microbe interactions reveals the specific response of the biocontrol strain *P. fluorescens* In5 to the phytopathogen *Rhizoctonia solani*. *BMC Res Notes* **10**: 376-376.

Hernandez M, Dumont MG, Yuan Q, Conrad R (2015). Different bacterial populations associated with the roots and rhizosphere of rice incorporate plant-derived carbon. *Appl Environ Microbiol* **81**: 2244-2253.

Hiltner L (1904). Über neue Erfahrungen und probleme auf dem gebiet der bodenback- teriologie und unter besonderer berucksichtigung der grundungung und brache. *Deut Landwirsch Ges* **98**: 59-78.

- Hoitink HAJ, Boehm MJ (1999). Biocontrol within the context of soil microbial communities: a substrate-dependent phenomenon. *Annu Rev Phytopathol* **37**: 427-446.
- Holmes NA, Innocent TM, Heine D, Bassam MA, Worsley SF, Trottmann F *et al* (2016). Genome analysis of two *Pseudonocardia* phylotypes associated with *Acromyrmex* leafcutter ants reveals their biosynthetic potential. *Front Microbiol* **7**: 2073.
- Holmes NA, Devine R, Qin Z, Seipke RF, Wilkinson B, Hutchings MI (2018). Complete genome sequence of *Streptomyces formicae* KY5, the formicamycin producer. *J Biotechnol* **265**: 116-118.
- Hooper LV, Littman DR, Macpherson AJ (2012). Interactions between the microbiota and the immune system. *Science* **336**: 1268-1273.
- Hopwood DA (2007). *Streptomyces in nature and medicine: the antibiotic makers*. Oxford University Press: New York.
- Hoster F, Schmitz JE, Daniel R (2005). Enrichment of chitinolytic microorganisms: isolation and characterization of a chitinase exhibiting antifungal activity against phytopathogenic fungi from a novel *Streptomyces* strain. *Appl Microbiol Biotechnol* **66**: 434-442.
- Huang AC, Jiang T, Liu Y-X, Bai Y-C, Reed J, Qu B *et al* (2019). A specialized metabolic network selectively modulates *Arabidopsis* root microbiota. *Science* **364**: eaau6389.
- Hulcr J, Adams AS, Raffa K, Hofstetter RW, Klepzig KD, Currie CR (2011). Presence and diversity of *Streptomyces* in *Dendroctonus* and sympatric bark beetle galleries across North America. *Microb Ecol* **61**: 759-768.
- Human ZR, Moon K, Bae M, de Beer ZW, Cha S, Wingfield MJ *et al* (2016). Antifungal *Streptomyces* spp. associated with the infructescences of *Protea* spp. in South Africa. *Front Microbiol* **7**: 1657.
- Igarashi Y, In Y, Ishida T, Fujita T, Yamakawa T, Onaka H *et al* (2005). Absolute configuration of TPU-0043, a pentaene macrolide from *Streptomyces* sp. *J Antibiot (Tokyo)* **58**: 523-525.
- Inderbitzin P, Ward J, Barbella A, Solares N, Izyumin D, Burman P *et al* (2018). Soil microbiomes associated with *Verticillium* wilt-suppressive broccoli and chitin amendments are enriched with potential biocontrol agents. *Phytopathology* **108**: 31-43.
- Ishiyama D, Vujaklija D, Davies J (2004). Novel pathway of salicylate degradation by *Streptomyces* sp. strain WA46. *Appl Environ Microbiol* **70**: 1297-1306.
- Itoh Y, Takahashi K, Takizawa H, Nikaidou N, Tanaka H, Nishihashi H *et al* (2003). Family 19 chitinase of *Streptomyces griseus* HUT6037 increases plant resistance to the fungal disease. *Biosci Biotechnol Biochem* **67**: 847-855.

- Jain C, Rodriguez RL, Phillipy AM, Konstantinidis KT, Aluru S (2018). High throughput ANI analysis of 90K prokaryotic genomes reveals clear species boundaries. *Nat Commun* **9**: 5114.
- Jing HC, Anderson L, Sturre MJ, Hille J, Dijkwel PP (2007). *Arabidopsis* CPR5 is a senescence-regulatory gene with pleiotropic functions as predicted by the evolutionary theory of senescence. *J Exp Bot* **58**: 3885-3894.
- Jing HC, Hebel R, Oeljeklaus S, Sitek B, Stuhler K, Meyer HE *et al* (2008). Early leaf senescence is associated with an altered cellular redox balance in *Arabidopsis* cpr5/old1 mutants. *Plant Biol (Stuttg)* **10 Suppl 1**: 85-98.
- Jirage D, Tootle TL, Reuber TL, Frost LN, Feys BJ, Parker JE *et al* (1999). *Arabidopsis thaliana* PAD4 encodes a lipase-like gene that is important for salicylic acid signaling. *Proc Natl Acad Sci U S A* **96**: 13583-13588.
- Jog R, Pandya M, Nareshkumar G, Rajkumar S (2014). Mechanism of phosphate solubilization and antifungal activity of *Streptomyces* spp. isolated from wheat roots and rhizosphere and their application in improving plant growth. *Microbiology* **160**: 778-788.
- Johnston-Monje D, Raizada MN (2011). Conservation and diversity of seed associated endophytes in *Zea* across boundaries of evolution, ethnography and ecology. *PLoS One* **6**: e20396.
- Joo GJ (2005). Purification and characterization of an extracellular chitinase from the antifungal biocontrol agent *Streptomyces halstedii*. *Biotechnol Lett* **27**: 1483-1486.
- Jousset A, Rochat L, Lanoue A, Bonkowski M, Keel C, Scheu S (2011). Plants respond to pathogen infection by enhancing the antifungal gene expression of root-associated bacteria. *Mol Plant Microbe Interact* **24**: 352-358.
- Kabat AM, Srinivasan N, Maloy KJ (2014). Modulation of immune development and function by intestinal microbiota. *Trends Immunol* **35**: 507-517.
- Kaltenpoth M, Göttler W, Herzner G, Strohm E (2005). Symbiotic bacteria protect wasp larvae from fungal infestation. *Curr Biol* **15**: 475-479.
- Kaltenpoth M, Goettler W, Dale C, Stubblefield JW, Herzner G, Roeser-Mueller K *et al* (2006). '*Candidatus Streptomyces philanthi*', an endosymbiotic streptomycete in the antennae of *Philanthus* digger wasps. *Int J Syst Evol Microbiol* **56**: 1403-1411.
- Kaltenpoth M (2009). Actinobacteria as mutualists: general healthcare for insects? *Trends Microbiol* **17**: 529-535.
- Kaltenpoth M, Goettler W, Koehler S, Strohm E (2010a). Life cycle and population dynamics of a protective insect symbiont reveal severe bottlenecks during vertical transmission. *Evol Ecol* **24**: 463-477.

- Kaltenpoth M, Schmitt T, Polidori C, Koedam D, Strohm E (2010b). Symbiotic streptomycetes in antennal glands of the South American digger wasp genus *Trachypus* (Hymenoptera, Crabronidae). *Physiol Entomol* **35**: 196-200.
- Kaltenpoth M, Yildirim E, Gürbüz MF, Herzner G, Strohm E (2012). Refining the roots of the beewolf-*Streptomyces* symbiosis: antennal symbionts in the rare genus *Philanthinus* (Hymenoptera, Crabronidae). *Appl Environ Microbiology* **78**: 822-827.
- Kanehisa M, Sato Y, Kawashima M, Furumichi M, Tanabe M (2016a). KEGG as a reference resource for gene and protein annotation. *Nucleic Acids Res* **44**: D457-462.
- Kanehisa M, Sato Y, Morishima K (2016b). BlastKOALA and GhostKOALA: KEGG Tools for Functional Characterization of Genome and Metagenome Sequences. *J Mol Biol* **428**: 726-731.
- Katz E (1967). Actinomycin. In: Gottlieb D, Shaw PD (eds). *Biosynthesis*. Springer Berlin Heidelberg: Berlin, Heidelberg. pp 276-341.
- Khan ST, Komaki H, Motohashi K, Kozone I, Mukai A, Takagi M *et al* (2011). *Streptomyces* associated with a marine sponge *Haliclona* sp.; biosynthetic genes for secondary metabolites and products. *Environ Microbiol* **13**: 391-403.
- Kieser T, Bibb MJ, Buttner MJ, Chater KF, Hopwood DA (2000). *Practical Streptomyces Genetics*. John Innes Foundation: Norwich.
- Kim D, Langmead B, Salzberg SL (2015). HISAT: a fast spliced aligner with low memory requirements. *Nat Methods* **12**: 357-360.
- Kinkel LL, Schlatter DC, Bakker MG, Arenz BE (2012). *Streptomyces* competition and co-evolution in relation to plant disease suppression. *Res Microbiol* **163**: 490-499.
- Kirik V, Bouyer D, Schobinger U, Bechtold N, Herzog M, Bonneville JM *et al* (2001). CPR5 is involved in cell proliferation and cell death control and encodes a novel transmembrane protein. *Curr Biol* **11**: 1891-1895.
- Kneip C, Lockhart P, Voss C, Maier UG (2007). Nitrogen fixation in eukaryotes--new models for symbiosis. *BMC Evol Biol* **7**: 55.
- Koch E, Ole Becker J, Berg G, Hauschild R, Jehle J, Köhl J *et al* (2018). Biocontrol of plant diseases is not an unsafe technology! *J Plant Dis and Protect* **125**: 121-125.
- Koehler S, Doubský J, Kaltenpoth M (2013). Dynamics of symbiont-mediated antibiotic production reveal efficient long-term protection for beewolf offspring. *Front Zool* **10**: 1.
- Kong D, Lee MJ, Lin S, Kim ES (2013). Biosynthesis and pathway engineering of antifungal polyene macrolides in actinomycetes. *J Ind Microbiol Biotechnol* **40**: 529-543.

- Konstantinidis KT, Tiedje JM (2005). Genomic insights that advance the species definition for prokaryotes. *Proc Nat Acad Sci USA* **102**: 2567.
- Kooij PW, Rogowska-Wrzesinska A, Hoffmann D, Roepstorff P, Boomsma JJ, Schiott M (2014). *Leucoagaricus gongylophorus* uses leaf-cutting ants to vector proteolytic enzymes towards new plant substrate. *ISME J* **8**: 1032-1040.
- Kortemaa H, Pennanen T, Smolander A, Haahtela K (1997). Distribution of antagonistic *Streptomyces griseoviridis* in rhizosphere and nonrhizosphere sand. *J Phytopathol* **145**: 137-143.
- Kost C, Lakatos T, Böttcher I, Arendholz W-R, Redenbach M, Wirth R (2007). Non-specific association between filamentous bacteria and fungus-growing ants. *Naturwissenschaften* **94**: 821-828.
- Kotani T, Yamamoto T, Yurimoto H, Sakai Y, Kato N (2003). Propane monooxygenase and NAD⁺-dependent secondary alcohol dehydrogenase in propane metabolism by *Gordonia* sp. strain TY-5. *J Bacteriol* **185**: 7120-7128.
- Kotani T, Kawashima Y, Yurimoto H, Kato N, Sakai Y (2006). Gene structure and regulation of alkane monooxygenases in propane-utilizing *Mycobacterium* sp. TY-6 and *Pseudonocardia* sp. TY-7. *J Biosci Bioeng* **102**: 184-192.
- Kranzler M, Syrowatka M, Leitsch D, Winnips C, Walochnik J (2015). Pentamycin shows high efficacy against *Trichomonas vaginalis*. *Int J Antimicrob Agents* **45**: 434-437.
- Kroiss J, Kaltenpoth M, Schneider B, Schwinger M-G, Hertweck C, Maddula RK *et al* (2010). Symbiotic streptomycetes provide antibiotic combination prophylaxis for wasp offspring. *Nat Chem Biol* **6**: 261-263.
- Kuester E, Williams ST (1964). Selection of Media for Isolation of Streptomycetes. *Nature* **202**: 928-929.
- Kumar S, Stecher G, Tamura K (2016). MEGA7: Molecular Evolutionary Genetics Analysis Version 7.0 for Bigger Datasets. *Mol Biol Evol* **33**: 1870-1874.
- Kurth F, Mailander S, Bonn M, Feldhahn L, Herrmann S, Grosse I *et al* (2014). *Streptomyces*-induced resistance against oak powdery mildew involves host plant responses in defense, photosynthesis, and secondary metabolism pathways. *Mol Plant Microbe Interact* **27**: 891-900.
- Kwak YS, Weller DM (2013). Take-all of wheat and natural disease suppression: a review. *Plant Pathol J* **29**: 125-135.
- Lahdenperä ML, Simon E, Uoti J (1991). Mycostop - a novel biofungicide based on *Streptomyces* bacteria. In: Beemster ABR, Bollen GJ, Gerlagh M, Ruissen MA, Schippers B, Tempel A (eds). *Developments in Agricultural and Managed Forest Ecology*. Elsevier. pp 258-263.

- Lanoue A, Burlat V, Henkes GJ, Koch I, Schurr U, Rose US (2010). *De novo* biosynthesis of defense root exudates in response to *Fusarium* attack in barley. *New Phytol* **185**: 577-588.
- Law JW, Ser HL, Khan TM, Chuah LH, Pusparajah P, Chan KG *et al* (2017). The potential of *Streptomyces* as biocontrol Agents against the Rice Blast Fungus, *Magnaporthe oryzae* (*Pyricularia oryzae*). *Front Microbiol* **8**: 3.
- Lebeis SL, Paredes SH, Lundberg DS, Breakfield N, Gehring J, McDonald M *et al* (2015). Salicylic acid modulates colonization of the root microbiome by specific bacterial taxa. *Science* **349**: 860-864.
- Lee MJ, Kong D, Han K, Sherman DH, Bai L, Deng Z *et al* (2012). Structural analysis and biosynthetic engineering of a solubility-improved and less-hemolytic nystatin-like polyene in *Pseudonocardia autotrophica*. *Appl Microbiol Biotechnol* **95**: 157-168.
- Li Z, Rawlings BJ, Harrison PH, Vederas JC (1989). Production of new polyene antibiotics by *Streptomyces cellulosa* after addition of ethyl (Z)-16-phenylhexadec-9-enoate. *J Antibiot (Tokyo)* **42**: 577-584.
- Lim SK, Kim SJ, Cha SH, Oh YK, Rhee HJ, Kim MS *et al* (2009). Complete genome sequence of *Rhodobacter sphaeroides* KD131. *J Bacteriol* **191**: 1118-1119.
- Lin DX, Wang ET, Tang H, Han TX, He YR, Guan SH *et al* (2008). *Shinella kummerowiae* sp. nov., a symbiotic bacterium isolated from root nodules of the herbal legume *Kummerowia stipulacea*. *Int J Syst Evol Microbiol* **58**: 1409-1413.
- Lin L, Xu X (2013). Indole-3-acetic acid production by endophytic *Streptomyces* sp. En-1 isolated from medicinal plants. *Curr Microbiol* **67**: 209-217.
- Little AE, Currie CR (2007). Symbiotic complexity: discovery of a fifth symbiont in the attine ant-microbe symbiosis. *Biol Lett* **3**: 501-504.
- Little AE, Currie CR (2008). Black yeast symbionts compromise the efficiency of antibiotic defenses in fungus-growing ants. *Ecology* **89**: 1216-1222.
- Liu CW, Murray JD (2016). The role of flavonoids in nodulation host-range specificity: an update. *Plants (Basel)* **5**.
- Liu H, Carvalhais LC, Crawford M, Singh E, Dennis PG, Pieterse CMJ *et al* (2017a). Inner plant values: diversity, colonization and benefits from endophytic bacteria. *Front Microbiol* **8**: 2552.
- Liu H, Carvalhais LC, Schenk PM, Dennis PG (2017b). Effects of jasmonic acid signalling on the wheat microbiome differ between body sites. *Sci Rep* **7**: 41766.
- Lloyd AB (1969). Behaviour of streptomycetes in soil. *Microbiology* **56**: 165-170.

- Long HH, Sonntag DG, Schmidt DD, Baldwin IT (2010). The structure of the culturable root bacterial endophyte community of *Nicotiana attenuata* is organized by soil composition and host plant ethylene production and perception. *New Phytol* **185**: 554-567.
- Lopera J, Miller IJ, McPhail KL, Kwan JC (2017). Increased biosynthetic gene dosage in a genome-reduced defensive bacterial symbiont. *mSystems* **2**.
- Lu Y, Conrad R (2005). In situ stable isotope probing of methanogenic archaea in the rice rhizosphere. *Science* **309**: 1088-1090.
- Lu Y, Rosencrantz D, Liesack W, Conrad R (2006). Structure and activity of bacterial community inhabiting rice roots and the rhizosphere. *Environ Microbiol* **8**: 1351-1360.
- Lueders T, Manefield M, Friedrich MW (2004). Enhanced sensitivity of DNA- and rRNA-based stable isotope probing by fractionation and quantitative analysis of isopycnic centrifugation gradients. *Environ Microbiol* **6**: 73-78.
- Lugtenberg B, Kamilova F (2009). Plant-growth-promoting rhizobacteria. *Annu Rev Microbiol* **63**: 541-556.
- Lundberg DS, Lebeis SL, Paredes SH, Yourstone S, Gehring J, Malfatti S *et al* (2012). Defining the core *Arabidopsis thaliana* root microbiome. *Nature* **488**: 86-90.
- Madhaiyan M, Hu CJ, Kim SJ, Weon HY, Kwon SW, Ji L (2013). *Jatrophihabitans endophyticus* gen. nov., sp. nov., an endophytic actinobacterium isolated from a surface-sterilized stem of *Jatropha curcas* L. *Int J Syst Evol Microbiol* **63**: 1241-1248.
- Mahadevan B, Crawford DL (1997). Properties of the chitinase of the antifungal biocontrol agent *Streptomyces lydicus* WYEC108. *Enzyme Microb Technol* **20**: 489-493.
- Manulis S, Shafrir H, Epstein E, Lichter A, Barash I (1994). Biosynthesis of indole-3-acetic acid via the indole-3-acetamide pathway in *Streptomyces* spp. *Microbiology* **140**: 1045-1050.
- Marchesi JR, Ravel J (2015). The vocabulary of microbiome research: a proposal. *Microbiome* **3**: 31.
- Marfetan JA, Romero A, Folgarait PJ (2015). Pathogenic interaction between *Escovopsis weberi* and *Leucoagaricus* sp.: Mechanisms involved and virulence levels. *Fungal Ecol* **17**: 52-61.
- Mark GL, Dow JM, Kiely PD, Higgins H, Haynes J, Baysse C *et al* (2005). Transcriptome profiling of bacterial responses to root exudates identifies genes involved in microbe-plant interactions. *Proc Natl Acad Sci U S A* **102**: 17454-17459.
- Marsh SE, Poulsen M, Pinto-Tomás A, Currie CR (2014). Interaction between workers during a short time window is required for bacterial symbiont transmission in *Acromyrmex* leaf-cutting ants. *PloS one* **9**: e103269.

- Martin MM (1970). The biochemical basis of the fungus-attine ant symbiosis. *Science* **169**: 16-20.
- Martin S, Drijfhout F (2009). A review of ant cuticular hydrocarbons. *J Chem Ecol* **35**: 1151-1161.
- Martin-Platero AM, Valdivia E, Ruiz-Rodriguez M, Soler JJ, Martin-Vivaldi M, Maqueda M *et al* (2006). Characterization of antimicrobial substances produced by *Enterococcus faecalis* MRR 10-3, isolated from the uropygial gland of the hoopoe (*Upupa epops*). *Appl Environ Microbiol* **72**: 4245-4249.
- Martin-Vivaldi M, Pena A, Peralta-Sanchez JM, Sanchez L, Ananou S, Ruiz-Rodriguez M *et al* (2010). Antimicrobial chemicals in hoopoe preen secretions are produced by symbiotic bacteria. *Proc Biol Sci* **277**: 123-130.
- Matamoros S, Gras-Leguen C, Le Vacon F, Potel G, de La Cochetiere MF (2013). Development of intestinal microbiota in infants and its impact on health. *Trends Microbiol* **21**: 167-173.
- Mateus ID, Masclaux FG, Aletti C, Rojas EC, Savary R, Dupuis C *et al* (2019). Dual RNA-seq reveals large-scale non-conserved genotype x genotype-specific genetic reprogramming and molecular crosstalk in the mycorrhizal symbiosis. *ISME J*.
- Matsukawa E, Nakagawa Y, Iimura Y, Hayakawa M (2007). Stimulatory effect of indole-3-acetic acid on aerial mycelium formation and antibiotic production in *Streptomyces* spp. *Actinomycetologica* **21**: 32-39.
- Mattes TE, Coleman NV, Spain JC, Gossett JM (2005). Physiological and molecular genetic analyses of vinyl chloride and ethene biodegradation in *Nocardioides* sp. strain JS614. *Arch Microbiol* **183**: 95-106.
- McLeod MP, Warren RL, Hsiao WW, Araki N, Myhre M, Fernandes C *et al* (2006). The complete genome of *Rhodococcus* sp. RHA1 provides insights into a catabolic powerhouse. *Proc Natl Acad Sci U S A* **103**: 15582-15587.
- Mendes R, Kruijt M, de Bruijn I, Dekkers E, van der Voort M, Schneider JH *et al* (2011). Deciphering the rhizosphere microbiome for disease-suppressive bacteria. *Science* **332**: 1097-1100.
- Mendes R, Garbeva P, Raaijmakers JM (2013). The rhizosphere microbiome: significance of plant beneficial, plant pathogenic, and human pathogenic microorganisms. *FEMS Microbiol Rev* **37**: 634-663.
- Mercado-Blanco J, Bakker PA (2007). Interactions between plants and beneficial *Pseudomonas* spp.: exploiting bacterial traits for crop protection. *Antonie Van Leeuwenhoek* **92**: 367-389.

- Miller IJ, Chevrette MG, Kwan JC (2017). Interpreting Microbial Biosynthesis in the Genomic Age: Biological and Practical Considerations. *Mar Drugs* **15**.
- Mishina TE, Zeier J (2007). Pathogen-associated molecular pattern recognition rather than development of tissue necrosis contributes to bacterial induction of systemic acquired resistance in *Arabidopsis*. *Plant J* **50**: 500-513.
- Mizrahi I, Jami E (2018). Review: The compositional variation of the rumen microbiome and its effect on host performance and methane emission. *Animal* **12**: s220-s232.
- Moeller CH, Mudd JB (1982). Localization of filipin-sterol complexes in the membranes of *Beta vulgaris* roots and *Spinacia oleracea* chloroplasts. *Plant Physiol* **70**: 1554-1561.
- Moriya Y, Itoh M, Okuda S, Yoshizawa AC, Kanehisa M (2007). KAAS: an automatic genome annotation and pathway reconstruction server. *Nucleic Acids Res* **35**: W182-185.
- Mortazavi A, Williams BA, McCue K, Schaeffer L, Wold B (2008). Mapping and quantifying mammalian transcriptomes by RNA-Seq. *Nat Methods* **5**: 621-628.
- Mueller UG, Rehner SA, Schultz TR (1998). The evolution of agriculture in ants. *Science* **281**: 2034-2038.
- Mueller UG, Gerardo NM, Aanen DK, Six DL, Schultz TR (2005). The evolution of agriculture in insects. *Annu Rev Ecol Evol Syst* **36**: 563-595.
- Mueller UG, Dash D, Rabeling C, Rodrigues A (2008). Coevolution between attine ants and actinomycete bacteria: a reevaluation. *Evolution* **62**: 2894-2912.
- Mueller UG, Ishak H, Lee JC, Sen R, Gutell RR (2010). Placement of attine ant-associated *Pseudonocardia* in a global *Pseudonocardia* phylogeny (Pseudonocardiaceae, Actinomycetales): a test of two symbiont-association models. *Antonie Van Leeuwenhoek* **98**: 195-212.
- Musat N, Musat F, Weber PK, Pett-Ridge J (2016). Tracking microbial interactions with NanoSIMS. *Curr Opin Biotechnol* **41**: 114-121.
- Muyzer G, de Waal EC, Uitterlinden AG (1993). Profiling of complex microbial populations by denaturing gradient gel electrophoresis analysis of polymerase chain reaction-amplified genes coding for 16S rRNA. *Appl Environ Microbiol* **59**: 695-700.
- Napflin K, Schmid-Hempel P (2018). Host effects on microbiota community assembly. *J Anim Ecol* **87**: 331-340.
- Neal AL, Ahmad S, Gordon-Weeks R, Ton J (2012). Benzoxazinoids in root exudates of maize attract *Pseudomonas putida* to the rhizosphere. *PLoS One* **7**: e35498.
- Nelson EB (2018). The seed microbiome: Origins, interactions, and impacts. *Plant and Soil* **422**: 7-34.

- Neufeld JD, Vohra J, Dumont MG, Lueders T, Manefield M, Friedrich MW *et al* (2007). DNA stable-isotope probing. *Nat Protoc* **2**: 860-866.
- Newitt JT, Prudence SMM, Hutchings MI, Worsley SF (2019). Biocontrol of cereal crop diseases using streptomycetes. *Pathogens* **8**.
- Nordlund I, Powlowski J, Shingler V (1990). Complete nucleotide sequence and polypeptide analysis of multicomponent phenol hydroxylase from *Pseudomonas* sp. strain CF600. *J Bacteriol* **172**: 6826-6833.
- Nupur LN, Vats A, Dhanda SK, Raghava GP, Pinnaka AK, Kumar A (2016). ProCarDB: a database of bacterial carotenoids. *BMC Microbiol* **16**: 96.
- Nygaard S, Zhang G, Schiott M, Li C, Wurm Y, Hu H *et al* (2011). The genome of the leaf-cutting ant *Acromyrmex echinatior* suggests key adaptations to advanced social life and fungus farming. *Genome Res* **21**: 1339-1348.
- Nygaard S, Hu H, Li C, Schiott M, Chen Z, Yang Z *et al* (2016). Reciprocal genomic evolution in the ant-fungus agricultural symbiosis. *Nat Commun* **7**: 12233.
- O'Callaghan M (2016). Microbial inoculation of seed for improved crop performance: issues and opportunities. *Appl Microbiol Biotechnol* **100**: 5729-5746.
- Oh D-C, Poulsen M, Currie CR, Clardy J (2009). Dentigerumycin: a bacterial mediator of an ant-fungus symbiosis. *Nat Chem Biol* **5**: 391-393.
- Onaka H, Mori Y, Igarashi Y, Furumai T (2011). Mycolic acid-containing bacteria induce natural-product biosynthesis in *Streptomyces* species. *Appl Environ Microbiol* **77**: 400-406.
- Paget MS, Chamberlin L, Atrih A, Foster SJ, Buttner MJ (1999). Evidence that the extracytoplasmic function sigma factor sigmaE is required for normal cell wall structure in *Streptomyces coelicolor* A3(2). *J Bacteriol* **181**: 204-211.
- Palaniyandi SA, Damodharan K, Yang SH, Suh JW (2014). *Streptomyces* sp. strain PGPA39 alleviates salt stress and promotes growth of 'Micro Tom' tomato plants. *J Appl Microbiol* **117**: 766-773.
- Patel JK, Madaan S, Archana G (2018). Antibiotic producing endophytic *Streptomyces* spp. colonize above-ground plant parts and promote shoot growth in multiple healthy and pathogen-challenged cereal crops. *Microbiol Res* **215**: 36-45.
- Payero TD, Vicente CM, Rumbero A, Barreales EG, Santos-Aberturas J, de Pedro A *et al* (2015). Functional analysis of filipin tailoring genes from *Streptomyces filipinensis* reveals alternative routes in filipin III biosynthesis and yields bioactive derivatives. *Microb Cell Fact* **14**: 114.

- Pedrini N, Ortiz-Urquiza A, Huarte-Bonnet C, Zhang S, Keyhani NO (2013). Targeting of insect epicuticular lipids by the entomopathogenic fungus *Beauveria bassiana*: hydrocarbon oxidation within the context of a host-pathogen interaction. *Front Microbiol* **4**: 24.
- Pellon A, Ramirez-Garcia A, Buldain I, Antoran A, Martin-Souto L, Rementeria A *et al* (2018). Pathobiology of *Lomentospora prolificans*: could this species serve as a model of primary antifungal resistance? *Int J Antimicrob Agents* **51**: 10-15.
- Peraud O, Biggs JS, Huguen RW, Light AR, Concepcion GP, Olivera BM *et al* (2009). Microhabitats within venomous cone snails contain diverse actinobacteria. *Appl Environ Microbiol* **75**: 6820-6826.
- Philippot L, Raaijmakers JM, Lemanceau P, van der Putten WH (2013). Going back to the roots: the microbial ecology of the rhizosphere. *Nat Rev Microbiol* **11**: 789-799.
- Pieterse CM, Van der Does D, Zamioudis C, Leon-Reyes A, Van Wees SC (2012). Hormonal modulation of plant immunity. *Annu Rev Cell Dev Biol* **28**: 489-521.
- Pieterse CM, Zamioudis C, Berendsen RL, Weller DM, Van Wees SC, Bakker PA (2014). Induced systemic resistance by beneficial microbes. *Annu Rev Phytopathol* **52**: 347-375.
- Pimentel D, McLaughlin L, Zepp A, Lakitan B, Kraus T, Kleinman P *et al* (1993). Environmental and economic effects of reducing pesticide use in agriculture. *Agriculture, Ecosystems & Environment* **46**: 273-288.
- Poole RK, Hughes MN (2000). New functions for the ancient globin family: bacterial responses to nitric oxide and nitrosative stress. *Mol Microbiol* **36**: 775-783.
- Poulsen M, Bot ANM, Currie CR, Nielsen MG, Boomsma JJ (2003). Within-colony transmission and the cost of a mutualistic bacterium in the leaf-cutting ant *Acromyrmex octospinosus*. *Funct Ecol* **17**: 260-269.
- Poulsen M, Cafaro M, Boomsma JJ, Currie CR (2005). Specificity of the mutualistic association between actinomycete bacteria and two sympatric species of *Acromyrmex* leaf-cutting ants. *Mol Ecol* **14**: 3597-3604.
- Preston GM (2004). Plant perceptions of plant growth-promoting *Pseudomonas*. *Philos Trans R Soc Lond B Biol Sci* **359**: 907-918.
- Promnuan Y, Kudo T, Chantawannakul P (2009). Actinomycetes isolated from beehives in Thailand. *World J Microbiol Biotechnol* **25**: 1685-1689.
- Promnuan Y, Kudo T, Ohkuma M, Chantawannakul P (2013). *Streptomyces Chiangmaiensis* sp. nov. and *Streptomyces lannensis* sp. nov., isolated from the South-East Asian stingless bee (*Tetragonilla collina*). *Int J Syst Evol Microbiol* **63**: 1896-1901.

- Quecine MC, Araujo WL, Marcon J, Gai CS, Azevedo JL, Pizzirani-Kleiner AA (2008). Chitinolytic activity of endophytic *Streptomyces* and potential for biocontrol. *Lett Appl Microbiol* **47**: 486-491.
- Quiza L, St-Arnaud M, Yergeau E (2015). Harnessing phytomicrobiome signaling for rhizosphere microbiome engineering. *Front Plant Sci* **6**: 507.
- R Core Team (2017). R: A language and environment for statistical computing. R Foundation for Statistical Computing, Vienna, Austria. <https://www.R-project.org/>.
- Radajewski S, Ineson P, Parekh NR, Murrell JC (2000). Stable-isotope probing as a tool in microbial ecology. *Nature* **403**: 646-649.
- Raina JB, Tapiolas D, Willis BL, Bourne DG (2009). Coral-associated bacteria and their role in the biogeochemical cycling of sulfur. *Appl Environ Microbiol* **75**: 3492-3501.
- Raina JB, Dinsdale EA, Willis BL, Bourne DG (2010). Do the organic sulfur compounds DMSP and DMS drive coral microbial associations? *Trends Microbiol* **18**: 101-108.
- Raina JB, Tapiolas DM, Foret S, Lutz A, Abrego D, Ceh J *et al* (2013). DMSP biosynthesis by an animal and its role in coral thermal stress response. *Nature* **502**: 677-680.
- Raina JB, Tapiolas D, Motti CA, Foret S, Seemann T, Tebben J *et al* (2016). Isolation of an antimicrobial compound produced by bacteria associated with reef-building corals. *PeerJ* **4**: e2275.
- Rangel-Castro JI, Killham K, Ostle N, Nicol GW, Anderson IC, Scrimgeour CM *et al* (2005). Stable isotope probing analysis of the influence of liming on root exudate utilization by soil microorganisms. *Environ Microbiol* **7**: 828-838.
- Remans R, Spaepen S, Vanderleyden J (2006). Auxin signaling in plant defense. *Science* **313**: 171.
- Rey T, Dumas B (2017). Plenty Is No Plague: *Streptomyces* Symbiosis with Crops. *Trends Plant Sci* **22**: 30-37.
- Reynolds HT, Currie CR (2004). Pathogenicity of *Escovopsis weberi*: The parasite of the attine ant-microbe symbiosis directly consumes the ant-cultivated fungus. *Mycologia* **96**: 955-959.
- Richter TK, Hughes CC, Moore BS (2015). Sioxanthin, a novel glycosylated carotenoid, reveals an unusual subclustered biosynthetic pathway. *Environ Microbiol* **17**: 2158-2171.
- Riley MA, Gordon DM (1999). The ecological role of bacteriocins in bacterial competition. *Trends Microbiol* **7**: 129-133.
- Ruby EG (1996). Lessons from a cooperative, bacterial-animal association: The *Vibrio fischeri*-*Euprymna scolopes* light organ symbiosis. *Annu Rev Microbiol* **50**: 591-624.

- Rudrappa T, Czymmek KJ, Pare PW, Bais HP (2008). Root-secreted malic acid recruits beneficial soil bacteria. *Plant Physiol* **148**: 1547-1556.
- Ruiz-Gonzalez MX, Male PJ, Leroy C, Dejean A, Gryta H, Jargeat P *et al* (2011). Specific, non-nutritional association between an ascomycete fungus and *Allomerus* plant-ants. *Biol Lett* **7**: 475-479.
- Rungin S, Indananda C, Suttiviriya P, Kruasuwan W, Jaemsaeng R, Thamchaipenet A (2012a). Plant growth enhancing effects by a siderophore-producing endophytic streptomycete isolated from a Thai jasmine rice plant (*Oryza sativa* L. cv. KDML105). *Antonie Van Leeuwenhoek* **102**: 463-472.
- Rungin S, Indananda C, Suttiviriya P, Kruasuwan W, Jaemsaeng R, Thamchaipenet A (2012b). Plant growth enhancing effects by a siderophore-producing endophytic streptomycete isolated from a Thai jasmine rice plant (*Oryza sativa* L. cv. KDML105). *Antonie van Leeuwenhoek* **102**: 463-472.
- Ryan PR, Dessaux Y, Thomashow LS, Weller DM (2009). Rhizosphere engineering and management for sustainable agriculture. *Plant and Soil* **321**: 363-383.
- Sanders JG, Powell S, Kronauer DJ, Vasconcelos HL, Frederickson ME, Pierce NE (2014). Stability and phylogenetic correlation in gut microbiota: lessons from ants and apes. *Mol Ecol* **23**: 1268-1283.
- Santhanam R, Groten K, Meldau DG, Baldwin IT (2014). Analysis of plant-bacteria interactions in their native habitat: bacterial communities associated with wild tobacco are independent of endogenous jasmonic acid levels and developmental stages. *PLoS One* **9**: e94710.
- Santhanam R, Baldwin IT, Groten K (2015). In wild tobacco, *Nicotiana attenuata*, variation among bacterial communities of isogenic plants is mainly shaped by the local soil microbiota independently of the plants' capacity to produce jasmonic acid. *Commun Integr Biol* **8**: e1017160.
- Sarwar A, Latif Z, Zhang S, Hao J, Bechthold A (2019). A Potential Biocontrol Agent *Streptomyces violaceusniger* AC12AB for Managing Potato Common Scab. *Front Microbiol* **10**: 202.
- Scherlach K, Hertweck C (2009). Triggering cryptic natural product biosynthesis in microorganisms. *Org Biomol Chem* **7**: 1753-1760.
- Scheuring I, Yu DW (2012). How to assemble a beneficial microbiome in three easy steps. *Ecol Lett* **15**: 1300-1307.
- Schiøtt M, Rogowska-Wrzesinska A, Roepstorff P, Boomsma JJ (2010). Leaf-cutting ant fungi produce cell wall degrading pectinase complexes reminiscent of phytopathogenic fungi. *BMC Biol* **8**: 156.

- Schlaeppli K, Dombrowski N, Oter RG, Ver Loren van Themaat E, Schulze-Lefert P (2014). Quantitative divergence of the bacterial root microbiota in *Arabidopsis thaliana* relatives. *Proc Natl Acad Sci U S A* **111**: 585-592.
- Schoenian I, Spitteller M, Ghaste M, Wirth R, Herz H, Spitteller D (2011). Chemical basis of the synergism and antagonism in microbial communities in the nests of leaf-cutting ants. *Proc Natl Acad Sci U S A* **108**: 1955-1960.
- Schrempf H (2001). Recognition and degradation of chitin by streptomycetes. *Antonie Van Leeuwenhoek* **79**: 285-289.
- Schrey SD, Tarkka MT (2008). Friends and foes: streptomycetes as modulators of plant disease and symbiosis. *Antonie Van Leeuwenhoek* **94**: 11-19.
- Schultz TR, Brady SG (2008). Major evolutionary transitions in ant agriculture. *Proc Natl Acad Sci U S A* **105**: 5435-5440.
- Scott JJ, Oh DC, Yuceer MC, Klepzig KD, Clardy J, Currie CR (2008). Bacterial protection of beetle-fungus mutualism. *Science* **322**: 63.
- Seipke RF, Barke J, Brearley C, Hill L, Douglas WY, Goss RJ *et al* (2011a). A single *Streptomyces* symbiont makes multiple antifungals to support the fungus farming ant *Acromyrmex octospinosus*. *PLoS One* **6**: e22028.
- Seipke RF, Crossman L, Drou N, Heavens D, Bibb MJ, Caccamo M *et al* (2011b). Draft Genome Sequence of *Streptomyces* Strain S4, a Symbiont of the Leaf-Cutting Ant *Acromyrmex octospinosus*. *JBacteriol* **193**: 4270-4271.
- Seipke RF, Barke J, Ruiz-Gonzalez MX, Orivel J, Yu DW, Hutchings MI (2012a). Fungus-growing *Allomerus* ants are associated with antibiotic-producing actinobacteria. *Antonie Van Leeuwenhoek* **101**: 443-447.
- Seipke RF, Kaltenpoth M, Hutchings MI (2012b). *Streptomyces* as symbionts: an emerging and widespread theme? *FEMS Microbiol Rev* **36**: 862-876.
- Selosse MA, Bessis A, Pozo MJ (2014). Microbial priming of plant and animal immunity: symbionts as developmental signals. *Trends Microbiol* **22**: 607-613.
- Sen R, Ishak HD, Estrada D, Dowd SE, Hong E, Mueller UG (2009). Generalized antifungal activity and 454-screening of *Pseudonocardia* and *Amycolatopsis* bacteria in nests of fungus-growing ants. *Proc Natl Acad Sci USA* **106**: 17805.
- Shaharoon B, Arshad M, Zahir ZA (2006). Effect of plant growth promoting rhizobacteria containing ACC-deaminase on maize (*Zea mays* L.) growth under axenic conditions and on nodulation in mung bean (*Vigna radiata* L.). *Lett Appl Microbiol* **42**: 155-159.

- Shahzad R, Khan AL, Bilal S, Asaf S, Lee I-J (2018). What is there in seeds? Vertically transmitted endophytic resources for sustainable improvement in plant growth. *Front Plant Sci* **9**: 24.
- Sharma SB, Sayyed RZ, Trivedi MH, Gobi TA (2013). Phosphate solubilizing microbes: sustainable approach for managing phosphorus deficiency in agricultural soils. *Springerplus* **2**: 587.
- Sharp JO, Sales CM, LeBlanc JC, Liu J, Wood TK, Eltis LD *et al* (2007). An inducible propane monooxygenase is responsible for nitrosodimethylamine degradation by *Rhodococcus* sp. Strain RHA1. *Appl Environ Microbiol* **73**: 6930.
- Shetty PR, Buddana SK, Tatipamula VB, Naga YV, Ahmad J (2014). Production of polypeptide antibiotic from *Streptomyces parvulus* and its antibacterial activity. *Braz J Microbiol* **45**: 303-312.
- Shields MS, Reagin MJ, Gerger RR, Campbell R, Somerville C (1995). TOM, a new aromatic degradative plasmid from *Burkholderia (Pseudomonas) cepacia* G4. *Appl Environ Microbiol* **61**: 1352-1356.
- Shih HD, Liu YC, Hsu FL, Mulabagal V, Dodda R, Huang JW (2003). Fungichromin: a substance from *Streptomyces padanus* with inhibitory effects on *Rhizoctonia solani*. *J Agric Food Chem* **51**: 95-99.
- Shimizu M, Igarashi Y, Furumai T, Onaka H, Kunoh H (2004). Identification of endophytic *Streptomyces* sp. R-5 and analysis of its antimicrobial metabolites. *J Gen Plant Pathol* **70**: 66-68.
- Siedenburg G, Jendrossek D (2011). Squalene-hopene cyclases. *Appl Environ Microbiol* **77**: 3905-3915.
- Sit CS, Ruzzini AC, Van Arnem EB, Ramadhar TR, Currie CR, Clardy J (2015). Variable genetic architectures produce virtually identical molecules in bacterial symbionts of fungus-growing ants. *Proc Natl Acad Sci U S A* **112**: 13150-13154.
- Smith TJ, Lloyd JS, Gallagher SC, Fosdike WL, Murrell JC, Dalton H (1999). Heterologous expression of alkene monooxygenase from *Rhodococcus rhodochrous* B-276. *Eur J Biochem* **260**: 446-452.
- Spadaro D, Gullino ML (2005). Improving the efficacy of biocontrol agents against soilborne pathogens. *Crop Protection* **24**: 601-613.
- Stanier RY (1942). Agar-decomposing strains of the *Actinomyces coelicolor* species-group. *J Bacteriol* **44**: 555-570.
- Strobel GA (2003). Endophytes as sources of bioactive products. *Microbes Infect* **5**: 535-544.

- Sugawara M, Tsukui T, Kaneko T, Ohtsubo Y, Sato S, Nagata Y *et al* (2017). Complete Genome Sequence of *Bradyrhizobium diazoefficiens* USDA 122, a Nitrogen-Fixing Soybean Symbiont. *Genome Announc* **5**.
- Sun J, Kelemen GH, Fernandez-Abalos JM, Bibb MJ (1999). Green fluorescent protein as a reporter for spatial and temporal gene expression in *Streptomyces coelicolor* A3(2). *Microbiology* **145 (Pt 9)**: 2221-2227.
- Tahvonen R, Hannukkala A, Avikainen H (1995). Effect of seed dressing treatment of *Streptomyces griseoviridis* on barley and spring wheat in field experiments. *Agr Food Sci* **4**: 419-427.
- Tahvonen Rk (1982). The suppressiveness of Finnish light coloured *Sphagnum* peat. *J Scient Agri Soc Finland* **54**: 345-356.
- Tamas I, Dedysh SN, Liesack W, Stott MB, Alam M, Murrell JC *et al* (2010). Complete genome sequence of *Beijerinckia indica* subsp. *indica*. *J Bacteriol* **192**: 4532-4533.
- Tannock GW, Lawley B, Munro K, Sims IM, Lee J, Butts CA *et al* (2014). RNA-stable-isotope probing shows utilization of carbon from inulin by specific bacterial populations in the rat large bowel. *Appl Environ Microbiol* **80**: 2240-2247.
- Temuujin U, Chi WJ, Chang YK, Hong SK (2012). Identification and biochemical characterization of Sco3487 from *Streptomyces coelicolor* A3(2), an exo- and endo-type beta-agarase-producing neoagarobiose. *J Bacteriol* **194**: 142-149.
- Thiemer B, Andreesen JR, Schrader T (2003). Cloning and characterization of a gene cluster involved in tetrahydrofuran degradation in *Pseudonocardia* sp. strain K1. *Arch Microbiol* **179**: 266-277.
- Timmis KN (2010). *Handbook of Hydrocarbon and Lipid Microbiology*. Springer-Verlag Berlin Heidelberg.
- Tokala RK, Strap JL, Jung CM, Crawford DL, Salove MH, Deobald LA *et al* (2002). Novel plant-microbe rhizosphere interaction involving *Streptomyces lydicus* WYEC108 and the pea plant (*Pisum sativum*). *Appl Environ Microbiol* **68**: 2161-2171.
- Tremaroli V, Bäckhed F (2012). Functional interactions between the gut microbiota and host metabolism. *Nature* **489**: 242.
- Uksa M, Buegger F, Gschwendtner S, Lueders T, Kublik S, Kautz T *et al* (2017). Bacteria utilizing plant-derived carbon in the rhizosphere of *Triticum aestivum* change in different depths of an arable soil. *Environ Microbiol Rep* **9**: 729-741.
- Umezawa S, Tanaka Y, Ooka M, Shiotsu S (1958). A new antifungal antibiotic, pentamycin. *J Antibiot (Tokyo)* **11**: 26-29.
- Valdes-Stauber N, Scherer S (1994). Isolation and characterization of Linocin M18, a bacteriocin produced by *Brevibacterium linens*. *Appl Environ Microbiol* **60**: 3809-3814.

- Van Arnam EB, Ruzzini AC, Sit CS, Horn H, Pinto-Tomas AA, Currie CR *et al* (2016). Selvamycin, an atypical antifungal polyene from two alternative genomic contexts. *Proc Natl Acad Sci U S A* **113**: 12940-12945.
- van der Meij A, Worsley SF, Hutchings MI, van Wezel GP (2017). Chemical ecology of antibiotic production by actinomycetes. *FEMS Microbiol Rev* **41**: 392-416.
- van der Meij A, Willemse J, Schneijderberg MA, Geurts R, Raaijmakers JM, van Wezel GP (2018). Inter- and intracellular colonization of *Arabidopsis* roots by endophytic actinobacteria and the impact of plant hormones on their antimicrobial activity. *Antonie Van Leeuwenhoek* **111**: 679-690.
- Van Minh N, Woo EE, Lee GS, Ki DW, Lee IK, Lee SY *et al* (2017). Control efficacy of *Streptomyces* sp. A501 against Ginseng damping-off and its antifungal substance. *Mycobiology* **45**: 44-47.
- Van Wees SC, Van der Ent S, Pieterse CM (2008). Plant immune responses triggered by beneficial microbes. *Curr Opin Plant Biol* **11**: 443-448.
- Varanda-Haifig SS, Albarici TR, Nunes PH, Haifig I, Vieira PC, Rodrigues A (2017). Nature of the interactions between hypocrealean fungi and the mutualistic fungus of leaf-cutter ants. *Antonie Van Leeuwenhoek* **110**: 593-605.
- Vardar G, Wood TK (2005). Protein engineering of toluene-o-xylene monooxygenase from *Pseudomonas stutzeri* OX1 for enhanced chlorinated ethene degradation and o-xylene oxidation. *Appl Microbiol Biotechnol* **68**: 510-517.
- Viaene T, Langendries S, Beirinckx S, Maes M, Goormachtig S (2016). *Streptomyces* as a plant's best friend? *FEMS Microbiology Ecology*: fiw119.
- Vieira AS, Morgan ED, Drijfhout FP, Camargo-Mathias MI (2012). Chemical composition of metapleural gland secretions of fungus-growing and non-fungus-growing ants. *J Chem Ecol* **38**: 1289-1297.
- Wan M, Li G, Zhang J, Jiang D, Huang H-C (2008). Effect of volatile substances of *Streptomyces platensis* F-1 on control of plant fungal diseases. *Biol Control* **46**: 552-559.
- Wang C, Wang Z, Qiao X, Li Z, Li F, Chen M *et al* (2013a). Antifungal activity of volatile organic compounds from *Streptomyces alboflavus* TD-1. *FEMS Microbiol Lett* **341**: 45-51.
- Wang D, Yuan J, Gu S, Shi Q (2013b). Influence of fungal elicitors on biosynthesis of natamycin by *Streptomyces natalensis* HW-2. *Appl Microbiol Biotechnol* **97**: 5527-5534.
- Wang H, Fewer DP, Holm L, Rouhiainen L, Sivonen K (2014). Atlas of nonribosomal peptide and polyketide biosynthetic pathways reveals common occurrence of nonmodular enzymes. *Proc Natl Acad Sci U S A* **111**: 9259-9264.

Wang Y, Dufour YS, Carlson HK, Donohue TJ, Marletta MA, Ruby EG (2010a). H-NOX-mediated nitric oxide sensing modulates symbiotic colonization by *Vibrio fischeri*. *Proc Natl Acad Sci U S A* **107**: 8375-8380.

Wang Y, Dunn AK, Wilneff J, McFall-Ngai MJ, Spiro S, Ruby EG (2010b). *Vibrio fischeri* flavohaemoglobin protects against nitric oxide during initiation of the squid-*Vibrio* symbiosis. *Mol Microbiol* **78**: 903-915.

Wang Y, Huang WE, Cui L, Wagner M (2016). Single cell stable isotope probing in microbiology using Raman microspectroscopy. *Curr Opin Biotechnol* **41**: 34-42.

Wang YL, Ruby EG (2011). The roles of NO in microbial symbioses. *Cell Microbiol* **13**: 518-526.

Watrous JD, Alexandrov T, Dorrestein PC (2011). The evolving field of imaging mass spectrometry and its impact on future biological research. *J Mass Spectrom* **46**: 209-222.

Watrous JD, Dorrestein PC (2011). Imaging mass spectrometry in microbiology. *Nature Rev Microbiol* **9**: 683-694.

Weber T, Blin K, Duddela S, Krug D, Kim HU, Brucoleri R *et al* (2015). antiSMASH 3.0-a comprehensive resource for the genome mining of biosynthetic gene clusters. *Nucleic Acids Res* **43**: W237-243.

Weinert N, Piceno Y, Ding G-C, Meincke R, Heuer H, Berg G *et al* (2011). PhyloChip hybridization uncovered an enormous bacterial diversity in the rhizosphere of different potato cultivars: many common and few cultivar-dependent taxa. *FEMS Microbiol Ecol* **75**: 497-506.

Weller DM, Raaijmakers JM, Gardener BB, Thomashow LS (2002). Microbial populations responsible for specific soil suppressiveness to plant pathogens. *Annu Rev Phytopathol* **40**: 309-348.

Wellington EM, Cresswell N, Saunders VA (1990). Growth and survival of streptomycete inoculants and extent of plasmid transfer in sterile and nonsterile soil. *Appl Environ Microbiol* **56**: 1413-1419.

Westermann AJ, Forstner KU, Amman F, Barquist L, Chao Y, Schulte LN *et al* (2016). Dual RNA-seq unveils noncoding RNA functions in host-pathogen interactions. *Nature* **529**: 496-501.

Westermann AJ, Venturini E, Sellin ME, Forstner KU, Hardt WD, Vogel J (2019). The major RNA-binding protein ProQ impacts virulence gene expression in *Salmonella enterica* serovar Typhimurium. *MBio* **10**.

Weyl EG, Frederickson ME, Yu DW, Pierce NE (2010). Economic contract theory tests models of mutualism. *Proc Natl Acad Sci U S A* **107**: 15712-15716.

- Wheatley RE (2002). The consequences of volatile organic compound mediated bacterial and fungal interactions. *Antonie Van Leeuwenhoek* **81**: 357-364.
- Whipps JM (1990). Carbon economy. In: Lynch JM (ed). *The Rhizosphere*. John Wiley & Sons Ltd: Essex, UK. pp 59-97.
- Wildermuth MC, Dewdney J, Wu G, Ausubel FM (2001). Isochorismate synthase is required to synthesize salicylic acid for plant defence. *Nature* **414**: 562-565.
- Worsley SF, Innocent TM, Heine D, Murrell JC, Yu DW, Wilkinson B *et al* (2018). Symbiotic partnerships and their chemical interactions in the leafcutter ants (Hymenoptera: Formicidae). *Myrmecological News* **27**: 59-74.
- Wu ZM, Yang Y, Li KT (2019). Antagonistic activity of a novel antifungal mycin N2 from *Streptomyces* sp. N2 and its biocontrol efficacy against *Rhizoctonia solani*. *FEMS Microbiol Lett* **366**.
- Xiao K, Kinkel LL, Samac DA (2002). Biological control of *Phytophthora* root rots on alfalfa and soybean with *Streptomyces*. *Biol Control* **23**: 285-295.
- Xiong ZQ, Zhang ZP, Li JH, Wei SJ, Tu GQ (2012). Characterization of *Streptomyces padanus* JAU4234, a producer of actinomycin X(2), fungichromin, and a new polyene macrolide antibiotic. *Appl Environ Microbiol* **78**: 589-592.
- Yamada Y, Kuzuyama T, Komatsu M, Shin-Ya K, Omura S, Cane DE *et al* (2015). Terpene synthases are widely distributed in bacteria. *Proc Natl Acad Sci U S A* **112**: 857-862.
- Yang J, Kloepper JW, Ryu CM (2009). Rhizosphere bacteria help plants tolerate abiotic stress. *Trends Plant Sci* **14**: 1-4.
- Yek SH, Boomsma JJ, Poulsen M (2012). Towards a better understanding of the evolution of specialized parasites of fungus-growing ant crops. *Psyche* **ID23939**.
- Yu Y, Lee C, Kim J, Hwang S (2005). Group-specific primer and probe sets to detect methanogenic communities using quantitative real-time polymerase chain reaction. *Biotechnol Bioeng* **89**: 670-679.
- Yuan J, Zhao J, Wen T, Zhao M, Li R, Goossens P *et al* (2018). Root exudates drive the soil-borne legacy of aboveground pathogen infection. *Microbiome* **6**: 156.
- Yuan WM, Crawford DL (1995). Characterization of *Streptomyces lydicus* WYEC108 as a potential biocontrol agent against fungal root and seed rots. *Appl Environ Microbiol* **61**: 3119-3128.
- Zhalnina K, Louie KB, Hao Z, Mansoori N, da Rocha UN, Shi S *et al* (2018). Dynamic root exudate chemistry and microbial substrate preferences drive patterns in rhizosphere microbial community assembly. *Nat Microbiol* **3**: 470-480.

Zhang S, Vallad GE, White TL, Huang C-H (2011). Evaluation of microbial products for management of powdery mildew on summer squash and cantaloupe in Florida. *Plant Disease* **95**: 461-468.

Zhao CZ, Huang J, Gyaneshwar P, Zhao D (2017). *Rhizobium* sp. IRBG74 alters *Arabidopsis* root development by affecting auxin signaling. *Front Microbiol* **8**: 2556.

Zhou N, Tootle TL, Tsui F, Klessig DF, Glazebrook J (1998). PAD4 functions upstream from salicylic acid to control defense responses in *Arabidopsis*. *Plant Cell* **10**: 1021-1030.

Zhou S, Song L, Masschelein J, Sumang FAM, Papa IA, Zulaybar TO *et al* (2019). Pentamycin biosynthesis in Philippine *Streptomyces* sp. S816: cytochrome P450-catalyzed installation of the C-14 hydroxyl group. *ACS Chem Biol*.

Supplementary Information

S1 Amino acid sequences of alkane monooxygenases used for phylogenetic analysis in Chapter 1

Ae707 *P. octospinosus*: PrmA (Holmes et al 2016)

VSRQSLAKAHQKIQELSWEPQYHEPYMKYGTDYTFKKAQKKDPLKQVLRSYFPMEEEKDH
RVYGAQDGAIRGNMFRQVQERWLEWQKLFSLIPLPEISAARSMPLFHVVPNPPELHNGQ
AIQMIDEVRHSTIQQNLKRLYMNNYIDPAGFNNSLRNFQSDYCGTIGRQFAEGFITGDAI
TAASIYLTIVAETAFTNTLFVAMPAAEAANGDYLLPTVFHHSVQSDSRHISNGYATLLMA
LSDEDNRQLLERDLRYAWWNNHRVVDAAIGTFIEYGTKDRRKDRESYAEMWRRWIYDDYY
RSYLLPLEKYGLVIPHDLVEESWNQIWNKGYVHEVAQFFATGWCANYWRIDGMTDEDFEW
FEYKYPGWYDRYGKWWENYNRLAKPNGHHAIVAEDVDYVYPHRCWTCMVPCLVREDMVVD
KVDGQWRTYCHEVCRWTDAAEFRPVYQGRETPNMGKLVGHREWETLYHGWNWADVVDQDM
GFVRDDGKTLTAQPHLDLDPKKMWTLDHMRRMPHLASPNVILNEMSDSEREFAADYNRQG
PAGRPAPTA

Ae356 *P. octospinosus*: PrmA (Holmes et al 2016)

LAKAHQKIQELSWEPQYHEPYMKYGTDYTFKKAQKKDPLKQVLRSYFPMEEKGRVYGA
QDGAIRGNMFRQVQERWLEWQKLFSLIPLPEISAARSMPLFHVVPNPPELHNGQAIQMI
DEVHRHSTIQQNLKRLYMNNYIDPAGFNNSLRNFQSDYCGTIGRQFAEGFITGDAITAASI
YLTIVAETAFTNTLFVAMPAAEAANGDYLLPTVFHHSVQSDSRHISNGYATLLMALSDDED

NRQLLERDLRYAWWNNHRVVDAAIGTFIEYGTKDRRKDRESYAEMWRRWIYDDYYRSYLL
PLEKYGLVIPHDLVEESWNQIWNKGYVHEVAQFFATGWCANYWRIDGMTDEDFEWFYKY
PGWYDRYGKWWENYNRLAKPNGHHAIVAEDVDYVYPHRCWTCMVPCLAREDMVVDKVDGQ
WRTYCHEVCRWTDAAEFRPVYQGRETPNMGKLVGHREWETLYHGWNWADV IQDMGFVRDD
GKTLTAQPHLDLDPKKMWTLDHMRRMPHLASPNVILNEMSDSREAFVADYNRQGPAGRP
APTDA

Ae263 *P. octospinosus*: PrmA (Holmes et al 2016)

LAKAHQKIQELSWEPQYHEPYMKYGTDYTFKKAQKKDPLKQVLSYFPMEEEEKGHRVYGA
QDGAIRGNMFRQVQERWLEWQKLFLSIPLPEISAARSMPLFHVVPNPELHNGQAIQMI
DEVRHSTIQQLKRLYMNNYIDPAGFNNSLRNFQSDYCGTIGRQFAEGFITGDAITAASI
YLTIVAETAFTNTLFVAMPAAEAANGDYLLPTVFHVSQSDSRHISNGYATLLMALSDED
NRQLLERDLRYAWWNNHRVVDAAIGTFIEYGTKDRRKDRESYAEMWRRWIYDDYYRSYLL
PLEKYGLVIPHDLVEESWNQIWNKGYVHEVAQFFATGWCANYWRIDGMTDEDFEWFYKY
PGWYDRYGKWWENYNRLAKPNGHHAIVAEDVDYVYPHRCWTCMVPCLAREDMVVDKVDGQ
WRTYCHEVCRWTDAAEFRPVYQGRETPNMGKLVGHREWETLYHGWNWADV IQDMGFVRDD
GKTLTAQPHLDLDPKKMWTLDHMRRMPHLASPNVILNEMSDSREAFVADYNRQGPAGRP
APTDA

Ae168 *P. octospinosus*: PrmA (Holmes et al 2016)

LAKAHQKIQELSWEPQYHEPYMKYGTDYTFKKAQKKDPLKQVLSYFPMEEEEKGHRVYGA
QDGAIRGNMFRQVQERWLEWQKLFLSIPLPEISAARSMPLFHVVPNPELHNGQAIQMI
DEVRHSTIQQLKRLYMNNYIDPAGFNNSLRNFQSDYCGTIGRQFAEGFITGDAITAASI
YLTIVAETAFTNTLFVAMPAAEAANGDYLLPTVFHVSQSDSRHISNGYATLLMALSDED
NRQLLERDLRYAWWNNHRVVDAAIGTFIEYGTKDRRKDRESYAEMWRRWIYDDYYRSYLL
PLEKYGLVIPHDLVEESWNQIWNKGYVHEVAQFFATGWCANYWRIDGMTDEDFEWFYKY
PGWYDRYGKWWENYNRLAKPNGHHAIVAEDVDYVYPHRCWTCMVPCLAREDMVVDKVDGQ
WRTYCHEVCRWTDAAEFRPVYQGRETPNMGKLVGHREWETLYHGWNWADV IQDMGFVRDD
GKTLTAQPHLDLDPKKMWTLDHMRRMPHLASPNVILNEMSDSREAFVADYNRQGPAGRP
APTDA

Ae150A *P. octospinosus*: PrmA (Holmes et al 2016)

LAKAHQKIQELSWEPQYHEPYMKYGTDYTFKKAQKKDPLKQVLSYFPMEEEEKGHRVYGA

QDGAIRGNMFRQVQERWLEWQKFLFSIPLPEISAARSMPLFHVVPNPELHNGQAIQMI
DEVRHSTIQQLKRLYMNNYIDPAGFNNSLRNFQSDYCGTIGRQFAEGFITGDAITAASI
YLTIVAETAFTNTLFVAMPAAEAANGDYLLPTVFHVSQSDSRHISNGYATLLMALSDED
NRQLLERDLRYAWWNNHRVVDAAIGTFIEYGTKDRRKDRESYAEMWRRWIYDDYYRSYLL
PLEKYGLVIPHDLVEESWNQIWNKGYVHEVAQFFATGWCANYWRIDGMTDEDFEWFYKY
PGWYDRYGKWWENYNRLAKPNGHHAIVAEDVDYVYPHRCWTCMVPCLAREDMVVDKVDGQ
WRTYCHEVCRWTDAAEFRPVYQGRETPNMGKLVGHREWETLYHGWNWADVIQDMGFVRDD
GKTLTAQPHLDLDPKKMWTLDHMRRMPHLASPNVILNEMSDSREAFVADYNRQGPAGRP
APTDA

Ae706 *P. echinator*: PrmA (Holmes et al 2016)

LAKAHQKIQELSWEPQYHEPYMKYGTDYTFKKAACKDPLKQVLSYFPMEEKDHRYGA
QDGAIRGNMFRQVQERWLEWQKFLFSIPLPEISAARSMPLFHVVPNPELHNGQAIQMI
DEVRHSTIQQLKRLYMNNYIDPAGFNNSLRNFQSDYCGTIGRQFAEGFITGDAITAASI
YLTIVAETAFTNTLFVAMPAAEAANGDYLLPTVFHVSQSDSRHISNGYATLLMALSDED
NRQLLERDLRYAWWNNHRVVDAAIGTFIEYGTKDRRKDRESYAEMWRRWIYDDYYRSYLL
PLEKYGLVIPHDLVEESWNQIWNKGYVHEVAQFFATGWCANYWRIDGMTDTEDFEWFYKY
PGWYDRYGKWWENYNRLAKPNGHHAIVAEDVDYVYPHRCWTCMVPCLVREDMVVDKVDGQ
WRTYCHEVCRWTDAAEFRPVYQGRETPNMGKLVGHREWETLYHGWNWADVIQDMGFVRDD
GKTLTAQPHLDLDPKKMWTLDHMRRMPHLASPNVILNEMSDAEREAFVADYNRQGPGRP
APTDA

Ae717 *P. echinator*: PrmA (Holmes et al 2016)

LAKAHQKIQELSWEPQYHEPYMKYGTDYTFKKAACKDPLKQVLSYFPMEEKDHRYGA
QDGAIRGNMFRQVQERWLEWQKFLFSIPLPEISAARSMPLFHVVPNPELHNGQAIQMI
DEVRHSTIQQLKRLYMNNYIDPAGFNNSLRNFQSDYCGTIGRQFAEGFITGDAITAASI
YLTIVAETAFTNTLFVAMPAAEAANGDYLLPTVFHVSQSDSRHISNGYATLLMALSDED
NRQLLERDLRYAWWNNHRVVDAAIGTFIEYGTKDRRKDRESYAEMWRRWIYDDYYRSYLL
PLEKYGLVIPHDLVEESWNQIWNKGYVHEVAQFFATGWCANYWRIDGMTDTEDFEWFYKY
PGWYDRYGKWWENYNRLAKPNGHHAIVAEDVDYVYPHRCWTCMVPCLVREDMVVDKVDGQ
WRTYCHEVCRWTDAAEFRPVYQGRETPNMGKLVGHREWETLYHGWNWADVIQDMGFVRDD
GKTLTAQPHLDLDPKKMWTLDHMRRMPHLASPNVILNEMSDAEREAFVADYNRQGPGRP
APTDA

Ae505 *P. echinaior*: PrmA (Holmes et al 2016)

LAKAHQKIQELSWEPQYHEPYMKYGTDYTFKKAACKDPLKQVLSYFPMEEKDHRYGA
QDGAIRGNMFRQVQERWLEWQKLFLSIPLPEISAARSMPLFHVVPNPELHNGQAIQMI
DEVRHSTIQQLKRLYMNNYIDPAGFNNSLRNFQSDYCGTIGRQFAEGFITGDAITAASI
YLTIVAETAFTNTLFVAMPAAEAANGDYLLPTVFHVSQSDSRHISNGYATLLMALSDED
NRQLLERDLRYAWWNNHRVVDAAIGTFIEYGTKDRRKDRESYAEMWRRWIYDDYYRSYLL
PLEKYGLVIPHDLVEESWNQIWNKGYVHEVAQFFATGWCANYWRIDGMTDTDFEWFYKY
PGWYDRYGKWWENYNRLAKPNGHHAIVAEDVDYVYPHRCWTCMVPCLVREDMVDKVDGQ
WRTYCHEVCRWTDAAEFRPVYQGRETPNMGKLVGHREWETLYHGWNWADVQDMGFVRDD
GKTLTAQPHLDLDPKKMWTLDHMRRMPHLASPNVILNEMSDAEREAADVADYNRQGGGRP
APTDA

Ae406 *P. echinaior*: PrmA (Holmes et al 2016)

LAKAHQKIQELSWEPQYHEPYMKYGTDYTFKKAACKDPLKQVLSYFPMEEKDHRYGA
QDGAIRGNMFRQVQERWLEWQKLFLSIPLPEISAARSMPLFHVVPNPELHNGQAIQMI
DEVRHSTIQQLKRLYMNNYIDPAGFNNSLRNFQSDYCGTIGRQFAEGFITGDAITAASI
YLTIVAETAFTNTLFVAMPAAEAANGDYLLPTVFHVSQSDSRHISNGYATLLMALSDED
NRQLLERDLRYAWWNNHRVVDAAIGTFIEYGTKDRRKDRESYAEMWRRWIYDDYYRSYLL
PLEKYGLVIPHDLVEESWNQIWNKGYVHEVAQFFATGWCANYWRIDGMTDTDFEWFYKY
PGWYDRYGKWWENYNRLAKPNGHHAIVAEDVDYVYPHRCWTCMVPCLVREDMVDKVDGQ
WRTYCHEVCRWTDAAEFRPVYQGRETPNMGKLVGHREWETLYHGWNWADVQDMGFVRDD
GKTLTAQPHLDLDPKKMWTLDHMRRMPHLASPNVILNEMSDAEREAADVADYNRQGGGRP
APTDA

Ae331 *P. echinaior*: PrmA (Holmes et al 2016)

LAKAHQKIQELSWEPQYHEPYMKYGTDYTFKKAACKDPLKQVLSYFPMEEKDHRYGA
QDGAIRGNMFRQVQERWLEWQKLFLSIPLPEISAARSMPLFHVVPNPELHNGQAIQMI
DEVRHSTIQQLKRLYMNNYIDPAGFNNSLRNFQSDYCGTIGRQFAEGFITGDAITAASI
YLTIVAETAFTNTLFVAMPAAEAANGDYLLPTVFHVSQSDSRHISNGYATLLMALSDED
NRQLLERDLRYAWWNNHRVVDAAIGTFIEYGTKDRRKDRESYAEMWRRWIYDDYYRSYLL
PLEKYGLVIPHDLVEESWNQIWNKGYVHEVAQFFATGWCANYWRIDGMTDTDFEWFYKY
PGWYDRYGKWWENYNRLAKPNGHHAIVAEDVDYVYPHRCWTCMVPCLVREDMVDKVDGQ

WRTYCHEVCRWTDAAEFRPVYQGRETPNMGKLVGHREWETLYHGWNWADVIQDMGFVRDD
GKTLTAQPHLDLDPKKMWTLDHMRRMPHLASPNVILNEMSDAEREAFVADYNRQGPGRP
APTDA

***Methylocella silvestris*: PrmA (Crombie and Murrell 2014)**

MSLSLNSITQQKGIPIAEATRRIADLGWTPTYVKEAMTFPTDYKISKHPKDPMKQVLSYFPMQEE
KDNRVYGALDAALRGDMFRNVEQRWVEWMKFLAIIPPEISAARSMAMLGRLAPGDELRTGFT
MQMVDEFHRSTIQMNLKKWYMENYIDPAGFDITEAAFGKCYATTIGRQFGAEFLTGDAVTAANI
YLQVVAESAFTNTLFVAMPSEAARNGDYALPTVFLSVQSDESRHIGNGHSFLMSVLNNPDNHL
ERDIRYAFWQNHGIVDAAVGTIVEYGTKHRDKKESYAELWHRWIYEDYRXYMLPLEKYGIKIH
DDVHAAWDRIVKEGYVHKVAQFFSAGWWANFWRLEGLDEYDFEWFYKYPGWYNEYGAWW
ENYRKLSPKGSVPITFADTGYVYPHRCWSNLVPCVIRDQFTTDVVDGELYTYGHEIDRWTHKEAFA
AEYKGRPTPAMGRFSGKRQWEELYDGWDVADAIDKDMGFVRPDGKTLMAQPHLSLEEKDMWT
LDHVRGYTIKAPIKVLRLDLSPADREKHIAEYKKGTYIKRL

***Beijerinckia indica*: PrmA (Tamas et al 2010)**

MAVSLTSITQQKGMPIAEATRISDLGWTPSYVQEAMTFPTDYKISKQPKDPMKQVLSYFPMQ
EEKDNRVYGALDAALRGDMFRNVEQRWVEWMKFLAIIPPEISAARSMAMLGRLAPGDDLRT
GFTMQMVDEFHRSTIQMNLKKWYMENYIDPAGFDITEKAFGKCYATTIGRQFGAEFITGDAITAA
NVYLQVVAETAFTNTLFVAMPSEAARNGDYALPTVFLSVQSDESRHIGNGHSLLMSILNNPDNHL
LLERDIRYAFWQNHAIVDAAVGTIIEYGTKNRDKKESYAELWHRWIYEDYRXYMLPLEKYGIKIH
HDDVHQAWEDITKNGYVHKVAQFFSAGWWANFWRIDPLDERDFDWFYKYPGWYNEYGAW
WENYRKLSPKGSIPITFADTGYVYPHRCWSNLVPCVIRDQIKVDEVDGQLYTYGSEVDRWTHKEA
FSGEYKGRSTPAMGRFSGRRQWEELYDGWDVADAIDKDMGFVRADGKTLIAQPHLSLDEKDLWT
LDHVRGNTIKAPLKTRELSPADREKHLAEYRKGVTIRRV

***Rhodococcus jostii* RHA1: PrmA (McLeod et al 2006, Sharp et al 2007)**

MSRQSLTCAHAKITELSWDPTFATPATRFGTDYTFEKAPKKDPLKQIMRSYFPMEEEEKDNRVYGA
MDGAIRGNMFRQVQQRWLEWQKFLSIIPPEISAARAMPMAIDAVPNPEIHNGLAVQMIDEV
RHSTIQMNLKKLYMNNYIDPAGFDMTEKAFANNYAGTIGRQFGEGFITGDAITAANIYLTVAET
AFTNTLFVAMPDEAAAANGDYLLPTVFHVSQSDSRHISNGYSILLMALADERNRPLLERDLRYAW
WNNHCVVDAAGTFIEYGTKDRRKDRESYAEMWRRWIYDDYRSYLIPLEKYGLTIPHDLVEEAW
KRITDKGYVHEVARFFATGWPVNYWRIDAMTDKDFEWFHFKYPGWYSKYGKWWEEYNRLAYP

GRNKPIAFEEVGYQYPHRCWTCMVPALIREDMVVEKVDDQWRTYCSETCYWTDVAVAFRSEYQG
RPTPNMGRLTGFREWELHHGKDLADIVSDLGYYRDDGKTLVGQPHLDLDDPKKMWTLDDVRG
NTFQSPNVLLNEMSDAERNAHIAAYRAGGAVPA

Pseudonocardia sp. TY-7: PrmA (Kotani et al 2006)

MSRQSMSIAHKKITELSWEPTFATPAKRFGTDYTFDNPAPKKDPLKQILRSYFPMEEKDSRVFGA
MDGAIRGNMFRQVQERWMEWQKFLSIIPFPEISAARAMPMAIDAVPNPEIHNGLAVQMIDEV
RHSTIQMNLKRLYMNHYIDPAGFDMTEKAFANNYASTIGRQFGEGFITGDAITAANIYLTVAETA
FTNTLFVAMPSEAAAANGDYLLPTVFHVSQSDSRHISNGYSILLMALADEDNRVLLERDLRYAWW
NNHCVVDAAGTIFIEYGSKDRRKDRDSYAEMWQRWIYDDYYRSYLIPLEKYGLTIPHDLVEKSWER
INNGFYVHRVAQFFATGWPVNYWRIDPMTDITDFEWFHFKYPGWYNQFGKWWEAYARLSKPN
GHKPIAFEDVQYQYPHRCWTCMVPCLIREDMVTDKVVDDQWRTYCSETCHWTDVAVAFRPEYEG
RATPNMGRLTGKREWESLHHGRDLADIVTDLGYIRDDGKTLIPQPHLDLSDPKKLWTIDKLRGIEF
QSPNVLLNEMTDAEREAHIAEYKANPNVTTSVA

Mycobacterium sp. TY-6: PrmA (Kotani et al 2006)

MRNLIRAHERVKDFDWEHSYAEKPDYPTKYVMPRKTCDPFRHLIRDYVSMEQEKDDRQYGAM
EDALARSNSAGKAQPRWMEILKIALPVVNFGEYAAMKCCGQLVDTVNNAELRQGYMAQMIDE
VRHTNQELYLNRYFAKHAADPEGFHIGMKARANNLFGVAGRAALETFFVGDVPEGALNLQVVAE
TAYTNPIFVTLTEVAAAANGDNVTPSVFLSVQSDEARHMANGYSTLAAVVSNEEDNLKYLQADFRA
FWRQHSFLDPFLGAVYDYFQKERGHSYLEKWTEWIEEDWVGSYISKMEPYGLAVPDCFHVAKEQ
MRWKHHTAAMLAAASWPLHFWRWDPLTESDFEWFENKYPGWYEHYGPFWENFRQITKAED
GVNPMAAFEALPPLCQVCQMPCIFPRLDCEVRFADYGGRTVPFCGPMCELTFFQEPYRQAQSRN
FWQHHDGVELADHLVENGLLRSDGKTLIAQPSLDAERMWTIDDIRAWGMEITDPMPAITAQLA
AAGASGNGARA

Pseudomonas sp. CF600: phenol-2-monooxygenase-P3-component (Nordlund et al 1990)

MATHNKKRLNLKDYRYLTRDLAWETTYQKKEDVPLEHFEGIKITDWDKWEDPFRLTMDTYWK
YQAEKEKKLYAIFDAFAQNNGHQNISDARYVNALKLFLTAVSPLYQAFQGFSSRVGRQFSGAGAR
VACQMQAIDELRHVQTQVHAMSHYNKHFDGLHDFAHMYDRVWYLSVPSYMDDARTAGPFE
FLTAVSFSFEYVLTNLLFVPFMSGAAAYNGDMATVTFGFSAQSDEARHMTLGLEVIKFMLEQHEDN
VPPIQRWIDKWFWRGYRLLTLIGMMMDYMLPNKVMWSWSEAWGVYFEQAGGALFKDLERYGIR

PPKYVEQTTIGKEHITHQVWGALYQYSKATSFHTWIPGDEELNWLSEKYPDTFDKYRPRFEFWR
EQQAKGERFYNDTLPHLCQVCQLPVIFTEPDDPTKLSLRSLVHEGERYQFCSDGCCDIFKNPVKYI
QAWLPVHQIYQGNCEGGDVETVVQKYYHIKSGVDNLEYLGSPEHQRWLALKGQTPTAAPADK
SLGAA

***Mycobacterium chubuense* NBB4: PrmA (Das et al 2015)**

MTASITTQHEKIKSFDWEPSYFRRDALYPTKYKIPPKTKDPFRTLREYVGMEEKDDRQYGALED
ALSRMNNSAQAEPRFMEIMKPVLLVDFGEYAAMKCTAMLVDTVENPELRQGYLAQMIDEVRH
TNQEAYLMRYFAKHAPDPAGFNSGFQTRASDPIGRPGRAVFEAFMNDPITNALNLQVVAETAY
TNPLFVAVTEVAAAANGDQATPSVFLSVQSDEARHMANGYSTLA AVLSEPENLPMLQEDFDATAFW
RQHSFLDNFQGAUVYDYFSKVRKLSYKEYWDQWIWDDWAGSYIERLEPFGLKVPRIWHDARHV
EWGGHSAAMVSAALWPVHAWRSYMTDEDFAYLEEKYPGWEQHFGPFWTAYREMGDPRKG
HLALELFPMPICRQCMPVFPDPDINEVRLSIDAAGQRHAFCEACQHIFRQAPHRHTGMTW
WEVNDGIELARYIEDNGLLRADGRTLMGQPHVHTEERWLWTIDDIRRTGIVIQDPLRAMPADAF
TDI

***Rhodococcus sp.* AD45: IsoA, isoprene monooxygenase hydroxylase, alpha sub-unit
(Crombie et al 2015)**

MQWKAQIMLLNRDDWYDTSRNLWDLSYVDPSEAFPASWSGAGDVPTEAWDKWDEPFRVSY
RDYVRIQREKESGVKAVSNALVRSPTYEKLDPAHVAASHLHMGTTCMVEHMAVTMQSRFCRFA
PTPRWRNLGVFGMLDETRHTQLDLRFSDLLKQDPRFDWSQKAFHTNEWGVLAVKNFFDDAM
LNADCVEAALATSLTVEHGFTNVQFVALAADAMAAGDINWSNLLSSIQTDEARHAQQGFPTLSIL
MEHDPARAQKALDIAFWRSTRLFQTLTGPAVDYYPDLQQRKMSFKEFMLEWIVNHHERILEDYG
LKKPWYWDQFMYSLEHGHAMHLGTWFWRPTLFWKPNAGVSKDEREWLREKYPTWEENWG
GMWDEIINKVNTDQIEKTLPATFPSLCNLTQLPLGSAFSLNDLADHSLTYNGRLYHFDSAISKWCFE
QDPERYAGHQNIIDRVIDGQIVPADLAGGLSYMGLTPEVMGEDVYNYAWAKDYLASPSLAATEF
VAQEKISI

***Pseudomonas sp.*: OX1, toluene-o-xylene monooxygenase component (Vardar and
Wood 2005)**

MSMLKREDWYDLTRTTNWTPKYVTENELFPEEMSGARGISMEAWEKYDEPKITYPEVSIQREK
DSGAYSIIKALERDGFVDRADPGWVSTMQLHFGAIALEEYAASTAEARMARFAKAPGNRMAT
FGMMDENRHGQIQLYFPYANVKRSRKWDWAHKAIHTNEWAAIAARSAFFDDMMMTRDSVAVS

IMLTFAFETGFTNMQFLGLAADAAEAGDHTFASLISSIQTDESRHAQQGGPSLKILVENGKKDEAQ
QMVDVAIWRSWKLFSVLTGPIMDYITPLESRNQSFKEFMLEWIVAQFERQLLDLGLDKPWYWD
QFMQDLDETHHGMHLGVWYWRPTVWWDPAAAGVSPEEREWLEEKYPGWNDTWGQCWDVI
TDNLVNGKPELTPETLPTICNMCNLPIAHTPGNKWNVKDYQLEYEGRLYHFGSEADRWCQIDP
ERYENHTNLVDRFLKGEIQPADLAGALMYMSLEPGVMGDDAHDYEWVKAYQKKTNA

Mycobacterium sp. M156: PmoC propene monooxygenase (Chan Kwo Chion et al 2005)

MASDATQLHEKTKAYDWDFTSVEQKPKFETKYKLPKKGKDPFRLLRDYMKMEAEKDDRTYGF
DGAIRTREATKMEPRFVELMKMILPILTNAEYQAVAGCGMIISAINNQEMRQGYAAQMLDEV
AQLMALRNFYVKHYHDPAGFDLGQVGLYQHPAGLLSIGEFQHFNTGDPDLCIIDLNIVVETAFT
ILLVAMPQVAVRNGDNALATTMSIQSDESRHMANGYGAIMSVLGEPDNVPMINESLERHFWH
AHKSLDAAIGWGSEYGAHDRAWSYKDQWDEWVVDFFIGGFVDRLSEFGLTPPSRLAAAAEVT
WTHHTVGQVLSAVWPLNFWRSAMGPADFEWFENNYPGWSAAYQGYWEAYKELADPAGGH
IMLQELPGLPPMCQVCQTPCIVPRLDNTVRIVELDGQNYALCSEGCEWIFGKWPDAYKDRKQL
WERYDGDWDLADVLDLGYVRPDGHTLIGQPLLKMDRFWTIDDIRRLGYEVKNPMLTI

Gordonia sp. TY5: PrmA (Kotani et al 2003)

MSRQSLTKAHAKITELSWEPTFATPATRFGTDYTFEKAPKKDPLKQIMRSYFPMEEKDNRYGA
MDGAIRGNMFRQVQERWLEWQKFLSIIPFEISAARAMPMAIDAVPNPEIHNGLAVQMIDEVR
HSTIQMNLKLYMNNYIDPAGFDITEKAFANNYAGTIGRQFGEGFITGDAITAANIYLTVAETAFT
NTLFVAMPDEAAANGDYLLPTVFHVSQSDESRHISNGYSILLMALADERNRPLLERDLRYAWWN
NHCVVDAAGTFIEYGTKDRRKDRESYAEMWRRWIYDDYRSYLLPLEKYGLTIPHDLVEEAWNRI
VDKHYVHEVARFFATGWPVNYWRIDAMTDTDFEWFEEKYPGWYNKFGKWWENYNRLAYPGK
NKPIAFEDVDYEPHRCWTCMVPCLIREDMVTDKVDGQWRTYCSETCAWTDKVAFRPEYEGRP
TPNMGRLTGFEWETLHHGKDLADIITDLGYVRDDGKTLIPQPHLDLDPKKMWTLDDVVRGIPFGS
PNVALNEMSDDEREAHIAAYMANKNGAVTV

Bradyrhizobium diazoefficiens USDA110: alkene monooxygenase hydroxylase (Sugawara et al 2017)

MVSDPIRRKDEMSGTLTLNKITAQRGISVGEAAKKIADLGWNPSYVQEAMTFPTDYKITKAPKDP
MKQVLRSYFPMQEEKDNRYGALDAALRGDMFRNVEPRWVEWMKLFLAIIPFEISAARSMAM
VGRLAPGEDLRTGFTMQMVDEFHSTIQMNLKWKYMENYIDPAGFDITEEAFGKCYATTIGRQF

GEGFITGDAITSANVYLTVAETAFTNTLTVAMPSEAARNGDYALPTVFLSVQSDSRHIGNGHSM
LMSMLKEPENHLLLERDMRYAFWQNHAIVDAAIGTFIEYGTTNRDKNKESYAEMWHRWIFEDYY
RTYMLPLEKYGIKIHDDVQAAWKRLTEKHVYHKVAQFFAVGWSANFWRIEAQTEKDFEWFH
KYPGWYAQFGEFWKWYEKLSHRGQTNILFNSDVGYVYPHRCWSCLVPCLIREDIVTDEIDGKLHT
FAHELDRWTAVEAFAGEYQGRPTPAMGRFSGRREWESVYHNVDIADAIDKDLGFVRTDGKTLVA
QPHLRFDQKEMWTLDDVVRGHILKSPLQTLREMSPADREKHLAEYRKGF TINPCN

***Rhodobacter sphaeroides* 2792: methane monooxygenase (Lim et al 2009)**

MEAHGMTSLTLNKITSQRGISVGEATKKISDLGWNPTYVQEATFPTDYKISKAPRDPMKQVLSY
FPMQEEKDNRVYGALDAALRGDMFRNVEPRWVEWMKFLAIIPFEISAARSMAMVARLAPGE
DLRTGFTMQMVDEFHSTIQMNLKKWYMENYIDPAGFDITEEAFGKCYATTIGRQFGEGFITGDT
MTAACMYLTVAETAFTNTLTVAMPSEAARNGDYALPTVFLSVQSDSRHIGNGHSLLMALKE
PENHLLLERDLRYAFWQNHAIVDAAIGTFIEYGTTNRDKNKESYAEMWHRWIFEDYYRTYMLPLE
KYGIKVHDDVQEAWNRIKHYVHKVAQFFAVGWPNFWRIEAQTDRDFEWFQKYPGWYA
EFGFWRWYAKLSKPGQKVITFNEEVGYVYPHRCWSCLVPCLIREDMVVDEIDGQLHTFAELDR
WTAVEAFSDEYQGRPTPAMGRFSGKREWETLYHGWDLADAIDKDLNFVRDDGRTLTPQPHLRFD
DKDMWTLDDVVRGHTLLSPLTLLREMSPEAREKHLAEYRAGFTINPCH

***Pseudonocardia* spK1: ThmA, tetrahydrofuran monooxygenase (Thiemer et al 2003)**

MTAPPMKRPRRSITASHAKIGELGWDRTYYPHERGKYPSRYKLPNKGRDPMKQIMGDYLMQ
NEKDDR VHGLDAAVRAEVP GKAPLRWLELLKPYLLTVISAEAAAATRCMGMLVDALDDPELQNA
YYIQQQLDEQRHTAMQMNLRYWYMKNMPEPVGWNLGLQAVGGDSILVAAQNLTGSFMTGDPF
QAAVALQVVETAFTNTILVAFPDVAVRNHDFALPTVMNSVQSDEARHINNGYATLLYLLQEPEN
APLLEQDIQQMFWTVHAFVDAFMGILVEYAPT DATDPESWTTKWDRWVNDYYRSYIVNLGKL
GLKIPDSIFKRARERIAADYHHKVAVGVWASWPFHYKYGNLEQKDYDWFESKYPGWNEKFGAF
WRGYADVRYPGSGPLQLPGLLEGAGPICWTCQLGCLRPEEQCHRIVDEHTRFYCSPECKWIDMT
NPGRYVGDRVWFDRYHGWEYSEIVRDLGFLRPDGKTLTGQPHVDP DPAKQWTIDDLRELGHIM
QSPNILTAERLGLPYKRVEYTGTKPGDMPPTIPPLFGV

***Burkholderia cepacia* G4: TomA3 toluene monooxygenase (Shields et al 1995)**

MDTSVQKKLGLKNRYAAMTRGLGWQTSYQPMKVFYDYKYEKIHWDKWKWEDPFRLTMDA
YWKYQGEKEKKLYAVIDAFAQNNGQLSISDARYVNALKVFIQGVTPLEYMAHRGFAHIGRHFTGE
GARVACQMQSIDELRHFQTEMHALSHYNKYFNGLHNSIHWYDRVWYLSVPKSFFEDAATGGPF

EFLTAVSFSFEYVLTNLLFVPFMSGAAAYNGDMSTVTFGFSAQSDSRHMTLGIIECIKFMLEQDPDN
VPIVQRWIDKWFWRGYRLLSIVAMMQDYMLPNRVMSWRESWEMYVEQNGGALFKDLARYGI
RKPKGWDQACEGKDHISHQTFVAFYNYNAAAPIHTWVPTKEEMGWLSEKYPETFDKYRPRWD
YWREQAAKGNRFYNKTLPMLCTTCQIPMIFTEPGDATKICYRESAYLGDKYHFCS DHCKEIFDNEP
EKFVQSWLPPQVYQGNCFKPDADPTKEGFDPLMALLDYNNLVGRDNFDFEGSEDQKNFAA
WRGEVLQGEAK

***Mycobacterium rhodesiae* JS60: EtnC methane monooxygenase (Coleman and Spain 2003)**

MANPTIEVVHEKSKRYDWGFDYARPDPKFPTRYIIPPKGKDPFRSMLRGYAAMETEKDNRVYGG
DSNVRYRNATSAEPRFIEGMKFGIPSFTDAEYQATCGSGFLIASMKNQELRQGYAGQMLDEV
RHTQIEVALRKYYLKNYHDPAGFDIGQIGLGNHPIGTLARASFQSFNTGDPVEVSMCLNIVLE
TAYTNPLVVALPQVA AVNGEHAMPTAFLSIQSDESRHMANGYGTLM SVIQEHDNLPFLQESL
DRHFHWQHQSMDTLVGV LSEYFAVERPWAYKDVWEEWVVD D FVGSYMSRLSPFGLKPPAR
LGDVARYVNDMHHSVAIALAAMWPLNFWRTDPMGPADYEW FENHYPGWTKSYGGLWDAFRD
MSDPSSARILQELPSLPPFCQVCHVPCVMPTLHAPETRIVY GEGKKFAVCSEGCEWIFNLNPT
IYSGCANWWERFDGMDLADVILALGYVRPDGKTLIGQPHLNAERMWTIDDIRRLEYEVDPLK

***Nocardioides* sp. JS614: EtnC methane monooxygenase (Coleman et al 2011, Mattes et al 2005)**

MVAPKLETVHEKSKRYDWGFDYAKPDPKFPSPRYIIPPKGKDPFRVMMRGYAAMENEKDN
RVYALDSNVRYRNANLAEPRFMEAMKFAVPAL TDAEYQAVCGAGFLISSVKNQELRQGYAG
QMLDEV RHAQLEINLRKYYLKNYHDPAGFDIGQIALGNHPIGTLARASFQPFNTGDP
IEVAMCLGVVLETA YTNPLVVALPQVAMVNGDHAMPTTFLSIQSDESRHMANGYATL
MACLESTENV PFLQESLERHF WHQHMSMDTLVGVVSEYYAVNRPWAYKDVWEEW
VVD D FVGSYMNRLAPYGLKPPERLPDVARFVEDMHHSVAIALAAIWPLNFWRIDP
MGPADYEW FENHYPGW TARYGGLW DAYREMSDPSS GRLLMQELPALPPFCQVCHV
PCVMPRIDAPETRIFDHEGKRYAVCSEGCDWIFKLNPTIYTGCAN WWERFDGMDLAD
VILALGYVRPDGKTLMGQPHLNADRMWTIDDIRALKYEIKDPLRV

***Rhodococcus rhodochrous* B276: AmoC alkene monooxygenase (Smith et al 1999)**

MASNPTQLHEKSKSYDWDFTSVERRPKFETKYKMPKKGKDPFRVLIRDYMKMEAEKDDRTHGFL
DGAVRTREATRIEPRFAEAMKIMVPQLTNAEYQAVAGCGMIISAVENQELRQGYAAQMLDEV
HAQLEMTLRNYAKHWCDPSGFDIGQRGLYQHPAGLVSIGEFQHFNTGDPLDVIIDLNIVAETA
TNILLVATPQVAVANGDNAMASVFLSIQSDEARHMANGYGSVMALLEENLPLLNQSLDRHF
WRAHKALDNAVWGCSEYGARKRPWSYKAQWEEWVVDVGGYIDRLSEFGVQAPACLGAAA
DEVKWSHHTLGQVLSAVWPLNFWRSAMDGPADFEWFENHYPGWSAAYQGYWEGYKALADP
AGGRIMLQELPGLPPMCQVCQVPCVMPRLDMNAARIIEFEGQKIALCSEPCQRIFTNWPEAYRH
RKQYWARYHGWDLADVIVDLGYIRPDGKTLIGQP LLEMERLWTIDDIRALQYEVKDPLQEA

S2 Buoyant density of RNA SIP gradient fractions

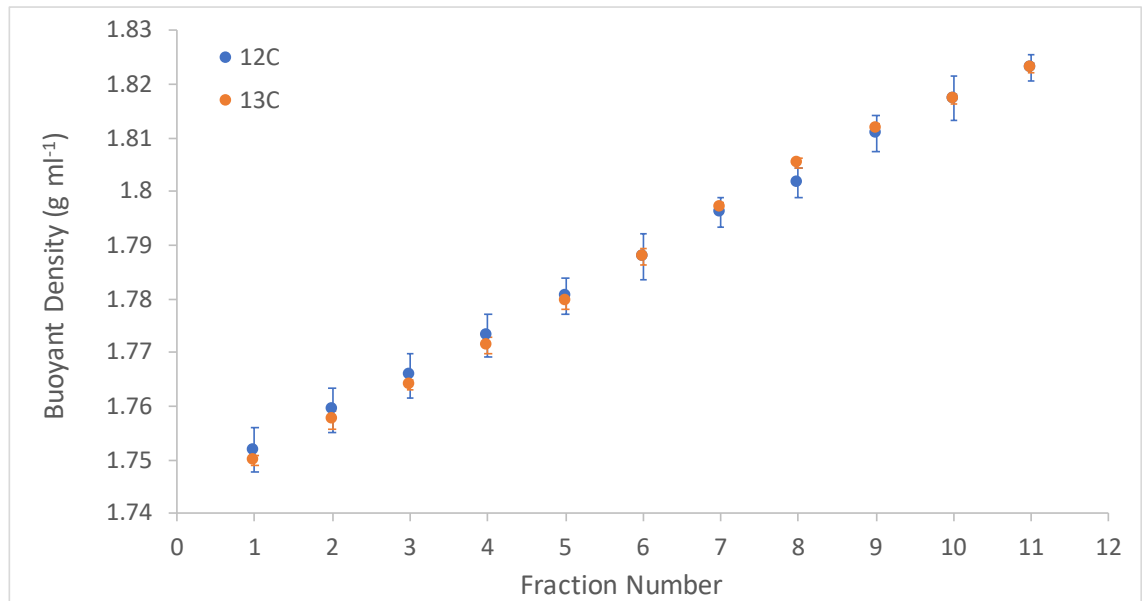


Figure S2.1 The relationship between SIP fraction number and buoyant density (in g ml⁻¹). Fractions were generated from density gradients containing RNA isolated from the laterocervical plates of *A. echinator* ants fed on either a ¹²C (blue) or ¹³C (orange) glucose water diet (see Chapter 2). Points represent averages (n=3 samples of 22 ants per dietary treatment) ± standard error.

S3 Biosynthetic gene clusters predicted for *Streptomyces* strain N2

Table S3.1 Biosynthetic Gene Clusters (BGCs) predicted to be encoded in the genome of *Streptomyces* strain N2. Analysis was carried out using antiSMASH 4.0. PKS = polyketide synthase, NRPS = non-ribosomal peptide synthase.

Cluster number	Cluster classification	Most similar known cluster (% of genes showing similarity)
Cluster 1	T1PKS-NRPS	Filipin (100%)
Cluster 2	NRPS	Herbimycin (13%)
Cluster 3	T1PKS	Borrelidin (9%)
Cluster 4	Terpene	-
Cluster 5	NRPS	Actinomycin (89%)
Cluster 6	Ectoine-NRPS	Pristinamycin (29%)
Cluster 7	T3PKS	Herboxidiene (7%)
Cluster 8	T1PKS-Other	Cinnamycin (19%)
Cluster 9	Ectoine	Ectoine (100%)
Cluster 10	Lantipeptide	-
Cluster 11	Melanin	Melanin (100%)
Cluster 12	Siderophore	Desferrioxamine_B (83%)
Cluster 13	Lassopeptide	-
Cluster 14	T2PKS-T1PKS	Spore_pigment (83%)
Cluster 15	NRPS	Phosphonoglycans (3%)
Cluster 16	Terpene	Albaflavenone (100%)
Cluster 17	Terpene	-
Cluster 18	NRPS-Siderophore-T1PKS	Kinamycin (22%)
Cluster 19	T1PKS-Other	Meilingmycin (5%)
Cluster 20	Bacteriocin	-
Cluster 21	Terpene	Herboxidiene (3%)
Cluster 22	Nrps-T1PKS	Meilingmycin (3%)
Cluster 23	Siderophore-NRPS	Friulimicin (18%)
Cluster 24	NRPS-Other	Kirromycin (16%)

Cluster 25	NRPS	-
Cluster 26	Terpene-Thiopeptide- Lantipeptide	Hopene (92%)
Cluster 27	PKS-NRPS-T1PKS	Cinnabaramide (18%)
Cluster 28	NRPS-Lantipeptide	Bleomycin (12%)
Cluster 29	NRPS	Mirubactin (78%)
Cluster 30	T1PKS	Tetronasin (3%)
Cluster 31	Bacteriocin	-
Cluster 32	NRPS	Fusaricidin (25%)
Cluster 33	NRPS-T1PKS	Pristinamycin (12%)
Cluster 34	NRPS-Terpene	2-methylisoborneol (100%)
Cluster 35	Lantipeptide	A-503083 (7%)

S4 UPLC-MS analysis of *Streptomyces* strain N2 extracts

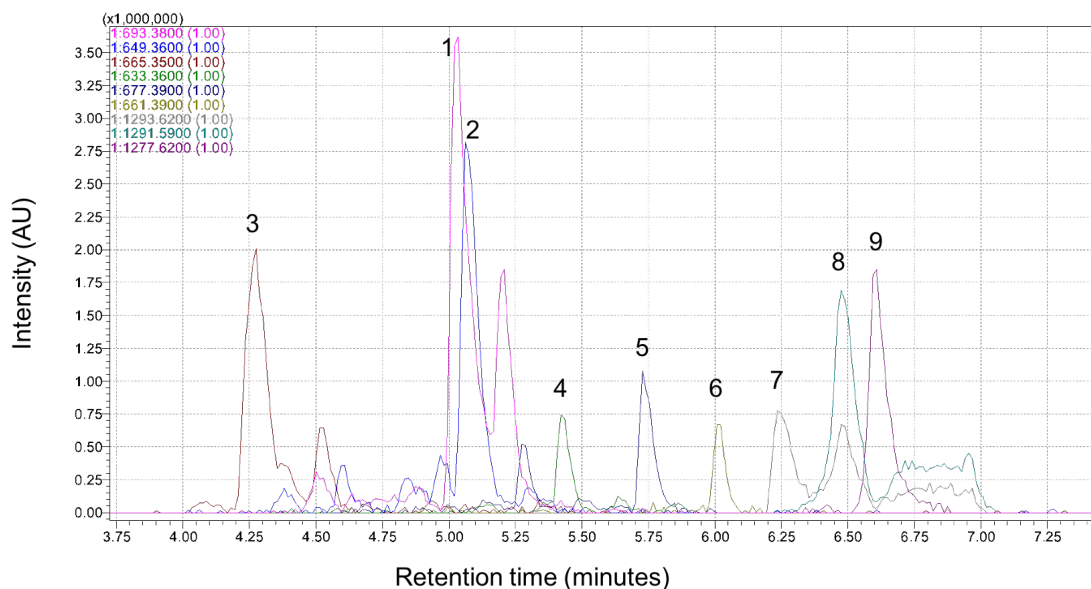


Figure S4.1 Ion chromatograms from UPLC-MS analysis summarising the metabolic profile of the crude ethyl acetate extract of *Streptomyces* strain N2 grown on SFM plates (work done by Johannes Rassbach, John Innes Centre). Numbers above peaks represent different compounds identified in the extract (see Table S4.1). Numbers in the key represent $[M + Na]^+$ masses and the colours of numbers relate to peaks. The y-axis is in absorbance (AU) units.

Table S4.1 Compounds identified in the crude extracts of *Streptomyces* N2 grown on SFM agar. Codes relate to peaks identified during UPLC-MS analysis (see Figure S4.1). Those shown in blue were successfully purified (work done by Johannes Rassbach, John Innes Centre).

Code	[M+Na] ⁺	Exact mass	Molecular formula	Potential compound (isomers possible)
1	693.3842	670.3928	C ₃₅ H ₅₈ O ₁₂	Fungichromin
2	649.3585	626.3666	C ₃₃ H ₅₄ O ₁₁	14-Hydroxy(iso)chainin
3	665.3491	642.3615	C ₃₃ H ₅₄ O ₁₂	1',14-Dihydroxy(iso)chainin
4	633.3624	610.3717	C ₃₃ H ₅₄ O ₁₀	(Iso)chainin
5	677.3845	654.3979	C ₃₅ H ₅₈ O ₁₁	Filipin III
6	661.3959	638.4030	C ₃₅ H ₅₈ O ₁₀	Filipin II
7	1293.6184	1270.6234	C ₆₂ H ₈₆ N ₁₂ O ₁₇	Actinomycin X ₀₈ = I
8	1291.5936	1268.6077	C ₆₂ H ₈₄ N ₁₂ O ₁₇	Actinomycin X ₂ = V
9	1277.6192	1254.6285	C ₆₂ H ₈₆ N ₁₂ O ₁₆	Actinomycin D = C ₁ = IV

S5 Analysis of rhizosphere SIP fractions using qPCR

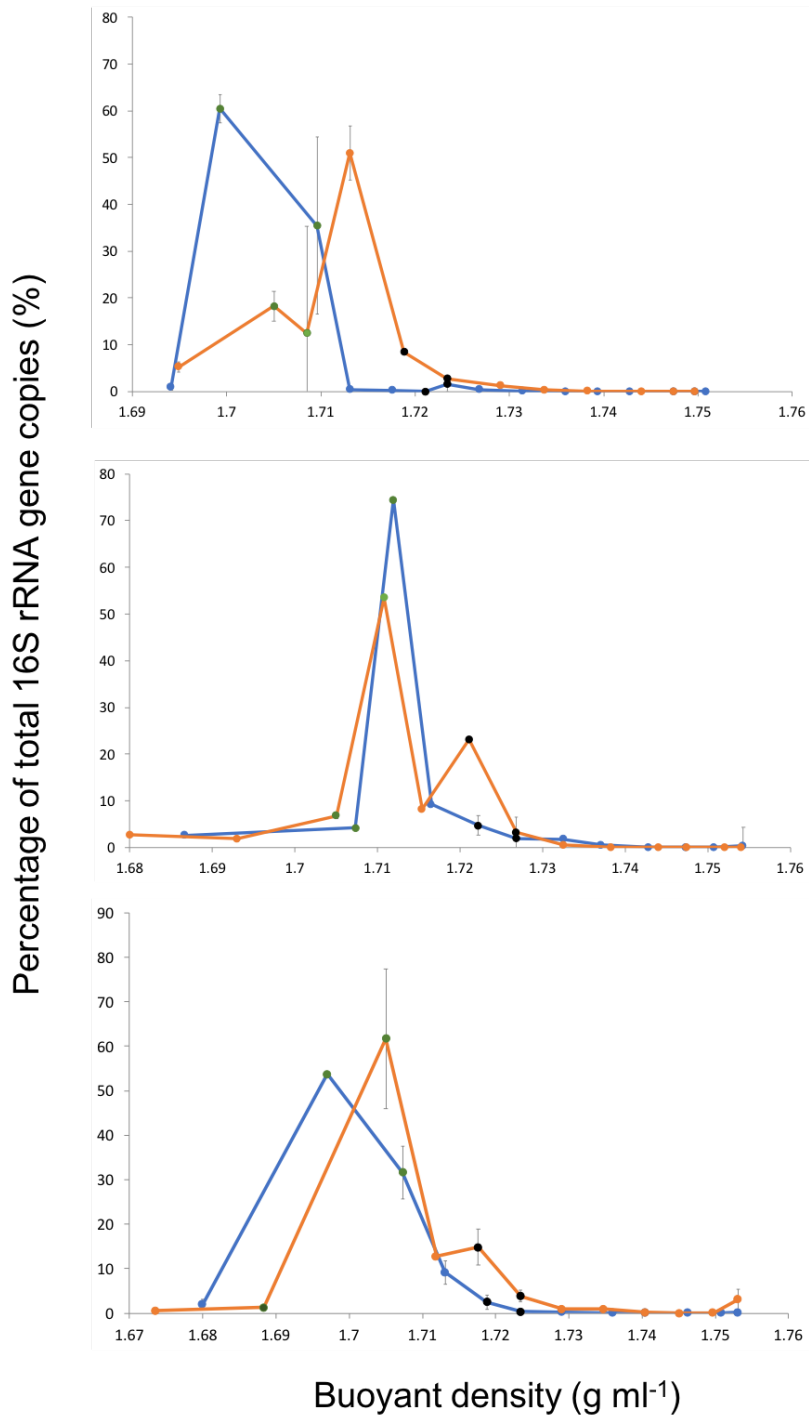


Figure S5.1 16S rRNA gene copy number across buoyant density fractions of DNA isolated from rhizosphere samples of *A. thaliana* plants incubated under either ¹²CO₂ (blue) or ¹³CO₂ (orange) conditions. Copy number is shown as a percentage of total copy number per sample. N=2 replicate measurements on the same fraction. Bars represent standard errors. Green and black dots represent the “light” and “heavy” fractions, respectively, that were pooled in each treatment and submitted for 16S rRNA gene amplicon sequencing.

S6 Growth of streptomycetes on agar minimal medium

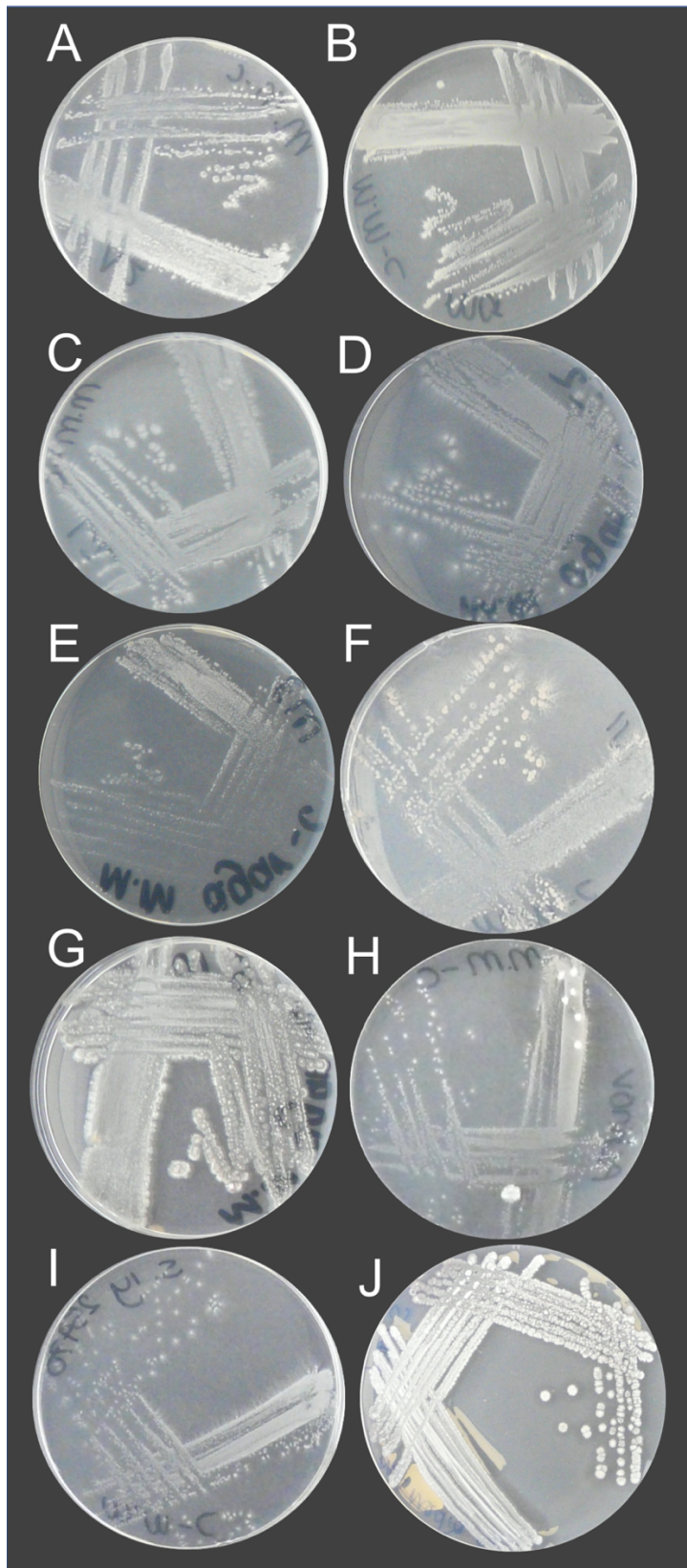


Figure S6.1 Growth of *Streptomyces* isolates on minimal medium with agar as a gelling agent and no additional carbon source. A) N2, B) MG, C) L2, D) M2, E) M3, F) N1, G) *S. lydicus* 31975, H) Actinovate I) *S. lydicus* 25470, J) *S. coelicolor* M145.